University of Alberta

Neural correlates of sensory specializations in birds.
By

Cristian Gutierrez-Ibanez

A thesis submitted to the Faculty of Graduate Studies and Research in partial fulfillment of the requirements for the degree of

Doctor of Philosophy

in

Neuroscience

Centre for Neuroscience

Fall, 2013
Edmonton, Alberta

Examining Committee

Dr. Douglas Wylie, Department of Psychology

Dr. Ian Winship, Department of Psychiatry

Dr. Peter Hurd, Department of Psychology

Dr. Christopher B. Sturdy, Department of Psychology

Dr. Gerog Striedter, Department of Neurobiology and Behavior at the University of California at Irvine

Abstract

A basic tenet of comparative studies of the brain is that the larger size of any neural structure is related to the need for progressing more complex or larger quantities of information, the so call Jerison's “principle of proper mass”. Base on this principle, variation of the absolute and relative size of the brain, as well as variation in individual regions, has been correlated with motor, sensory and cognitive specializations. A large amount of these comparative studies have been focused on birds. Birds have become powerful models in many aspects of neurobiology as they display a large diversity of sensory, behavioural, motor and cognitive specializations. This provides the perfect opportunity to study changes in the brain related to these specializations.

This dissertation seeks to further advance our understanding of the principles that govern brain evolution using birds as a model. We performed five studies on the variation of cytoarchitectonic organization, relative volume and cell numbers in different sensory nuclei in birds. We found differences in the relative size of somatosensory, auditory and visual nuclei among birds. We show the independent enlargement of a somatosensory nucleus in three groups of birds related to different feeding behaviors. Our results also show variation in the relative size of nuclei that belong to parallel visual and auditory pathways within owls (Strigiforms). Additionally, we performed a comparison of the cytoarchitectonic organization, size and cell numbers in the isthmo optic nucleus in a large sample of birds which throws new light on the function of the projection from the isthmo optic nucleus to the retina. Lastly, we use a combination of phylogenetically corrected principal component analysis and evolutionary rates of

change to show that the relative size of 9 visual nuclei evolve in a combination of concerted and mosaic manner. The current dissertation adds greatly to our knowledge of the forces that drive differences in morphology and cytoarchitecture of the brain between different species.

Acknowledgements

First and foremost, I would like to thank my supervisor, Dr. Doug Wylie and my co-supervisor Dr. Andy Iwaniuk. Dr. Wylie always gave me complete liberty to pursuit any research avenues. He was also incredible generous and supportive all along my program. Dr. Iwaniuk was equally important in me completing this degree. He provided constant support, feedback and discussion for my research with incredible patience. Thanks to Dr. Pete Hurd who always provided advice when needed and not only about stats. Very big thanks to everyone in the lab over the years, Tom, Jeffrey, Erin, and everyone who came along the years. Special thanks to David Graham, who not only painfully proofread all of my manuscripts but provided technical, and more importantly, moral support all along. Thanks to the Centre for Neuroscience. Thank you to all the staff in the psychology department main office and shop for always being available and willing to help. Thanks to the long list of researchers and institutions that have provided specimens. Thanks to everyone in el “El rayo” lab back in Chile for helping making me the biologist I am. Thank to Macarena Faunes for her constant support. Finally, thanks to all my family who have always encourage and support my carrier. Thanks to Jessica Thomson, my incredible wife who for great part of this thesis was there to support me, encourage me and keep me grounded.

Table of content

List of tables

List of Figures

List of abbreviations

AIC	Akaike Information Criterion
BC	brachium conjunctivum
Cb	cerebellum
CE	coefficient of error
DLL	nucleus dorsolateralis anterios thalami
DLP	posterior part of the dorsolateral thalamic nucleus
E	entopallium
f	frontal
GLv	nucleus geniculatus lateralis, pars ventralis
IC	inferior colliculus
ICc-core	core of the central nucleus of the inferior colliculus
ICc-ls	lateral shell of the central inferior colliculus
ICx	external nucleus of the inferior colliculus
ILD	interaural level difference
ION	isthmo optic nucleus
Ipc	parvocellular part of the nucleus isthmi
Imc	magnocellular part of the nucleus isthmi
Imc-in	internal subdivision of the Imc
Imc-ex	external subdivision of the Imc
ITD	interaural time difference
LLDa	anterior dorsal lateral lemniscus
LLDp	posterior dorsal lateral lemniscus
LLIc	caudal part of the intermediate lateral lemniscus
LLIr	rostral part of the intermediate lateral lemniscus
LLv	ventral part of the lateral lemniscus
LM	nucleus lentifomis mesencephali
MLd	nucleus mesencephalicus lateral pars dorsalis (MLd
MV	Motor nuclei of the fifth nerve
nIV	abducens nerve nucleus

NA	nucleus angularis
nBOR	nucleus of the basal optic root
NL	nucleus laminaris
NM	nucleus magnocellularis
nRt	nucleus rotundus
NV	root of the trigeminal nerve
OMv	ventral part of the oculomotor nucleus
OU	Ornstein-Uhlenbeck
OV	nucleus ovoidalis
op	orbital process
PE	nucleus pontine externus
p	parietal
PCA	principal component analysis
PGLS	phylogenetic generalized least squares
p.o.p.	Postorbital process
pP	nucleus paraprincipalis
PrV	principal sensory nucleus of the trigeminal nerve
PrVi	inferior part of principal sensory nucleus of the trigeminal nerve
PrVs	superior part of principal sensory nucleus of the trigeminal nerve
PT	nucleus pretectalis
RA	robust nucleus of arcopallium
RGC	retinal ganglion cell
RP	nucleus reticularis pontis
sIXd	nucleus sensorius of nIX
Slu	nucleus semi lunaris
SO	superior olive
sq.o.w.	squamo-occipital wing
SP	nucleus subpretectalis.
SPL	nucleus spiriformis lateralis
sT	nucleus supratrigeminalis
Tel	telencephalon
TeO	optic tectum

TOv	tractus ovoidalis
TTD	descending tract of the trigeminal nerve
VeM	nucleus vestibularis medialis

Chapter 1: Introduction

Even before Darwin published "On the origin of the species" [1876] and evolution was widely accepted, biologists have been comparing the shape and size of vertebrate brains. For example, Owen [1857], one of the most famous anatomists of the eighteen century and someone who did not actually believe in evolution [Panchen, 1994], classified mammals into four groups base on the gyri of the cortex. Since then, many studies have attempted to elucidate why vertebrate brains vary in size and conformation, how evolution acts on neural tissue to effectuate these conformational differences, and ultimately, what are the principles behind brain evolution.

One of the most evident variation among vertebrates' brains is in the absolute size. Within vertebrates, the absolute brain size can vary by several orders of magnitude, from a few milligrams in small fishes and amphibians to seven kilograms in the sperm whale. It is fairly intuitive that brain size is correlated with body size in all animals, but it was also clear from very early on that brains do not scale directly with body size. In fact, Cuvier [1845] noticed that small animals have proportionally larger brains than bigger ones. This becomes very clear when the weight of the brain (log transformed) is plotted against body size (log transformed; Figure 1.1). Data points tend to fall in a straight line with a slope different than one. Therefore the brain scales allometrically with body size rather than isometrically, meaning that the proportion of the body that the brains occupies does not remains constant as body size increases. In this case, because

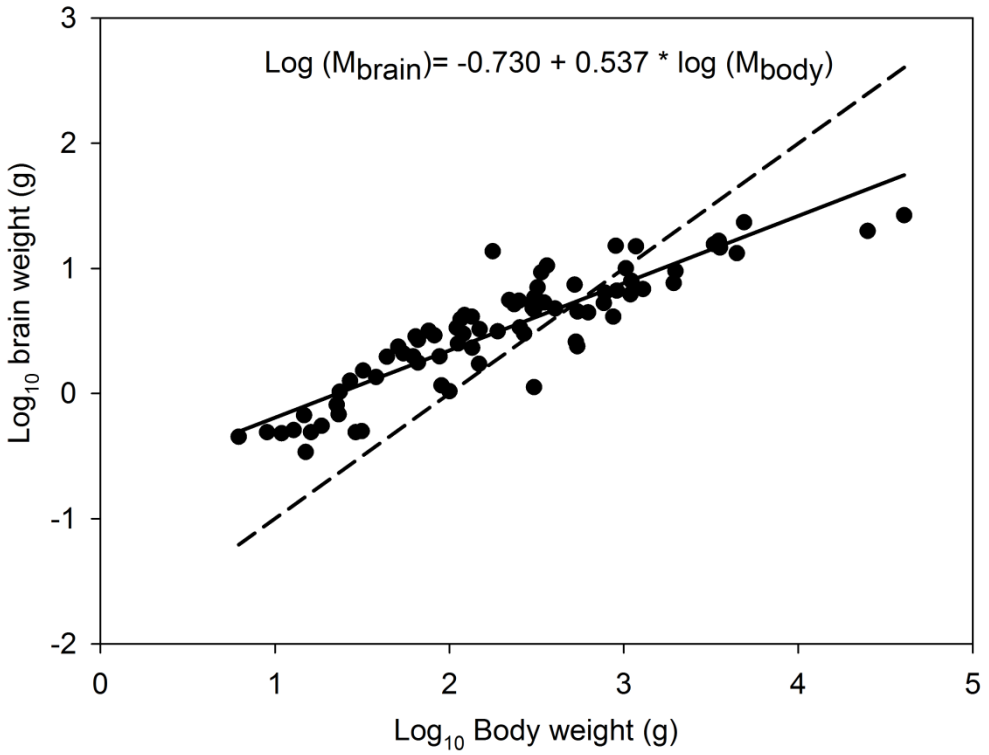

Figure 1.1. Allometric relationship between body and brain weight in birds. Scatterplot of the log10 body weight vs. log10 brain weight in 82 species of birds [data from Iwaniuk and Nelson 2002]. The solid lines show the regression through the mean. The slope is = 0.537, indicating negative allometry between body and brain weight in birds. The dotted line shows what an isometric relationship (slope = 1) between brain and body weight for the same data set would look like. M_{brain} = brain weight. M_{body} = brain weight

the slope is less than one is said that the brain scales with negative allometry with respect to body size, and means that the brain gets proportionally smaller as the body size grows. The relationship between brain and body size can be described by an equation of the form:

$$\mathrm{Log}(M_{brain}) = \mathrm{Log}(a) + b*\mathrm{Log}\,(M_{body})$$

where b is the slope, a the intercept, M_{brain} the brain weight and M_{body} the body weight. Several studies have shown the slope for the relationship between brain and body size in vertebrates to be somewhere between 2/3 and 3/4 [e.g. Jerison 1973; Martin, 1981], and many explanations have been offered for the particular value of the slope. For example, initial studies found the value of the slope to be close to 2/3, and because the surface of any Euclidean body scales to its volume with an exponent of 2/3, it has been proposed that brain size scales to body surface [Jerison, 1973]. Later studies [Martin, 1981; Mink et al., 1981] found the slope to be 3/4 for placental mammals but less than 2/3 for reptiles and birds, and thus dismissed the body surface explanation. Martin [1981] proposed that at least in placental mammals the relationship between brain and body size would be explained by the basal metabolic rate as this also scales with a slope of 3/4 with body size. It must be noted that the variation of the slope between different groups and its variation with the species sampled has led some authors to discard any significance of the brain body slope [Pagel and Harvey, 1989].

1.1 Variation in relative size of neural structures.

From studying the relationship between brain and body size, it is also clear that some species lie above the regression line while others lie under the same line, meaning that some species have relatively larger brains than other species even after allometric effects have been accounted for. Variation in the relative size of the brain has been studied extensively in almost all groups of vertebrates and has been attributed to a large diversity of factors [see Healey and Rowe, 2007; Dechmann and Safi, 2009]. Differences in diet and ecology have been one of the most common factors used to explain differences in relative brain size. For example, in bats, insect eating species have relatively smaller brains than species that feed on fruit, nectar, or meat [Eisengberg and Wilson, 1978; Hutcheon et al., 2002]. Among primates, species that feed on leaves tend to have smaller brains than those that feed on fruit or insects [Clutton-Brock and Harvey, 1980]. As a general rule, Striedter [2005] proposed that species that hunt or forage more strategically (i.e. have to actively hunt or search for food) have larger brains than those that graze or hunt opportunistically. Habitat complexity has also been correlated to relative brain size. In sharks and teleosts (bony fish), species that live in reefs tend to have larger brains than species that live in open waters [Bauchot et al., 1977, 1989; Yopak et al., 2007]. Alternatively, Dunbar and Shultz [2007] proposed that in mammals, particularly primates, the relative size of the brain is directly related to living in large, complex societies. In general, all these studies make the assumption that a larger brain means more processing power, and indicate that larger brains must evolve related to an increased necessity to process

more complex or larger quantities of information, either by memorizing several foraging locations, navigating a complex environment or tracking individuals in a social group.

In contrast, Healy and Rowe [2007] suggested that correlations between behavioural or ecological factors and relative brain size are meaningless because the brain is composed of multiple, distinct functional units, and therefore changes in the size of the entire brain tell us little about the relationship between brain and behavior. These same authors point out that, on the other hand, studies of specific sensory or motor regions, with clearly defined function are much more useful as they can point out directly when and where selection is acting upon neural structures.

1.1.1 Variation of specific brain regions

Apart from variation in the absolute and relative size of the brain, it is also clear that among vertebrates there is large variation in different parts of the brain. Vertebrate brain architecture is highly conserved and the same main subdivisions (telencephalon, thalamus, mesencephalon, cerebellum, etc.), can be found in all vertebrates. Upon observation of the brain of several unrelated species it is obvious that some of these areas vary greatly in size, sometimes quite dramatically. For example in the weakly electric fish (Mormyrids), the cerebellar valvula is greatly enlarged to the point that it covers the entire anteroposterior extent of the brain [Nieuwenhuyis et al., 1998]. This hypertrophy of the cerebellar valvula is associated with the use of electric signals to navigate in their

environment and communicate with other individuals [Heiligenberg and Bastian, 1984; Hopkins, 1988; Bell, 1989]. However is not always clear why some parts of the brain are larger in some species than others, especially when the differences are not as pronounced as in the weakly electric fish. As with the variation of the brain as a whole, several studies have tried to correlate the variation of individual regions of the brain with ecological and behavioral factors. In mammals the size of the neocortex has been associated with the size of the social group in carnivores and insectivores [Dunbar and Bever, 1998], and social skills and social group size in primates [Pawlowski et al., 1998; Kudo and Dumbar, 2001]. Similarly, the size of the telencephalon in birds has been associated with social complexity, measured by flock size [Beauchamp and Fernandez-Juricic, 2004], and also with rates of feeding innovations [Lefebvre et al., 1997]. In primates, the size of the olfactory bulb has been associated with activity period, diet, social system and mating strategy [Barton, 2006]. A problem with this approach is that, as with variation of the whole brain, the large subdivisions of the brain are not functionally homogeneous and consist of many different sensory and motor pathways. Further, they are all interconnected, which means that variation of the size of one structure can affect the size of others.

One approach to overcome these limitations has been the recognition of "cerebrotypes" [Clark et al., 2001]. Clark used the proportion of the total brain volume that different brain regions occupy (12 in total) and defined the cerebrotype of a species or group as the particular combination of these proportions. Several studies have showed that the proportions of these different

brain regions vary within different vertebrates groups, and are associated to particular clades or ecological niches. The existence of cerebrotypes has been shown in sharks [Yopak et al., 2007], bony fish [Huber et al., 1997; Wagner, 2001a, b], amphibians [Doré et al., 2002], birds [Iwaniuk and Hurd, 2005], and mammals [Legendre et al., 1994; Lapointe et al., 1999; Clark et al., 2001; de Winter and Oxnard, 2001]. In birds for example, several species have similarities in brain composition related to similarities in flight behaviour, cognitive abilities, hunting strategies and the ecological niches they occupy [Iwaniuk and Hurd, 2005]. In other groups, phylogeny seems to have stronger influence. Among mammals, primates have larger isocortex, striatum, cerebellum and diencephalon volumes independent of ecology or behavior. [Clark et al., 2001; de Winter and Oxnard, 2001]. In general, cerebrotypes analyses are useful in that they can reveal the influence of phylogeny, behavior and ecology in brain evolution.

A main question that emerges in examining the variation of the different parts of the brain has been to what extent the different areas of the brain vary in size with respect to each other. Two main models have been proposed in this regard. The concerted evolution model proposes that developmental constraints cause different parts of the brain to vary in size in a coordinated manner [Finlay and Darlington 1995; Finlay et al., 2001]. Therefore, if there is selective pressure to increase the size of a specific brain region, the rest of the brain will increase in size as well. Finlay and Darlington [1995] showed that in mammals, up to 96 % of the variation of the relative size of different brain part is predicted by changes in the absolute size of the brain. Recently, Powell and Leal [2012] have shown a

similar pattern in anole lizards with up to 98 % variation of individual brain parts explained by variation in the absolute size of the brain. Finlay and Darlington [1995], proposed that any differences in the proportions of the different regions of the brain can be explained by differences in the allometric slope of each part. Thus, the disproportionally large neocortex in primates and humans for example [Finlay and Darlinton, 1995], would be explained by a slope of the neocortex in its scaling with brain size larger than the slope of other parts of the brain.

The second model proposed to explain changes in the size of different regions of the brain is the mosaic evolution model, where there are no developmental constraints and individual brain structures can vary in size independently of each other [Harvey and Krebs, 1990; Barton et al., 1995; Barton and Harvey, 2000]. Barton and Harvey [2000] showed that primates have disproportionally large neocortex compared to insectivores, and that variation in absolute brain size is not enough to explain these differences, as proposed by the concerted evolution model. Further these same authors showed that not all parts of the brain evolve together and anatomically and functionally related structures, such as the cortex and the diencephalon, vary in size together, independent of other structures.

While these models are still sometimes presented as a dichotomy [e.g. Hager et al., 2012], in recent years a more integrative view has emerged and it is clear that both mechanisms can simultaneously explain brain evolution. The mosaic evolution model can be used to explain large changes in the relative size of specific brain region, like the cerebellar valve of mormyrid fish (see above),

while the similarities between other species, especially closely related ones, are probably better explain by a concerted model [Striedter, 2005].

1.1.2 Principle of proper mass

A basic assumption behind the study of differences in the size of either the brain as a whole or its different parts is that larger means better; *i.e*. that a bigger relative volume results in more neurons and in a better and faster processing of information. This principle is known as the "principle of proper mass" [Jerison, 1973]. Jerison [1973] defines this principle as: "The mass of a neural tissue controlling a particular function is appropriate to the amount of information processing involved in performing the function". While this may seem unequivocal at first glance there are some problems with Jerison's definition. For instance, it is not clear if Jerison refers to the absolute or relative size of the neural structure [Striedter, 2005]. While in most studies it is the relative size of a neural structure that is assumed to be correlated with higher information processing [e.g. Iwaniuk and Wylie, 2007; Iwaniuk et al., 2006; 2008], in recent years it has been proposed that, for example, the absolute size of the brain (and therefore number of cells), and not the relative size, are important to explain the higher cognitive abilities of primates and humans [Herculano-Houzel et al., 2007; 2010]. Another problem with the principle of proper mass is the impossibility to actually quantify the amount of information processing required by a neural structure to perform a task and/or the fact that the neural computation underlying most behaviors is poorly known.

Empirically, in some cases the correlation between the size of a structure and the amount of information being processed is clear while in other it is less straightforward than initially assumed. For example the star-nosed mole (*Condylura cristata*) has a complex rhinarium comprised of 22 fleshy appendages cover in specialized mechanoreceptors used for detecting prey [Catania, 2005]. Concordantly, there is a large representation of the rhinarium in the brainstem and somatosensory cortex where sensory information from the rhinarium is processed [Catania, 2012]. On the other hand, in bats for example, species that echolocate have a much larger inferior colliculus (IC, the auditory portion of the mesencephalon) than species that do not echolocate [Baron, 1996] but in birds, species that echolocate do not present a relatively larger IC [Iwaniuk et al., 2006]. Another interesting example is the song system in passerines [MacDougall-Shackleton and Ball, 1999]. In the telencephalon of songbirds, the song production circuit consists of the high vocal center (HVc) and the robust nucleus of the arcopallium [RA; review by DeVoogd and Szekely, 1998]. Comparative studies have shown that the sizes of the different components of the song motor pathway are correlated to the number and complexity of the songs for each species [e.g Devoogd et al., 1993]. Interestingly, Moore et al. [2011] recently showed, using a multiple regression analysis, that the complexity of the song is better predicted by the degree of convergence in the song motor pathways. Repertoire size is better predicted by the proportion between the number of cells in higher motor areas (HVc, RA) and that of downstream targets, than the overall number of neurons in the song motor pathway. This shows that even if the

correlation between relative size and complexity of a behavior appears straight forward, other factors should always be considered, such as variation of other structures in the same pathways or sensory modality.

Another some how ambiguous example of the principle of proper mass is the correlation of the size of the hippocampus and food storing behavior in passerines; species that engage in food storing appear to have a much larger hippocampus than species that do not [Sherry et al., 1989; Healy and Krebs, 1992; Sherry et al., 1993; Basil et al. 1996; Healy et al., 1996]. Some songbirds (Parids and Corvids) find and then store food in large areas and find it again days or months later. Some birds are capable of remembering the spatial location of thousands of scattered food caches [Smith and Reichman, 1984; Sherry, 1985]. The hippocampus has been historically associated with memory formation and retrieval [reviewed in Jarrard, 1993] and therefore the ability to successfully retrieve food caches in this species would require a large amount of processing from this structure. Later studies have put into question these findings [Brodin and Lundborg, 2003] while other studies seem to confirm the correlation between food storing behavior and relative size of the hippocampus, but also found differences in the size of the hippocampus between North American and Eurasian species even among non-storing species [Garamszegi and Eens, 2004; Lucas et al., 2004; Garamszegi and Lucas, 2005]. This shows that one should be cautious when correlating variation of the size of a structure and behavior, and other factors, like ecology, anatomy and phylogeny, should always be considered.

As mentioned above, association between the size of the whole brain (or parts of it) and more complex environment or behaviors is obscured by the fact that regions of the brain are not functionally homogeneous and therefore are subject to a combination of selective pressures [Healey and Rowe, 2007; Dechmann and Safi, 2009]. On the other hand, individual sensory or motor nuclei show a much clearer correlation between size variation and complexity of the task or function to which they are related.

1.2 Birds as models for comparative studies.

In recent years there has been a renewed interest in using comparative studies to understand the evolution of the vertebrate brain [Striedter, 2005; Iwaniuk and Hurd, 2005] and a particularly large amount of these studies have focused on birds [Iwaniuk et al., 2009]. Birds are among the most diverse groups of vertebrates with more than 10,000 living species [Clements, 2007]. They occupy a wide range of ecological positions and many groups are highly specialized in their habitat or food requirements [Sekerciogluet al., 2006]. This results in a great diversity of sensory, behavioural, motor and cognitive specializations [Wyles et al., 1983] thus providing an excellent opportunity to study changes in the brain related to these specializations.

Further, birds have always been powerful models in neurobiology to study a wide range of subjects. Songbirds (and hummingbirds and parrots) learn their vocalizations from their parents [reviewed in Jarvis, 2004] and this has led them to become important models for the study of both learning in general [e.g. Fee and

Scharff, 2010; Kubikova and Kostál, 2010], and language acquisition [reviewed in Doupe and Kuhl, 1999; Brainard and Doupe, 2002]. The anatomy and physiology of the neural pathways involved in vocal learning have been studied extensively [e.g. Brenowitz et al., 1997; Wild, 1997], particularly in the zebra finch (*Taeniopygia guttata*), and therefore songbirds have provided important insights into neural and molecular mechanisms of learning [reviewed in Olveczky and Gardner, 2011; Moorman et al., 2011; Tschida and Mooney, 2012]. Also, the nuclei that form part of the song control system undergo seasonal anatomical and physiological changes under hormonal control, and have become models for the study the endocrine control of neural plasticity [reviewed in DeVoogd, 1991; Ball., 1999; Ball and Hahn 1997; Tramontin and Brenowitz, 2000]. Since the demonstration that owls, particularity, the barn owl (*Tyto alba*), can hunt in complete darkness and locate a sound within 1-2 degrees [Payne and Drury, 1958; Payne, 1971; Knonishi, 1973], they have become an established model for the study of sound localization. Like the song system of songbirds, the anatomy and physiology of auditory pathways involved in sound localization has been studied extensively [e.g. Moiseff and Konishi, 1983; Sullivan and Konishi, 1984; Takahashi et al., 1984; Sullivan, 1985; Manley et al., 1988; Takahashi and Konishi, 1988a, b; Takahashi and Keller, 1992; Adolphs, 1993; Mazer, 1998], and has also led to barn owls becoming an important model to the understanding of neuroplasticity and neural computation [Knudsen and Brainard, 1995; Konishi, 2003; Takahashi, 2010].

Birds are also important models in understanding visual processing. For instance, the accessory optic system and vestibulocerebellum of pigeons has been an important model in the study neural processing of visual signals that result from self-motion [reviewed in Wylie et al., 2013]. Recently, studies in pigeons, chickens and owls have revealed a circuit between the optic tectum and the isthmal nuclei as an important model to study visual spatial attention and competitive stimulus selection [Sereno and Ulinski, 1987; Marin et al., 2005, 2012; Gruberg et al., 2006; Salas et al., 2007; Asadollahi et al., 2010, 2011; Mysore et al., 2011; Knudsen, 2011]. Thus, besides what we can learn about brain evolution, comparative studies in birds can have a direct impact on other areas of neurobiology.

1.2.1 Comparative studies in birds

Comparative studies in birds have shown an increase in the size of neural structures in several groups and sensory systems related to very specific sensory tasks. For example, the cochlear nuclei in the brainstem and their target in the mesencephalon, the IC, are hypertrophied in owls but not in other auditory specialists, like vocal learners or species that echolocate [Kubke et al., 2004; Iwaniuk et al., 2006]. In the visual system of hummingbirds (and a few other hovering species), the pretectal nucleus lentifomis mesencephali (LM) is relatively larger than other birds [Iwaniuk and Wylie, 2007]. LM forms part of the accessory optic system and neurons respond most to optic flow in the temporal-to-nasal direction [Wylie and Frost, 1996; Wylie and Crowder, 2000], suggesting

that the increase in size is directly related to increased need to detect and minimize optic flow resulting from drifting backward during hovering [Iwaniuk and Wylie, 2007]. Also in the visual system, owls and some caprimulgiforms shown an enlarged visual Wulst compared to other birds [Iwaniuk et al, 2006, 2008]. In owls, the visual Wulst is related to stereopsis, *i.e.* depth perception. Owls and some caprimulgiforms, like owlet-nightjars and frogmouths, have frontal eye positions with a large binocular visual field [Martin, 1984; Petttigrew and Konishi, 1984; Wallman and Pettigrew, 1985; Wylie et al., 1994 Martin et al., 2004a, b] and the size of the visual Wulst is directly correlated with this overlap [Iwaniuk et al., 2008]. Other studies have shown variation in the olfactory [Cobb, 1968; Healey and Guilford, 1990; Zelenitsky et al., 2011] or somatosensory system of birds [Stingelin, 1961, 1965; Boire, 1989; Dubbeldam, 1998].

Several studies in birds have also shown variation in different brain structures associated with higher cognitive abilities [e.g. Lefevbre et al., 2002 ; Timmermans et al., 2000; Sol et al., 2002; Lefebvre et al., 2004; Iwaniuk et al., 2004; Cnotka et al., 2008; Overingtona et al., 2009]. For example, the size of the telencephalon, and specifically of the nidopallium which plays an important role in different kinds of learning [Horn, 1990; Nottebohm et al., 1990], is associated with the use of tools [Lefevbre et al., 2002]. Also in the telencephalon, the relative size of the mesopallium which is also involved in. learning, [McCabe et al., 1982;

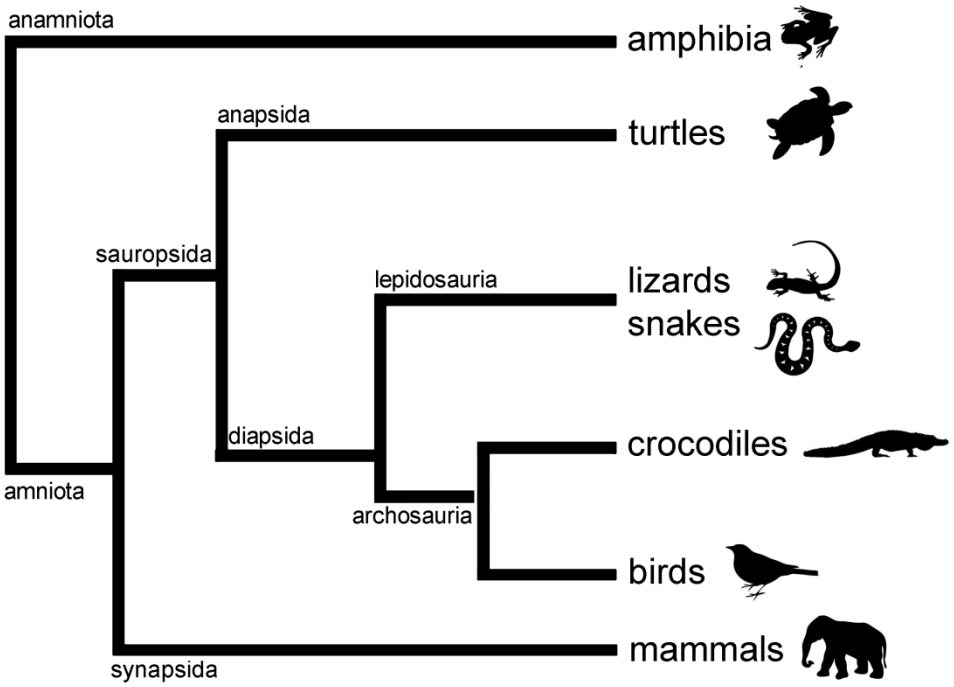

Figure 1.2. Phylogenetic relationships between the tetrapods. Phylogenetic tree depicting relationships between the major groups of tetrapods (land vertebrates). The tree is based on the topology proposed by several studies [see Zardoya and Meyer, 2001, Kumar and Hedges, 1998; Lou et al., 2001] See section 1.3 for details.

MacPhail et al., 1993], has been correlated with the amount of feeding innovations in different species [Timmermans et al., 2000]. In general, all these studies show that the great diversity of sensory, behavioural, motor and cognitive specialization in birds is indeed reflected in their brains, making them suitable models to study the different aspects of brain evolution.

Several of the studies listed above were done either comparing only a few species or were performed before statistical procedures that account for phylogenetic relatedness [e.g. Garland et al., 1992] were implemented or widely used [e.g. Stingelin, 1961, 1965; Kubke et al., 2004]. This means that comparative studies with larger data sets that use appropriated statistical procedures are needed to confirm or test some of these results. Also, as pointed out in section 1.1.2, these type of studies are focused mostly on the variation of only one region and therefore fail to assess how entire neural pathways evolve.

1.3 Birds phylogenetic relationships

It is now largely accepted that birds evolved from sauropod dinosaurs about 100 million years ago [Holtz, 1998; Sereno, 1999; Witmer, 2002]. Figure 1.2 shows the phylogenetic relationships of birds to other vertebrates. Birds belong to the archosauria from which the other extant members are crocodriles. The sister group of archosauria remains contentious, and is proposed to be either the lepidosauria (lizard and snakes) or the anapsids (turtles) [Zardoya and Meyer, 2001]. Together all these groups form the sauropsida which is the sister group to the synapsids from which mammals evolved. This separation occurred at least 300 million years ago [Kumar and Hedges 1998; Lou et al., 2001].

The class Aves is represented by around 30 orders. Many different phylogenies have been proposed for these orders [e.g. Sibley and Ahlquist 1990, Livezey and Zusi, 2007; Davis, 2008; Hackett et al., 2008; McCormack et al., 2013], and the relationship between many clades remains controversial [McCormack et al., 2013]. Figure 1.3 shows the phylogenetic relationship between major avian orders proposed by Hackett at al., [2008]. A major consensus is that aves are divided into two main taxa; paleognatha and neognatha. Paleognatha are basal to the neognatha and are constitute a group of mostly gondwanic birds, including kiwis (Apterygiformes), ostriches (Struthioniformes) and tinamous (Tinamiformes). Among neognatha, it is well accepted that waterfowl (Anseriformes) and gallinaceous birds (i.e. chicken, turkey, grouse (Galliformes)) are sister groups and are the most basal group in this taxon [Sibley and Ahlquist 1990; Ericson et al., 2006; Livezey and Zusi, 2007; Davis, 2008; Hackett et al., 2008; McCormack et al., 2013]. While many of the relationships are not clear, some groups within the rest of neoghnatha are well supported. For example, waterbirds, which include pelicans (Pelecaniformes), herons (Ciconiiformes), puffins (Procellariiformes), penguins (Sphenisciformes) and cormorants (Phalacrocoraciformes), among others, form a consistent monophyletic group [Ericson et al., 2006; Hackett 2008; McCormack et al., 2013]. Another well supported group is the close relatedness of hummingbirds and swift (Apodiformes), and caprimulgiformes, a group of mostly nocturnal species like nightjars and frogmouths [Ericson et al., 2006; Hackett 2008; McCormack et al., 2013]. Also, the so-called group of land birds, which

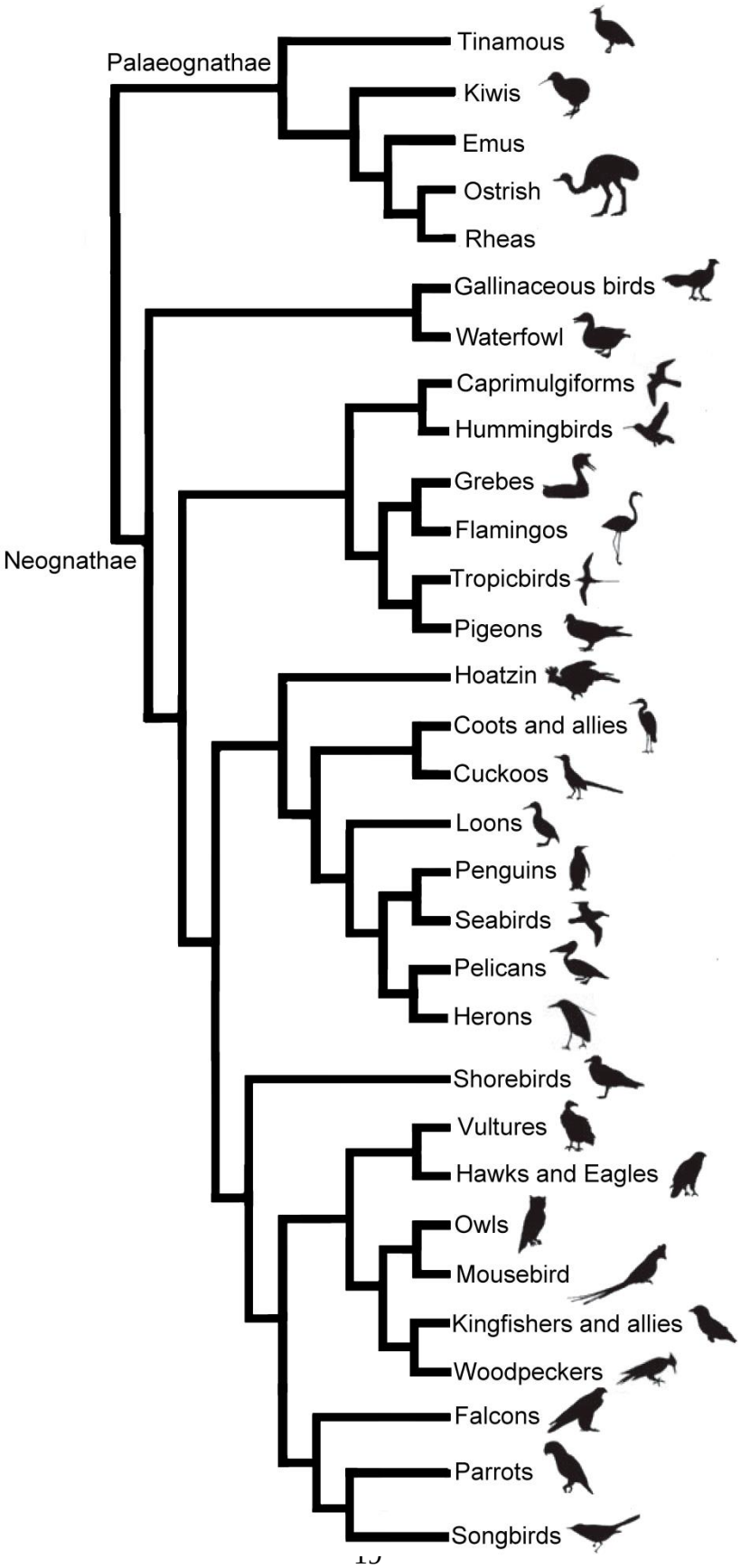
Palaeognathae
Neognathae
Tinamous
Kiwis
Emus
Ostrish
Rheas
Gallinaceous birds
Waterfowl
Caprimulgiforms
Hummingbirds
Grebes
Flamingos
Tropicbirds
Pigeons
Hoatzin
Coots and allies
Cuckoos
Loons
Penguins
Seabirds
Pelicans
Herons
Shorebirds
Vultures
Hawks and Eagles
Owls
Mousebird
Kingfishers and allies
Woodpeckers
Falcons
Parrots
Songbirds

Figure 1.3. A phylogenetic tree of the principal orders of the class aves.

Phylogenetic tree depicting the phylogenetic relationships between the major orders of birds. The tree is based on the topology proposed as by Hackett et al., [2008]. See section 1.3 for details. Adapted from Zelenitsky et al., [2011].

includes songbirds, parrots (Psittasiformes), hawks (Accipitridae), falcons (Falconidae), owls (Strigiformes), woodpeckers (Piciformes) and Kingfishers (Coraciiformes) and others orders is well supported [Ericson et al., 2006; Hackett 2008; McCormack et al., 2013]. Among this group, two relationships that have been controversial since first proposed [Ericson et al., 2006; Hackett et al., 2008] are that parrots and songbirds are sister groups (fig. 1.3), and that falcons and hawks are not closely related (fig. 1.3). Several recent studies support these two proposals [Suh et al., 2011; Wang et al., 2012; McCormack et al., 2013] which have interesting implications. On the one hand, songbirds and parrots share many characteristics, like an enlarged telencephalon [Iwaniuk and Hurd, 2005] and the learning of their vocalization [Jarvis, 2004]. The close relationship of these two groups implies these characters may have a common origin. On the other hand, falcons and hawks are very similar in ecology and hunting behaviors [del Hoyo et al., 1999] and a large phylogenetic distance between the two groups implies these common characteristics are the result of convergent evolution.

1.4 Summary and Outline of Chapters

Variation of brain size and morphology has been studied in all vertebrates with the aim to understand the principles that govern brain evolution. A major goal has been to find behavioral or ecological correlates to variation of neural structures, particularly to the variation of the brain size as a whole or a gross anatomical subdivision (telencephalon, cerebellum, etc.) [Reviewed in Healy and Rowe, 2007; Dechmann and Safi, 2009]. A problem with this approach is that the

brain is comprised of many parallel motor and sensory pathways and the size of the brain as a whole, or its main subdivisions, are the result of a complex combination of multiple selection pressures and constraints affecting the different motor and sensory pathways at the same time. Comparative analyses of more functionally defined sensory or motor areas has been more successful in showing the direct impact of natural selection on neural structures [Healy and Rowe, 2007], but they also have some limitations. For instance most of these studies have dealt with variation in only a few structures, neglecting how variation of one nucleus might affect other anatomically and functionally related structures.

Birds have become powerfull models in many aspects of neurobiology, including comparative studies. Birds show a large diversity of sensory, behavioural, motor and cognitive specializations. This provides the perfect opportunity to study changes in the brain related to these specializations. This dissertation seeks to further advance our understanding of the principles that govern brain evolution using birds as models.

This dissertation includes five studies on the variation of cytoarchitectonic organization, relative volume and cell numbers in different sensory nuclei in birds. In Chapter 2, we measure the relative size of the principal nucleus of the trigeminal nerve (PrV) in a large sample of birds. PrV receives somatosensory projections from the orofacial region (the beak), mainly from the trigeminal nerve [Bout and Dubbeldam, 1985; Dubbeldam et al., 1979; Wild, 1981, 1990]. Previous studies have suggested that birds that depend heavily on tactile input when feeding have an enlarged PrV [Stingelin, 1961, 1965; Boire, 1989;

Dubbeldam, 1998], but no broad systematic analysis across species has been carried out.

In Chapter 3 we investigate the variation of the size of parallel auditory pathways in owls. Within owls, vertical ear asymmetries have evolved independently several times [Norberg, 1978]. These ear asymmetries result in interaural level differences (ILD) between the two ears when the sound source is above or below the head, allowing the localization of sound in elevation [Knudsen and Konishi, 1979, 1980; Moiseff and Konishi, 1981; Moiseff, 1989]. In barn owls, azimuth and elevation are computed using interaural time differences (ITDs) and ILDs, respectively [Knudsen and Konishi, 1979, 1980; Moiseff and Konishi, 1981; Moiseff, 1989]. ITDs and ILDs are processed independently along two separate parallel pathways. Previous studies have shown that some auditory nuclei are larger in asymmetrically eared owls compared to symmetrically eared ones [Cobb, 1964; Wagner and Luksch, 1998; Iwaniuk et al., 2006], but is not clear how the ITD and ILD pathways vary with respect to each other, or if different ear morphologies result in difference in the size of the auditory pathway among asymmetrically eared owls. To test this we measured the size of 11 different auditory nuclei.

Owls also vary with respect to their activity pattern, (*i.e.* at which times of the day they are more active [de Hoyo et al., 1999]). Previous research has shown that differences in activity pattern are reflected in eye morphology and retinal organization both in birds in general, and specifically in owls [see Lisney et al., 2011; Oehme, 1961; Bravo and Pettigrew, 1981], but is not known if this

difference is reflected in the relative size of the visual pathways. Previous research has shown that species with a more nocturnal activity pattern have a reduced number of retinal ganglion cells (RGCs) compared to more diurnal species, and also have a reduced tectofugal pathway [Kay and Kirk, 2000; Kirk and Kay, 2004; Hall et al., 2009; Iwaniuk et al., 2010; Corfield et al., 2011] but this has not been tested within owls. Also, there is some evidence that there are differences in the number of RGCs that project to the optic tectum and the dorsal thalamus between diurnal and nocturnal species [Bravo and Pettigrew, 1981]. In Chapter 4, we compare the relative size of 8 visual nuclei in 9 species of owls (and one Caprimulgiform) with different activity patterns. This includes the two main visual pathways, the tectofugal and thalamofugal pathways, as well as other retinorecipient nuclei.

In Chapter 5 we compare the cytoarchitectonic organization, relative size and cell number of the isthmo optic nucleus (ION) in a large sample of bird species in an effort to clarify the function of this structure. In birds, ION gives rise to a centrifugal projection to the retina. Despite extensive research of the anatomy, physiology and histochemistry of this structure [Reviewed in Reperant et al., 2006; Wilson and Lindstrom, 2011], the function of this centrifugal system remains unclear. Previous research has shown that there is large variation in the size and cell numbers of the ION among birds [egg Shortess and Klose, 1977; Weidner et al., 1987; Reperant et al., 1989] but no broad comparative analysis of the relative size and organization of the ION has been carried out. We use a sample of 81 species of bird with different ecological niches and feeding habits in

order to test some of the functional hypotheses previously proposed, such as the involvement of ION in ground feeding [Shortess and Klose, 1977; Weidner et al., 1987; Reperant et al., 1989; Hahmann and Gunturkun, 1992; Miceli et al., 1999] or its involvement in the detection of aerial predators [Wilson and Lindstrom, 2011].

Finally, in Chapter 6 we test if visual nuclei evolved in a concerted or mosaic manner (see section 1.1.1). Several studies have shown variation in the relative size of visual neural structures in birds, both among and within orders [e.g. Iwaniuk and Wylie 2006, 2007; Iwaniuk et al., 2008, 2010], however no study to date has tested how variation of the relative size of one structure affects other anatomically and functionally related structures. Previous studies have suggested that the covariation in the size of different neural structures is related to the functional inter-connectivity of these structures [Barton and Harvey, 2000; Whiting and Barton, 2003]. To test this we use a combination of phylogenetically corrected principal component analysis and evolutionary rates of change on the absolute and relative size of the 9 visual nuclei in 98 species of birds that belong to 16 different orders.

1.5 References

Adolphs R (1993): Acetylcholinesterase staining differentiates functionally distinct auditory pathways in the barn owl. J Comp Neurol 329: 365–377.

Asadollahi A, Mysore SP, Knudsen EI. (2010): Stimulus-driven competition in a cholinergic midbrain nucleus. Nat neurosci. 13: 889–95.

Asadollahi A, Mysore SP, Knudsen EI. (2011): Rules of competitive stimulus selection in a cholinergic isthmic nucleus of the owl midbrain. J Neurosci: 31:6088–97.

Ball GF (1999): Neuroendocrine basis of seasonal changes in vocal behavior among songbirds. In *The Design of Animal Communication*, M Hauser and M Konishi, eds, pp 213-253, MIT Press, Cambridge, MA.

Ball GF and Hahn TP (1997) GnRH neuronal systems in birds and their relation to the control of seasonal reproduction. In *GnRH Neurons: Gene to Behavior*, IS Parhar and Y Sakuma, eds, pp 325-342, Brain Shuppan, Tokyo.

Baron G, Stephan H, Frahm HD (1996): Comparative Neurobiology in Chiroptera. Basel: Birkh¨auser Verlag. 1596 pp.

Barton RA, Purvis A, Harvey PH (1995): Evolutionary radiation of visual and olfactory brain systems in primates, bats and insectivores. Proc R Soc Lond B. 348: 381-392.

Barton RA, Harvey PH (2000): Mosaic evolution of brain structure in mammals. Nature. 405: 1055-1058.

Barton RA (2006): Olfactory evolution and behavioral ecology in primates. Amer. J. Primatology. 68: 545-558.

Bauchot R, Bauchot ML, Platel R, Ridet, J. M. (1977): Brains of Hawaiian tropical fishes; brain size and evolution. Copeia, 42-46.

Bauchot R, Randall JE, Ridet JM, Bauchot ML (1989): Encephalization in tropical teleost fishes and comparison with their mode of life. J Hirnforsch. 30: 645.

Bell, C. C. (1989): Sensory coding and corollary discharge effects in mormyrid electric fish. J Exp Biol. 146: 229-253.

Beauchamp G, Fernández-Juricic E. (2004): Is there a relationship between forebrain size and group size in birds?. Evol Eco Res, 6: 833-842.

Brainard MS, Doupe AJ (2002): What songbirds teach us about learning. Nature. 417: 351-358.

Brenowitz EA, Margoliash D, Nordeen, KW (1997): An introduction to birdsong and the avian song system. J Neurobiol. 33: 495-500.

Basil JA, Kamil AC, Balda RP, Fite KV (1996): Differences in hippocampal volume among food storing corvids. Brain Behav Evol 47: 156–164.

Bravo H, Pettigrew JD (1981): The distribution of neurons projecting from the retina and visual cortex to the thalamus and tectum opticum of the barn owl, *Tyto alba*, and burrowing owl, *Speotyto cunicularia*. J Comp Neurol 199:419–441.

Boire D (1989): Comparaison quantitative de l'encephale de ses grades subdivisions et de relais visuals, trijumaux et acoustiques chez 28 especes. PhD Thesis, Universite de Montreal, Montreal.

Bout RG, Dubbeldam JL (1985): An HRP study of the central connections of the facial nerve in the mallard (*Anas platyrhynchos L.*): Acta Morphol Neerl Scand 23:181-93.

Brodin A, Lundborg K (2003): Is hippocampus volume affected by specialization for food hoarding in birds? Proc R Soc Lond B 270: 1555–1563.

Clark DA, Mitra PP, Wang SSH (2001): Scalable architecture in mammalian brains. Nature, 411: 189-193.

Clements JF (2007): The Clements Checklist of Birds of the World (6th ed.). Ithaca: Cornell University

Clutton-Brock TH, Harvey, PH (1980): Primates, brains and ecology. J Zool. 190: 309-323.

Cnotka J, Güntürkün O, Rehkämper G, Gray RD, Hunt GR (2008): Extraordinary large brains in tool-using New Caledonian crows (Corvus moneduloides). Neurosci lett. 433: 241-245.

Cobb S (1964): A comparison of the size of an auditory nucleus (n. mesencephalicus lateralis, pars dorsalis) with the size of the optic lobe in twenty-seven species of birds. J Comp Neurol. 122:271–279.

Cobb S. (1968): The size of the olfactory bulb in 108 species of birds. The Auk. 85: 55-61.

Corfield JR, Gsell AC, Brunton D, Heesy CP, Hall MI, Acosta ML, Iwaniuk AI (2011): Anatomical specializations for nocturnality in a critically endangered parrot, the kakapo (*Strigops habroptilus*). PLoS ONE 6:e22945.

Darwin CR (1876): The origin of species by means of natural selection, or the preservation of favoured races in the struggle for li*e*. London: John Murray. 6th ed.

Davis KE (2008): Reweaving the tapestry: a supertree of birds. PhD Thesis, University of Glasgow, UK.

DeVoogd TJ (1991): Endocrine modulation of the development and adult function of the avian song system. Psychoneuroendocrino. 16: 41-66.

DeVoogd TJ, Krebs JR, Healy SD, Purvis A (1993): Relations between song repertoire size and the volume of brain nuclei related to song: comparative evolutionary analyses amongst oscine birds. Proc R Soc Lond B 254: 75-82.

DeVoogd TJ, Székely T (1998): Causes of avian song: using neurobiology to integrate proximate and ultimate levels of analysis. In: Balda RP , Pepperberg IM , editors. Animal cognition in nature. San Diego: Academic Press. p. 337-380.

Dechmann DK, Safi K. (2009): Comparative studies of brain evolution: a critical insight from the Chiroptera. Biol Rev. 84: 161-172.

de Winter W, Oxnard CE (2001): Evolutionary radiations and convergences in the structural organization of mammalian brains. Nature 409:710–714.

del Hoyo J, Elliott A, Sargatal J (eds) (1999): Handbook of the Birds of the World. Volume 5: Barn-owls to Hummingbirds. Barcelona, Lynx Editions.

Doré J-C, Ojasoo T, Thireau M (2002): Using the volumetric indices of telencephalic structures to distinguish Salamandridae and Plethodontidae: comparison of three statistical methods. J Theor Biol 214:427–439.

Doupe AJ, Kuhl PK (1999): Birdsong and human speech: common themes and mechanisms. Ann Rev Neurosci, 22: 567-631.

Dubbeldam JL, Brus ER, Menken SB, Zeilstra S (1979): The central projections of the glossopharyngeal and vagus ganglia in the mallard, *Anas platyrhynchos* L. J Comp Neurol. 183:149-68.

Dubbeldam JL (1998): The sensory trigeminal system in birds: input, organization and effects of peripheral damage. A review. Arch Physiol Biochem. 106:338-45.

Dunbar RIM, Bever J (1998): Neocortex size predicts group size in carnivores and some insectivores. Ethology. 104(8), 695-708.

Dunbar RIM, Shultz S (2007) Evolution in the Social Brain. Science 317: 1344-1347.

Eisenberg JF, Wilson DE (1978): Relative brain size and feeding strategies in the Chiroptera. Evolution 32: 740-751.

Ericson PG, Anderson CL, Britton T, Elzanowski A, Johansson US, Källersjö M, Mayr, G. (2006): Diversification of Neoaves: integration of molecular sequence data and fossils. Biol lett. 2L 543-547.

Fee MS, Scharff C (2010): The songbird as a model for the generation and learning of complex sequential behaviors. ILAR Journal, 51: 362-377.

Finlay BL, Darlington RB. (1995): Linked regularities in the development and evolution of mammalian brains. Science. 268:1578–1584.

Finlay BL, Hersman MN, Darlington RB (1998): Patterns of vertebrate neurogenesis and the paths of vertebrate evolution. Brain Behav Evol. 52: 232-242.

Finlay BL, Darlington RB, Nicastro N. (2001): Developmental structure in brain evolution. The Behavioral and brain sciences 24:263–78; discussion 278–308.

Garland TJr, Harvey PH, Ives AR (1992): Procedures for the analysis of comparative data using phylogenetically independent contrasts. Syst Biol 41:18–32.

Gruberg E, Dudkin E, Wang Y. (2006): Influencing and interpreting visual input: the role of a visual feedback system. J neurosci 26:10368–10371.

Hackett SJ, Kimball RT, Reddy S, Bowie RCK, Braun EL, et al. (2008): A phylogenomic study of birds reveals their evolutionary history. Science 320: 1763–1768.

Hager R, Lu L, Rosen GD, Williams RW (2012): Genetic architecture supports mosaic brain evolution and independent brain–body size regulation. Nature Comm. 3: 1079.

Hahmann U, Gunturkun O (1992): Visual-discrimination deficits after lesions of the centrifugal visual system in pigeons (Columba livia). Vis Neurosci 9: 225–233.

Hall MI, Gutiérrez-Ibáñez C, Iwaniuk AN (2009): The morphology of the optic foramen and activity pattern in birds. Anat Rec 292:1827-1845.

Harvey PH, Krebs JR (1990): Comparing brains. Science. 249: 140-146.

Healy SD, Krebs JR (1992): Food storing and the hippocampus in corvids: amount and volume are correlated. Proc R Soc Lond B 248: 241–245.

Healy S, Guilford T, (1990): Olfactory-bulb size and nocturnality in birds. Evolution, 339-346.

Healy SD, Rowe C (2007): A critique of comparative studies of brain size. Proc R Soc Lond B 274: 453-464.

Heiligenberg W, Bastian J (1984): The electric sense of weakly electric fish. Ann Rev Physiol. 46: 561-583.

Holtz TR (1998): A new phylogeny of the carnivorous dinosaurs. Gaia 15:5–61.

Hopkins CD (1988): Neuroethology of electric communication. Ann Rev Neurosci. 11: 497-535.

Horn G. (1990): Neural bases of recognition memory investigated through an analysis of imprinting. Proc R Soc Lond B. 329: 133-142.

Hutcheon JM, Kirsch JA, Garland Jr, T (2002): A comparative analysis of brain size in relation to foraging ecology and phylogeny in the Chiroptera. Brain Behav Evol. 60: 165-180.

Huber R, van Staaden MJ, Kaufman LS, Liem KF (1997): Microhabitat use, trophic patterns, and the evolution of brain structure in African cichlids. Brain Behav Evol. 50:167–182.

Iwaniuk AN, Nelson JE (2002): Can endocranial volume be used as an estimate of brain size in birds? Can J Zool. 80: 16-23.

Iwaniuk AN, Dean KM, Nelson JE (2004): Interspecific allometry of the brain and brain regions in parrots (Psittaciformes): comparisons with other birds and primates. Brain behav evol 65: 40-59.

Iwaniuk AN, Hurd PL. (2005): The evolution of cerebrotypes in birds. Brain behav evol 65:215-230.

Iwaniuk AN, Clayton DH, Wylie DRW (2006a): Echolocation, vocal learning, auditory localization and the relative size of the avian auditory midbrain nucleus (Mld). Behav Brain Res 167: 305-317

Iwaniuk AN, Wylie DRW (2006b): The evolution of stereopsis and the wulst in caprimulgiform birds: a comparative analysis. J Comp Physiol [A] 192:1313-1326.

Iwaniuk AN, and Wylie DRW (2007): Comparative evidence of a neural specialization for hovering in hummingbirds: hypertrophy of the pretectal nucleus lentiformis mesencephali. J Comp Neurol. 50:11-221.

Iwaniuk AN, Heesy CP, Hall MI, Wylie DR (2008): Relative Wulst volume is correlated with orbit orientation and binocular visual field in birds. J Comp Physiol A 194: 267-82 .

Iwaniuk AN, Lefebvre L, Wylie DR (2009): The comparative approach and brain–behaviour relationships: A tool for understanding tool use. Can J Exp Psychol 63*:* 150-159.

Iwaniuk AN, Gutiérrez-Ibáñez C, Pakan JMP, Wylie DR (2010b): Allometric scaling of the tectofugal pathway in birds. Brain Behav Evol 75:122-137.

Jarrard LE (1993): On the role of the hippocampus in learning and memory in the rat. Behavioral and neural biology, 60: 9-26.

Jarvis ED (2004): Learned birdsong and the neurobiology of human language. Ann Ny Acad Sci. 1016: 749-777.

Jerison HJ (1973): Evolution of the brain and intelligence. New York: Academic Press.

Kay RF, Kirk EC (2000): Osteological evidence for the evolution of activity pattern and visual acuity in primates. Am J Physical Anthropol 113:235–262.

Kirk EC, Kay RF (2004): The evolution of high visual acuity in the Anthropoidea; In: Ross CF, Kay RF (eds) Anthropoid origins: new visions. New York, Kluwer Academic/Plenum, pp 539–602.

Konishi M (1973): How the owl tracks its prey. Am Sci 6: 414–424.

Konishi, M. (2003): Coding of auditory space. Ann Rev Neurosci. 26: 31-55.

Kubikova L, Kostal L. (2010): Dopaminergic system in birdsong learning and maintenance. Journal of chemical Neuroanatomy. 39: 112-123.

Kudo H, Dunbar RIM (2001): Neocortex size and social network size in primates. Anim. Behav. 62: 711-722.

Kumar S, Hedges SB (1998): A molecular timescale for vertebrate evolution. Nature. 392: 917-920.

Knudsen EI. (2011): Control from below: the role of a midbrain network in spatial attention. The European journal of neuroscience 33:1961–72.

Knudsen EI, Blasdel GG, Konishi M. (1979): Sound localization by the barn owl (Tyto alba) measured with the search coil technique. J Comp Physiol A 133:1-11

Knudsen EI, Konishi M. (1980): Monaural occlusion shifts receptive-field locations of auditory midbrain units in the owl. J Neurophysiol 44:687-95.

Knudsen EI, Brainard MS (1995): Creating a unified representation of visual and auditory space in the brain. Ann Rev of Neurosci. 18: 19-43.

Lapointe F-J, Baron G, Legendre P (1999): Encephalization, adaptation and evolution of Chiroptera: A statistical analysis with further evidence for bat monophyly. Brain Behav Evol 54: 1191–1226.

Legendre P, Lapointe F-J, Casgrain P (1994): Modeling brain evolution from behavior: a permutational regression approach. Evol. 48: 1487–1499.

Lefebvre L, Nicolakakis N, Boire D (2002): Tools and brains in birds. Behav.. 139: 939-974.

Lefebvre, L., Reader, SM,Sol D (2004): Brains, innovations and evolution in birds and primates. Brain Behav Evol, 63(4), 233-246.

Livezey, B C,Zusi RL (2007): Higher-order phylogeny of modern birds (Theropoda, Aves: Neornithes) based on comparative anatomy. II. Analysis and discussion. Zool J Linn Soc-Lond. 149: 1-95.

Luo ZX, Crompton AW, Sun AL (2001): A new mammaliaform from the early Jurassic and evolution of mammalian characteristics. Science 292:1535–1540.

Lisney TJ, Rubene D, Rózsa J, Løvlie H, Håstad O, Ödeen A (2011): Behavioural assessment of flicker fusion frequency in chicken *Gallus gallus domesticus*. Vision Res 51:1324-1332.

Lisney TJ, Iwaniuk AN, Bandet MV, Wylie DR (2012): Eye shape and retinal topography in owls (Aves: Strigiformes). Brain Behav Evol 79:218-236

Manley GA, Köppl C, Konishi M (1988): A neural map of interaural intensity differences in the brain stem of the barn owl. J Neurosci 8: 2665–2676.

Marín G, Mpodozis J, Mpdozis J, Sentis E, Ossandón T, Letelier JC. (2005): Oscillatory bursts in the optic tectum of birds represent re-entrant signals from the nucleus isthmi pars parvocellularis. J Neurosci 25:7081–9.

Marín GJ, Dura E, Morales C, González-cabrera C, Sentis E, Mpodozis J, Letelier JC. (2012): Attentional Capture ? Synchronized Feedback Signals from the Isthmi Boost Retinal Signals to Higher Visual Areas. J Neurosci 32:1110–1122.

Martin RD (1981): Relative brain size and basal metabolic rate in terrestrial vertebrates. Nature. 293(5827), 57-60.

Martin GR (1984): The visual Welds of the tawny owl, Strix aluco L. Vision Res 24:1739–1751

Martin G, Rojas LM, Figueroa YMR, McNeil R (2004a): Binocular vision and nocturnal activity in oilbirds (Steatornis caripensis) and pauraques (Nyctidromus albicollis): Caprimulgiformes. Orn Neo 15:233–242

Martin G, Rojas LM, Ramirez Y, McNeil R (2004b): The eyes of oilbirds (Steatornis caripensis): pushing at the limits of sensitivity. Naturwiss 91:26–29

MacDougall-Shackleton SA, Ball GF (1999): Comparative studies of sex differences in the song-control system of songbirds. Trends Neurosci. 22, 432–436.

Mazer JA (1998): How the owl resolves auditory coding ambiguity. Proc Natl Acad Sci USA 95: 10932–10937.

McCabe BJ, Cipolla-Neto J, Horn G, Bateson P (1982): Amnesic effects of bilateral lesions placed in the hyperstriatum ventrale of the chick after imprinting. Experimental Brain Res. 48: 13-21.

McCormack JE, Harvey MG, Faircloth BC, Crawford NG, Glenn TC, Brumfield, RT (2013): A phylogeny of birds based on over 1,500 loci collected by target enrichment and high-throughput sequencing. PloS one, 8(1), e54848.

Macphail EM, Reilly S, Good M (1993): Lateral hyperstriatal lesions disrupt simultaneous but not successive conditional discrimination learning of pigeons (*Columba livia*). Behav Neurosci. 107:289–298.

Miceli D, Reperant J, Bertrand C, Rio JP (1999): Functional anatomy of the avian centrifugal visual system. Behav Brain Res 98: 203–210.

Mink JW, Blumenschine RJ, Adams DB (1981): Ratio of central nervous system to body metabolism in vertebrates: its constancy and functional basis. Am J Physiol-Reg I. 241: R203-R212.

Moiseff A. (1989): Bi-coordinate sound localization by the barn owl. J Comp Physiol A 64:637-644.

Moiseff A, Konishi M. (1981): Neuronal and behavioral sensitivity to binaural time differences in the owl. J Neurosci 1:40-8.

Moiseff A, Konishi M (1983): Binaural characteristics of units in the owl's brainstem auditory pathway: precursors of restricted spatial receptive fields. J Neurosci 12: 2553–2562.

Moore JM, Székely T, Büki J, DeVoogd TJ (2011): Motor pathway convergence predicts syllable repertoire size in oscine birds. Proc. natl Acad. Sci. U.S.A. 108: 16440-16445.

Moorman S, Mello CV, Bolhuis, JJ (2011): From songs to synapses: Molecular mechanisms of birdsong memory. Bioessays. 33: 377-385.

Mysore SP, Asadollahi A, Knudsen EI. (2011): Signaling of the strongest stimulus in the owl optic tectum. J Neurosci. 31:5186–96.

Nieuwenhuyis R, ten Donkelaar HJ, Nicholson C (1998): The Central Nervous System of Vertebrates: With Posters (Vol. 1). Springer

Norberg RA. (1978): Skull asymmetry, ear structure and function, and auditory localization in Tengmalm's owl, Aegolius funereus (Linne). Phil Trans R Soc Lond B 282:325-410.

Overington SE, Morand-Ferron, J, Boogert, NJ, Lefebvre L (2009):. Technical innovations drive the relationship between innovativeness and residual brain size in birds. Anim Behav. 78: 1001-1010.

Oehme H (1961): Vergleichend-histologische Untersuchungen an der Retina von Eulen. Zool Jb Anat 79:439-478.

Owen R, (1857). On the characters, principles of division and primary groups of the class mammalia. J. Linnaean Soc. 2: 1–37.

Panchen AL. 1994. Richard Owen and the concept of homology. In Homology: The Hierarchical Basis of Comparative Biology, ed. BK Hall, pp. 21–62. San Diego: Academic

Pawłowski B, Lowen CB, Dunbar RIM (1998): Neocortex size, social skills and mating success in primates. Behaviour. 357-368

Pagel MD, Harvey PH (1989): Taxonomic differences in the scaling of brain on body weight among mammals. Science. 244: 1589-1593.

Payne RS (1971): Acoustic location of prey by barn owls (*Tyto alba*).. J Exp Biol 54: 535–573.

Payne RS, Drury WH Jr (1958): Marksman of the darkness. Part 2. Nat Hist NY 67: 316–323.

Pettigrew JD, Konishi M (1976): Neurons selective for orientation and binocular disparity in the visual Wulst of the barn owl (*Tyto alba*). Science 193:675–678

Powell BJ, Leal M (2012): Brain Evolution across the Puerto Rican Anole Radiation. Brain Behav Evol. 80: 170-180.

Reperant J, Miceli D, Vesselkin NP, Molotchnikoff S (1989): The centrifugal visual system of vertebrates: a century-old search reviewed. Int Rev Cytol 118: 115–171.

Reperant J, Ward R, Miceli D, Rio JP, Medina M, et al. (2006): The centrifugal visual system of vertebrates: A comparative analysis of its functional anatomical organization. Brain Res Rev. 52: 1–57.

Salas C, Sentis E, Rojas X, Letelier JC, Mpodozis J. (2007): A Cholinergic Gating Mechanism Controlled by Competitive Interactions in the Optic Tectum of the Pigeon. J Neurosci. 27:8112–8121.

Sereno PC. 1993. Shoulder girdle and forelimb of Herrerasaurus. J Vert Paleont 13:425–450.

Sereno M, Ulinski P. (1987): Caudal topographic nucleus isthmi and the rostral nontopographic nucleus isthmi in the turtle, Pseudemys scripta. J Comp Neurol.

Sekercioglu CH (2006): "Foreword". in Josep del Hoyo, Andrew Elliott & David Christie (eds.). Handbook of the Birds of the World, Volume 11: Old World Flycatchers to Old World Warblers. Barcelona: Lynx Edicions. pp.48.

Sherry DF (1985): Food storage by birds and mammals. Adv Stud Behav. 15: 153-188.

Sherry DF, Vaccarino AL, Buckenham K, Herz RS (1989): The hippocampal complex of food-storing birds. Brain Behav Evol 34: 308-317.

Sherry DF, Forbes MRL, Khurgel M, Ivy GO (1993): Females have a larger hippocampus than males in the brood-parasitic brownheaded cowbird. Proc. natl Acad. Sci. U.S.A. 90: 7839–7843.

Shortess GK, Klose EF (1975): The area of the nucleus isthmoopticusin the american kestrel (Falco sparverius) and the redtailed hawk (Buteo jamaicensis). Brain Res 88: 525–531.

Sibley CG, Ahlquist JE (1990): Phylogeny and Classification of Birds. New Haven CT: Yale University Press.

Sidor CA, Hopson JA (1998): Ghost lineages and "mammalness": Assessing the temporal pattern of character acquisition in the Synapsida. Paleobiol 24:254–273.

Smith CC, Reichman OJ (1984): The evolution of food caching by birds and mammals. Annu Rev Eecol Syst, 15: 329-351.

Sol D, Timmermans S, Lefebvre L (2002): Behavioural flexibility and invasion success in birds. Anim behav. 63: 495-502.

Stingelin W (1961): Grossenunterschiede des sensiblen Trigeminuskerns bei verschiedenen Vogeln. Rev Suisse Zool 68:247-251.

Stingelin W (1965): Qualitative und quantitative Untersuchungen an Kerngebieten der Medulla oblongata bei VSgeln. Bibl Anat 6:1-116.

Striedter GF (2005): Principles of brain evolution. In: Sunderland , editor. Mass. Sinauer Associates. 436 pp.

Suh A, Paus M, Kiefmann M, Churakov G, Franke FA, et al. (2011): Mesozoic retroposons reveal parrots as the closest living relatives of passerine birds. Nature Comm 2: 443

Sullivan WE (1985): Classification of response patterns in cochlear nucleus of barn owl: correlation with functional response properties. J Neurophysiol 53: 201–216.

Sullivan WE, Konishi M (1984): Segregation of stimulus phase and intensity coding in the cochlear nucleus of the barn owl. J Neurosci 4: 1787–1799.

Takahashi, T. T. (2010): How the owl tracks its prey–II. J Exp Biol. 213: 3399-3408.

Takahashi TT, Moiseff A, Konishi M (1984): Time and intensity cues are processed independently in the auditory system of the owl. J Neurosci. 4: 1781–1786.

Takahashi TT, Konishi M (1988a): Projections of nucleus angularis and nucleus laminaris to the lateral lemniscal nuclear complex of the barn owl. J Comp Neurol 274: 212–238.

Takahashi TT, Konishi M (1988b): Projections of the cochlear nuclei and nucleus laminaris to the inferior colliculus of the barn owl. J Comp Neurol 274: 190–211.

Takahashi TT, Keller CH (1992): Commissural connections mediate inhibition for the computation of interaural level difference in the barn owl. J Comp Physiol A 170: 161–169.

Timmermans S, Lefebvre L, Boire D, Basu P (2000): Relative size of the hyperstriatum ventrale is the best predictor of feeding innovation rate in birds. Brain Behav Evol. 56(4), 196-203.

Tschida K, Mooney R (2012): The role of auditory feedback in vocal learning and maintenance. Curr Opin Neurobiol. 22: 320-327.

Tramontin, A. D., & Brenowitz, E. A. (2000): Seasonal plasticity in the adult brain. Trends neurosci. 23: 251-258.

Wallman J, Pettigrew JD (1985): Conjugate and disjunctive saccades in two avian species with contrasting oculomotor strategies. J Neurosci 5:1418–1428

Wagner H-J (2001a): Sensory brain areas in mesopelagic fishes. Brain Behav Evol. 57:117–133.

Wagner H-J (2001b): Brain areas in abyssal demersal fishes. Brain Behav Evol 57:301–316.

Wagner H, Luksch H. (1998): Effect of ecological pressures on brains: examples from avian neuroethology and general meanings. Z Naturforsch C 53:560–81.

Wang N, Braun EL, Kimball RT (2012): Testing hypotheses about the sister group of the Passeriformes using an independent 30-locus data set. Mol Biol Evol., 29: 737-750.

Weidner C, Repe´rant J, Desroches AM, Miceli D, Vesselkin NP (1987): Nuclear origin of the centrifugal visual pathways in birds of prey. Brain Res 43:153–160.

Whiting B., Barton R. (2003): The evolution of the cortico-cerebellar complex in primates: anatomical connections predict patterns of correlated evolution. J Hum Evol. 44:3–10.

Wild JM (1981): Identification and localization of the motor nuclei and sensory projections of the glossopharyngeal, vagus, and hypoglossal nerves of the cockatoo (*Cacatua roseicapilla*), Cacatuidae. J Comp Neurol 203:351-77.

Wild JM (1990): Peripheral and central terminations of hypoglossal afferents innervating lingual tactile mechanoreceptor complexes in Fringillidae J Comp Neurol 298:157-71.

Wild JM (1997): Neural pathways for the control of birdsong production. Journal of neurobiology, 33: 653-670.

Wilson M, Lindstrom SH (2011): What the bird's brain tells the bird's eye: the function of descending input to the avian retina Vis Neurosci 28: 337–50.

Witmer LM. (2002): The debate on avian ancestry: phylogeny, function, and fossils. In: Chiappe LM, Witmer LM, editors. Mesozoic birds: above the heads of dinosaurs. Berkeley:University of California Press. pp 3–30.

Wyles JS, Kunkel JG, Wilson AC (1983): Birds, behavior and anatomical evolution. Proc. natl Acad. Sci. U.S.A. 80: 4394–4397.

Wylie DR, Shaver SW, Frost BJ (1994): The visual response properties of neurons in the nucleus of the basal optic root of the northern saw-whet owl (Aegolius acadicus). Brain Behav Evol 43:15–25

Wylie DR, Frost BJ (1996): The pigeon optokinetic system: visual input in extraocular muscle coordinates. Vis Neurosci 13:945–953.

Wylie DR, Crowder NA (2000): Spatiotemporal properties of fast and slow neurons in the pretectal nucleus lentiformis mesencephali in pigeons. J Neurophysiol 84:2529–2540.

Wylie DR (2013): Processing of visual signals related to self-motion in the cerebellum of pigeons. Frontiers in Behavioral Neuroscience 7:4. doi: 10.3389/fnbeh.2013.00004

Yopak KE, Lisney TJ, Collin SP, Montgomery JC (2007): Variation in brain organization and cerebellar foliation in chondrichthyans: sharks and holocephalans. Brain Behav Evol. 69: 280-300.

Zardoya R, Meyer A (2001): The evolutionary position of turtles revised. Naturwissenschaften. 88: 193-200.

Zelenitsky DK, Therrien F, Ridgely RC, McGee AR, Witmer LM (2011): Evolution of olfaction in non-avian theropod dinosaurs and birds. Proc R Soc Lond B, 278: 3625-3634.

Chapter 2: **The Independent Evolution of the Enlargement of the Principal Sensory Nucleus of the Trigeminal Nerve in Three Different Groups of Birds**

A version of this chapter has been published:

Gutiérrez-Ibáñez C, Iwaniuk AN, Wylie DRW (2009): The independent evolution of the enlargement of the principal sensory nucleus of the trigeminal nerve (PrV) in three different groups of birds. Brain, Behav and Evol 74:280–294.

In vertebrates, sensory specializations are usually correlated with increases in the brain areas associated with that specialization. This correlation is called the 'principle of proper mass' whereby the size of a neural structure is a reflection of the complexity of the behaviors that it subserves [Jerison, 1973]. Examples of this correlation are found in all sensory systems and in all vertebrates [e.g., somatosensory: Pubols et al., 1965; Pubols and Pubols, 1972; visual: Barton, 1998; Iwaniuk and Wylie, 2007; gustatory: Finger, 1975; auditory: Kubke et al., 2004]. Some of the best-studied examples of this correlation between sensory systems and behavior come from examinations of the trigeminal system in small mammals and its representation in the primary somatosensory cortex [Catania and Henry, 2006]. For example, a comparison between Norway rats *(Rattus norvegicus)* and naked molerats *(Heterocephalus glaber)* revealed a large representation of the vibrissae in the somatosensory cortex of the former, but a large representation of the incisor in the latter [Henry et al., 2006]. Similarly, Catania [2000, 2005] compared the representation of the trigeminal system in the somatosensory cortex of several species of insectivores and found that the cortical representation of the vibrissae and the rhinarium was a reflection of species' differences in both facial morphology and ecology. For example, the masked shrew *(Sorex sinereus)* hunts above ground during the night for small invertebrates and has a large representation of the vibrissae in the somatosensory cortex, but a very small representation of the rhinarium. In contrast, the eastern mole *(Scalopus aquaticus)*, which has an enlarged rhinarium and hunts underground, has equal representations of both the vibrissae and the rhinarium. Finally, the star-nose mole (*Condylura cristata*) has a large representation of the

rhinarium and little of the vibrissae, related to the complex rhinarium comprised of 22 fleshy appendages used for detecting prey [Catania, 2005].

The correlated evolution of the trigeminal system and ecology has been studied in some detail in mammals, but there is relatively little information for other vertebrate groups, particularly for birds. Even though birds do have a well-developed trigeminal system [Dubbeldam, 1998], studies have been restricted to the anatomy and physiology in pigeons [*Columba livia*; Zeigler and Witkovsky, 1968; Silver and Witkovsky, 1973; Dubbeldam and Karten, 1978] and the mallard duck [*Anas platyrhynchus*; Dubbeldam, 1980; Arends et al., 1984; Kishida et al., 1984]. In addition, comparative studies of sensory specializations in birds have focused on other sensory systems [e.g., visual: Iwaniuk and Wylie, 2006, 2007; Iwaniuk et al., 2008; auditory: Kubke et al., 2004; Iwaniuk et al., 2006] and thus a detailed comparative analysis of the correlation between trigeminal system specialization and behavior is completely lacking in birds.

One of the unique characteristics of birds is the presence of a beak, and the form and size of the beak is strongly correlated with species-specific feeding behaviors. This correlation between beak morphology and feeding behavior even extends to the number and distribution of mechanoreceptors in the beak and tongue [Gottschaldt, 1985]. For example, in shorebirds (Charadriiformes, such as snipe and sandpipers) that use their beak for probing, mechanoreceptors are numerous and concentrated in the tip of the beak [Bolze, 1968; Pettigrew and Frost, 1985]. In ducks and geese (Anseriformes) mechanoreceptors are concentrated in the tip and ridges of the beak, as well as on their large, fleshy tongue [Berkhoudt, 1980]. Even in grain-feeding songbirds, which have relatively

low numbers of mechanoreceptors in the beak, they are located exactly in the parts of the beak involved in seed-opening [Krulis, 1978]. Not only does the overall number of mechanoreceptors vary among species, but also the abundance of specific types of mechanoreceptors. In the domestic goose *(Anser anser)*, Grandry corpuscles, which are velocity detectors, are ten times more abund ant than Herbst corpuscles, which detect pressure [Gottschaldt and Lausmann, 1974; Gottschaldt, 1985]. In contrast, Herbst corpuscles are much more abundant than Grandry corpuscles in shorebirds [Bolze, 1968; Piersma et al., 1998]. Finally, the presence and degree of development of the bill tip organ also varies among bird groups. The bill tip organ itself is a complex sensory structure at the tip of the beak that is covered by a horny plate and contains several touch papillae, with both Grandry and Herbst corpuscles [Iggo and Gottschald, 1974]. The bill tip organ is highly developed in waterfowl, shorebirds and parrots (Psittaciformes) and is completely lacking in most other birds [Gottschaldt and Lausmann, 1974; Gottschaldt, 1985].

The mechanoreceptors in the beak are innervated by the three branches of the trigeminal nerve [Dubbeldam and Karten, 1978]. These nerves also convey nociceptive information from the beak and proprioceptive information from jaw muscles to the gasserian ganglion [Bout and Dubbeldam, 1991]. From there, trigeminal efferents reach three main targets: the mesencephalic nucleus of the trigeminal nerve, which receives information exclusively from the proprioceptive component; the descending tract of the trigeminal nerve (TTD); and the principal sensory nucleus of the trigeminal nerve (PrV). Both PrV and TTD receive projections from the three branches of the trigeminal nerve, but differ in the type

of information they receive. Although the TTD receives proprioceptive and nociceptive information, PrV is the main target of mechanoreceptive afferents [Zeigler and Witkovsky, 1968; Silver and Witkovsky, 1973; Kishida et al., 1985; Dubbeldam, 1998]. The trigeminal nerve is not, however, the only afferent of PrV. Information from the tongue is conveyed to PrV via afferents from the facial [Bout and Dubbeldam, 1985], glossopharyngeal [Dubbeldam et al., 1979; Wild, 1981] and hypoglossal nerves [Wild, 1981, 1990]. Previous studies found that PrV is enlarged in some species that rely heavily on tactile input when feeding. For example, Stingelin [1961, 1965] found that the common snipe *(Gallinago gallinago)* and Fisher's lovebird *(Agapornis fisheri)* have relatively larger PrVs than the carrion crow *(Corvus corone)*, European bee-eater, *(Merops apiaster)* and the tawny owl *(Strix aluco)* . Similarly, using the ratio between the volume of PrV and the nucleus rotundus,as a measure of tactile versus visual specialization, Dubbeldam [1998] found that the mallard and the snipe had high ratios and the budgerigar *(Melopsittacus undulatus)* had a ratio between that of the tactile and visual specialists. Finally, Boire [1989] compared the size of PrV in 27 species and found high values in the mallard, a sandpiper *(Limnodromus griseus)* and the budgerigar. Thus, there is some evidence that PrV is hypertrophied in at least three groups of birds, waterfowl, shorebirds and parrots, but a broad systematic analysis across species has not been performed. The use of a large sample could not only reveal differences among groups, but also within groups in relation to feeding behavior and/or beak morphology. In the present study we build on previous analyses of PrV by measuring PrV volume in dozens of additional

species and present a detailed analysis of size variation of PrV across 73 species using both conventional and phylogenetically based statistics.

2.1 Methods

2.1.1 *Specimens*

We measured PrV in 47 specimens representing 46 species (table 2.1). For all specimens, the head was immersion-fixed in 4% paraformaldehyde in 0.1 M phosphate buffer (PB). The brain was then extracted, weighed to the nearest milligram, cryoprotected in 30% sucrose in PB, embedded in gelatin and sectioned in the coronal or sagittal plane on a freezing stage microtome at a thickness of 40 μm. Sections were collected in 0.1 M phosphate buffered saline, mounted onto gelatinized slides, stained with thionin and coverslipped with Permount.

The olfactory bulbs were intact in all of the specimens that we collected and sectioned. In the case of the spinal cord, all brains were cut following bird brain atlases [e.g., Pigeon: Karten, 1967], in which the brainstem ends at the same rostro-caudal point as the cerebellum. As a result, brain weight measurements were consistent among our specimens.

Photomicrographs of every second section were taken throughout the rostrocaudal extent of PrV using a Retiga EXi *FAST* Cooled mono 12-bit camera (Qimaging, Burnaby, B.C., Canada) and OPENLAB Imaging system (Improvision, Lexington, Mass., USA) attached to a compound light microscope (Leica DMRE, Richmond Hill, Ont., Canada). Measurements of the PrV were

taken directly from these photos with ImageJ, (NIH, Bethesda, Maryland, USA, http://rsb.info.nih.gov/ij/) and volumes were calculated by multiplying the area in each section by the thickness of the section (40 μm) and the sampling interval.

Additional data for 31 specimens was obtained from several sources [table 2.1; Boire, 1989; Carezzano and Bee-de-Speroni, 1995; Pistone et al., 2002]. This included 27 additional species. In the event that there was more than one specimen for our measurements or there was data from both studies, the number used was the average of both measurements. A paired t test between the four species that coincided between Boire [1989] and our measurements (see table 2.1) showed no significant differences ($p > 0.05$). Because neither Dubbeldam [1998] nor Stingelin [1965] used brain volume to standardize their results, we could not include their data in the current analysis.

2.1.2 Defining PrV

The limits of PrV were established using the descriptions of Dubbeldam and Karten [1978], Boire [1989] and Dubbeldam [1980]. In birds with small PrV volumes (e.g., Passeriformes, Columbiformes), PrV can be identified as a round or oval mass of large cells in the dorsolateral part of the anterior brainstem (fig. 2.1 D). It lies dorsal to the root of the fifth nerve and the motor nuclei of the fifth nerve (mV). The dorsal border of PrV is defined by the brachium conjunctivum (BC) and the caudo-lateral borders are defined by the TTD.

In waterfowl, PrV lies more lateral than in other birds, just above the root of the trigeminal nerve (fig. 2.1 A). Dubbeldam [1980] describes three cell groups

that form part of PrV in the mallard, but show differences in the connections with the main part of the PrV: nucleus paraprincipalis (pP), nucleus sensorius of nIX (sIXd) and nucleus supratrigeminalis (sT). The pP lies ventral to the rostral part of the PrV and receives few projections from the gasserian ganglion. sIXd lies dorsal and medial to the caudal PrV and receives projections from the glossopharyngeal nerve. Finally, sT is a small round group of cells that is located dorsomedial to PrV and receives projections from the mesencephalic nucleus of the trigeminus. Because these three groups cannot be distinguished easily with a Nissl stain, they were all included in our measurements.

In beak-probing shorebirds, PrV size and position is similar to waterfowl (fig. 2.1 C). Some subdivisions are apparent, but we cannot confirm if they correspond with the ones found in waterfowl. As in waterfowl, the entire cell mass was included in the measurements. In parrots, PrV has several subdivisions and appears to extend more caudally than in other birds (fig. 2.2 A–C). Because there is no detailed description of PrV in parrots, we used coronal and sagittal sections through the brainstem of the galah *(Eolophus roseicapillus)* to aid in determining the extent and limits of the PrV in parrots.

2.13 Statistical Analyses

To test for significant differences in the relative size of PrV, we performed analyses of covariance between log 10 -transformed PrV volumes and log 10 -transformed brain volume minus PrV volume [Deacon, 1990; Iwaniuk et al., 2005, 2006; Iwaniuk and Wylie, 2007]. The species were separated into four

categories; waterfowl, parrots, beak-probing shorebirds and non-specialists. Because comparative analyses using species as independent data points are subject to inflated type II error [Harvey and Pagel, 1991], we also used phylogenetic generalized least squares (PGLS) regressions [Garland and Ives, 2000; Garland et al., 2005]. PGLS assumes that residual variation among species is correlated, with the correlation given by a process that acts like Brownian motion evolution along the phylogenetic tree. Analyses were performed using the MATLAB program Regressionv2.m [available from T. Garland, Jr., on request; Ives et al., 2007, Lavin et al., 2008]. Currently, there is no consensus regarding the phylogenetic relationships among most orders of birds. To account for phylogenetic relatedness in our analyses, we therefore used five different phylogenetic trees that all differed in their inter-ordinal and inter-familial relationships: Sibley and Ahlquist [1990], Cracraft et al. [2004], Livezey and Zusi [2007], Davis [2008] and Hackett et al. [2008]. Resolution at the species level within orders and families was derived from additional taxon-specific studies [Johnson and Sorenson, 1999; Donne-Goussé et al., 2002; Barker et al., 2004; Thomas et al., 2004; Pereira et al., 2007; Kimball and Braun, 2008; Wink et al., 2008; Wright et al., 2008]. Phylogenetic trees, character matrix and phylogenetic

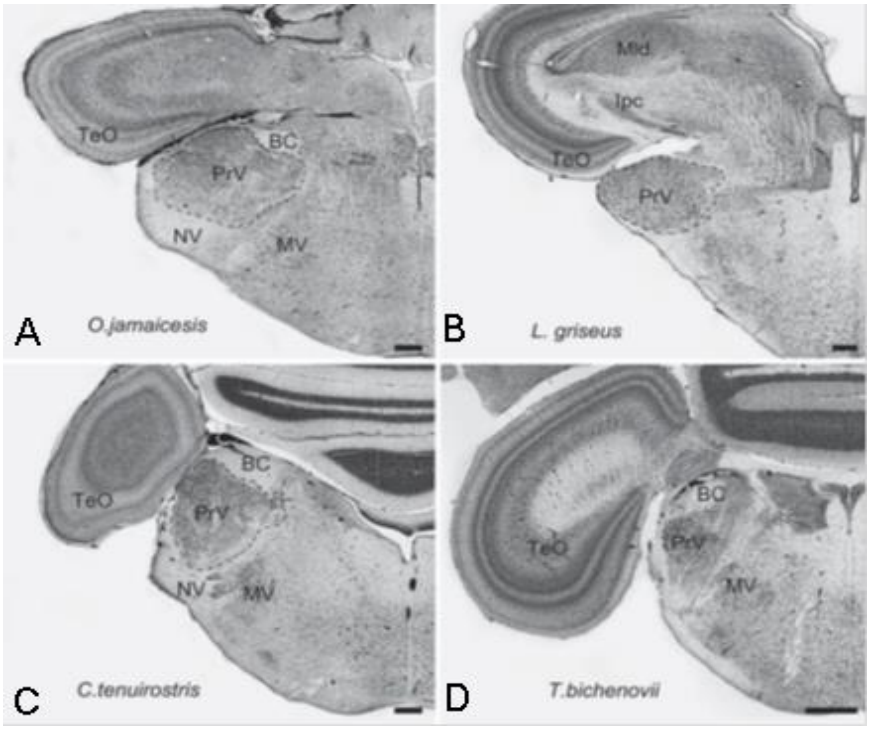

Figure 2.1. Photomicrographs of coronal sections through PrV of four species of birds. Photomicrographs of coronal sections through the principal sensory nucleus of the trigeminal nerve (PrV) of four species of birds, the three somatosensory specialists (A–C) and a non-specialist (D). Pictures were taken approximately midway along the antero-posterior extent. The dotted black lines indicate the borders of PrV. A Ruddy duck (Oxyura jamaicesis) ;B Long-billed corella (Cacatua tenuirostris) ; C Short-billed dowitcher (Limnodromus griseus) ; D the double-barred finch (Taeniopygia bichenovii) . Abbreviations are as follows: TeO = optic tectum; BC = brachium conjunctivum; NV = root of the trigeminal nerve; MV = motor nucleus of the trigeminal nerve; Mld = nucleus mesencephalicus lateralis pars dorsalis; Ipc = nucleus isthmi parvocellularis. Scale bars = 600 μm.

variance-covariance matrix were constructed using Mequite/PDAP:PDTREE software [Midford et al., 2002; Maddison and Maddison, 2009] and the PDAP software package (available from T. Garland upon request). Because the phylogeny was constructed from multiple sources, branch lengths were all set at 1 to provide adequately standardized branch lengths [Garland et al., 1992]. We applied two models of evolutionary change as implemented in Regressionv2.m: Brownian motion (phylogenetic generalized least-squares or PGLS) and Ornstein-Uhlenbeck [Lavin et al., 2008; Swanson and Garland, 2009]. Akaike Information Criterion was then used to determine which model best fit the data [Lavin et al., 2008].

2.3 Results

Figure 2.1 shows coronal sections through the PrV of a waterfowl, the ruddy duck (A; *Oxyura jamaicensis*); a parrot, the long-billed corella (B; *Cacatua tenuirostris*); a beak-probing shorebird, the short-billed dowitcher (C; *Limnodromus griseus*); and the double-barred finch (D, *Taeniopygia bichenovii*). This last one represents a nonspecialist bird. PrV looks similar in most species: an oval cell mass dorsal to the root of the V nerve and ventral to the BC [for detailed description in pigeons see Dubbeldam and Karten, 1978]. In the three specialist groups, PrV is greatly expanded, both laterally and rostro-caudally. In waterfowl and beak-probing shorebirds, the lateral part of the nucleus is expanded against the brainstem wall, forming a protuberance ventrally and caudally to the optic tectum (fig. 2.1 A, C). In these groups, the anterior part PrV continues rostrally to

the root of the V nerve and BC and can be followed to the level of isthmo-optic nucleus. The most caudal parts of the nucleus extend to the level of the root of the VII nerve and lie laterally to the nucleus vestibularis medialis (VeM) [see Dubbeldam, 1980, for detailed description in the mallard]. In parrots, PrV is also expanded, but presents some differences when compared to the waterfowl and shorebirds. Figure 2.2 shows three sagittal sections at different mediolateral planes (medial to lateral, A–C) and three coronal sections at different rostro-caudal planes (anterior to posterior, D–F) from the galah *(Eolophus roseicapillus*)

.

In parrots, PrV does not extend as far laterally (fig. 2.2 B) or rostrally as in the other two groups (fig. 2.2 A). The caudal portion extends to a similar extent in waterfowl and beakprobing shorebirds, dorsally to the root of the VII nerve (fig. 2.2 C), but lies in a much more dorsal position, inside the cerebellar peduncle and dorsal to the VeM (fig. 2.2 C). Sagittal sections show that this most caudal portion of PrV is separated from the main part of PrV by a bundle of fibers that course from the posterior part of the brainstem to join the BC (fig. 2.2 A–C). Because this group of cells is of similar size and organization to the main part of the PrV, we considered it to be part of the nucleus and divided PrV in parrots into superior and inferior components (PrVi, PrVs). These two components could be distinguished in the coronal section of all the parrots examined, but not in any other species (see fig. 2.1, 2.2).

Our statistical analysis showed that the three somatosensory specialists have a significantly larger PrV, relative to brain volume, than the non-specialist birds. The regression lines describing the relation between PrV volume and brain

volume for the three specialist taxa are significantly higher than those for the non-specialists (fig. 2.3; table 2.2), with waterfowl and beak-probing shorebirds having the largest PrV and parrots falling between these two groups and the non-specialists. ANCOVA shows a significant effect for the group ($F = 111.06$, d.f. = 3, 68, $p > 0.0001$) on the size of PrV relative to brain size. Tukey HSD post-hoc comparisons revealed that all three specialist groups, the waterfowl, beak-probing shorebirds and parrots, have significantly larger relative PrV volumes compared to non-specialists. In addition, the beakprobing shorebirds and waterfowl have significantly larger relative PrV volumes than the parrots.

These results were corroborated by the PGLS approach. We detected a significant effect of group on the relative size of PrV for all five phylogenies and both models of evolutionary change (table 2.2). Thus, even though our categorization of species is largely based on taxonomy, a phylogenetically based approach also detects a significant difference between the specialists and non-specialists. Based on the lower Akaike Information Criterion, ordinary least square regressions fit the data better than both models of evolutionary change (table 2.2).

The hypertrophy of PrV in these three groups is also evident when comparing the average volume occupied by the PrV relative to total brain size for each group (fig. 2.4). Beak-probing shorebirds show the highest average (0.3864 8 0.0183), almost twice that for waterfowl (0.2229 8 0.0867) and four times that for parrots (0.0957 8 0.0282).

Waterfowl show the largest variation among the three specialist groups (fig. 2.5). The ruddy duck has the largest PrV relative to brain size, followed by

species within the genera *Anas* and *Aythya*. At the low end, the red-breasted merganser *(Mergus serrator)* and the Australian wood duck *(Chenonetta jubata)* have the smallest PrV volumes, more similar to the volumes we observed in parrots. Thus, although waterfowl all have relatively large PrV volumes, there appears to be considerable variation among species within the order, which might reflect differences in feeding behavior.

2.4 Discussion

Our results showed that at least three groups of birds possess a hypertrophied PrV: waterfowl, beak-probing shorebirds and, to a lesser degree, parrots. Although this was suggested by Stingelin [1965], Dubbeldam [1998] and Boire [1989] only one or two species of each specialist group and a few non-specialists were used in these studies. Our study therefore corroborates previous observations, but adds to these studies by analyzing a broader range of species and using sophisticated analytical techniques to test for differences among groups.

We found that the PrV in parrots has a unique anatomical feature whereby the posterior part continues more caudally than other species, lying dorsally to the VeM and separated from the main part by a bundle of fibers (fig. 2.2 D–F). We named this the superior part of PrV (PrVs). In all the parrot species analyzed PrVs and the main part of PrV had similar cell shape and size. Wild [1981] considered PrVs to be part of the nucleus vestibularis superior in the galah, but we found

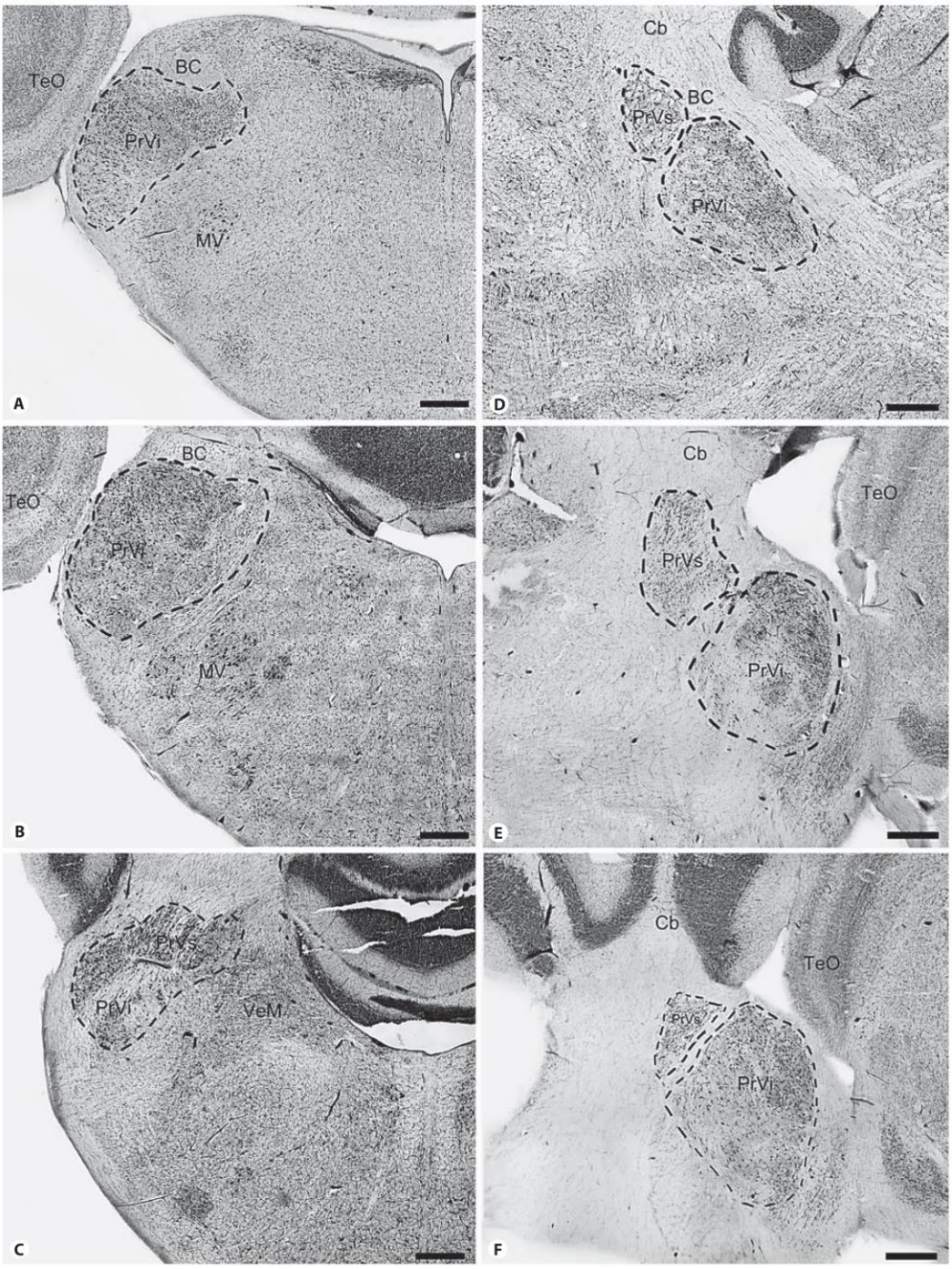
TeO
BC
PrVi
MV
A
Cb
BC
PrVs
PrVi
D
BC
TeO
PrVi
MV
B
Cb
TeO
PrVs
PrVi
E
PrVs
PrVi
VeM
C
Cb
TeO
PrVs
PrVi
F

Figure. 2.2. Photomicrograph of PrV in the Galah (*Eolophus roseicapillus*). Photomicrograph of the principal sensory nucleus of the trigeminal nerve (PrV) in the Galah (Eolophus roseicapillus). Coronal sections at three different antero-posterior levels through are shown in **A** (anterior) to **C** (posterior), and sagittal sections at three different medio-lateral levels are shown in **D** (medial) to **F** (lateral). The dotted black lines indicate the borders of PrV. Abbreviations are as follows: PrVi = inferior part of principal sensory nucleus of the trigeminal nerve; PrVs = superior part of the principal sensory nucleus of the trigeminal nerve; TeO = optic tectum; BC = brachium conjunctivum; NV = root of the trigeminal nerve; MV = motor nucleus of the trigeminal nerve; Cb = cerebellum; VeM = nucleus vestibularis medialis. Scale bars = 600 μm.

that this nucleus lies more caudally and can be distinguished from PrVs due to very different cytoarchitectonic features. Furthermore, Stingelin [1965] also considered this cell mass to be part of PrV. Also, Boire's [1989] measurement of the volume of PrV in the budgerigar is very similar to ours, and thus Boire [1989] must have considered this cell mass to be part of PrV. Tracer studies, however, would be necessary to confirm this as part of PrV.

As noted previously (see-introduction), PrV receives projections not only from the trigeminal nerve, which innervates the upper and lower beak, but also from the facial [Bout and Dubbeldam, 1985], glossopharyngeal [Dubbeldam et al., 1979; Wild, 1981] and hypoglossal nerves [Wild, 1981, 1990]. PrV therefore gathers information from the beak, palate, tongue and pharynx. This convergence of sensory information from the orofacial region into PrV is clear in waterfowl and parrots [Dubbeldam et al., 1979; Wild, 1981], but seems to be lacking in the pigeon [Arends et al., 1984, 1998]. Dubbeldam [1992] proposed that these differences in the innervation of PrV among species are correlated with the functional demands of specific feeding behaviors. The alternative is that non-trigeminal afferents to PrV are present in the pigeons, but are too small to be detected, and therefore the relative contribution of each nerve to PrV would vary in concert with different feeding behaviors.

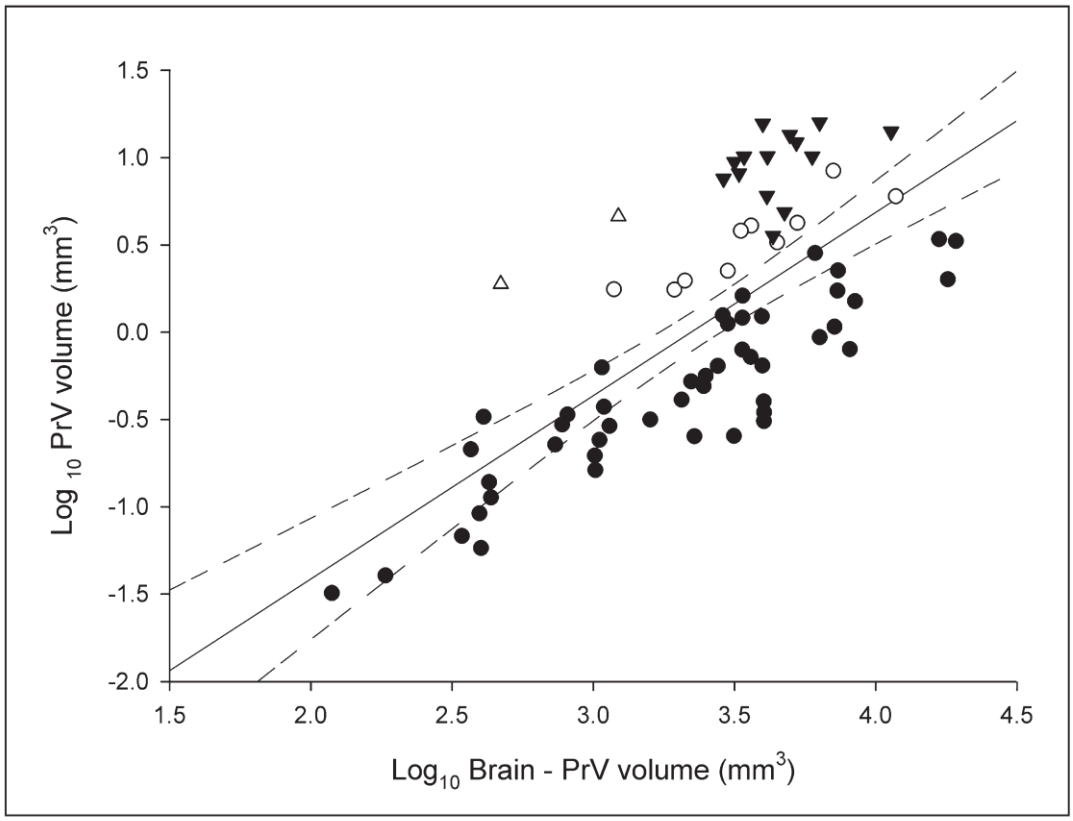

Figure. 2.3. PrV volume plotted vs brain minus PrV volume for all species. Scatterplot of the volume of principal sensory nucleus of the trigeminal nerve (PrV) volume plotted as a function of brain minus PrV volume for all species examined (see table 2.1). Waterfowl are indicated by black triangles, beak-probing shorebirds by white triangles, parrots by white circles and non-specialists by black circles. The solid lines indicate the least squares linear regression line for all species and the dotted lines are the 95% confidence interval around the regression line.

2.4.1 Feeding Mechanism and PrV Hypertrophy

To understand the hypertrophy of PrV in beak-probing shorebirds, waterfowl and parrots, we must consider the particular feeding behaviors of each group and the sensory demands these behaviors place on different parts of the orofacial region. These three groups are very specialized with respect to their feeding behaviors and present several related anatomical and behavioral adaptations.

In the case of beak-probing shorebirds, we could only include two species, the least sandpiper *(Calidris minutilla)* and the short-billed dowitcher *(Limnodromus griseu),* both of which belong to the family of the Scolopacidae. Feeding behavior in most scolopacids consists of inserting the beak into a soft substrate (e.g., sand or mud) to capture invertebrates that live below the sediment surface [Barbosa and Moreno, 1999; Nebel and Thompson, 2005]. To detect their prey, they use a complex array of sensory pits in the tip of the bill, which are filled with Herbst corpuscles. These mechanoreceptors sense pressure or vibrationalcues from buried invertebrate prey [Gerritsen and Meiboom, 1986; Zweers and Gerritsen, 1997; Piersma et al., 1998]. In some cases, such as the red knot *(Calidris canutus)* and sanderling *(C. alba)* , it has been suggested that the high density of mechanoreceptors is used to detect changes in pressure patterns produced by buried objects, allowing these species to detect immobile bivalves without direct contact [Gerritsen and Meiboom, 1986; Piersma et al., 1998]. Thus, scolopacids depend highly upon the trigeminal system for foraging and this has likely placed increased demands on the processing capacity of PrV thereby leading to its enlargement. Beakprobing as a feeding strategy is not, however,

limited to scolopacids. Within Charadriiforms, oystercatchers (Haematopodidae) have long, narrow beaks that are used to capture buried worms and bivalves [Hulscher, 1976; Boates and Goss-Custard, 1989; Zweers et al., 1994]. Although not related to shorebirds, ibis (Threskiornithidae) also have long narrow beaks that are used to probe in mud and shallow waters in search of small invertebrates [Bildstein, 1987; Bildstein et al., 1989; Zweers et al., 1994]. Stingelin [1965] measured PrV volume in the sacred ibis (*Threskiornis aethiopica)*, using a cerebral index approach and found it was of similar relative size to a snipe (*G. gallinago*).

Recently, Cunningham et al. [2007] found that kiwis *(Apteryx spp.)* have a large number of sensory pits in the tip of the beak and the number of Herbst corpuscles per pit was similar to beak-probing shorebirds. Based on this, they proposed that kiwis must use tactile information in a similar fashion to beak-probing shorebirds. Martin et al. [2007] analyzed the brain of kiwis and reported a 'large and well-defined' PrV, but no measurements were provided. Because kiwis also have an enlarged olfactory system system [Martin et al., 2007] and there is some controversy regarding the use of olfactory versus tactile information in foraging [see Cunningham et al., 2007], a comparison of the relative size of PrV to other beak-probing birds could be useful in determining the relative importance of tactile information in the feeding behavior of kiwis.

Waterfowl exhibit a great diversity of diets and feeding behaviors, and this is reflected in a large variation in the size of PrV (fig. 2.5). Waterfowl from the

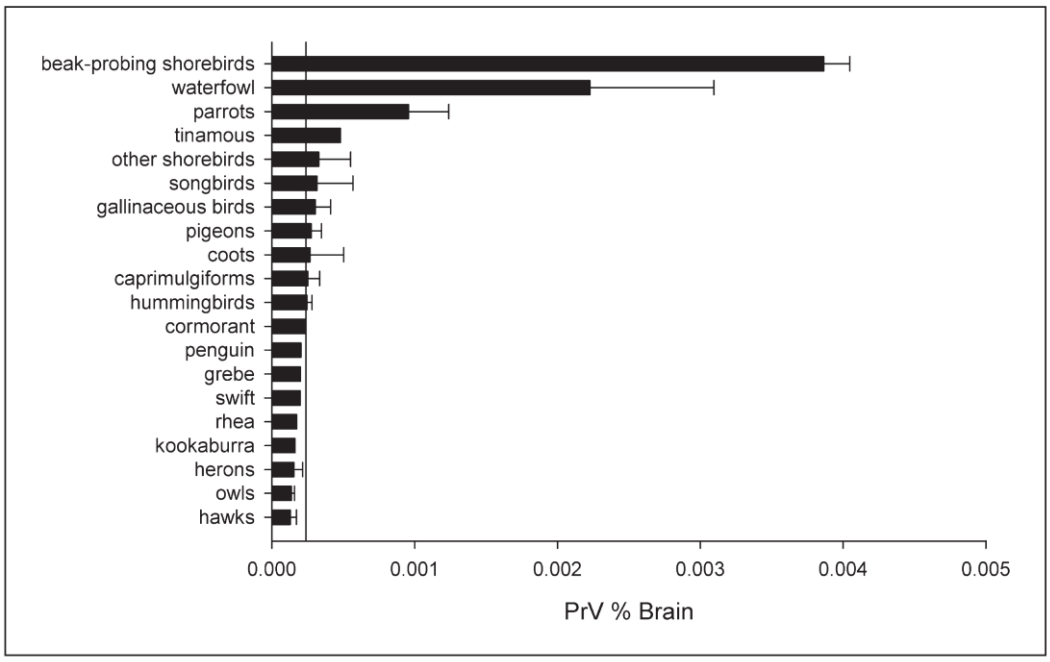

Figure 2.4. Relative size of PrV expressed as a percentage of total brain. Bar graph of the relative size of PrV expressed as a percentage of total brain volume. The solid line indicates the mean for all non-specialists (0.0239) and the error bars indicate standard deviations.

genera *Oxyura* , *Anas* and *Aythya* are mostly filter feeders or search for food items in the sediment while diving [Tome and Wrubleski, 1988; Kooloos et al., 1989; Barbosa and Moreno, 1999]. The general foraging behavior of these birds consists of inserting the tip of the bill into the substrate while moving their head from side to side and opening and closing the bill. The bill movements are coordinated with tongue movements; when the bill opens, the tongue retracts and acts as a piston, sucking water and food particles inside the mouth. When the bill closes, the tongue expels the water through the sides of the bill and the lamellae that line the bill trap any food items. As the mouth opens again and the tongue is retracted, horny spines on the lateral edge of the caudal tongue are used to sweep food out of the lamellae [Zweers et al., 1977; Tome and Wrubleski, 1988; Kooloos et al., 1989]. This complex behavior is associated with a large number of mechanoreceptors in the beak and tongue of waterfowl, especially Grandry's corpuscles, which detect velocity [Gottschaldt and Lausmann, 1974; Gosttchaldt, 1985]. Mechanoreceptors in the beak, and especially in the bill tip organ, are used to detect and discriminate food items, whereas those in the tongue and palate are used for monitoring the transport and flow of water and food into the oral cavity [Zweers et al., 1977; Berckhoudt, 1980]. Given the complexity of these coordinated movements for filter feeding and their reliance on somatosensory input throughout the oral cavity, it is therefore of little surprise that the PrV is enlarged in all filter-feeding species. Not all waterfowl, however, share an equally large PrV. As indicated in our results, there is significant variation among species. In the middle range are the bufflehead (*Bucephala albeola*), the common

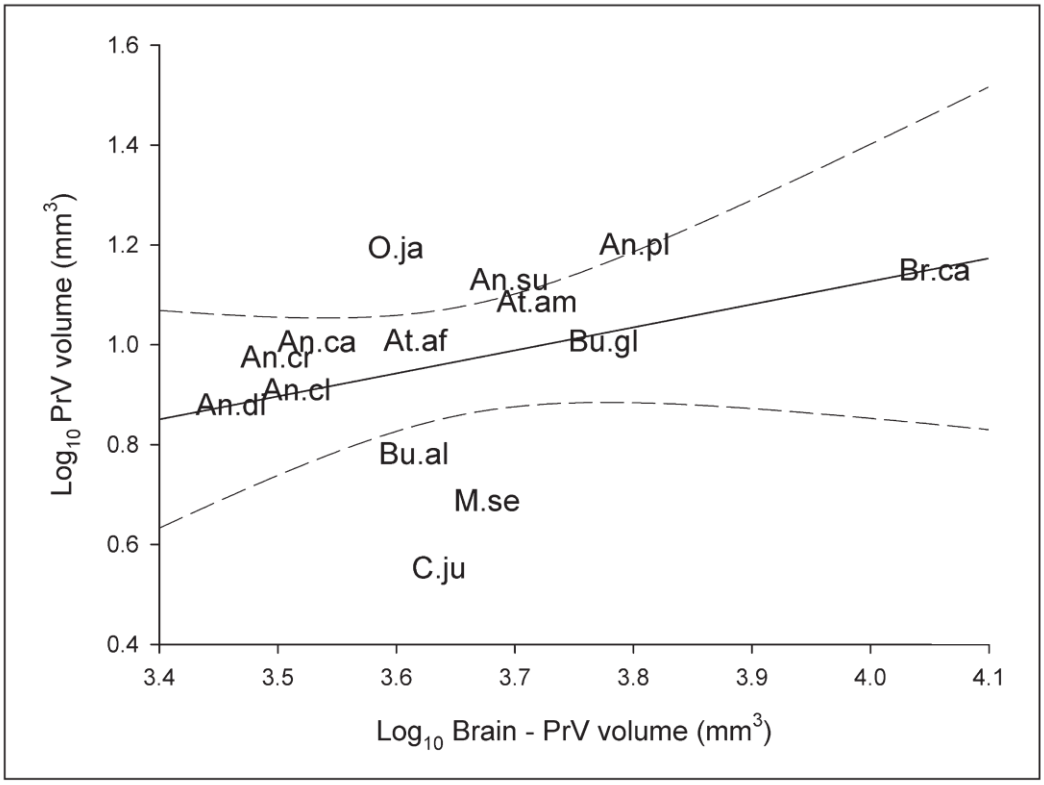

Figure 2.5. PrV plotted vs brain minus PrV volume for waterfowl. Scatterplot of the volume of principal sensory nucleus of the trigeminal nerve (PrV) volume plotted as a function of brain minus PrV volume for all waterfowl (Anseriformes) species examined. Abbreviations are as follows: O.ja = *Oxyura jamaicensis* ; An.pl = *Anas platyrhynchus* ; An.su = *Anas superciliosa* ; An.ca = *Anas castanea* ; An.cl = *Anas clypeata* ; An.di = *Anas discors* ; An.cr = *Anas carolinensis* ; At.am = *Aythya americana* ; At.cl = *Aythya affinis* ; Br.ca = *Branta canadensis* ; Bu.cl = *Bucehala clangula* ; Bu.al = *Bucephala albeola* ; M.se = *Mergus serrator* ; C.ju = *Chenonetta jubata.*

goldeneye (*Bucephala clangula*) and the Canada goose *(Branta canadiensis,* Bufflehead and goldeneye feed by diving and actively trapping small invertebrates [Goodman and Fisher, 1962; Pehrsson, 1976] whereas Canada geese are terrestrial grazers [Goodman and Fisher, 1962]. At the lower end of PrV size among the waterfowl are the red-breasted merganser and the Australian wood duck. The former is a diving duck with an elongated narrow beak and it feeds exclusively on fish mainly using visual cues [Goodman and Fisher 1962; Sjöberg, 1988], whereas the Australian wood duck has a short beak and is a terrestrial grazer, feeding mostly on grass and occasionally on insects [Dawson et al., 1989; Marchant and Higgins, 1990]. Previously, Dubbeldam [1998] used the ratio between PrV volume and the volume of a visual nucleus, the nucleus rotundus, as a measurement of somatosensory specialization in nine species of waterfowl and found a similar degree of variation. The ratio was high in filtering species in the genera *Anas* and *Aythya,* and low in the Mandarin duck (*Aix galericulata*), a short-billed duck that feeds on small invertebrates [Delacour, 1954]. Filter feeding is thought to the ancestral feeding method of Anseriformes and all other feeding behaviors are secondarily derived [Olson and Feduccia, 1980; Zweers and Vandenberg, 1996]. This suggests that the expansion of PrV in all waterfowl is probably an ancestral feature that also reflects the consequences of enhanced somatosensory processing for filter feeding, and that smaller PrV sizes are due to the loss of this behavior. Why non-filter feeding waterfowl retain relatively large PrV volumes compared to other avian taxa is, however, unclear. One possible explanation is that a larger PrV can be used for other feeding strategies too, such as enhanced sensitivity in the bill tip of mergansers which would probably aid in

the capturing of fish. It should also be noted that just as probe feeding is not exclusive to scolopacid shorebirds; filter feeding has also evolved in other groups of birds [Zweers et al., 1994]. For example, both flamingos [Phoenicopteridae; Zweers et al., 1995] and Antarctic prions [Procellariidae; Morgan and Ritz, 1982; Harper, 1987; Klages and Cooper, 1992] have evolved some form of filtering that involves straining water through lamellae in the sides of their beaks, but the species differ greatly in the form of the beak, how they use it, and in their water pumping mechanism [Zweers et al., 1994]. These differences should be reflected in the sensory requirements from the orofacial region during feeding and, ultimately, in the size of PrV. Lastly, we found parrots have a hypertrophied PrV, but not as large as waterfowl or beak-probing shorebirds (fig. 2.3, 2.4). Contrary to the other two specialist groups, parrots do not rely on mechanosensory information from the beak to find their food. Instead, they use mechanosensory information in the processing of food items, such as seeds, nuts and fruit. Indeed, the feeding apparatus (*i.e.*, beak, palate and tongue) of parrots is highly adapted to seed husking in all species, irrespective of diet [Homberger, 1980a]. The tongue is specially adapted to the seed-husking task and possesses a series of cavernous bodies and a large number of muscles, making it fleshy and highly mobile [Homberger, 1980a, b, 1986; Zweers et al., 1994]. When husking seeds and fruits, parrots use the tip of their tongue to constantly rotate and position the food item against the palate, and use coordinated movements of the lower jaw and tongue to break and remove the husk [Homberger, 1980b, 1983; Zweers et al., 1994]. The distribution of mechanoreceptors in the parrot orofacial region corresponds to this feeding mechanism, with a high concentration of touch papillae in the tip of the

lower beak [Gottschhaldt, 1985] and in the tip of the tongue [Zweers et al., 1994]. Parrots also use the tongue to drink water by shaping the tip of their tongue to resemble a spoon, to pick up small seeds against the upper jaw, and even in the control of vocalizations [Homberger, 1980b, 1983; Zweers et al., 1994; Beckers et al., 2004]. Mechanoreceptors in the dorsal part of the tongue are innervated by the lingual branch of the glossopharyngeal nerve, whereas receptors in the ventral and lateral parts are innervated by the lingual branch of the hypoglossal nerve [Wild, 1981]. Wild [1981] found that in the galah *(E.roseicapillus)* , both nerves send projections to PrV, but contrary to the situation in the mallard duck [Dubbeldam et al., 1979], this projection overlaps with that from the trigeminal nerve. Wild [1981] proposed that this particular organization serves as the anatomical substrate for sensory integration during seed-husking behavior. The relatively large PrV of parrots therefore seems to be directly correlated with the evolution of the sensory and morphological specializations for seed husking. What is surprising, however, is that nectar-feeding species, such as the rainbow *(Trichglossus haematodus)* and purplecrowned lorikeets *(Glossopsitta porphyrocephala)* have a PrV that is similar in size to all of the species feeding on seeds and nuts. Perhaps these species require similar somatosensory processing for tongue-feeding in flowers or for climbing around thin branches using the beak as an additional ‘limb’.

2.5 Conclusions

Enlargement of the PrV in birds appears to be related to at least three very specific feeding behaviors: beakprobing, filtering and seed husking. Even though each specific feeding strategy is restricted to a separate taxonomic group in our study, each has evolved several times within birds. Analyses of the relative size of PrV in some of these groups (e.g., flamingos in the case of filtering or oystercatchers in the case of beak-probing) could reveal further convergence of somatosensory specializations related to feeding behaviors. Furthermore, other birds might present other specialized feeding mechanisms that require an increased amount of somatosensory information from the orofacial region. PrV enlargement could therefore have evolved independently several times in response to the somatosensory requirements of a range of feeding behaviors in birds.

Table 2.1. Species, sample size and volumes of the brain and PrV. List of the species surveyed, sample size and volumes (in mm3) of the brain and the principal sensory nucleus of the trigeminal nerve (PrV)

Order	Common name	Species	n	PrV (mm^3)	Brain (mm^3)	Source
Anseriformes	Green-winged Teal	*Anas carolinensis*	1	9.43	3165.83	This study
	Chestnut teal	*Anas castanea*	1	10.138	3424.71	This study
	Northern shoveler	*Anas clypeata*	1	8.117	3288.51	This study
	Blue-winged teal	*Anas discors*	1	7.573	2895.75	This study
	Mallard	*Anas platyrhynchos*	2	15.882	6343.98	This study, Boire 1989
	Australian black duck	*Anas superciliosa*	1	13.496	4973.94	This study
	Lesser scaup	*Aythya affinis*	1	10.186	4141.89	This study
	Redhead	*Aythya americana*	1	12.194	5245.17	This study
	Canada goose	*Branta canadensis*	1	14.091	11346.91	This study
	Bufflehead	*Bucephala albeola*	1	6.045	4122.97	This study
	Common goldeneye	*Bucephala clangula*	1	10.153	5961.39	This study
	Australian wood duck	*Chenonetta jubata*	1	3.568	4329.15	This study

	Red-breasted merganser	*Mergus serrator*	1	4.872	4754.34	This study
	Ruddy duck	*Oyura jamaicensis*	1	15.637	3993.73	This study
Apodiformes	Chimney swift	*Chaetura pelagica*	1	0.068	342.66	Boire, 1989
Caprimulgiformes	Nightjar	*Caprimulgus sp.*	1	0.228	733.59	Boire, 1989
	Spotted nightjar	*Eurostopodus argus*	1	0.197	1012.55	This study
Charadriiformes	Least sandpiper [a]	*Calidris minutilla*	1	1.885	472.01	Boire, 1989
	Killdeer	*Charadrius vociferus*	1	0.629	1073.36	Boire, 1989
	Short-billed dowitcher [a]	*Limnodromus griseus*	2	4.59	1230.79	This study, Boire, 1989
	Common tern	*Sterna hirundo*	1	0.316	1592.66	Boire, 1989
	Southern lapwing	*Vanellus chilensis*	1	0.492	2461.00	Pistone et al., 2002
Ciconiiformes	Grey heron	*Ardea cinerea*	1	1.504	8445.95	Boire, 1989
	Cattle egret	*Bubulcus ibis*	1	0.348	4025.10	This study
	Snowy Egret	*Egretta thula*	1	0.722	3610.00	Carezzano and Bee-de-speroni, 1995
Columbiformes	Rock dove	*Columba livia*	2	0.523	2219.55	This study, Boire, 1989
	Peaceful dove	*Geopelia placida*	1	0.296	776.06	This study
	Superb Fruit-dove	*Ptilinopus superbus*	1	0.242	1052.12	This study
	Ringneck dove	*Streptopelia risoria*	1	0.291	1140.93	Boire, 1989

Coraciiformes	Laughing kookaburra	*Dacelo novaeguineae*	1	0.644	3970.08	This study
Falconiformes	Swainson's hawk	*Buteo swainsoni*	1	0.800	8099.42	This study
	American Kestrel ()	*Falco sparverius*	1	0.163	1017.00	This study
Galliformes	Chukar	*Alectoris chukar*	1	0.563	2500.00	Boire, 1989
	Ruffed grouse	*Bonasa umbellus*	2	0.255	3146.72	This study
	Golden pheasant	*Chrysolophus pictus*	1	0.795	3368.73	Boire, 1989
	Northern bobwhite	*Colinus virginianus*	1	0.374	1090.73	Boire, 1989
	Common quail	*Coturnix coturnix*	1	0.34	810.81	Boire, 1989
	Chicken	*Gallus domesticus*	1	1.120	2993.00	Boire, 1989
	Turkey	*Meleagris gallopavo*	1	2.839	6096.95	Boire, 1989
	Helmeted guineafowl	*Numida meleagris*	1	1.231	3950.77	Boire, 1989
	Chaco chachalaca	*Ortalis canicollis*	1	1.209	3373.55	Boire, 1989
	Indian peafowl	*Pavo meleagris*	1	2.258	7355.21	Boire, 1989
	Ring-necked pheasant	*Phasianus colchicus*	1	0.641	2761.58	Boire, 1989
Gruiformes	American coot	*Fulica americana*	1	1.249	2875.00	This study
	The Red-gartered Coot	*Fulica armillata*	1	0.402	4015.00	Carezzano and Bee-de-speroni, 1995

Passeriformes	Brown thornbill	*Acanthiza pusilla*	1	0.11	434.36	This study
	Eastern spinebill	*Acanthorhynchus tenuirostris*	1	0.092	395.75	This study
	Gouldian finch	*Erythrura gouldiae*	1	0.139	427.61	This study
	Australian magpie	*Gymnorhina tibicen*	1	0.310	4017.37	This study
	Noisy miner	*Manorina melanocephala*	1	0.254	2278.96	This study
	Spotted pardalote	*Pardalotus punctatus*	1	0.058	400.58	This study
	Double-barred finch	*Taeniopygia bichenovii*	1	0.328	409.27	This study
	Zebra finch	*Taeniopygia guttata*	1	0.214	368.73	Boire, 1989
Pelecaniformes	Double-crested cormorant	*Phalacrocorax auritus*	1	1.728	7323.36	Boire, 1989
Podicipediformes	White-tufted Grebe	*Rollandia rolland*	1	0.411	2056.00	Carezzano and Bee-de-speroni, 1995
Psittaciformes	Australian king parrot	*Alisterus scapularis*	1	3.27	4478.76	This study
	Long-billed Corella	*Cacatua tenuirostris*	1	6.001	11777.99	This study
	Galah	*Eolophus roseicapillus*	2	8.404	7083.98	This study
	Purple-crowned Lorikeet	*Glossopsitta porphyrocephala*	1	1.753	1939.19	This study

	Budgerigar	*Melopsittacus undulatus*	2	1.760	1185.77	This study, Boire, 1989
	Cockatiel	*Nymphicus hollandicus*	1	1.97	2111	This study
	Blue-headed parrot	*Pionus menstruus*	1	4.230	5282.82	Boire, 1989
	Crimson rosella	*Platycercus elegans*	1	4.082	3628.38	This study
	Superb parrot	*Polytelis swainsonii*	1	2.248	2996.14	This study
	Rainbow lorikeet	*Trichoglossus haematodus*	2	3.805	3333.98	This study
Rheiformes	Greater rhea	*Rhea americana*	1	0.242	1052.12	Boire, 1989
Sphenisciformes	Magellanic penguin	*Spheniscus magellanicus*	1	3.412	16756.76	Boire, 1989
Strigiformes	Great horned owl	*Bubo virginianus*	1	2.012	17994.21	This study
	Boobook owl	*Ninox boobook*	1	0.936	6338.80	This study
	Barn owl	*Tyto alba*	1	1.075	7142.86	This study
Tinamiformes	Red-winged tinamou	*Rhynchotus rufescens*	1	1.620	3377.41	Boire, 1989
Trochiliformes	Anna's hummingbird	*Calypte anna*	1	0.040	183.88	This study
	Blue-tailed emerald	*Chlorostilbon melisugus*	1	0.032	118.73	Boire, 1989

[a] Beak-probing shorebirds.

Table 2.2. Least-squares linear regression results of the volume of PrV vs the brain. Results of least-squares linear regression performed on species as independent data points ('No phylogeny') and Generalise least square with five different phylogenetic trees and two models of evolutionary change, Brownian [OU, Lavin et al., 2008; Swanson and Garland 2009].

PrV	evolutionary change models	F	df	Slope	r^2	AIC
No phylogeny		111.06	3,68	0.82	0.919	-21.04
Sibley and Ahlquist, 1990	PGLS	15.78	3,68	0.725	0.695	1.04
	OU	80.76	3,68	0.801	0.883	-19.43
Davis, 2008	PGLS	14.23	3,68	0.746	0.698	-1.52
	OU	70.27	3,68	0.805	0.882	-19.35
Livezey and Zusi, 2007	PGLS	16.17	3,68	0.716	0.690	-0.51
	OU	70.13	3,68	0.796	0.881	-19.3
Hackett et al., 2008	PGLS	16.71	3,68	0.718	0.699	-3.84
	OU	60.86	3,68	0.795	0.868	-19.7
Cracraft et al., 2004	PGLS	16.67	3,68	0.724	0.699	-2.16
	OU	74.57	3,68	0.797	0.884	-19.44

2.6 References

Arends JJ, Woelders-Blok A, Dubbeldam JL (1984): The efferent connections of the nuclei of the descending trigeminal tract in the mallard (*Anas platyrhynchos L.*). Neuroscience 13:797-817.

Barbosa A, Moreno E (1999): Evolution of foraging strategies in shorebirds: An ecomorphological approach. Auk 116:712-725.

Barton RA (1998): Visual specialization and brain evolution in primates. Proc Biol Sci. 265:1933-7.

Barker FK, Cibois A, Schikler P, Feinstein J, Cracraft J (2004): Phylogeny and diversification of the largest avian radiation. Proc Nat Acad Sci USA 101: 11040-11045.

Beckers GJ, Nelson BS, Suthers RA (2004): Vocal-tract filtering by lingual articulation in a parrot. Curr Biol 14:1592-7.

Berkhoudt H (1980): The morphology and distribution of cutaneous mechanoreceptors (Herbst and Grandry corpuscles) in bill and tongue of the mallard (*Anas platyrhynchos L.*). Neth J Zool 50;1–34.

Bildstein KL, (1987): Energetic consequences of sexual size dimorphism in white ibises (*Eudocimus albus*). *Auk* 104:771-775.

Bildstein KL, McDowell SG, Brisbin IL (1989): Consequences of sexual dimorphism in sand fiddler crabs, *Uca pugilator*: differential vulnerability to avian predation. Anim Behav 37:133–139.

Boates JS, Goss-Custard JD (1989): Foraging behaviour of oystercatchers *Haematopus ostralegus* during a diet switch from worms *Nereis diversicolor* to clams *Scrobicularia plana*. Can J Zool 67:2225-2231

Boire D (1989): Comparaison quantitative de l'encephale de ses grades subdivisions et de relais visuals, trijumaux et acoustiques chez 28 especes. PhD Thesis, Universite de Montreal, Montreal.

Bolze G (1968): Anordnung und Bau der Herbstchen Korperchen in Limicolenschnabeln im Zusammenhang mit der Nahrungsfindung. Zool Anz 181:313–355.

Bout RG, Dubbeldam JL (1985): An HRP study of the central connections of the facial nerve in the mallard (*Anas platyrhynchos L*.). Acta Morphol Neerl Scand 23:181-93.

Bout RG, Dubbeldam JL (1991) Functional morphological interpretation of the distribution of muscle spindles in the jaw muscles of the mallard (*Anas platyrhynchos*). J Morphol. 210:215-26.

Carezzano F, Bee-De-Speroni N (1995): Composición volumétrica encefálica e índices cerebrales en tres aves de ambiente acuático (Ardeidae, Podicipedide, Rallidae). Facena 11:75-83.

Catania KC (2000): Cortical-organization in moles: evidence of new areas and a specialized S2. Somatosens Mot Res 17:335-47.

Catania KC (2005) Evolution of sensory specializations in insectivores. Anat Rec 287:1038-50.

Catania KC, Henry EC (2006): Touching on somatosensory specializations in mammals. Curr Opin Neurobiol. 16:467-73.

Cracraft J, Barker FK, Braun MJ, Harshman J, Dyke G, Feinstein J, Stanley S, Cibois A, Schikler P, Beresford P, García-Moreno J, Sorenson MD, Yuri T, Mindell DP (2004): Phylogenetic relationships among modern birds

(Neornithes): toward an avian tree of life. In: Assembling the tree of life (Cracraft J, Donoghue MJ, eds), pp 468-489. New York:Oxford Univ Press.

Cunningham S, Castro I, Alley M (2007): A new prey-detection mechanism for kiwi (*Apteryx* spp.): suggests convergent evolution between paleognathous and neognathous birds. J Anat 211:493-502.

Davis KE (2008) Reweaving the tapestry: a supertree of birds. PhD Thesis, University of Glasgow, UK.

Dawson TJ, Johns AB, Beal AM (1989): Digestion in the Australian wood duck (*Chenonetta jubata*): a small avian herbivore showing selective digestion of the hemicellulose component of fiber. Physiol Zool 62:522-540.

Deacon TW (1990): Fallacies of progression in theories of brain-size evolution. Int J Primatol 11:193–236.

Delacour J (1954): The waterfowl of the world. London: Country Life.

Donne-Goussé C, Laudet V, Hänni C (2002): A molecular phylogeny of anseriformes based on mitochondrial DNA analysis. Mol Phylogenet Evol 23: 339-356.

Dubbeldam JL (1980): Studies on the somatotopy of the trigeminal system in the mallard, *Anas platyrhynchos* L. II. Morphology of the principal sensory nucleus. J Comp Neurol 191:557-71.

Dubbeldam JL (1992): Nerves and sensory centres—a matter of definition? Hypoglossal and other afferents of the avian sensory trigeminal system. Zool JB Anat 122:179-186.

Dubbeldam JL (1998): The sensory trigeminal system in birds: input, organization and effects of peripheral damage. A review. Arch Physiol Biochem 106:338-45.

Dubbeldam JL, Karten HJ (1978): The trigeminal system in the pigeon (*Columba livia*). I. Projections of the gasserian ganglion. J Comp Neurol 180:661-78.

Dubbeldam JL, Brus ER, Menken SB, Zeilstra S (1979): The central projections of the glossopharyngeal and vagus ganglia in the mallard, *Anas platyrhynchos* L. J Comp Neurol 183:149-68

Finger TE (1975): Feeding patterns and brain evolution in ostariophysean fishes. Acta Physiol Scand Suppl 638:59–66.

Garland TJr, Harvey PH, Ives AR (1992): Procedures for the analysis of comparative data using phylogenetically independent contrasts. Syst Biol 41:18–32.

Garland TJr, Ives AR (2000): Using the past to predict the present: Confidence intervals

for regression equations in phylogenetic comparative methods. Am Nat 155:346-364.

Garland TJr, Bennett AF, Rezende EL (2005): Phylogenetic approaches in comparative physiology. J Exp Biol 208:3015-3035.

Gerritsen AFC, Meiboom A (1986): The role of touch in prey density estimation by *Calidris alba.* Neth J Zool 36: 530-562.

Goodman DC, Fisher HI **(**1962**):** Functional Anatomy of the Feeding Apparatus in Waterfowl (Aves:Anatidae). Carbondale: Southern Illinois Univ Press.

Gottschaldt KM (1985): Structure and function of avian somatosensory receptors. In: Form and function in birds vol. 3. (King AS, McLelland J, eds), pp 375–461 London: Academic Press.

Gottschaldt KM, Lausmann S (1974): The peripheral morphological basis of tactile sensibility in the beak of geese. Cell Tissue Res 153:477-496.

Hackett SJ, Kimball RT, Reddy S, Bowie RCK, Braun EL, Braun MJ, Chojnowski JL, Cox WA, Han KL, Harshman J, Huddleston CJ, Marks BD, Miglia KJ, Moore WS, Sheldon FH, Steadman DW, Witt CC, Yuri T (2008) A phylogenomic study of birds reveals their evolutionary history. Science 320:1763-1768.

Harper PC, (1987): Feeding behaviour and other notes on 20 species of Procellariiformes at sea. Notornis 34:169-192.

Harvey PH, Pagel MD (1991): The comparative method in evolutionary biology. Oxford: Oxford University Press.

Henry EC, Remple MS, O'Riain MJ, Catania KC (2006): Organization of somatosensory cortical areas in the naked mole-rat (*Heterocephalus glaber*). J Comp Neurol 495: 434-52.

Homberger DG (1980a): Funktionell-morphologische Untersuchungen zur Radiation der Ernährungs- und Trinkmethoden der Papageien. Bonn Zool Monogr 13:1–192

Homberger DG (1980b): Functional morphology and evolution of the feeding apparatus in parrots, with special reference to the Pesquet's parrot, *Psttrichas fuligidus* (Lesson). In: Conservation of New World parrots

(Pasquier RF, ed). pp 471-485. Washington, DC: Smithsonian Institution Press,..

Homberger DG (1983): Nonadaptive evolution of avian drinking methods. Am Zool 23:894.

Homberger DG (1986): The lingual apparatus of the African grey parrot, *Psittacus erithacus* Linné (Aves: Psittacidae): description and theoretical mechanical analysis. Ornithol monogr 39; 1-233

Hulscher JB (1976): Localization of cockles (*Cardium edule*) by an oystercatcher (*Haematopus ostralegus*) in darkness and daylight. Ardea 64:292-310.

Iggo A, Gottschald KM (1974): Cutaneous mechanoreceptors in simple and in complex sensory structures. In: Symposium: Mechanoreception. (Schwartzkopff J, ed), pp 153–176, Opladen: Westdeutscher Verlag.

Ives AR, Midford PE, Garland TJr (2007) Within-species variation and measurement error in phylogenetic comparative methods. *Syst Biol* 56:252-270.

Iwaniuk AN, Dean KM, Nelson JE (2005): Interspecific allometry of the brain and brain regions in parrots (Psittaciformes): comparisons with other birds and primates. Brain Behav Evol 65:40–59.

Iwaniuk AN, Clayton DH, Wylie DRW (2006): Echolocation, vocal learning, auditory localization and the relative size of the avian auditory midbrain nucleus (Mld). Behav Brain Res 167: 305-317

Iwaniuk AN, Wylie DRW (2006): The evolution of stereopsis and the wulst in caprimulgiform birds: a comparative analysis. J Comp Physiol [A] 192:1313-1326.

Iwaniuk AN, and Wylie DRW (2007): Comparative evidence of a neural specialization for hovering in hummingbirds: hypertrophy of the pretectal nucleus lentiformis mesencephali. J Comp Neurol. 50:11-221.

Iwaniuk AN, Heesy CP, Hall MI, Wylie DR (2008): Relative Wulst volume is correlated with orbit orientation and binocular visual field in birds. J Comp Physiol [A] 194: 267-82

Jerison HJ (1973): Evolution of the brain and intelligence. New York: Academic Press.

Johnson KP, Sorenson MD (1999): Phylogeny and biogeography of dabbling ducks (Genus: *Anas*): a comparison of molecular and morphological evidence. Auk 116: 792-805.

Kimball RT, Braun EL (2008): A multigene phylogeny of Gallifomes supports a single origin of erectile ability in non-feathered facial traits. J Avian Biol 39: 438-445.

Kishida R, Dubbeldam JL, Goris RC (1985): Primary sensory ganglion cells projecting to the principal trigeminal nucleus in the mallard, *Anas platyrhynchos.* J Comp Neurol 240:171-9.

Klages NTW, Cooper J (1992): Bill morphology and the diet of filter-feeding seabird: the Broad-billed Prion *Pachyptila vittata* at South Atlantic Gough Island. J Zool (Lond) 227:385-396.

Kooloos JGM, Kraaijeveld AR, Langenbach GEJ (1989): Comparative mechanics of filter feeding in *Anas platyrhynchos*, *Anas clypeata* and *Aythya fuligula (Aves, Anseriformes*). Zoomorphology 108:269-290.

Krulis, V (1978): Struktur und Verteilung von Tastrezeptoren im Schnabel-Zungenbereich von Singvogeln im besonderen der Fringillidae. Rev Suisse Zool 85:385-447.

Kubke MF, Massoglia DP, Carr CE (2004): Bigger brains or bigger nuclei? Regulating the size of auditory structures in birds. Brain Behav Evol 63:169–80.

Lavin SR, Karasov WH, Ives AR, Middleton KM, Garland TJr (2008): Morphometrics of the avian small intestine, compared with non-flying mammals: a phylogenetic approach. Physiol Biochem Zool 81:526-550.

Livezey BC, Zusi RL (2007): Higher-order phylogeny of modern birds (Theropoda, Aves: Neornithes) based on comparative anatomy. II. Analysis and discussion. Zool J Linn Soc 149:1-95.

Maddison WP, Maddison DR (2009): Mesquite: a modular system for evolutionary analysis. Version 2.6 http://mesquiteproject.org

Marchant S, Higgins P (1990): Handbook of Australian, New Zealand and Antarctic birds, Vol 1., Melbourne: Oxford Univ Press.

Martin GR, Wilson KJ, Wild MJ, Parsons S, Kubke FM, Corfield J (2007): Kiwi forego vision in the guidance of their nocturnal activities. PLoS One. 2:e198

Midford, PE, Garland TJr, Maddison WP (2002): PDAP:PDTREE for Mesquite, version 1.00. http://mesquiteproject.org/mesquite/pdap/.

Morgan WL, Ritz DA (1982): Comparison of the feeding apparatus in the Mutton-bird, *Puffinus tenuirostris* (Temminck) and the Fairy Prion, *Pachyptila turtur* (Kuhl) in the relation to the capture of krill, *Nyctyphanes australis*. J Exp Mar Biol Ecol 59:61-76.

Nebel S, Thompson GI (2005): Foraging behaviour of Western Sandpipers changes with sediment temperature: implications for their hemispheric distribution. Ecol Res 20:503-507.

Olson SL, Feduccia A (1980): *Presbyornis* and the Origin of the Anseriformes (Aves: Charadriomorphae). Smithson Contrib Zool323:1-24.

Pereira SL, Johnson KP, Clayton DH, Baker AJ (2007): Mitochondrial and nuclear DNA sequences support a Cretaceous origin of Columbiformes and a dispersal-driven radiation in the Paleogene. Syst Biol 56: 656-672.

Pehrsson O (1976): Food and feeding grounds of the Goldeneye *Bucephala clangula* (L.) on the Swedish west coast. Ornis Scand 7:91-112.

Pettigrew JD, Frost BJ (1985): Tactile Fovea in the *Scolopacidae?*. Brain Behav Evol 26:185-195.

Piersma T, van Aelst R, Kurk K, Berkhoudt H, Maas LRM (1998): A new pressure sensory mechanism for prey detection in birds: the use of seabed-dynamic principles?. Proc R Soc Lond B 265:1377-1383.

Pistone E, Carezzano F, Bee-de-speroni N (2002): Relative encephalic size and cerebral indices of *Vanellus c. chilensis* (Aves: Charadriidae) Rev Chil Hist Nat 7:595-602.

Pubols BH, Welker WI, Johnson JI (1965): Somatic sensory representation of forelimb in dorsal root fibers of raccoon, coatimundi, and cat. J Neurophysiol. 28:312-41.

Pubols BH, Pubols LM (1972): Neural organization of somatic sensory representation in the spider monkey. Brain Behav Evol 5:342-66.

Sibley CG, Ahlquist JE (1990): Phylogeny and Classification of Birds. New Haven CT: Yale University Press.

Silver R, Witkovsky P (1973): Functional characteristics of single units in the spinal trigeminal nucleus of the pigeon. Brain Behav Evol 8:287-303.

Sjöberg K, (1988): Food selection, food-seeking patterns and hunting success of captive Goosanders *Mergus merganser* and Red-breasted Mergansers *M. serrator* in relation to the behaviour of their prey. Ibis 130:79-93

Stingelin W (1961): Grossenunterschiede des sensiblen Trigeminuskerns bei verschiedenen Vogeln. Rev Suisse Zool 68:247-251.

Stingelin W (1965): Qualitative und quantitative Untersuchungen an Kerngebieten der Medulla oblongata bei VSgeln. Bibl Anat 6:1-116.

Swanson DL, Garland TJr (2009): The evolution of high summit metabolism and cold tolerance in birds and its impact on present-day distributions. Evolution 63:184-194.

Thomas GH, Wills MA, Székely TA (2004): Supertree approach to shorebird phylogeny. BMC Evol Biol 4:28

Tome MW, Wrubleski DA (1988): Underwater foraging behavior of canvasbacks, lesser scaups, and ruddy ducks. Condor 90:168-172.

Wild JM (1981): Identification and localization of the motor nuclei and sensory projections of the glossopharyngeal, vagus, and hypoglossal nerves of the cockatoo (*Cacatua roseicapilla*), Cacatuidae. J Comp Neurol 203:351-77.

Wild JM (1990): Peripheral and central terminations of hypoglossal afferents innervating lingual tactile mechanoreceptor complexes in Fringillidae J Comp Neurol 298:157-71.

Wink M, Heidrich P, Sauer-Gurth H, Elsayed A-A, Gonzalez J (2008): Molecular phylogeny and systematics of owls (Strigiformes). In: Owls of the World (Konig C, Weick F, eds) pp 42-63. London: Christopher Helm.

Wright TF, Schirtzinger EE, Matsumoto T, Eberhard JR, Graves GR, Sanchez JJ, Capelli S, Muller H, Scharpegge J, Chambers GK, Fleischer RC (2008): A multilocus molecular phylogeny of the parrots (Psittaciformes): support for a Gondwanan origin during the Cretaceous. Mol Biol Evol 25: 2141-2156.

Zeigler HP, Witkovsky P (1968): The main sensory trigeminal nucleus in the pigeon: a single-unit analysis. J Comp Neurol 134:255-64.

Zweers GA, Gerritsen AFC, Van Kranenburg-Vood PJ (1977): Mechanics of feeding of the Mallard (*Anas platyrhynchos L.*; Aves, Anseriformes). Contrib Vertebr Evol3:1-109

Zweers GA, Berkhoudt H, Vanden Berge JC (1994): Behavioral mechanisms of avian feeding. In: Biomechanics of Feeding in Vertebrates, Advances in Comparative Environmental Physiology (Bels VL, Chardon M, Vandewalle P, eds) 18:241-279.

Zweers G, de Jong F, Berkhoudt H, Vanden Berge JC (1995): Filter Feeding in Flamingos (*Phoenicopterus ruber*). Condor 97: 297-324

Zweers GA, Gerritsen AFC (1997): Transition from pecking to probing mechanisms in waders. Neth J Zool 47:161-208.

Zweers GA, Vanden Berge JC (1996): Evolutionary transitions in the trophic system of the wader-waterfowl complex Neth J Zool 47:255-287.

Chapter 3**: Relative Size of Auditory Pathways in Symmetrically and Asymmetrically Eared Owls**

A version of this chapter has been published:

Gutiérrez-Ibáñez C, Iwaniuk AN, Wylie DR (2011): Relative size of auditory pathways in symmetrically and asymmetrically-eared owls.Brain Behav Evol 78:286–301.

It is well known that owls have extremely sophisticated auditory systems that enable them to hunt, such that some species can accurately localize sounds in complete darkness [Payne and Drury, 1958; Payne, 1971]. In fact, their ability to precisely localize sounds, combined with the developmental plasticity of the underlying neural mechanisms, has made owls, especially the barn owl *(Tyto alba)* , a model for studying the neural mechanisms of sound localization and, more generally, the plasticity of sensory systems [reviewed in Knudsen, 1999; Takahashi, 2010]. To facilitate their auditory abilities, owls possess a suite of anatomical specializations. Externally, the feathers in the preaural skin folds are sparse and modified to be 'acoustically transparent', while in the postaural flaps, the feathers are densely packed and form a concave surface that helps to direct sound to the ears and increase the intensity of sound [Norberg, 1977, 2002]. The peripheral auditory system is characterized by a unique columella footplate morphology, a long cochlea, a long interaural canal and a relatively large tympanic membrane [Schwartzkopf, 1955, 1968; Schwartzkopf and Winter, 1960; Payne, 1971]. Perhaps the most unique anatomical feature of the owl auditory system is the presence, in some species, of vertically asymmetrical ears. These ear asymmetries have evolved independently several times and are based on a variety of anatomical adaptations [Kelso, 1940; Norberg, 1977, 1978]. In some species the asymmetry is due to differences in the soft tissue. For example, in the eagle owl *(Bubo bubo*), the genus *Cicabba* and some *Strix* species, the differences between the two ears are mostly in the size of the ear openings in the skin. In the genus *Asio*, the ear asymmetry is caused entirely by differences in the orientation of an intra-aural septum in the skin of the two ears,

which results in different shapes and vertical positions of the ear openings [Norberg, 2002]. In contrast, in the genus *Aegolius*, ear asymmetry does not arise from the soft tissues. Instead, the ear openings in the skulls of these species are dramatically different in both shape and vertical position [Norberg, 1977, 1978].

Most of what we know of the neural mechanisms underlying auditory localization comes from the extensive research on the barn owl *(T. alba*). Several studies have shown that the external ear morphology provides directional cues in azimuth and elevation [Payne, 1971; Coles and Guppy, 1988; Moiseff, 1989; Keller et al., 1998]. Behavioural studies have shown that barn owls can localize sounds with great precision both in azimuth and elevation [Knudsen et al., 1979; Bala et al., 2003; Whitchurch and Takahashi, 2006] and electrophysiological studies revealed that there is a map of auditory space in the external nucleus of the inferior colliculus (ICx) where neurons have spatial receptive fields that are restricted in both azimuth and elevation [Knudsen et al., 1977; Knudsen and Konishi, 1978a, b]. Other asymmetrically eared owls including the northern saw-whet owl *(Aegolius acadicus)* and the long-eared owl *(Asio otus)* have ICx neurons with receptive fields restricted in elevation [Wise et al., 1988; Volman and Konishi, 1990]. However, in symmetrically eared owls, such as the great horned owl *(Bubo virginianus)* and the burrowing owl *(Athene cunicularia)* , the receptive fields of ICx neurons are much less restricted in elevation [Volman and Konishi, 1990]. Thus, vertical asymmetry of the ear openings facilitates localization in elevation.

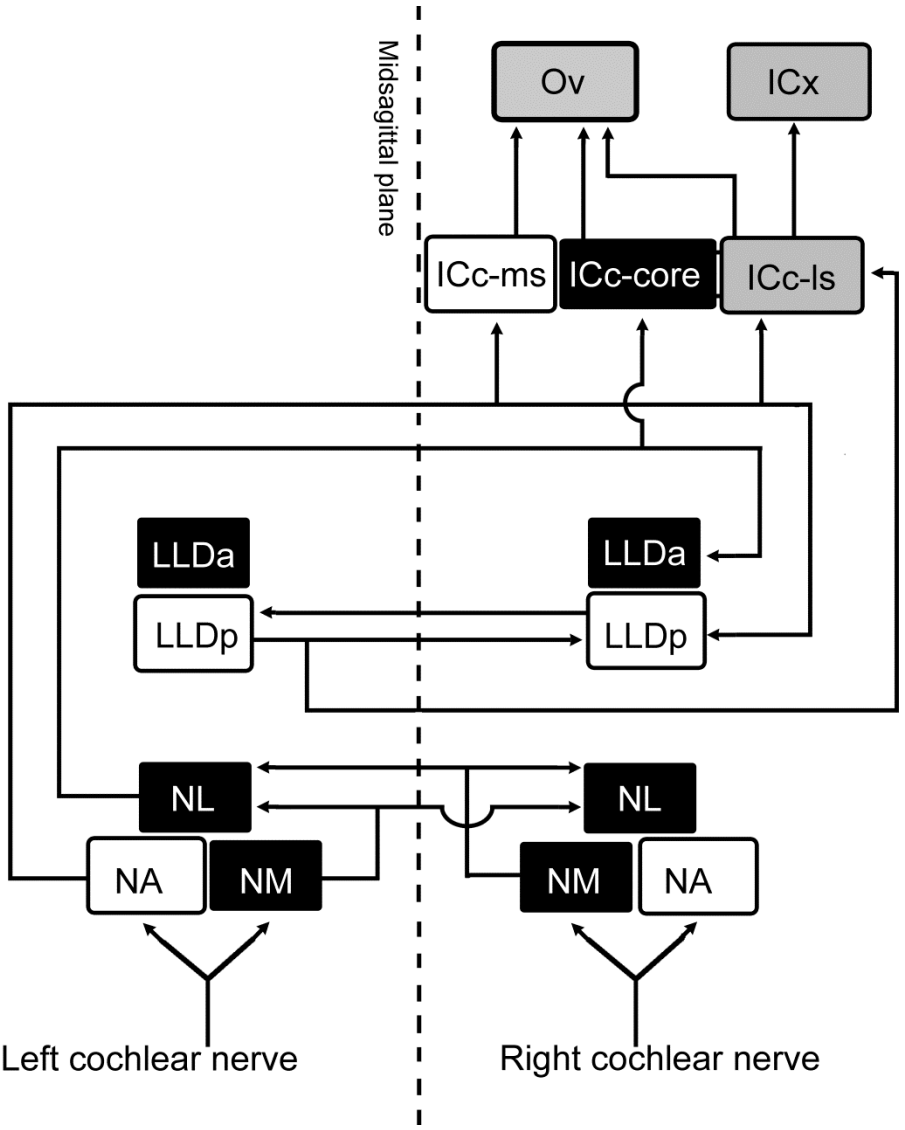

Figure 3.1. Neural pathways in owls for the processing of ITD and ILD. Parallel neural pathways in owls for the processing of ITD (black) and ILD (white). ITD is first computed at the NL and ILD at the LLDp. A second level of coincidence detection exists in the LLDa. Information in the ITD and ILD pathways is combined at the level of the ICc-ls (grey). ICc-ls projects to the external nucleus of the ICx. ICc-ls, ICc-core and the medial shell of the central nucleus of the IC project to the ipsilateral OV.

In barn owls, azimuth and elevation are computed using interaural time differences (ITDs) and interaural level differences (ILDs), respectively [Knudsen and Konishi, 1979, 1980; Moiseff and Konishi, 1981; Moiseff, 1989]. Moreover, ITDs and ILDs are processed independently along two separate pathways from the cochlear nuclei to the ICx [Moiseff and Konishi, 1983; Takahashi et al., 1984; Takahashi and Konishi, 1988a, b; Adolphs, 1993; Mazer, 1998]. The time and intensity pathways are shown in figure 3.1. The cochlear nerve projects directly to 2 nuclei in the brainstem: nucleus angularis (NA) and nucleus magnocellularis (NM) [Carr and Boudreau, 1991]. Cells in NA are mainly sensitive to stimulus intensity and this nucleus is the starting point of the ILD pathway [Sullivan and Konishi, 1984; Sullivan, 1985]. NA projects to the contralateral dorsal lateral lemniscus (LLDp) and the medial shell of the central IC and the lateral shell of the central inferior colliculus (ICc-ls) [Takahashi and Konishi, 1988a, b; Takahashi and Keller, 1992; Adolphs, 1993]. LLDp receives an inhibitory projection from the contralateral LLDp and is the first place where ILDs are computed [Manley et al., 1988]. NM cells show phase locking properties [Sullivan and Konishi, 1984; Sullivan, 1985] and represent the start of the ITD pathway. NM projects bilaterally to the nucleus laminaris (NL) [Carr and Konishi, 1988, 1990] where interaural differences in the phase of each spectral component are computed by a binaural cross-correlation-like mechanism [Jeffress, 1948; Carr and Konishi, 1990; Yin and Chan, 1990]. NL cells project to the contralateral anterior dorsal lateral lemniscus (LLDa) and the core of the central nucleus of the inferior colliculus (ICc-core) [Takahashi and Konishi, 1988b]. Information from both the ILD and ITD pathways are combined in ICc-ls, as it receives input from NA,

LLDp, and the ICc-core [Knudsen, 1983; Takahashi and Konishi, 1988a, b; Takahashi et al., 1989]. ICc-ls projects to ICx, the site of an auditory space map [Knudsen and Konishi, 1978a; Knudsen, 1983]. All divisions of ICc project to the nucleus ovoidalis (OV) [Proctor and Konishi, 1997; Cohen et al., 1998; Arthur, 2005], which in turn projects to field L in the telencephalon [Cohen et al., 1998] where auditory space is also processed [Pérez et al., 2009].

Previous work has shown that the relative size of some of these auditory nuclei is not only larger in owls, but also differs between asymmetrically and symmetrically eared owls. For example, the asymmetrically eared barn owl and long-eared owl *(A. otus)* have a larger number of cells in the auditory brainstem nuclei than species with symmetrical ears *(B. bubo* and *Athene noctua)* [Winter, 1963; Kubke et al., 2004]. The inferior colliculus (IC) is also enlarged in owls compared to other birds and is much larger in asymmetrically eared owls than symmetrically eared owls [Cobb, 1964; Wagner and Luksch, 1998; Iwaniuk et al., 2006]. While these previous studies suggest a hypertrophy (*i.e.* enlargement) of the auditory system associated with ear asymmetry, they fail to reveal several aspects of evolution of the auditory system relative to ear asymmetry.

First, as mentioned above, vertical ear asymmetry allows for sound localization in elevation, and the system has evolved such that ILD varies with elevation and not azimuth [Coles and Guppy, 1988]. Even though symmetrically eared owls use ILD in addition to ITD to locate sounds in azimuth [Volman and Konishi, 1989], the increased use of ILD in asymmetrically eared owls to localize sounds in elevation could result in a greater hypertrophy of the ILD pathway. Second, ear asymmetry has evolved independently many times in owls [Norberg,

1977] and arises from various changes in ear morphology (see above). Given that there are differences in the manner in which the external auditory apparatus has evolved; one might expect central differences as well. Finally, there is a great degree of variation in activity patterns within asymmetrically eared owls. In this paper, we present a comparison of the relative volume of eleven auditory nuclei in both the ITD and the ILD pathways of 8 species of symmetrically and asymmetrically eared owls. This includes 5 species from 4 different genera that vary in ear asymmetry (table 3.1). Based on previous studies and the functional organization of the ITD and ILD pathways, we predict that both the ILD and ITD auditory pathways will be enlarged in asymmetrically eared owls compared to symmetrically eared owls, with an emphasis on the enlargement of the ILD pathway. Moreover, highly nocturnal asymmetrically eared species, such as the barn owl and the northern saw-whet owl, will have larger auditory pathways than more diurnal asymmetrically eared owls, such as the short-eared owl *(Asio flammeus)* and the great grey owl *(Strix nebulosa)* .

3.1 Materials and Methods

We measured the relative volume of 11 auditory nuclei in 12 specimens representing 8 species (table 3.1), including 4 species that appear to have a marked ear asymmetry. Within the asymmetrically eared species, each species differs in how the asymmetry is manifested. In the barn owl the ear asymmetry is due to soft tissue, the ear openings are the same shape, but are at different vertical levels (*i.e.*, left is higher than right). Also, the skin flaps in front of the ears are of

a different shape and the left ear is higher than the right [Konishi, 1973; Norberg, 1977]. In the short-eared owl, ear asymmetry is also caused by differences in the soft tissue. A horizontal intra-aural septum is oriented in a different manner in the left versus the right ear, which results in a different shape, and the left ear opening being higher than the right [Norberg, 1977, 2002]. As described above, the ear asymmetry in the northern saw-whet owl is inherent in the skull, as the auditory canals differ in shape and position such that the right ear is much higher than the left ear [Norberg, 1977, 1978]. Together these three species are classified as having a high degree of ear asymmetry.

We examined two *Strix* species that appear to have different degrees of ear asymmetry. The great grey owl *(S. nebulosa)* has an obvious asymmetry that is present in both the soft tissue and the skull. The right ear opening in the skin is larger than the left and the preaural skin flaps are asymmetrical [Voous, 1964; Norberg, 1977]. In the skull, the asymmetry is dramatic: the postorbital process on the right side extends further laterally than on the left side. On the right side, the postorbital process is connected to the squa mo-occipital wing, but not on the left side. Together the asymmetry in soft tissue and skull results in the left external auditory meatus being directed more dorsally than the right (fig. 3.2 A–D) [Collett, 1881; Norberg, 1977]. In the barred owl *(Strix varia*), the ear asymmetry is quite subtle. There is no asymmetry in the skull, but with respect to soft tissue, the right ear opening in the skin is larger than the left and is a few millimeters higher [Voous, 1964; Norberg, 1977]. Because of the more apparent aural asymmetry in the great grey owl, for convenience it has been grouped with the barn owl, northern saw-whet owl, and short-eared owl, which are labelled in bold

letters in figures 3.5 and 3.6. The barred owl is labelled in italics, whiles the 3 species with symmetrical ears, the snowy owl (*Bubo scandiacus*), the great horned owl (B. virginianus) and the northern hawk owl (*Surnia ulula*), are labeled in plain letters.

For all specimens, the head was immersion-fixed in 4% paraformaldehyde in 0.1 M phosphate buffer. The brain was then extracted, weighed to the nearest milligram, cryoprotected in 30% sucrose in phosphate buffer, embedded in gelatin and sectioned in the coronal or sagittal plane on a freezing stage microtome at a thickness of 40 μm. Sections were collected in 0.1 M phosphatebuffered saline, mounted onto gelatinized slides, stained with thionin and coverslipped with Permount. The olfactory bulbs were intact in all of the specimens that we collected and sectioned. All brains were cut following bird brain atlases [e.g. Karten and Hodos, 1967; Puelles et al., 2007], in which the brainstem ends at the same rostrocaudal point as the cerebellum. In this manner, brain measurements were consistent among our specimens. Photomicrographs of every fourth section were taken throughout the rostrocaudal extent of each nucleus using a Retiga EXi *FAST* Cooled mono 12-bit camera (Qimaging, Burnaby, B.C., Canada) and OPENLAB Imaging system (Improvision, Lexington, Mass., USA) attached to a compound light microscope (Leica DMRE, Richmond Hill, Ont., Canada). Measurements of all the nuclei were taken directly from these photos with ImageJ (NIH, Bethesda, Md., USA; http://rsb.info.nih.gov/ij/) and volumes were calculated by multiplying the area in each section by the thickness of the section (40 μm) and the sampling interval. For those species represented by more than

one specimen (table 3.1), the average of the measurements was taken as the species' given value.

3.1.1 Borders of Nuclei in the Auditory System

We measured nuclei in the time and intensity pathways as indicated in figure 3.1 , as well as other auditory nuclei not explicitly associated with sound localization including the superior olive (SO), which receives input from both NA and NL and projects back to NA, NL and NM [Takahashi and Konishi, 1988a; Carr et al., 1989; Carr and Boudreau, 1993; Lachica et al., 1994], and 3 lemniscal subnuclei: the ventral part of the lateral lemniscus (LLv), the caudal part of the intermediate lateral lemniscus (LLIc) and the rostral part of the intermediate lateral lemniscus (LLIr). All three receive input primarily from NA but do not analyze ILDs [Moiseff and Konishi, 1983; Takahashi and Konishi, 1988a; Wild et al., 2001].

Borders for NA, NM and NL were established using the descriptions of Takahashi and Konishi [1988a, b] and Köppl and Carr [1997]. Cells in these 3 nuclei are surrounded by thick bundles of fibers and therefore the borders are easily distinguished by the presence of cells (fig. 3.3 A–D). In the case of the lemniscal complex and SO, we followed the descriptions and nomenclature of Wild et al. [2001]. Even though the nucleus pontine externus (PE) does not receive auditory projections [Wild et al., 2001], it was included in the measurement of the volume of the LLIr because it was impossible to distinguish the border between these 2 nuclei in Nissl-stained material (fig. 3.3G, H). The

LLIc can be identified as a group of cells lateral to the principal sensory nucleus of the trigeminal nerve. The anterior part of LLIc is surrounded by the faciculus uncinatus [Karten and Hodos, 1967] and it lies ventral to a fiber tract, the brachium conjunctivum (fig. 3.3E, F). LLv was easily distinguished as a group of darkly stained cells anterior to SO and dorsal to the lateral pontine nucleus (fig. 3.3H). In all species, LLDa could be followed from its anterior border as an oval group of cells ventral and lateral to the nucleus semilunaris (fig. 3.3G, H). LLDp could be identified as the group of cells dorsal and lateral to LLDa. The borders of the SO were clearly delineated (fig. 3.4 A, B).

In most studies of the avian auditory system, the IC is named the nucleus mesencephalicus lateral pars dorsalis (MLd) after Karten [1967]. Because MLd is homologous to the IC in mammals [Karten, 1967], Knudsen [1983] recommended that the term IC be applied to refer to the MLd in birds. Since then, this terminology has been used in most owl studies [Wagner et al., 2003] and will be adopted here. In the IC, the caudal and rostral poles were defined as the regions ventral to the third ventricle that had larger, darker and more densely packed cells than adjacent regions. The ventral and lateral borders were defined by the presence of a distinct lamina that forms a fibre bundle surrounding the IC [Knudsen, 1983] and the dorsal and lateral borders were defined by the tectal ventricle (fig. 3.4C, D). Although IC has several subdivisions [Knudsen, 1983; Wagner et al., 2003], the border between the central and external nuclei is very faint in Nissl preparations and we were unable to distinguish the subdivisions, and therefore our measurements are restricted to the entire volume of the IC. We attempted to define the different subdivision of IC by using

immunohistochemistry against a calcium-binding protein, calretinin, which is expressed at higher levels in ICx and ICc-core [Wagner et al., 2003]. Unfortunately, because of the various states of fixation and time that the brains have been stored in fixative we could not reliably discern the subdivisions across all species.

OV is a well-defined group of dark-stained cells in the posterior part of the dorsal thalamus, lateral and dorsal to nucleus rotundus (fig. 3.4E, F). Finally, we were unable to reliably measure field L, the telencephalic target of OV, due to the diffuse borders of this nucleus in Nissl stain preparations.

3.12 Cell Counts

We counted cells in the 2 cochlear nuclei (NA and NM) and NL for comparison with previous studies (table 3.3) [Winter, 1963; Kubke et al., 2004]. Cells were counted in the same sections used for volume estimation. The cells were counted using an unbiased stereological method, the optical fractionator [West et al., 1991; Howard and Reed, 2005]. An unbiased counting frame [Gundersen, 1977] with an area of 0.0088 mm^2 was positioned on the coordinates of a rectangular lattice randomly superimposed on the section. The distance between the coordinates was 282 μm along each axis of the lattice. At each sampling point, the thickness of the sections was determined as the distance between that of the first particle coming into focus and the last particle coming out of focus [West et al., 1991]. An unbiased brick-counting rule [Gundersen and Osterby, 1981; Howard et al., 1985] was used. That is, an unbiased counting

frame was projected onto the thickness of the section resulting in a cube with the upper, top and left planes as acceptable surfaces and all others as no acceptable surfaces. Thus, if a cell contacted the lower, bottom or right planes, it was not counted. The upper plane refers to the first section in the plane of focus and the lower plane to the last. Top, bottom, right and left refer the sides on the counting frame. The height of the counting brick was two thirds of the total thickness. Nuclear profiles containing a nucleolus were counted using a 100 X oil immersion objective. At least 100 cells were counted per cochlear nucleus across all specimens. Coefficients of error were calculated with the quadratic approximation formula [Gundersen and Hensen, 1986; West et al., 1991]. As with the volumetric measurements, for those species represented by more than one individual, we used the average of the measurements as the species' given value.

3.1.3 Statistical Analyses

In most comparative studies dealing with relative size of brain structures, allometric effects are accounted by comparing residuals from least-squares linear regressions between the structure and body mass or brain volume [e.g. Iwaniuk et al., 2005, 2006; Iwaniuk and Wylie, 2007]. With a relatively small number of species, such comparisons become problematic because a single data point can have a huge influence on the slope and intercept of an allometric line. Instead, we have taken a qualitative approach by examining the relative size of each nucleus as a percentage of overall brain volume.

Also, in recent years comparative analyses have used phylogenetically corrected statistics [e.g. Garland et al., 1992, 2005] to account for possible phylogenetic effects. The small number of species examined herein has low statistical power that would be even further reduced with such a correction. The sample size of our subgroups (e.g. asymmetrical vs. symmetrical) further constrains our statistical power, therefore making such phylogenetic corrections impractical. Instead, we compared the results of a hierarchical cluster analysis to the most complete phylogenetic tree available for owls [Wink et al., 2008]. Using a similar approach to Iwaniuk and Hurd [2005], we performed a hierarchical cluster analysis of the proportional size of all auditory nuclei measured, with JMP (Version 7, SAS Institute Inc., Cary, N.C., USA). Although the dendrograms produced by hierarchical cluster analyses are based on similarities among species, comparing the dendrogram with a phylogeny of the species of interest can reveal whether interspecific differences have arisen largely through phylogenetic relatedness or independent evolution [e.g. Iwaniuk and Hurd, 2005]. Here, we show the results generated using an average linkage method, but the dendrograms arising from other linkage methods (e.g. Ward's, UPGMA) shared the same topology.

3. 2 Results.

We found marked differences in the relative size of all auditory nuclei among owl species (fig. 3.3–3.6). For illustrative purposes, in figures 3.5 and 3.6, nuclei in the intensity pathway and time pathway are shown in white and black, respectively, and nuclei that integrate information from both pathways are shown

in grey. Finally, auditory nuclei that have not been explicitly associated with sound localization are indicated with cross-hatching. Overall, the barn owl, the northern saw-whet owl and the short-eared owl have hypertrophied auditory nuclei when compared to the other species. Both *Strix* species also have auditory nuclei that are somewhat larger than the 3 symmetrically eared species and generally, the great grey owl had relatively larger nuclei than the barred owl (fig. 3.5, 3.6). In the great grey owl, for some nuclei, the relative volume approached that of the other asymmetrically eared owls.

3.2.1 Cochlear Nuclei and NL

Shown in figure 3.5A–C, the volume occupied by NA, NM and NL relative to total brain volume was largest in the barn owl, the northern saw-whet owl and short-eared owl. These values were 4–5 times larger than those of the 3 symmetrically eared species (see fig. 3.3A–D). The 2 species of *Strix* owls had relative NA, NM and NL volumes that were larger than those of the symmetrically eared species, but by a factor of less than two (see also table 3.2). The hypertrophy of these nuclei in asymmetrically eared owls is readily evident in coronal sections through the brainstem. When compared to symmetrically eared owls (fig. 3.3A–D) the dorsal part of brainstem of the barn owl, the northern saw-whet owl and the short-eared owl is greatly expanded dorsoventrally, and all 3 nuclei extend much further rostrally. Figure 3.5D–I shows a scatterplot of the logarithm of the total cell numbers (fig. 3.5D–F) and cell densities (fig. 3.5G–I) of

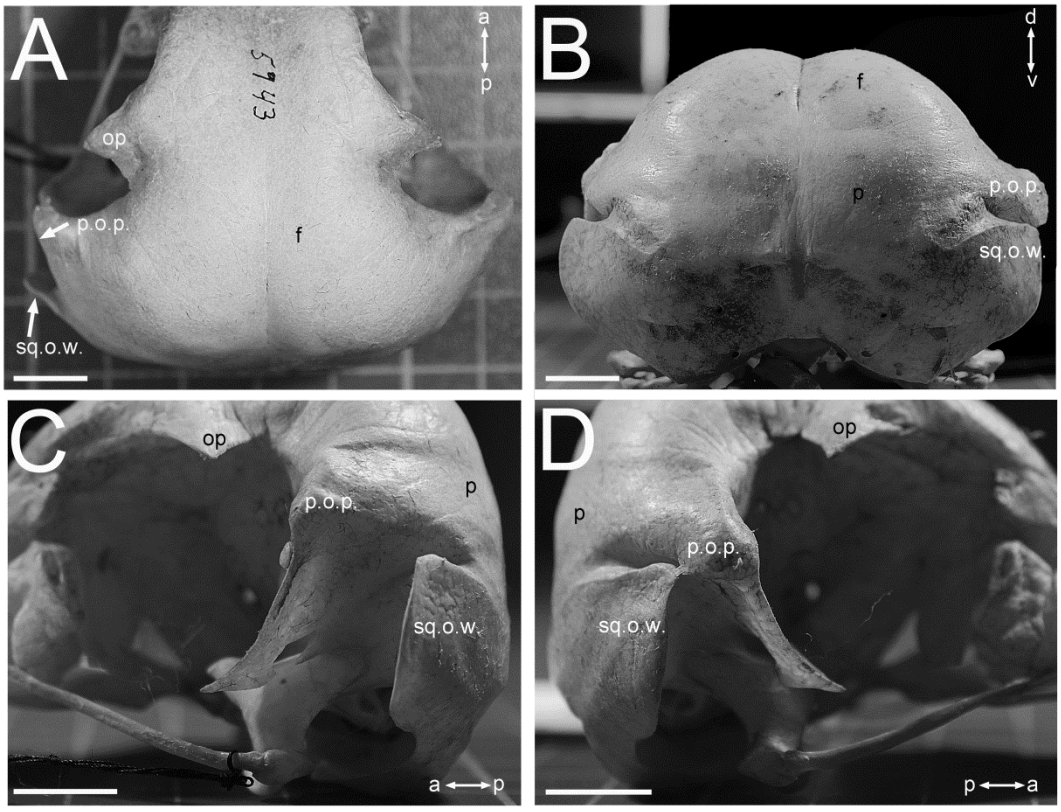

Figure. 3.2. Ear Asymmetry in the skull of the great grey owl. Dorsal (A), posterior (B), left (C) and right (D) views of the skull of the great grey owl (S. nebulosa) . Specimen number: 5943 (Museum of Zoology, University of Alberta). Scale bars = 1 cm. p.o.p. = Postorbital process; sq.o.w. = squamo-occipital wing; op = orbital process; f = frontal; p = parietal.

NA, NM and NL plotted against the logarithm of the brain volume. Overall, the barn owl has the highest total number of cells for the 3 nuclei, although for NL, there was little difference between the barn owl and shorteared owl (table 3.3). The great grey owl (fig. 3.5) has a large number of cells in NA, especially when compared to the barred owl, which has both a similar relative volume of NA (fig. 3.5) and overall brain size (table 3.2). When we examined cell density within the cochlear nuclei and NL, it was clear that the barn owl and the northern saw-whet owl have the highest cell densities in NA and NM, almost twice those of the short-eared owl. The northern saw-whet owl also had the highest cell density for NL (table 3.3).

3.2.2 Lemniscal and Midbrain Nuclei in the ITD and ILD Pathways

In all other nuclei of both auditory pathways, the results were similar to those of the cochlear nuclei in that they were hypertrophied in the barn owl, short-eared owl and northern saw-whet owl. However, some nuclei in the great grey owl were also hypertrophied to a similar degree (fig. 3.6). For both the LLDa and LLDp, the relative sizes were largest in the barn owl, on the order of 5 times larger than those in the symmetrically eared owls. The LLDa was also large in the northern saw-whet owl, short-eared owl and great grey owl, 4 times larger than that in the symmetrically eared species. Similarly, compared to the symmetrically eared owls LLDp was about 3.5 times larger in the northern saw-whet and short-eared owls, and 2.5 times larger in the great grey owl. The LLDa and LLDp in the barred owl were only slightly larger compared to the symmetrically eared species

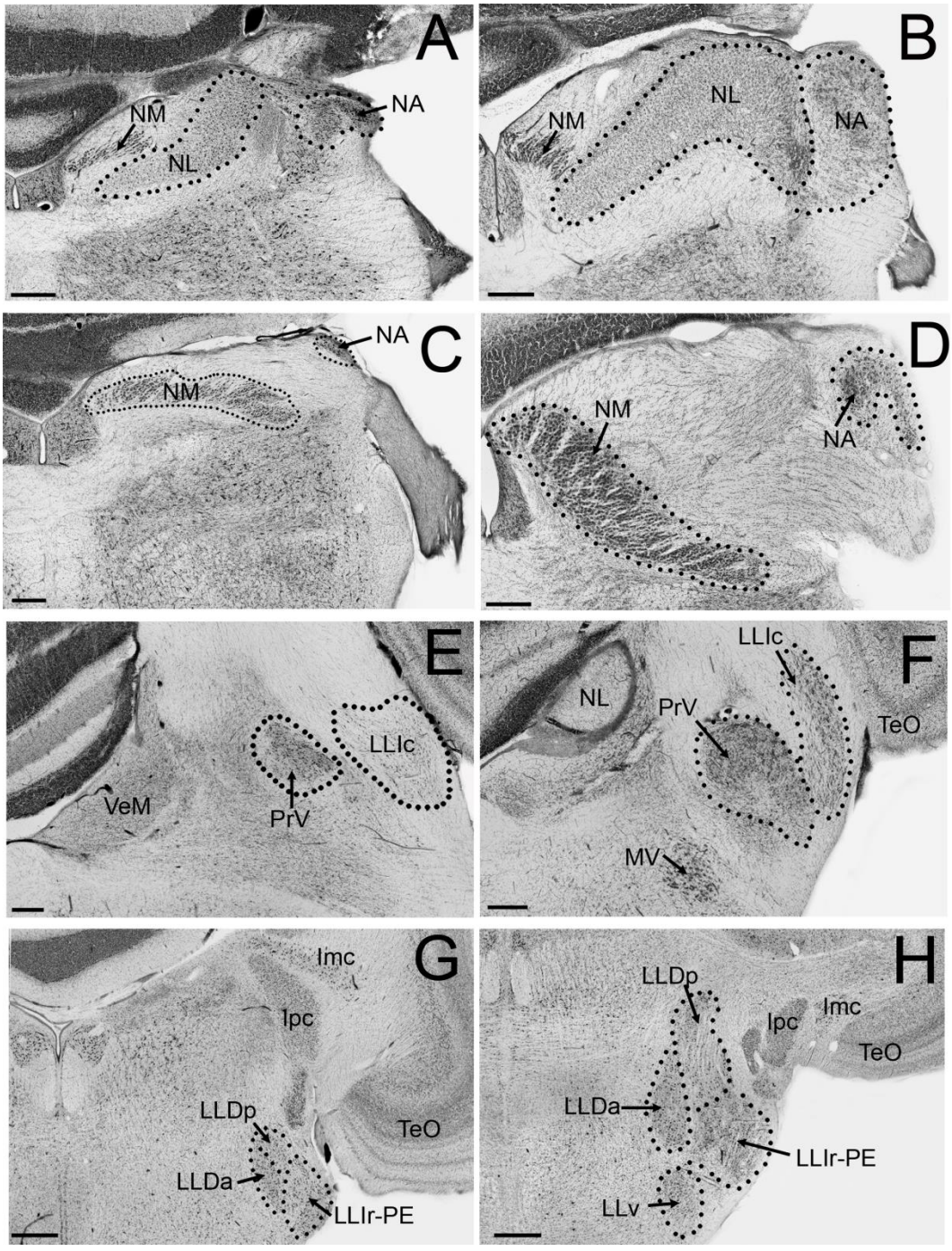
A
NM
NA
NL
B
NL
NM
NA
C
NA
NM
D
NM
NA
E
LLIc
VeM
PrV
F
LLIc
NL
PrV
TeO
MV
G
Imc
Ipc
LLDp
TeO
LLDa
LLIr-PE
H
LLDp
Imc
Ipc
TeO
LLDa
LLIr-PE
LLv

Figure. 3.3. Borders of NA, NM and NL in symmetrically and asymmetrically eared species. Photomicrographs of coronal section through the following: NA, NM and NL of a symmetrically eared owl, the hawk owl (S. ulula) (A) and an asymmetrically eared owl, the northern saw-whet owl *(A. acadicus)* (**B**). NM and NA in the hawk owl (**C**) and an asymmetrically eared owl, the barn owl *(T. alba)* (D). Caudal part of the LLIc in a symmetrically eared owl, the snowy owl *(B. scandiacus)* (E) and the northern saw-whet owl (**F**). Rostral part of the LLIr, the PE, the LLDp and the LLDa in the hawk owl (**G**) and the barn owl (**H**). Letter in brackets next to the scientific name of the species indicate symmetric (S) or asymmetric (A) ears. TeO = Optic tectum; Ipc = parvocellular part of the nucleus isthmi; Imc = magnocellular part of the nucleus isthmi; PrV = motor nucleus of the trigeminal nerve; MV = motor nucleus of the trigeminal nerve; VeM = nucleus vestibularis medialis. Scale bars = 400 μm.

(fig. 3.6D, E). This difference in the relative size of LLDp and LLda are reflected in the organization of both nuclei. In the asymmetrically eared owl and the barred owl, both nuclei appear as two very distinct, independent cell groups all along the anteroposterior axis. Furthermore, in all these species LLDp extends dorsally to lie lateral to the nucleus semilunaris (fig. 3.3H). In contrast, in symmetrically eared owls both nuclei appear as a one group of cells, ventral to the nucleus semilunaris (fig. 3.3G). The IC and OV showed a similar pattern. The relative sizes of both of these nuclei were largest in the northern saw-whet owl, but also larger in the barn owl, short-eared owl, and great grey owl. Compared to the symmetrically eared owls, the IC was 2–3.5 times larger in these 4 species, and the OV was 3–5 times larger (fig. 3.6C, F). For the barred owl, the IC was only slightly larger compared to the symmetrically eared species, but the OV was almost as large as that of the great grey owl and 2.5 times larger than that of the symmetrically eared species. In asymmetrically eared species IC appears much larger along the dorsoventral axis than in symmetrically eared owls (fig. 3.4C, D) and it extends further rostrally.The auditory nuclei not explicitly associated with sound localization also showed some degree of hypertrophy in the asymmetrically eared owls. Compared to the symmetrically eared owls, the relative size of SO was 4–5 times larger in the northern saw-whet owl, barn owl and short-eared owl, and 2 times larger in the great grey owl (fig. 3.6A). The LLv and LLlr-PE were largest in the barn owl and short-eared owl and about the same size in the great grey owl and the northern saw-whet owl (fig. 3.6B, G). Nonetheless, these were still larger than those of the symmetrically eared owls. The LLIc was the only nucleus to be approximately the same relative size in all species (fig. 3.6H). In

addition to examining the proportional sizes of all of the individual auditory nuclei, we calculated the proportional sizes of the entire ITD and ILD pathways (fig. 3.6I). The relative volume of the ITD pathway, calculated as the sum of the volume of NM, NL and LLDa, is correlated with the total volume of the ILD pathway, calculated as the sum of NA and LLDp (fig. 3.6I, $r^2 = 0.958$; $p < 0.001$). Note that the barn owl, northern saw-whet owl and short-eared owl have the largest ILD and ITD pathways, followed by the great grey owl, the barred owl, and the three symmetrically eared owls in that order. The slope of the regression line describing the relationship between the volumes of the ITD and the ILD pathways is not statistically different from 1 (one-tailed t test, $t = 0.986$, $p = 0.181$), which indicates that both pathways are equally enlarged in the asymmetrically eared owls. Lastly, we compared a dendrogram resulting from a hierarchical cluster analysis with a molecular phylogeny of the species we examined. Figure 3.7A depicts the phylogenetic relationships among the 8 species used in this study [Wink et al., 2008] and figure 3.7B illustrates the similarity among the 8 species based on a cluster analysis of the relative size of all auditory nuclei. This dendrogram has two main clusters, but does not separate symmetrically and asymmetrically eared owls completely. The barn owl, northern saw-whet owl and short-eared owl comprise one group and all other species are in a second group. Within this second group, the two *Strix* species come out at a basal position relative to the 3 symmetrically eared species. This dendrogram contrasts greatly with the phylogeny where the 3 species with greatly enlarged auditory pathways are not closely related, but are distributed across the phylogenetic tree.

3.3 Discussion

Overall, our results indicate that asymmetrically eared owls have much larger auditory nuclei than owls with symmetrical ears. In doing so, this study significantly expands upon previous studies [Winter and Schwartzkopf, 1961; Winter, 1963; Kubke et al., 2004; Iwaniuk et al., 2006], which examined only cochlear nuclei or IC, and a smaller number of species. Our study is therefore the first to compare the relative size of all the auditory nuclei from the brainstem to the thalamus among multiple owl species.

Previously, Kubke et al. [2004] compared the relative number of cells in the cochlear nuclei and NL and found that the barn owl had a larger relative number of cells than the long-eared owl in NA and NM, but not NL, and that the tawny owl had a relative number of cells just slightly larger that symmetrically eared owls. While we found similar differences among asymmetrically eared species in the relative volume of the cochlear nuclei (fig. 3.5A–C), our results suggest that the total number of cells in the cochlear nuclei is not entirely related to ear asymmetry. This is well illustrated by the northern sawwhet owl; this species has a similar number of cells in the two cochlear nuclei and NL to both *Bubo* species (table 3.3), but the relative volume of the nuclei is 5 times larger (fig. 3.5A–C). We also found that while there is little variation in cell density in the NA, NM and NL between asymmetrically and symmetrically eared owls, there are some exceptions. The northern saw-whet owl has particularly high cell densities in NA, NM and NL, despite having relative volumes similar to that of the barn owl (fig. 3.5D–F). The northern saw-whet owl has the smallest brain of all species sampled, about half the size of the barn owl and the short-eared owl,

and this difference in density could therefore be related to overall brain size. In mammals,

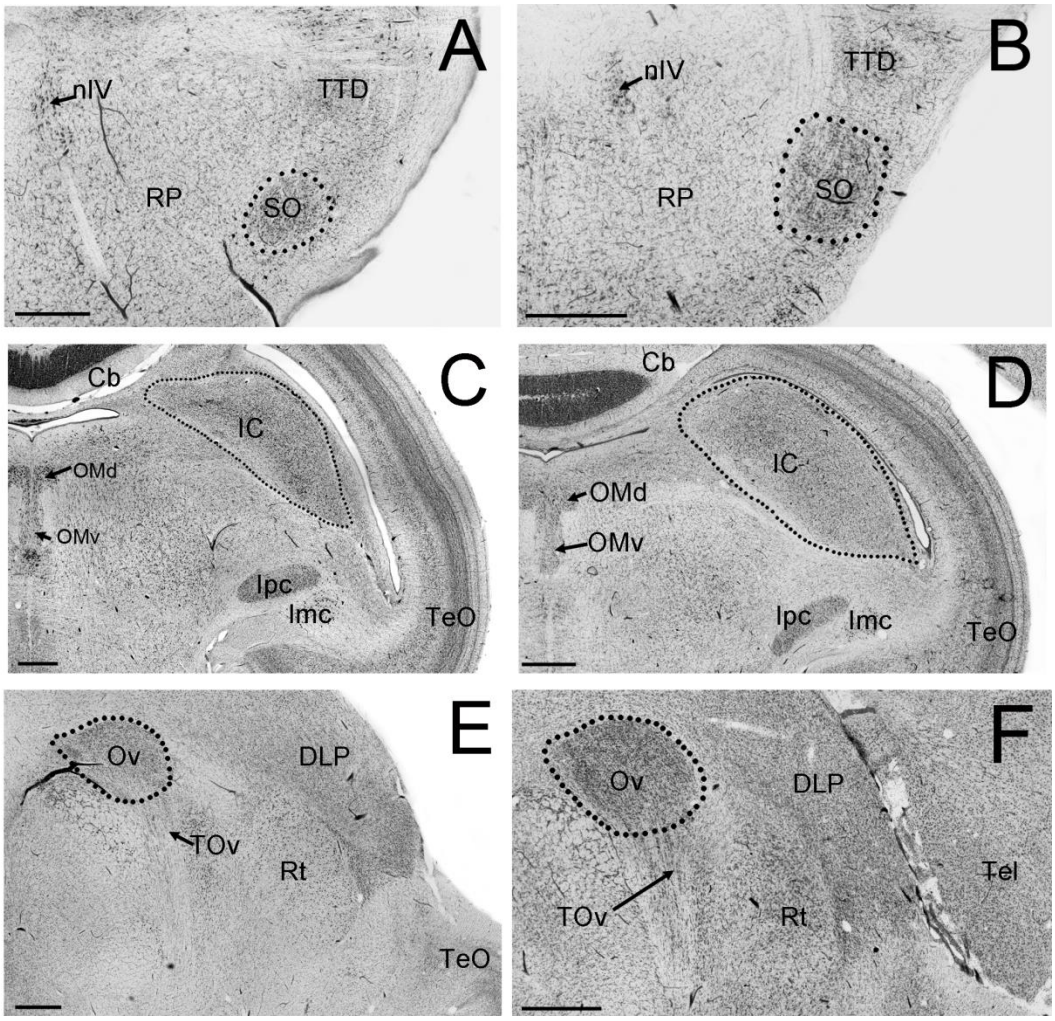

Figure 3.4. Photomicrographs of SO, IC and OV in asymmetrically and symmetrically eared owls. Photomicrographs of coronal sections through: the SO of a symmetrically eared owl, the hawk owl (*S. ulula*) (**A**) and an asymmetrically eared owl, the northern saw-whet owl (A. acadicus) (**B**). IC of the hawk owl (C) and the northern saw-whet owl (**D**). The OV of the symmetrically eared owl, the great horned owl (*B. virginianus*) (**E**) and the northern saw-whet owl (*A. acadicus*) (**F**). Letter in brackets next to the scientific name of the species indicate symmetric (S) or asymmetric (A) ears. TeO = Optic tectum; Ipc = parvocellular part of the nucleus isthmi; Imc = magnocellular part of the nucleus isthmi; Rt = nucleus rotundus; Tel = telencephalon; Cb = cerebellum; OMd = dorsal part of the oculomotor nucleus; OMv = ventral part of the oculomotor nucleus; nIV = abducens nerve nucleus; TOv = tractus ovoidalis; DLP = posterior part of the dorsolateral thalamic nucleus; RP = nucleus reticularis pontis; TTD = nucleus of the descending trigeminal tract. Scale bars = 400 μm.

cell density is inversely proportional to the cubic root of the brain volume [Shariff, 1953; Tower, 1954; Bok, 1959] and the same rule could apply to birds, although this has not been tested to date. Despite previous suggestions that the total number of cells is important for auditory coding [Kubke et al., 2004; Kubke and Carr, 2006], our results suggest that cell numbers may vary according to some scaling function (see above) or other unknown variables. Further research is necessary to determine if other factors, like cell size or the shape of cells and dendritic trees, play more important roles in auditory coding in asymmetrically eared owls.

Our results show that the hypertrophy of auditory pathways is not equal in all asymmetrically eared owls. In the barn owl, the northern saw-whet owl and the short shorteared owl, the difference in the relative size of all auditory nuclei is similar when compared to the symmetrically eared owls (fig. 3.5, 3.6). In contrast, both *Strix* species present little difference compared to symmetrically eared owls in the 2 cochlear nuclei and NL (fig 3.5A–C), but the difference is much more pronounced in nuclei further upstream, especially for the great grey owl (e.g. C, OV; fig. 3.5 , 3.6). These species represent at least four independent examples of the evolution of ear asymmetry [Norberg, 1977, 2002], and in each case this has arisen from different morphological adaptations (see Materials and Methods for details). Furthermore, in some cases, like the barred owl, the asymmetry is much more subtle than other species. While it is possible that the differences in the relative size of the auditory pathways are related to the different

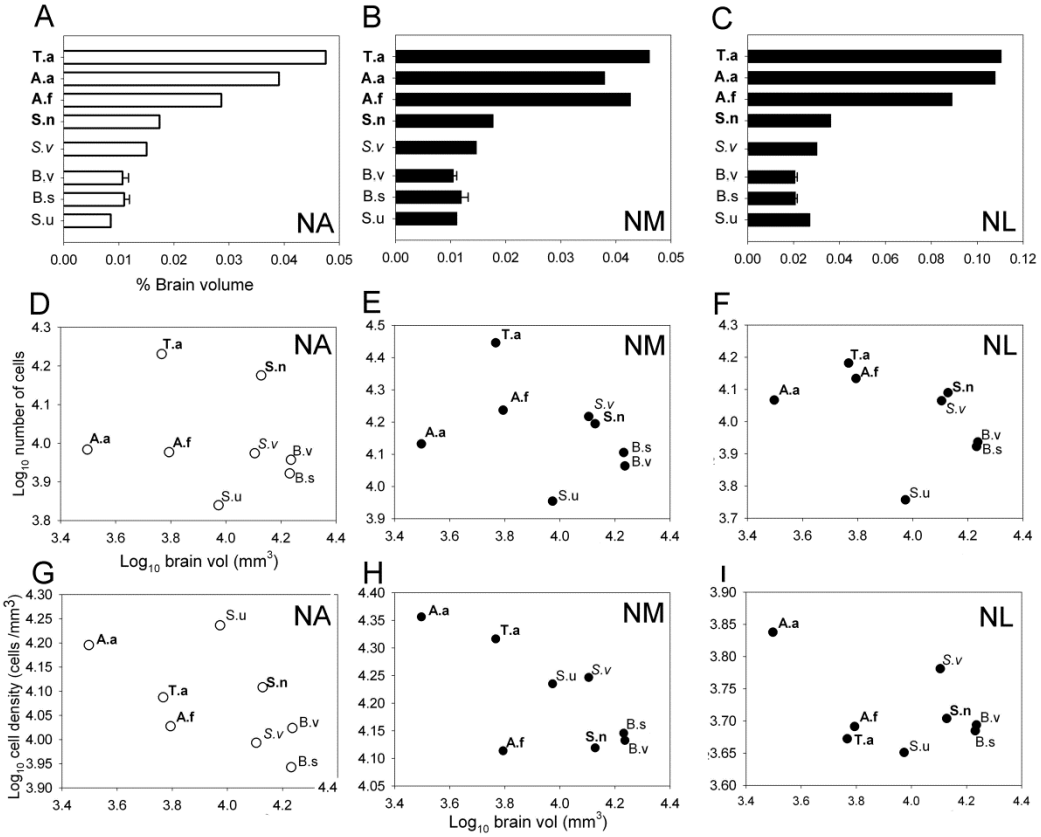

Figure 3.5. Relative size, cells numbers and cell density in the cochlear nuclei. Bar graphs show the relative size of the NA, NM and NL in 8 species of owls expressed as a percentage of total brain volume. Scatterplots show the number of cells and cell density (cells/mm 2) of NA, NM and NL plotted as a function of the logarithms of the brain volume for all species examined. White bars and dots indicate the nucleus belongs to the ILD pathway. Black bars and dots indicate the nucleus belongs to the ITD pathway. Bold letters indicate a high degree of ear asymmetry, italic letters a moderate degree of ear asymmetry, and plain text symmetrical ears. T.a = Barn owl *(T. alba)*; A.a = northern saw-whet owl *(A. acadicus)* ; A.f = short-eared owl *(A. flammeus)* ; S.n = great grey owl *(S. nebulosa)* ; S.v = barred owl *(S. varia)* ; B.v = great horned owl *(B. virginianus)* ; B.s = snowy owl *(B. scandiacus)* ; S.u = hawk owl *(S. ulula).*

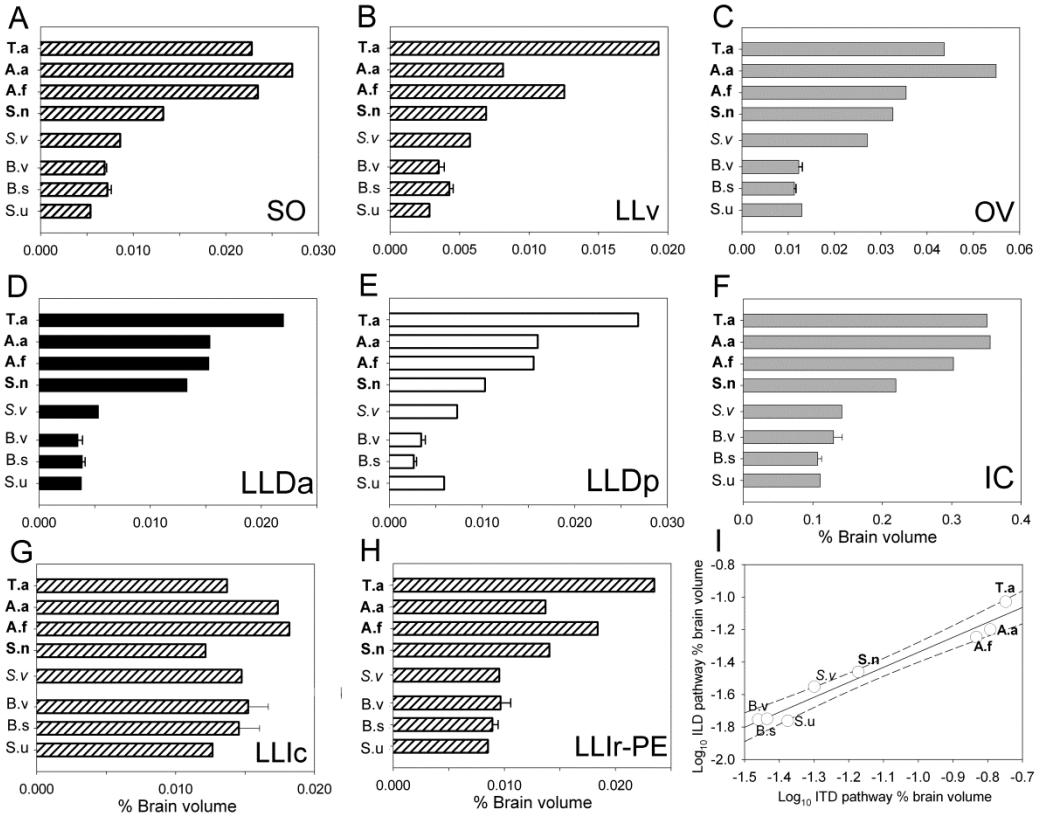
A
T.a
A.a
A.f
S.n
S.v
B.v
B.s
S.u
SO
0.000 0.010 0.020 0.030
B
LLv
0.000 0.005 0.010 0.015 0.020
C
OV
0.00 0.01 0.02 0.03 0.04 0.05 0.06
D
LLDa
0.000 0.010 0.020
E
LLDp
0.000 0.010 0.020 0.030
F
IC
0.0 0.1 0.2 0.3 0.4
% Brain volume
G
LLIc
0.000 0.010 0.020
% Brain volume
H
LLIr-PE
0.000 0.010 0.020
% Brain volume
I
Log10 ILD pathway % brain volume
-0.8 -1.0 -1.2 -1.4 -1.6 -1.8 -2.0
-1.5 -1.4 -1.3 -1.2 -1.1 -1.0 -0.9 -0.8 -0.7
Log10 ITD pathway % brain volume

Figure.3.6. Relative size of other auditory nuclei. Bar graphs show the relative size of the SO (a), the LLv (b), the OV (c), the LLDa (d), the LLDp (e), the IC (f), and the caudal part of the intermediate lateral lemniscus (LLIc) (g). **h** The LLIr- PE expressed as a percentage of total brain volume for all species examined (see table 2). White bars indicate the nucleus belongs to the ILD pathway. Black bars indicate the nucleus belongs to the ITD pathway. Striped bars indicate the nucleus is not directly involved in binaural comparisons. Grey bars indicate the nucleus receives projections from both the ILD and the ITD pathways (see text and fig. 3.1). **i** Scatterplot of the total volume of the ILD pathway plotted as a function of the total volume of the ITD pathway in 8 species of owls. The solid lines indicate the least squares linear regression line for all species and the dotted lines are the 95% confidence interval around the regression line. Bold letters indicate a high degree of ear asymmetry, italic letters a moderate degree of ear asymmetry, and plain text symmetrical ears. T.a = Barn owl *(T. alba)*; A.a = northern saw-whet owl *(A. acadicus)*; A.f = shorteared owl *(A. flammeus)*; S.n = great grey owl *(S. nebulosa)*; S.v = barred owl *(S. varia)*; B.v = great horned owl *(B. virginianus)*; B.s = snowy owl *(B. scandiacus)*; S.u = hawk owl *(S. ulula)* .

ear morphologies, or the degree of ear asymmetry, we currently lack the appropriate data to test this hypothesis. To do so, one would need (1) behavioural studies showing the accuracy of sound localization in azimuth and elevation; (2) acoustical studies showing how (or if) ILD varies with a function of elevation and frequency, and (3) neurophysiological data indicating the spatial precision of cells in ICx. Currently these data are only available for the barn owl [Knudsen et al., 1977, 1979; Knudsen and Konishi, 1978b; Coles and Guppy, 1988]. Indeed, the data for barn owls goes beyond this. Measurement of ILDs in barn owls, where the facial ruff and the preaural flaps are removed (which leaves only a small difference in the vertical level of the ear opening), results in much smaller ILDs than in barn owls with unmodified ears, and the ILDs change much more slowly with elevation, providing half the spatial resolution [Coles and Guppy, 1988]. For the saw-whet owl, it is known that they can precisely localize sound in elevation and the receptive fields in ICx are restricted in elevation [Wise et al., 1988; Frost et al., 1989]. One would predict that acoustical studies would show that ILD varies as a function of elevation in this species with a high degree of spatial resolution. In the long-eared owl *(A. otus)*, a close relative of the shorteared owl with very similar ear morphology [Norberg, 1977], the receptive fields are much less restricted in elevation than those of the barn owl [Volman and Konishi, 1990]. One would predict that ILD would vary as a function of elevation, but not affording the same resolution as that of the barn owl. One would also predict that this species would not be as precise in the elevational component of sound localization, but behavioural data is only available for their localization in azimuth (2°) [Rice, 1982]. None of these data are available for the other

asymmetrically eared owls in our sample, although it is known that the long-eared owl can hunt in complete darkness [Payne, 1971] and the great grey owl often hunts by hovering over a spot and then plunging into deep snow to capture prey [Nero, 1980]. However, without empirical data it is impossible to assess if different ear morphologies, and especially more subtle ear asymmetries, provide different degrees of spatial resolution. Detailed studies on the variation of ILD and ITD in different asymmetrically eared species, as well as behavioral studies of auditory spatial resolution and electrophysiological studies of the properties of space-specific neurons are needed in order to assess the spatial cues available to each species and whether this explains the differences in the relative size of the auditory pathways.

Because of the increased use of ILDs by asymmetrically eared owls, we expected a greater enlargement of the ILD pathway. In contrast, our results show that the ITD and ILD pathways are equally enlarged in asymmetrically and symmetrically eared owls (fig. 3.6I). This equal expansion of both auditory pathways might be related to the expansion of hearing range in asymmetrically eared owls. Published audiograms for 13 owl species (table 3.4) suggest there is an association between ear asymmetry and both a higher range of sensitive hearing (threshold below 0 dB) and a high frequency cutoff (where threshold rises to 6 30 dB above the lowest threshold) [Van Dijk, 1973; Volman and Konishi, 1990; Dyson et al., 1998; Gleich et al., 2005]. In symmetrically eared owls, hearing deteriorates rapidly over 6 kHz and the high-frequency cutoff lies between 7 and 9.5 kHz. By contrast, in symmetrically eared owls, high-sensitivity hearing goes up to 8–9 kHz and their high-frequency cutoff lies between 10 and

13 kHz [Van Dijk, 1973; Konishi, 1973; Dyson et al., 1998]. This expansion in the hearing range is probably related to the fact that only sounds with short wavelengths can be shadowed enough by the small outer ear structures to produce ILDs that vary with elevation [Norberg, 1978; Volman and Konishi, 1990]. This means that in order to use ILDs to detect sounds in elevation, an asymmetrically eared owl must have high sensitivity at frequencies above 5 kHz [Volman and Konishi, 1990]. In the barn owl, this expansion of the hearing range results in a long cochlea where high frequencies are overrepresented, dedicating more cells per octave than any other bird [Manley et al., 1987; Gleich, 1989; Köppl et al., 1993; Smolders et al., 1995]. It is likely that a similar overrepresentation of high frequencies is present in other asymmetrically eared owls [Kubke and Carr, 2006]. In all birds, each auditory nerve bifurcates as it enters the brain and directly innervates both NM and NA [Whitehead and Morest, 1981; Carr and Boudreau, 1991]. These projections are organized tonotopically, so an expansion of the hearing range should result in a bigger NA and NM. Furthermore, ITDs in NL and ILDs in LLDp are computed by frequency [Manley et al., 1988; Carr and Konishi, 1990; Yin and Chan, 1990], and other auditory nuclei, like LLDa, LLv, SO and the core and shell of ICc, are also organized tonotopically [Moiseff and Konishi, 1983; Fischer and Konishi, 2008]. Thus, the expansion of the hearing range would explain not only the equal enlargement of the ITD and ILD pathways, but may also explain the hypertrophy of all auditory nuclei.

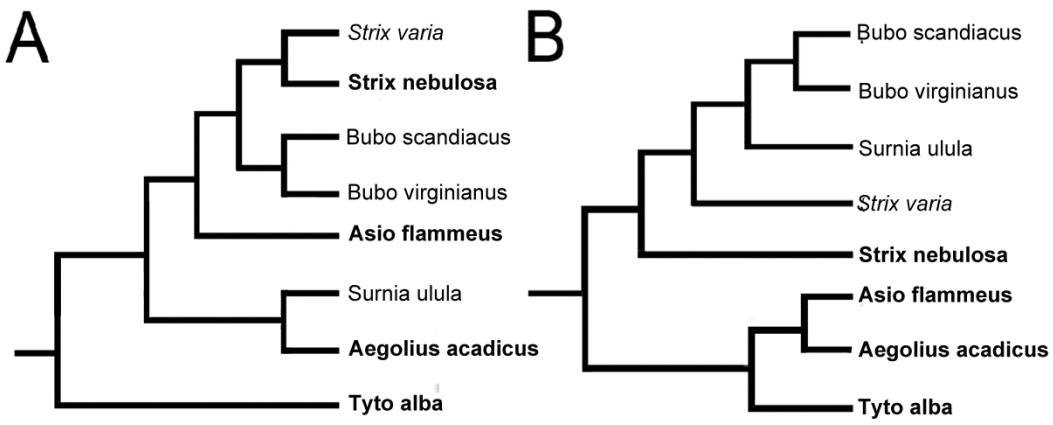

Figure 3.7. Phylogenetic relations and cluster analysis. A Phylogenetic relations among the 8 species used in this study based on Wink et al. [2008]. **B** Phenogram based on a hierarchical cluster analysis of the relative size of all auditory nuclei. Bold letters indicate a high degree of ear asymmetry, italic letters a moderate degree of ear asymmetry, and plain text symmetrical ears.

Unfortunately, the hearing range has not been reported for the great grey owl, but has for other *Strix* species that have only subtle ear asymmetries like the barred owl. These species have a lower high-sensitivity cutoff, very close to that of symmetrically eared owls (table 3.4). In the great grey owl, there was no hypertrophy of the cochlear nuclei or NL, but there was hypertrophy of the auditory nuclei further upstream. If the hearing range of the great grey owl is close to that of other *Strix* species, then the expansion of lemniscal and midbrain nuclei related to the computation of sound in space may have preceded the expansion of the hearing range and the cochlear nuclei.

The only nucleus in the barred owl that showed a substantial hypertrophy was OV. OVreceives projections from ICc and forms part of a sound localization pathway to field L in the telencephalon [Cohen et al., 1998], independent of the ICx-tectal pathway [Knudsen et al., 1993; Wagner, 1993; Cohen and Knudsen, 1999; Pérez et al., 2009]. Cells in OV show spatially selective fields that are as sharp as neurons in ICx [Proctor and Konishi, 1997; Pérez et al., 2009], but their ITD and ILD tunings vary more across frequencies and respond to a much broader frequency range than ICx neurons, especially lower frequencies [Pérez et al., 2009]. The enlargement of OV in both *Strix* species may reflect a greater reliance on the OV-forebrain pathway for sound localization.

We also found differences in the cytoarchitectonic organization of LLDa and LLDp between asymmetrically and symmetrically eared owls. In all the asymmetrically eared owls, LLDa and LLDp are clearly distinguishable in a Nissl's stain preparation, but in symmetrically eared owls they appear as one group of cells throughout the anteroposterior axis (fig 3.3G, H). Takahashi and

Konishi [1988a] had previously reported that in the barn owl these 2 nuclei are clearly distinguishable cytoarchitectonically and hodologically in the posterior region, where high frequencies are represented, but not in the most anterior part where low frequencies are found. As mentioned before, ILDs vary with elevation in asymmetrically eared owls at high frequencies, but vary with azimuth at low ones. This would suggest that in owls a distinct LLDa and LLDp are characteristic of a functional ear asymmetry and the use of ILD to detect sounds in elevation.

Additionally, we found LLDa is differentially hypertrophied in the barn owl. This nucleus appears as particularly large when compared to other asymmetrically eared owls, especially the northern saw-whet owl and the short-eared owl, even though the relative size of NL (the main afferent to LLDa) [Takahashi and Konishi, 1988a] in these species is very similar to the barn owl (fig. 3.5C). In the barn owl, LLDa is involved in noise reduction of coincidence detector responses to ITDs [Fischer and Konishi, 2008]. It is possible that the larger relative size of LLDa in the barn owl reflects higher noise reduction capabilities in the ITD pathway compared to the other two species.

We also found hypertrophy in auditory nuclei not directly involved in binaural comparisons, like SO, LLv and LLIr-PE. SO receives projections from NA and NM [Takahashi and Konishi, 1988a] and sends inhibitory projections to the cochlear nuclei, NL, and the contralateral SO [Conlee and Parks, 1986; Monsivais et al., 2000; Burger et al., 2005]. This inhibitory projection is involved in enhanced phase locking to the waveform in NM and NL, improved coincidence detection in NL, and offsetting of intensity levels in the ITD pathway [Reyes et al., 1996; Funabiki et al., 1998; Yang et al., 1999; Monsivais et al., 2000; Burger

et al., 2005]. This tight correlation with the ITD pathway suggests that the expansion of SO is related to the hypertrophy of NM and NL. Unfortunately, much less information is available for LLv and LLIr. LLv receives bilateral projections from NA [Takahashi and Konishi, 1988a], but cells respond only to monoaural stimuli [Moiseff and Konishi, 1983], and it projects to the contralateral ICc-core [Takahashi and Konishi, 1988b; Adolphs, 1993]. This suggests that LLv is associated with the ILD pathway, and therefore the higher relative volume in asymmetrically eared owls is probably associated with the increase in relative size of NA. This is probably also the case for LLIr, which receives projections from NA too [Wild et al., 2001]. It should be noted that we included PE when measuring this nucleus (see Materials and Methods), even though it is not an auditory nucleus [Wild et al., 2001], and this may have affected the smaller difference in size between asymmetrically eared and symmetrically eared owls in this nucleus. Finally, the only auditory nucleus where we found no marked difference in relative size between asymmetrically and symmetrically eared owls was LLIc. This nucleus receives projections from the ipsilateral NA, but also somatosensory information from the sciatic and radial nerves, and projects to nucleus basalis [Wild et al., 2001]. The lack of hypertrophy of LLIc in asymmetrically eared owls would suggest this nucleus is not related to sound localization.

3.3.1 Evolution of Ear Asymmetry

The cluster analysis of the relative size of all auditory nuclei revealed that the barn owl, northern saw-whet owl and short-eared owl share a similar

expansion of their auditory pathways (fig. 3.7). These species represent three independent events of the evolution of ear asymmetry and therefore three independent expansions of the auditory pathways. At least two studies suggest that this independent enlargement of auditory pathway associated with ear asymmetry could be facilitated by adaptation already present in the auditory pathways of symmetrically eared owls. Kubke and Carr [2006] showed that in both symmetrically and asymmetrically eared owls, NL is organized differently than most other birds and this is related to the ability to detect ITDs above 2 kHz. Second, the neural circuitry that underlies ILD selectivity is already present in symmetrically eared owls, but because ILDs vary with azimuth in these species, it serves as an additional cue to detect sounds in azimuth [Volman and Konishi, 1989]. Because ILD is not essential to sound localization in azimuth in symmetrically eared owls, the ILD pathways can be co-opted to detect differences in elevation in asymmetrically eared owls [Volman and Konishi, 1989]. Therefore, the independent enlargement of auditory pathways in asymmetrically eared owls and the accompanying increase in the ability to detect sounds do not depend on the evolution of novel neural circuitry, but rather the exaptation of preexisting traits in the auditory pathways.

Table 3.1: Owls species surveyed and ear asymmetry in each specie. List of owls species surveyed and a description of the different structures that contribute to the ear asymmetry in each species.

Species	Common name	Ear asymmetry
Tyto alba	Barn Owl	-Only soft anatomy -Left ear opening in the skin higher -Left pre-aural flap different shape than right and higher
Aegolius acadicus	Saw-whet Owl	-Only skull structure. -Ear openings in the skull of different shape. Right opening higher.
Asio flammeus	Short-eared Owl	-Only soft anatomy -Different orientation of skin septum in the ear openings.
Strix nebulosa	Great Grey Owl	-Soft anatomy and skull structures -Right ear opening in the skin bigger -Pre-aural flaps different shape -Slightly different position of an horizontal skin fold above the ear openings in the skull -Ear openings in the skull are of different shape -Left ear canal is directed more upward than the right.
Strix varia	Barred Owl	-Only soft structures -Right skin ear opening bigger.
Bubo virginianus	Great Horned Owl	none
Bubo scandiacus	Snowy Owl	none
Surnia ulula	Hawk Owl.	none

Table 3.2: Volumes of auditory nuclei in owls. List of the owl species surveyed, sample size and volumes (in mm3) of the brain and all nuclei measured; nucleus angularis (**NA**), nucleus magnocellularis (**NM**), nucleus laminaris **(NL**), superior olive (**SO**), ventral part of the lateral lemniscus (**LLv**), caudal part of the intermediate lateral lemniscus (**LLIc**), rostral part of the intermediate lateral lemniscus and pontine externus (**LLIr-PE**), posterior part of the dorsal lateral lemniscus (**LLDp**), anterior part of the dorsal lateral lemniscus (**LLDa**), inferior colliculus (**IC**) and nucleus ovoidalis (**OV**).

Common name	Species	n	Brain volume (mm3)	NA (mm3)	NM (mm3)	NL (mm3)	SO (mm3)	LLv (mm3)	LLIc (mm3)	LLIr-PE (mm3)	LLDp (mm3)	LLDa (mm3)	IC (mm3)	OV (mm3)
Barn Owl	Tyto alba	1	5849.81	2.781	2.695	6.464	1.334	1.131	0.802	1.374	1.571	1.287	19.623	2.557
Saw-whet Owl	Aegolius acadicus	1	3142.86	1.228	1.193	3.389	0.854	0.256	0.546	0.431	0.503	0.484	11.172	1.726
Short-eared Owl	Asio flammeus	1	6221.04	1.779	2.654	5.541	1.460	0.780	1.132	1.144	0.969	0.951	18.815	2.206
Great Grey Owl	Strix nebulosa	1	13433.40	2.334	2.380	4.863	1.780	0.929	1.633	1.889	1.385	1.788	29.508	4.381
Barred Owl	Strix varia	1	12727.12	1.913	1.869	3.844	1.094	0.732	1.878	1.214	0.930	0.679	18.040	3.450
Great horned Owl	Bubo virginianus	3	16323.47	1.740	1.714	3.370	1.127	0.571	2.486	1.577	0.559	0.571	21.200	2.008
Snowy Owl	Bubo scandiacus	3	17065.09	1.869	2.040	3.558	1.231	0.728	2.484	1.523	0.448	0.663	18.272	1.931

Hawk Owl.	Surnia ulula	1	9408.30	0.802	1.048	2.554	0.506	0.266	1.192	0.801	0.556	0.357	10.414	1.216

Table 3.3: Number and density of cells in the three cochlear nuclei. List of the owls species surveyed, sample size, number of cells, and cell density (in cells/mm2) in the three cochlear nuclei, nucleus angularis (**NA**), nucleus magnocellularis (**NM**) and nucleus laminaris (**NL**). On brackets next to the cells numbers appears the coefficient of error (CE) for the estimation of the cell numbers.

Common name	Species	n	NA number of cells (CE)	NM number of cells (CE)	NL number of cells (CE)	NA density (cells /mm2)	NM density (cells /mm2)	NL density (cells /mm2)
Barn owl	Tyto alba	1	17005.01 (0.020)	27915 (0.052)	15199 (0.046)	12227.49	20716.31	4703.10
Saw-wet owl	Aegolius acadicus	1	9627.36 (0.059)	13550.41 (0.064)	11666.55 (0.033)	15685.88	22711.20	6884.06
Short eared owl	Asio flammeus	1	9480.21 (0.047)	17246.55 (0.034)	13612.34 (0.082)	10656.71	12994.69	4913.49
Great grey owl	Strix nebulosa	1	14973.19 (0.049)	15654.30 (0.064)	12294.43 (0.066)	12828.30	13153.99	5056.61
Barred owl	Strix varia	1	9418.23	16484.95	11612.90	9848.41	17642.28	6041.84
Great horned owl	Bubo virginiatus	2	9058.79 (0.093)	11578.98 (0.088)	8646.08 (0.079)	10563.95	13569.97	4941.75
Snowy owl	Bubo scandicus	2	8351.89 (0.065)	12743.58 (0.059)	8369.54 (0.060)	8767.10	13983.04	4839.45
Hawk owl.	Surnia ulula	1	6909.80 (0.098)	8999.81 (0.088)	5717.71 (0.102)	17233.14	17180.46	4478.16

Table 3.4: Ear asymmetry and audiograms parameters. Degree of ear asymmetry and audiograms parameters of 13 species of owls. (1) Dyson et al., [1998]; (2) Konishi, [1973]; (3) van Dijk, [1973]; (4) Trainer, [1946]; (5) Nieboer and Van der Paardt, [1977].

Species	Ear asymmetry	Best frequency (KHz)	Low-frequency sensitivity (dB SPL)	High sensitivity cut off (kHz)	High frequency cut off (kHz)	Source
Tyto alba guttata	yes	6.3	7.0	10.6	13.8	1
Tyto alba pratincola	yes	4	4.8	10.6	12.9	2
Asio otus	yes	6	-6.5	8.5	11.1	3
Strix virgata	yes	0.5	-7.5	6.9	11.3	3
Strix seloputo	yes	2	-7.5	6.6	9.4	3
Strix aluco	yes	6	-1	8	10.3	3
Strix woodfordii	yes	6	-9.5	6.7	10.0	5
Bubo bubo	yes	2	-1.5	6.3	8.6	3
Otus scops	None	4	-0.5	6.3	9.5	3
Otus leucotis	None	2	-9.5	6.3	9.3	3
Bubo scandiacus	None	4	-8.0	6.3	8.5	3
Bubo virginianus	None	1	-1.6	2.3	7.0	4
Bubo nipalensis	None	0.5	-5	3.2	7.7	3
Ketupa zeylonensis	None	1	7.5	1.5	6	3

3.4 References

Adolphs R. (1993): Acetylcholinesterase staining differentiates functionally distinct auditory pathways in the barn owl. J Comp Neurol 329:365-377.

Arthur BJ. (2005): Distribution within the barn owl's inferior colliculus of neurons projecting to the optic ectum and thalamus. J Comp Neurol 492:110-121.

Bala AD, Spitzer MW, Takahashi TT. (2003): Prediction of auditory spatial acuity from neural images on the owl's auditory space map. Nature 424: 771-774.

Bok ST. (1959): Histonomy of the Cerebral Cortex. Amsterdam, Elsevier.

Burger RM, Cramer KS, Pfeiffer JD, Rubel EW. (2005): Avian superior olivary nucleus provides divergent inhibitory input to parallel auditory pathways. J Comp Neurol 481:6-18.

Carr CE, Konishi M. (1988): Axonal delay lines for time measurement in the owl's brainstem. Proc Natl Acad Sci U S A 85:8311-315.

Carr CE, Fujita I, Konishi M. (1989): Distribution of GABAergic neurons and terminals in the auditory system of the barn owl. J Comp Neurol 286:190-207.

Carr CE, Konishi M. (1990): A circuit for detection of interaural time differences in the brain stem of the barn owl. J Neurosci 10:3227-3246.

Carr CE, Boudreau RE. (1991): Central projections of auditory nerve fibers in the barn owl. J Comp Neurol 314:306-18.

Carr CE, Boudreau RE. (1993): Organization of the nucleus magnocellularis and the nucleus laminaris in the barn owl: encoding and measuring interaural time differences. J Comp Neurol. 334:337-55.

Cobb S. (1964): A comparison of the size of an auditory nucleus (*n. mesencephalicus lateralis, pars dorsalis*) with the size of the optic lobe in twenty-seven species of birds. J Comp Neurol 122:271–279.

Cohen YE, Miller GL, Knudsen EI. (1998) Forebrain pathway for auditory space processing in the barn owl. J Neurophysiol 79:891-902.

Cohen YE, Knudsen EI. (1999): Maps versus clusters: different representations of auditory space in the midbrain and forebrain. Trends Neurosci 22:128-135.

Coles RB, Guppy A. (1988): Directional hearing in the barn owl (Tyto alba). J Comp Physiol A 163:117-133.

Collett R. (1881): Craniets og 0reaabningernes bygning hos de nordeuropaeiske arter af familien Strigidae. Forh. vidensk. Selsk. Krist. 3:1-38.

Conlee JW, Parks TN. (1986): Origin of ascending auditory projections to the nucleus mesencephalicus lateralis pars dorsalis in the chicken. Brain Res 367:96-113.

Dyson ML, Klump GM, Gauger B. (1998): Absolute hearing thresholds and critical masking ratios in the European barn owl: a comparison with other owls. J Comp Physiol A 182:695-702.

Funabiki K, Koyano K, Ohmori H. (1998): The role of GABAergic inputs for coincidence detection in the neurones of nucleus laminaris of the chick. J Physiol 508:851-69.

Fischer BJ, Konishi M. (2008): Variability reduction in interaural time difference tuning in the barn owl. J Neurophysiol 100:708-715.

Frost BJ, Baldwin J, Csizy M. (1989): Auditory localization in the Saw-whet Owl Aegolius acadicus, Canadian J Zool 67:1955-1959.

Garland T Jr, Harvey PH, Ives AR. (1992): Procedures for the analysis of comparative data using phylogenetically independent contrasts. Syst Biol 41:18–32.

Garland T Jr, Bennett AF, Rezende EL. (2005): Phylogenetic approaches in comparative physiology. J Exp Biol 208:3015–3035.

Gleich O. (1989): Auditory primary afferents in the starling: correlation of function and morphology. Hear Res 37:255-267.

Gleich O, Dooling RJ, Manley GA. (2005): Audiogram, body mass, and basilar papilla length: correlations in birds and predictions for extinct archosaurs. Naturwissenschaften 92:595–598

Gundersen HJG. (1977): Notes on the estimation of the numerical density of arbitrary profiles: the edge effect. J Microsc 111:219-223.

Gundersen HJ, Osterby R. (1981): Optimizing sampling efficiency of stereological studies in biology: or 'do more less well! J Microsc 121:65-73.

Gundersen HJG, Hensen EB (1986): The efficiency of systematic sampling in stereology and its prediction. J Micros 147:22-63.

Howard CV, Reed MG. *(2005): Unbiased Stereology. Three-Dimensional Measurement in Microscopy. New York, Springer.*

Howard VS, Reid A, Baddeley A, Boyde A. (1985): Unbiased estimation of particle density in the tandem scanning reflected light microscope. J. Microsc 138:20-12.

Iwaniuk AN, Dean KM, Nelson JE. (2005):. Interspecific allometry of the brain and brain regions in parrots (Psittaciformes): comparisons with other birds and primates. Brain Behav Evol 65:40–59.

Iwaniuk AN, Hurd PL. (2005): The evolution of cerebrotypes in birds. Brain behav evol 65:215-230.

Iwaniuk AN, Clayton DH, Wylie DRW. (2006): Echolocation, vocal learning, auditory localization and the relative size of the avian auditory midbrain nucleus (MLd). Behav Brain Res 167:305–317.

Iwaniuk AN, Wylie DRW. (2007): Comparative evidence of a neural specialization for hoverin in hummingbirds: hypertrophy of the pretectal nucleus lentiformis mesencephali. J Comp Neurol 50:211–221.

Jeffress L. (1948): A place theory of sound localization. J Comp Physiol Psychol 41:35-39.

Karten HJ. (1967): The organization of the ascending auditory pathway in the pigeon (*Columba livia*). I. Diencephalic projections of the inferior colliculus (nucleus mesencephali lateralis, pars dorsalis). Brain Res 6:409-427.

Karten H, Hodos W. (1967): A stereotaxic atlas of the brain of the pigeon *(Columba livia)***.** Baltimore, Johns Hopkins University Press.

Keller CH, Hartung, K, Takahashi TT. (1998):. Head-related transfer functions of the barn owl: measurement and neural responses. Hear Res 118*:13-34.*

Kelso L. (1940): Variation of the external ear-opening in the Strigidae. Wilson Bull 52:24-29.

Knudsen EI. (1983): Subdivisions of the inferior colliculus in the barn owl (Tyto alba). J Comp Neurol 218:174-86.

Knudsen EI. (1999): Mechanisms of experience-dependent plasticity in the auditory localization pathway of the barn owl. J Comp Physiol A 185:305-321.

Knudsen EI, Konishi M, Pettigrew JD. (1977): Receptive fields of auditory neurons in the owl. Science 198:1278-1280.

Knudsen EI, Konishi M. (1978a): A neural map of auditory space in the owl. Science 200:795-797.

Knudsen EI, Konishi M. (1978b): Space and frequency are represented separately in auditory midbrain of the owl. J Neurophysiol 41:870-84.

Knudsen E, Konishi, M. (1979): Mechanisms of sound localization in the barn owl (*Tyto alba*). Journal of Comp Physiol 133:13-21.

Knudsen EI, Blasdel GG, Konishi M. (1979): Sound localization by the barn owl (Tyto alba) measured with the search coil technique. J Comp Physiol A 133:1-11

Knudsen EI, Konishi M. (1980): Monaural occlusion shifts receptive-field locations of auditory midbrain units in the owl. J Neurophysiol 44:687-95.

Knudsen EI, Knudsen PF, Masino T. (1993): Parallel pathways mediating both sound localization and gaze control in the forebrain and midbrain of the barn owl. J Neurosci 13:2837-2852.

Konishi M. (1973): How the owl tracks its prey. Am Sci 61:414-424.

Köppl C, Gleich O, Manley GA. (1993): An auditory fovea in the barn owl cochlea. J Comp Physiol A 171:695-704.

Köppl C, Carr CE. (1997): Low-frequency pathway in the barn owl's auditory brainstem. J Comp Neurol 378:265-282.

Kubke MF, Massoglia DP, Carr CE. (2004): Bigger brains or bigger nuclei? Regulating the size of auditory structures in birds. Brain Behav Evol 63:169–180.

Kubke MF, Carr CE. (2006): Morphological variation in the nucleus laminaris of birds. Int J Comp Psychol 19:83–97.

Lachica EA, Rübsamen R, Rubel EW. (1994): GABAergic terminals in nucleus magnocellularis and laminaris originate from the superior olivary nucleus. J Comp Neurol 348:403-18.

Mazer JA. (1998): How the owl resolves auditory coding ambiguity. Proc Natl Acad Sci USA. 95:10932-7.

Manley GA, Brix J, Kaiser A. (1987): Developmental stability of the tonotopic organization of the chick's basilar papilla. Science 237:655-656.

Manley GA, Köppl C, Konishi M. (1988): A neural map of interaural intensity differences in the brain stem of the barn owl. J Neurosci 8:2665-76.

Moiseff A. (1989): Bi-coordinate sound localization by the barn owl. J Comp Physiol A 64:637-644.

Moiseff A, Konishi M. (1981): Neuronal and behavioral sensitivity to binaural time differences in the owl. J Neurosci 1:40-8.

Moiseff A, Konishi M. (1983): Binaural characteristics of units in the owl's brainstem auditory pathway: precursors of restricted spatial receptive fields. J Neurosci 12:2553-2562.

Monsivais P, Yang L, Rubel EW. (2000): GABAergic inhibition in nucleus magnocellularis: implications for phase locking in the avian auditory brainstem. J Neurosci 20:2954-63.

Nero RW. (1980): The great gray owl-phantom of the northern forest. Washington, D.C, Smithsonian Inst. Press.

Nieboer E, Van der Paardt M. (1977): Hearing of the african wood owl, Strix woodfordii. Neth J Zool 27:227-229

Norberg RA. (1977): Occurrence and independent evolution of bilateral ear asymmetry in owls and implications on owl taxonomy. Phil Trans R Soc London B 280:375–408.

Norberg RA. (1978): Skull asymmetry, ear structure and function, and auditory localization in Tengmalm's owl, Aegolius funereus (Linne). Phil Trans R Soc Lond B 282:325-410.

Norberg RA. (2002): Independent evolution of outer ear asymmetry among five owl lineages; Morphology, function and selection; in Newton I, Kavanagh R, Olsen J, Taylor I (ed): Ecology and Conservation of Owls. Collingwood, CSIRO Publishing, pp 329-342

Payne RS. (1971): Acoustic location of prey by barn owls (Tyto alba). J exp Biol 54;535-573.

Payne RS, Drury WH Jr. (1958): Marksman of the darkness: Part 2. Nat Hist NY 67;316-323.

Pérez ML, Shanbhag SJ, Peña JL. (2009): Auditory spatial tuning at the crossroads of the midbrain and forebrain. J Neurophysiol 102:1472-1482.

Proctor L, Konishi M. (1997): Representation of sound localization cues in the auditory thalamus of the barn owl. Proc Natl Acad Sci U S A 94:10421-5.

Puelles L, Martinez-de-la-Torre M, Paxinos G, Watson C, Martinez S. (2007): The Chick Brain in Stereotaxic Coordinates: An Atlas featuring Neuromeric Subdivisions and Mammalian Homologies. San diego, Academic Press.

Reyes AD, Rubel EW, Spain WJ. (1996): In vitro analysis of optimal stimuli for phase-locking and time-delayed modulation of firing in avian nucleus laminaris neurons. J Neurosci. 16:993-1007.

Rice WR. (1982): Acoustical location by the Marsh Hawk: adaptation to concealed prey. Auk 99: 403–413.

Schwartzkopf J. (1955): On the hearing of birds. Auk 72:340–347.

Schwartzkopf J. (1968): Structure and function of the ear and of the auditory brain areas in birds. In: DeReuck AVS, Knight J (ed): Hearing mechanisms in vertebrates. London, J&A Churchill Ltd., pp. 41–63.

Schwartzkopf J, Winter P. (1960): Zur Anatomie der Vogel-Cochlea unter nat¨urlichen Bedgingungen. Biol Zentral-bl 79:607–625.

Shariff GA. (1953): Cell counts in the primate cerebral cortex. J Comp Neurol 98:381–400.

Smolders JW, Ding-Pfennigdorff D, Klinke R. (1995): A functional map of the pigeon basilar papilla: correlation of the properties of single auditory nerve fibres and their peripheral origin. Hear Res 92:151-169.

Sullivan WE. (1985): Classification of response patterns in cochlear nucleus of barn owl: correlation with functional response properties. J Neurophysiol 53:201-216.

Sullivan WE, Konishi M. (1984): Segregation of stimulus phase and intensity coding in the cochlear nucleus of the barn owl. J Neurosci 4:1787-799.

Takahashi TT. (2010): How the owl tracks its prey-II. J Exp Biol 213:3399-3408.

Takahashi TT, Moiseff A, Konishi M. (1984): Time and intensity cues are processed independently in the auditory system of the owl. J Neurosci 4:1781-786.

Takahashi TT, Konishi, M. (1988a): Projections of nucleus angularis and nucleus laminaris to the lateral lemniscal nuclear complex of the barn owl. J Comp neurol 274:212-238.

Takahashi TT, Konishi, M. (1988b): Projections of the cochlear nuclei and nucleus laminaris to the inferior colliculus of the barn owl. J Comp Neurol. 274:190-211.

Takahashi TT, Wagner H, Konishi M. (1989): Role of commissural projections in the representation of bilateral auditory space in the barn owl's inferior colliculus. J Comp Neurol 281:545-54.

Takahashi TT, Keller CH. (1992): Commissural connections mediate inhibition for the computation of interaural level difference in the barn owl. J Comp Physiol A 170:161-169.

Tower DB. (1954): Structural and functional organization of mammalian cerebral cortex: The correlation of neuron density with brain size. J Comp Neurol 101:19–51.

Van Dijk T. (1973): A comparative study of hearing in owls of the family Strigidae. Neth J Zool 23: 131-167

Volman SF, Konishi M. (1989): Spatial selectivity and binaural responses in the inferior colliculus of the great horned owl. J Neurosci 9:3083–3096.

Volman SF, Konishi M. (1990): Comparative physiology of sound localization in four species of owls. Brain Behav Evol. 36:196-215.

Voous KH. (1964): Wood owls of the genera Strix and Ciccaba. Zool Meded 39, 471-478.

Voous KH. (1989): Owls of the Northern Hemisphere. Cambridge, MIT Press.

Wagner H. (1993): Sound-localization deficits induced by lesions in the barn owl's auditory space map. J Neurosci. 13:371-86.

Wagner H, Luksch H. (1998): Effect of ecological pressures on brains: examples from avian neuroethology and general meanings. Z Naturforsch C 53:560–81.

Wagner H, Gunturkun O, Nieder B. (2003): Anatomical markers for the subdivisions of the barn owl’s inferior–collicular complex and adjacent periand subventricular structures. J Comp Neurol 465:145–59.

West MJ. (1991): Unbiased stereological estimation of the total number of neurons in the subdivisions of the rat hippocampus using the optical fractionator. Anat. Rec 231:482–497.

Whitchurch EA, Takahashi TT. (2006): Combined auditory and visual stimuli facilitate head saccades in the barn owl (Tyto alba). J Neurophysiol, 96: *730-745.*

Whitehead MC, Morest DK. (1981): Dual populations of efferent and afferent cochlear axons in the chicken. Neuroscience 6:2351-65.

Wild JM, Kubke MF, Carr CE. (2001): Tonotopic and somatotopic representation in the nucleus basalis of the barn owl, Tyto alba. Brain Behav Evol 57:39-62.

Wink M, Heidrich P, Sauer-Gurth H, Elsayed AA, Gonzalez J (2008): Molecular phylogeny and systematics of owls (Strigiformes). In Konig C, Weick F, (ed): Owls of the world. London: Christopher Helm. pp 42–63.

Winter P. (1963): Vergleichende Qualitative und quantitative untersuchungen an der horbahn von vogeln. Z Morph Okol Tiere 52:365–400.

Winter P, Schwartzkopf J. (1961): Form und Zellzahl der akustischen Nervenzentren in der Medulla oblongata von Eulen (Striges). Experientia 17:515-516.

Wise LZ, Frost BJ, Shaver SW (1988): The representation of sound frequency and space in the mid brain of the Saw-Whet Owl. Society for Neuroscience Abstracts 14:1095.

Yang L, Monsivais P, Rubel EW (1999): The superior olivary nucleus and its influence on nucleus laminaris: a source of inhibitory feedback for coincidence detection in the avian auditory brainstem. J Neurosci 19:2313-25.

Yin TC, Chan, JC (1990): Interaural time sensitivity in medial superior olive of cat. J Neurophysiol. 64:465-488.

Chapter 4: **Comparative study of visual pathways in owls (Aves:Strigiformes)**

A version of this chapter has been published:

Gutiérrez-Ibáñez C, Iwaniuk AN, Lisney TJ, Wylie DR. (2013): Comparative study of visual pathways in owls (Aves:Strigiformes). Brain behav evol 81:27-39.

In birds, several studies have shown that differences in activity pattern are correlated with differences in the visual system. For example, compared to diurnal birds, nocturnal species tend to exhibit a number of adaptations that serve to enhance visual sensitivity, such as: a larger cornea relative to total eye size, high rod:cone photoreceptor ratios, relatively fewer retinal ganglion cells (RGCs) and a relatively smaller optic foramen [Tansley and Erichsen, 1985; Rojas de Azuaje et al., 1993; Hall and Ross, 2007; Hall et al., 2009; Iwaniuk et al., 2010a; Corfield et al., 2011]. Although within most avian orders activity pattern is fairly uniform (e.g. all members are diurnal), in a few orders species vary widely in activity pattern along the nocturnal-diurnal gradient. One order of specific interest in this respect is that of the owl: Strigiformes. Although owls are generally regarded as nocturnal birds, only about 30% of owl species are strictly nocturnal; the rest of the species exhibit a wide range of activity patterns, from crepuscular or cathemeral, to diurnal [Martin, 1986; Voous, 1988; del Hoyo et al., 1999; König and Weick, 2008]. Past studies have shown that these differences in activity pattern are associated with the organization of the visual system of these birds. Owl species with different activity patterns differ in their photoreceptor density, shape and depth of the fovea [Oehme, 1961], rod:cone ratios, critical flicker fusion frequency [see Lisney et al., 2011] and number and distribution of RGCs [Oehme, 1961; Bravo and Pettigrew, 1981]. Recently, a detailed study [Lisney et al., 2012] of the eyes and retinas of eight species of owl with different activity patterns showed that nocturnal owls have relatively larger corneal diameters than diurnal species. Further, it was shown by these authors that the topographic

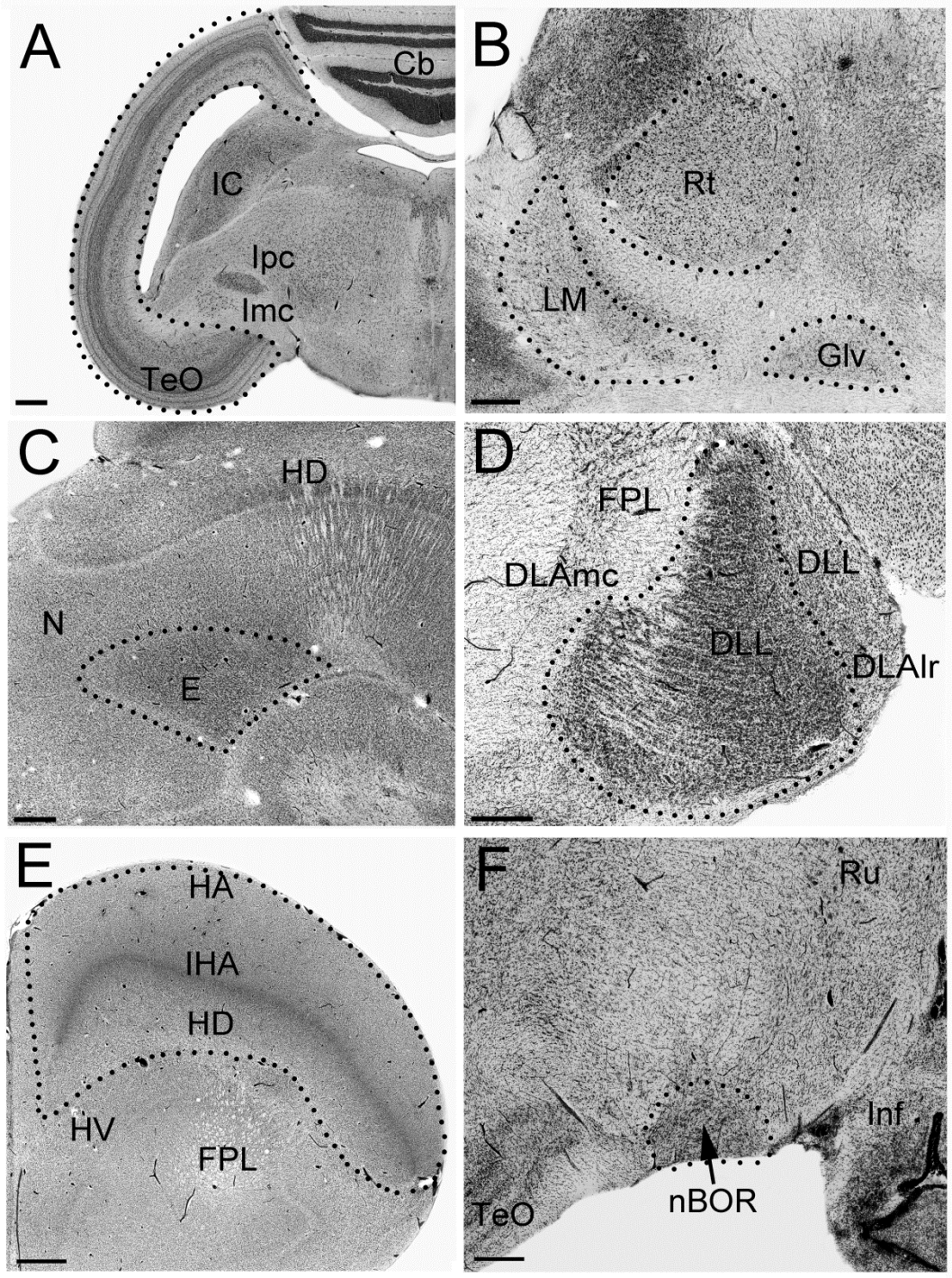
A
Cb
IC
Ipc
Imc
TeO
B
Rt
LM
Glv
C
HD
N
E
D
FPL
DLAmc
DLL
DLL
DLAlr
E
HA
IHA
HD
HV
FPL
F
Ru
Inf
nBOR
TeO

Figure. 4.1. Photomicrographs of coronal sections through the different components of the tectofugal pathway in owls. **a** The TeO of the northern hawk owl *(S. ulula)* . Scale bar = 800 μm. **b** The nRt of the great horned owl *(B. virginianus)*. Scale bar =600 μm. **c** The E in the short-eared owl *(A.flammeus)*. Scale bar = 800 μm. **d** The dotted lines show the portion of the nucleus DLL measured (see Methods for details) in the northern hawk owl *(S. ulula)*. Scale bar = 400 μm. **e** The three components of the wulst, the hyperpallium apicale (HA), the nucleus interstitialis hyperpallii apicalis (IHA) and the hyperpallium densocellulare (HD) also in the northern hawk owl. **f** The borders of the nBOR in the snowy owl *(B. scandiacus)* . Scale bar = 600 μm. DLAmc = Nucleus dorsolateralis anterior, pars magnocellularis; DLAlr = nucleus dorsolateralis anterior, pars lateralis rostralis; FPL = fasciculus prosencephali lateralis; HV = hyperstriatum ventral; Ipc = parvocellular part of the nucleus isthmi; Imc = magnocellular part of the nucleus isthmi; IC = inferior colliculus; LM = nucleus lentiformis mesencephali; N = nidopallium; Ru = nucleus ruber; Inf = infundibulum.

distribution of neurons in the RGC layer among owl species is related to both activity pattern and habitat preference. Species that live in open habitats and/or are more diurnal have well-defined, elongated visual streaks, while more nocturnal and/or forest-dwelling species have a poorly defined visual streak and exhibit a more radially symmetrical retinal topography pattern.

In recent years, several studies have shown that different demands on the visual system in birds are correlated with variation in the relative size of visual areas in the brain [Iwaniuk and Wylie, 2006, 2007; Iwaniuk et al., 2008, 2010b; Corfield et al., 2011]. However, despite the compelling evidence that differences in activity patterns among owl species are reflected in the organization of the eyes, there has been no attempt so far to correlate these differences with variation in the relative size of visual regions in the brain. Owls, like all vertebrates, have several visual pathways from the retina to the brain [Bravo and Pettigrew, 1981; Bagnoli et al., 1990]. One of the main visual pathways in birds is the tectofugal pathway, which is comprised of three main structures: optic tectum (TeO), nucleus rotundus (nRt) and entopallium (E). This pathway is involved in processing brightness, colour, pattern discrimination, simple motion and looming stimuli [Wang et al., 1993; Bischof and Watanabe, 1997; Sun and Frost, 1998; Husband and Shimizu, 2001; Nguyen et al., 2004]. A second pathway is the thalamofugal pathway, which includes the dorsal thalamus and the wulst (also known as the hyperpallium) [Reiner et al., 2004].

In owls, contralateral retinal projections reach the lateral part of the nucleus dorsolateralis anterios thalami (DLL) [Karten and Nauta, 1968; Karten,

1969], which in turn give rise to ipsilateral and contralateral projections to the visual wulst [Karten et al., 1973]. Several studies show that cells in the visual wulst of owls respond to binocular disparity which suggest that this structure is involved in stereopsis [e.g. Pettigrew and Konishi, 1976; Pettigrew, 1979; Wagner and Frost, 1994; Nieder and Wagner, 2001; Baron et al., 2007]. This is further supported by the presence of an enlarged wulst in owls and other bird species with large binocular fields [Iwaniuk et al., 2008]. There is also some evidence that the visual wulst is involved in the representation of illusory contours [Nieder and Wagner, 1999] and learning of visual discrimination tasks [Budzynski and Bingman, 2004]. Other retinorecipient nuclei in birds include the nucleus lentiformis mesencephali (LM) and the nucleus of the basal optic root (nBOR) [Karten et al., 1977; Fite et al., 1981; McKenna and Wallman, 1985; Gamlin and Cohen, 1988], which are involved in the generation of the optokinetic response [Frost et al., 1994], as well as the nucleus geniculatus lateralis, pars ventralis (GLv), the function of which remains largely unclear [but for some proposed functions see Maturana and Varela, 1982; Gamlin et al., 1984; Wakita et al., 1992; Vega-Zuniga et al., 2011].

Given the variation among activity patterns, eye morphology and retinal organization in owls, there are likely corresponding differences in the size of retinorecipient and other brain regions processing visual information. For example, several studies suggest that a transition from diurnality to nocturnality results in a reduction of the number of RGCs and a reduction of the tectofugal pathway [Kay and Kirk, 2000; Kirk and Kay, 2004; Hall et al., 2009; Iwaniuk et

al., 2010b; Corfield et al., 2011]. Therefore, we would expect that nocturnal owl species have a relative smaller tectofugal pathway than more diurnal species. With respect to the thalamofugal pathway, Bravo and Pettigrew [1981] compared the amount of RGCs that project to the TeO and the thalamus between the burrowing owl *(Athene cunicularia)* and the barn owl *(Tyto alba*). These authors found that while both species have a peak density of RGCs that project to the TeO of around 10,000 cells/mm^2, the peak density of RGCs that project to the thalamus is much smaller in the barn owl, around 4,000 cells/mm^2. These two species differ in activity pattern with the burrowing owl being diurnal while the barn owl is strictly nocturnal, but they also belong to the two different families within the order Strigiformes: Strigidae and Tytonidae, respectively [del Hoyo et al., 1999; König and Weick, 2008]. On the basis of Bravo and Pettigrew's [1981] results, we expect differences in the relative size of the thalamofugal pathway, between diurnal and nocturnal species and/or between strigid and tytonid owls. Finally, we have recently shown that asymmetrically eared owls have enlarged auditory pathways when compared to symmetrically eared ones [Gutiérrez-Ibáñez et al., 2011]. Several studies in mammals [Eisenberg, 1981; Baron et al., 1996; Barton, 1998; Catania, 2005] have shown that trade-offs can occur between different sensory systems, and species that rely heavily on one sensory modality (with a corresponding enlargement of associated brain areas) have relatively smaller brain regions dedicated to other sensory modalities. If such a 'trade-off' exists in owls, we expect that asymmetrically eared owls will have relatively smaller visual pathways compared to symmetrically eared owls because of the presumably

greater reliance on auditory rather than visual cues when foraging in asymmetrically eared species. Here, we test all of the predictions discussed above across nine owl species that vary in activity pattern.

4.1 Methods

We measured the relative volume of eight visual nuclei in 12 specimens representing nine species of owl and the tawny frogmouth *(Podargus strigoides)* , a caprimulgiform (see below). All specimens were provided to us dead by conservation authorities or wildlife veterinarians, or were donated by other researchers. In some cases the head without the eyes was provided to us. Owls are classified into two extant families: Tytonidae (barn and bay owls) and Strigidae ('typical' owls) [del Hoyo et al., 1999; König and Weick, 2008]. The barn owl is the most studied species with respect to the visual system [for review see Harmening and Wagner, 2011] and we include one individual in our analyses as a representative tytonid owl. Within the Strigidae, we examined eight species: the northern saw-whet owl *(Aegolius acadicus)*, the shorteared owl *(Asio flammeus)*, the snowy owl *(Bubo scandiacus)*, the great horned owl *(Bubo virginianus)*, the great grey owl *(Strix nebulosa)*, the barred owl *(Strix varia)*, the northern hawk owl *(Surnia ulula)* and the boobook owl *(Ninox boobook)*. This last species was not included in our previous work on the relative size of the auditory system [Gutiérrez-Ibáñez et al., 2011] or retinal organization of owls [Lisney et al., 2012] because we had no access to the eyes of this specimen and there was some tissue damage to the cochlear nuclei during processing of the brain. Finally, we included the tawny frogmouth *(P. strigoides)* for comparative purposes. This is a nocturnal

bird with feeding habits and morphology similar to owls [Cleere, 1998; Higgins, 1999]. They have frontally oriented eyes with similar binocular overlap to owls [Wallman and Pettigrew, 1985] and the relative size of the brain, telencephalon and wulst are similar to that of owls [Iwaniuk and Hurd, 2005; Iwaniuk and Wylie, 2006; Iwaniuk et al., 2008].

For all specimens, the head was immersion-fixed in 4% paraformaldehyde in 0.1 M phosphate buffer. The brain was then extracted, weighed to the nearest milligram, cryoprotected in 30% sucrose in phosphate buffer, embedded in gelatin and sectioned in the coronal or sagittal plane on a freezing stage microtome at a thickness of 40 μm. Sections were collected in 0.1 M phosphatebuffered saline, mounted onto gelatinized slides, stained with thionine and coverslipped with Permount. The olfactory bulbs were intact in all the specimens we collected and sectioned. All brains were cut following bird brain atlases [e.g. Karten and Hodos, 1967; Puelles et al., 2007] in which the brainstem ends at the same rostrocaudal point as the cerebellum. In this manner, brain measurements were consistent among our specimens. Photomicrographs of every fourth section were taken throughout the rostrocaudal extent of each nucleus using a Retiga EXi *FAST* Cooled mono 12-bit camera (Qimaging, Burnaby, B.C., Canada) and OPENLAB Imaging system (Improvision, Lexington, Mass., USA) attached to a compound light microscope (Leica DMRE, Richmond Hill, Ont., Canada). Measurements of all the nuclei were taken directly from these photos with ImageJ (NIH, Bethesda, Md., USA; http://rsb.info.nih.gov/ij/) and volumes were calculated by multiplying the area in each section by the thickness of the section (40 μm) and the sampling

interval. For those species represented by more than one specimen (table 4.1), the average of the measurements was taken as the species' given value. Brain volume for each specimen was calculated by dividing the mass of the brain by the density of brain tissue (1.036 g/mm 3) [Stephan, 1960] as in previous studies [Iwaniuk and Wylie, 2006; Iwaniuk et al., 2007, 2008, 2010b].

We measured the volume of all the nuclei comprising the two main visual pathways in birds (see Introduction), the tectofugal pathway (TeO, nRt and E) and the thalamofugal pathway (DLL and wulst). Additionally, we measured the relative size of three retinorecipient nuclei, LM, nBOR and GLv in order to assess whether differences in the relative size of visual areas between owl species apply to all retinorecipient areas or are independent for each pathway. We also tested for a correlation between the relative volume of all the visual nuclei measured in this study and the relative volume of auditory pathways for some of the same species, which were obtained from Gutiérrez-Ibáñez et al. [2011]. The total relative volume of auditory pathways is the sum of the relative volume of the nucleus angularis, the nucleus magnocellularis, the nucleus laminaris, the posterior part of the dorsal lateral lemniscus, the anterior part of the dorsal lateral lemniscus, the ventral part of the lateral lemniscus, the superior olive, inferior colliculus and the nucleus ovoidalis.

4.1.2 Activity Pattern

We classified the nine different owl species measured in this study into three different activity pattern categories following the same classification used in

our previous work with the same species (table 4.1) [for details see Lisney et al., 2012]. Briefly, species where classified as: (1) diurnal, meaning active during the day in photopic conditions, (2) crepuscular, meaning active during dawn and dusk periods and (3) nocturnal, meaning active during the night in scotopic conditions. Within the crepuscular category there is some variation as some species can be classified as crepuscular- nocturnal while others as crepuscular-diurnal [for details see Lisney et al., 2012]. It should also be noted that the short-eared owl is included in the crepuscular category even though it can be considered crepuscular-cathemeral because some reports suggest that this species is most active around dawn and dusk [Clark, 1975; Voous, 1988; Reynolds and Gorman, 1999; König and Weick, 2008] whereas others have reported that this owl is active at various times of the day and night [Clark, 1975; del Hoyo et al., 1999].

4.1.3 Borders of Visual Nuclei

The borders of the different nuclei were determined based on descriptions of the nuclei in the literature (see below) and several stereotaxic atlases [Karten and Hodos, 1967; Stokes et al., 1974; Matochik et al., 1991; Puelles et al., 2007] (www.bsos.umd.edu/psyc/Brauthlab/atlas.htm). Figure 4.1 shows examples of the visual nuclei in several owl species. Detailed descriptions of the borders of TeO, nRt, E, GLv, LM and nBOR can be found in previous works [Iwaniuk and Wylie, 2007; Iwaniuk et al., 2010b]. For the borders of the lateral part of the nucleus DLL, we measured the area distinguished by the presence of densely packed, darkly stained cells (fig. 4.1D). We chose this area because according to the

results of Bagnoli et al. [1990], this corresponds to the retinorecipient part of DLL in owls. This is in contrast to the more lateral and dorsal part of DLL, which shows less densely packed and less darkly stained cells, and does not receive retinal projections (fig. 4.1D) [Bagnoli et al., 1999]. For the borders of the wulst we followed Iwaniuk et al. [2008], which include the hyperpallium apicale, the nucleus interstitialis hyperpallii apicalis and the hyperpallium densocellulare (fig. 4.1E). It must be noted that this includes both the visual portions of the wulst as well as the rostral most part of it, which is not visual but rather receives somatosensory information [Karten et al., 1978; Manger et al., 2002; Wild et al., 2008]. Figure 4.1E shows an example of the borders of the wulst in an owl.

4.1.4 RGC Distribution and Total Number

We also compared the relative size of the different visual pathways to both the topographic distribution and total number of neurons in the RGC layer for the different species of owls, using data from Lisney et al. [2012]. To the best of our knowledge, similar data have not been published for the tawny frogmouth or the boobook owl and we had no access to retinas of either of these species, so we were not able to include them in this part of our analysis. Retinal topography is related to activity pattern in owls, with more diurnal species having a well-defined, elongated visual streak, while more nocturnal species have a poorly defined visual streak and a more radially symmetrical arrangement [Lisney et al., 2012]. The pattern can be quantified using a ‘H:V ratio’; the ratio of the maximum horizontal (H) and vertical (V) extent of the area enclosed by an

isodensity contour line [Stone and Keens, 1980; Fischer and Kirby, 1991]. In this sense, a perfectly circular distribution of RGCs would result in an H:V ratio of 1, whereas a visual streak results in an H:V ratio greater than 1. We also compared the relative size of visual pathways with the number of cells in the RGC layer reported by Lisney et al. [2012]. The RGC layer in the retina contains not only RGCs, but also displaced amacrine cells [Bravo and Pettigrew, 1981; Hayes, 1984; Chen and Naito, 1999], which account for about 50% of the cells in the ganglion cell layer in the barn owl [Wathey and Pettigrew, 1989]. In addition, a population of displaced RGCs resides in the amacrine cell layer in birds [Karten et al., 1977; Reiner et al., 1979; Fite et al., 1981]. As detailed in Lisney et al. [2012], we were unable to reliably distinguish amacrine from RGCs within the RGC layer, so the total number of cells in the RGC layer is an overestimate of RGC number. Because the number of cells in the brain correlates positively with the absolute size of the brain [reviewed in Herculano- Houzel, 2011] we divided the total number of cells in the RGC layer by the brain volume of each species as a way to account for the differences in cell numbers related to the size of each species.

4.1.5 Statistical Analyses

In many comparative studies dealing with relative size of brain structures, allometric effects are accounted for by comparing residuals from least-square linear regressions between the structures and body mass or brain volume [e.g. Iwaniuk et al., 2005, 2006; Iwaniuk and Wylie, 2007]. With a relatively small

number of species, such comparisons become problematic because a single data point can have a huge influence on the slope and intercept of an allometric line. Instead, we have taken a qualitative approach by examining the relative size of each nucleus as a percentage of overall brain volume. Also, in recent years comparative analyses have used phylogenetically corrected statistics [e.g. Garland et al., 1992, 2005] to account for possible phylogenetic effects. The small number of species examined herein has low statistical power that would be even further reduced with such a correction. The low sample size of each of our activity pattern subgroups further constrains our statistical power, therefore making such phylogenetic corrections impractical. Instead, we compared the results of a hierarchical cluster analysis to the most complete phylogenetic tree currently available for owls [Wink et al., 2008]. Using a similar approach to Iwaniuk and Hurd [2005], we performed a hierarchical cluster analysis of the proportional size of all auditory nuclei measured, with JMP (Version 7, SAS Institute Inc., Cary, N.C., USA). Although the dendrograms produced by hierarchical cluster analyses are based on similarities among species, comparing the dendrogram with a phylogeny of the species of interest can reveal whether interspecific differences have arisen largely through phylogenetic relatedness or independent evolution [Iwaniuk and Hurd, 2005; Gutiérrez-Ibáñez et al., 2011]. Here, we show the results generated using an average linkage method, but the dendrograms arising from other linkage methods (e.g. Ward's and UPGMA) shared the same topology.-

4.2 Results

We found marked differences in the relative size of all visual brain structures among the species studied (fig. 4.2). In the thalamofugal pathway, the boobook and the northern saw-whet owls have the largest DLL relative volume (fig. 4.2A), more than twice the size of that of the barn owl, the species with the smallest relative volume. The situation is very similar regarding the wulst, which was largest in the boobook and the northern saw-whet owls and smallest in the barn owl (fig. 4.2B). In the case of the TeO the tawny frogmouth has the largest relative volume, almost twice that of the two closest owl species (the boobook and the northern saw-whet owl; fig. 4.2C), and more than four times larger than the owls with the smallest TeO, the great grey owl and the barn owl. The situation is similar for the Rt and E, the other components of the tectofugal pathway. The relative size of both of these structures is four to five times greater in the tawny frogmouth, compared to the owls (fig. 4.2D, E). Among owls, as with the TeO, the boobook and the northern saw-whet owls have the largest relative Rt volume (fig. 4.2D), but in the case of E, the owls with the largest relative volume are the snowy and northern hawk owls.

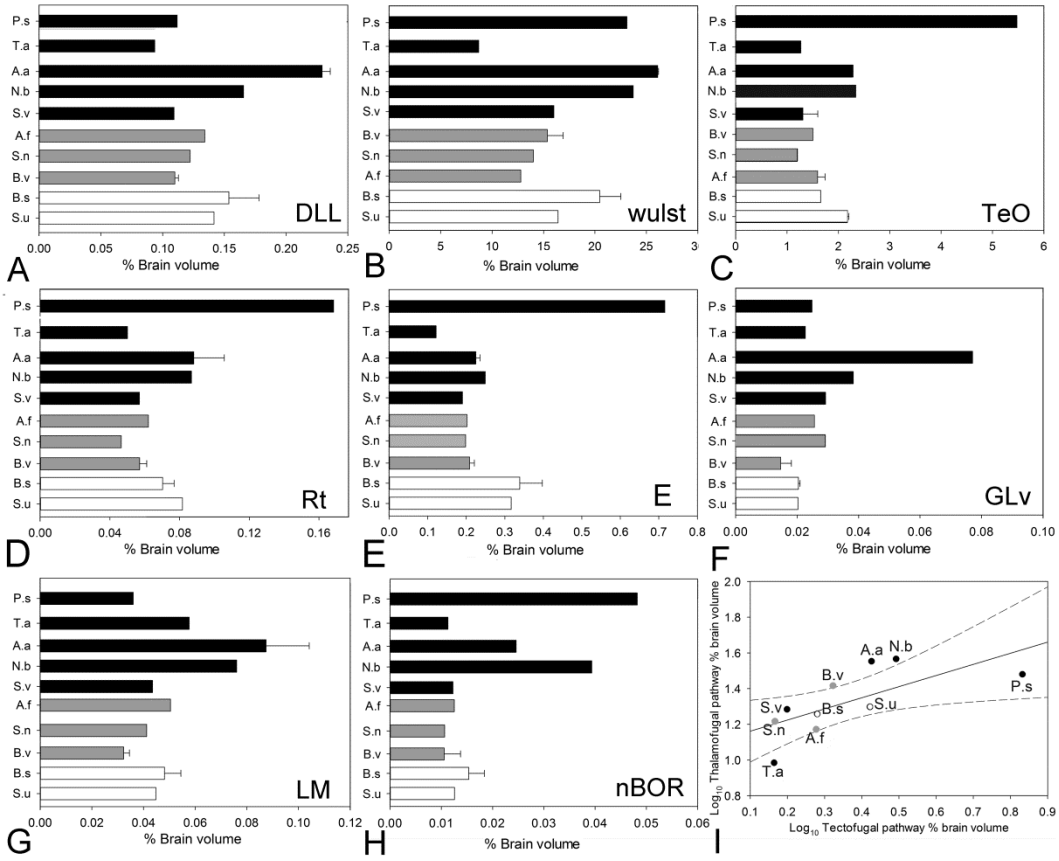
P.s
T.a
A.a
N.b
S.v
A.f
S.n
B.v
B.s
S.u
DLL
% Brain volume
A
wulst
B
TeO
C
Rt
D
E
GLv
F
LM
G
nBOR
H
Log10 Thalamofugal pathway % brain volume
Log10 Tectofugal pathway % brain volume
I

Figure. 4.2. Relative size of the tectofugal and thalamofugal pathways.

Bar graphs showing the relative size of visual nuclei in the tawny frogmouth (P. strigoides) and nine species of owls expressed as a percentage of total brain volume. **A** Nucleus DLL. **B** Wulst. **C** TeO. **D** nRt. **E** E. Bar graphs also show the relative size of three additional retinorecipient nuclei in the same species: nucleus GLv (**F**), nucleus LM (**G**) and nBOR (**H**). The shading of the bars shows the activity pattern of each species: black = nocturnal, grey = crepuscular, white = diurnal. **i** A logarithmic scatter plot of the total volume of the thalamofugal pathway expressed as a percentage of total brain volume, plotted as a function of the total volume of the tectofugal pathway expressed as a percentage of total brain volume in the same species as above. The solid line indicates the least squares linear regression line for all species and the dotted lines are the 95% confidence interval around the regression line. The colour of the dot indicates the activity pattern of each species: black = nocturnal, grey = crepuscular, white = diurnal. T.a = Barn owl *(T. alba)* ; A.a = northern saw-whet owl *(A. acadicus)* ; A.f = short-eared owl *(A. flammeus)* ; S.n = great grey owl *(S. nebulosa)* ; S.v = barred owl *(S. varia)* ; B.v = great horned owl *(B. virginianus)* ; B.s = snowy owl *(B. scandiacus)* ; S.u = northern hawk owl *(S. ulula)* ; N.b = boobook owl *(N. boobook)* ; P.s = tawny frogmouth *(P.strigoides)* .

We also found marked differences in the relative size of the other three visual nuclei we measured. In the case of GLv, the northern saw-whet owl has the largest relative volume; almost four times that of the great horned owl, the species with the smallest relative volume (fig. 4.2). For LM (fig. 4.2F) the boobook and northern saw-whet owls have the largest relative volumes, about twice that of other species. Finally, in the case of nBOR, the situation is more similar to the structures in the tectofugal pathway; the tawny frogmouth has the largest relative volume, followed by the boobook and northern saw-whet owls.

Figure 4.2I shows a scatterplot of the logarithm of the total relative volume of the tectofugal pathway (TeO + Rt + E) versus the total relative volume of the Thalamofugal pathway (DLL + wulst) among the species studied. We found a significant positive correlation between the relative volume of these two pathways ($R^2 = 0.472$, $F_{1,8} = 7.148$, $p < 0.05$). This is also true when the tawny frogmouth is excluded ($R^2 = 0.619$, $F_{1,7} = 11.391$, $p < 0.05$). The barn owl appears as an outlier as it falls well below the confidence intervals with both the smallest tectofugal and thalamofugal pathways.

4.2.1 Visual Pathways and Neurons in the RGC Layer

We found no correlation between H:V ratio and the relative volume of any of the nuclei belonging to either the thalamofugal pathway or the tectofugal pathway (table 4.2), nor with the total volume of the thalamofugal pathway (table 4.2 ; fig. 4.3A) or the tectofugal pathway (table 4.2; fig. 4.3B). We found a significant positive correlation between the relative volume of all the visual nuclei

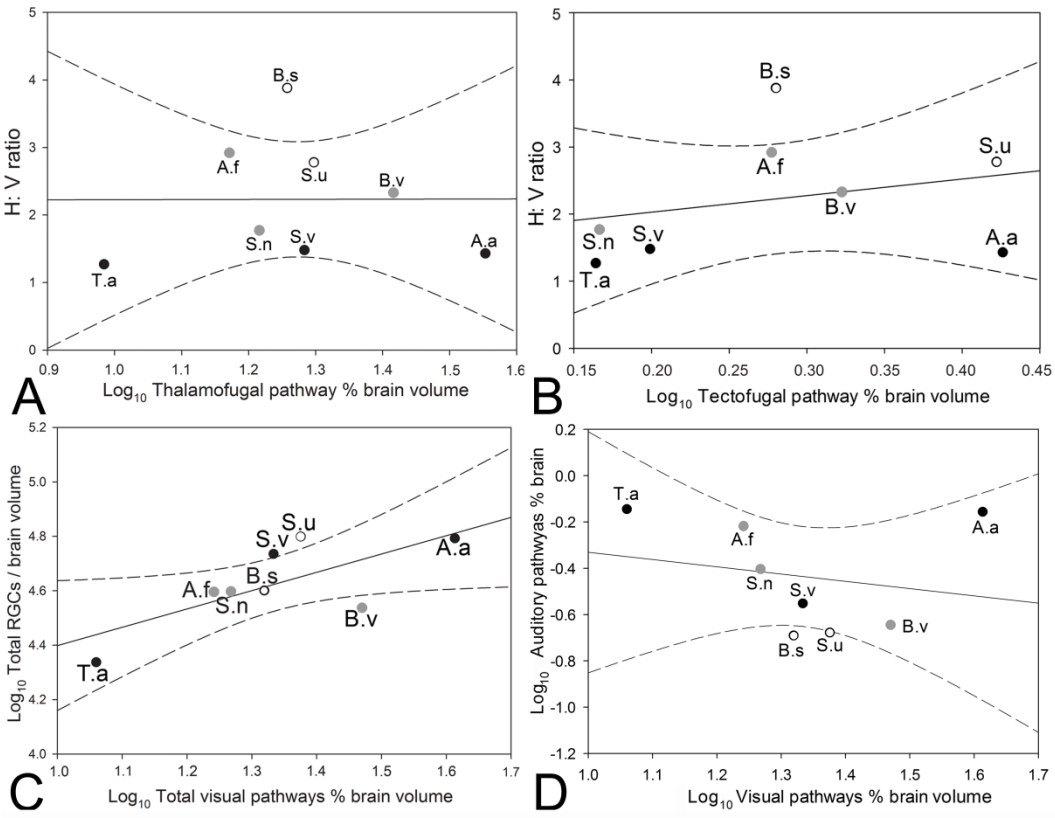
A
H: V ratio
Log10 Thalamofugal pathway % brain volume
B.s
A.f
S.u
B.v
S.n
S.v
A.a
T.a
B
H: V ratio
Log10 Tectofugal pathway % brain volume
C
Log10 Total RGCs / brain volume
Log10 Total visual pathways % brain volume
D
Log10 Auditory pathwyas % brain
Log10 Visual pathways % brain volume

Figure. 4.3. Relative volume of visual nuclei vs retinal topography, RGC numbers and relative volume of auditory nuclei. A scatter plot of H:V ratio plotted as a function of the logarithm of the total volume of the thalamofugal pathway expressed as a percentage of total brain volume for eight species of owl. **B** A scatter plot of H:V ratio plotted as a function of the logarithm of the total volume of the tectofugal pathway expressed as a percentage of total brain volume for eight species of owl. **C** A scatter plot of the logarithm of the total number of neurons in the retinal ganglion cell layer divided by the brain volume plotted as a function of the logarithm of the total volume of the visual pathway expressed as a percentage of total brain volume for the same eight species of owl. **D** A scatter plot of the logarithm of the total volume of the auditory nuclei expressed as a percentage of total brain (see Results) plotted as a function of the logarithm of the total volume of the visual pathway expressed as a percentage of total brain volume (see Results) for the same eight species of owl. The solid lines indicate the least squares linear regression line for all species and the dotted lines are the 95% confidence interval around the regression line. The colour of the dot indicates the activity pattern of each species: black = nocturnal, grey = crepuscular, white = diurnal. T.a =Barn owl *(T. alba)* ; A.a = northern saw-whet owl *(A. acadicus)* ; A.f = short-eared owl *(A. flammeus)* ; S.n = great grey owl *(S. nebulosa)* ; S.v = barred owl *(S. varia)* ; B.v = great horned owl *(B. virginianus)* ; B.s = snowy owl *(B. scandiacus)* ; S.u = northern hawk owl *(S. ulula)* ; N.b = boobook owl *(N. boobook)* ; P.s = tawny frogmouth *(P. strigoides)*

measured (tectofugal pathway + thalamofugal pathway + GLv + LM +nBOR) and the total number of RGC layer neurons, relative to brain volume (R^2 = 0.523, F 1,8 = 6.586, p > 0.05; fig. 4.3C). Finally, figure 4.3D shows a scatterplot of the relative size of all the visual brain structures measured plotted against the total volume of all auditory nuclei measured in Gutiérrez-Ibáñez et al. [2011]. We found no correlation between the total volumes of the visual and auditory pathways (R^2 = 0.0449, F 1,7 = 0.282, p = `0.614). In this comparison, the northern saw-whet owl appears as an outlier with both enlarged visual and auditory areas. When this owl is excluded, there is a significant, negative correlation between the total volume of all auditory and visual areas among the remaining species (R^2 = 0.736, F 1,6 = 13.960, p > 0.05). Lastly, we compared a dendrogram resulting from a hierarchical cluster analysis with a molecular phylogeny of the owl species we examined. Figure 4.4A depicts the phylogenetic relationships among the nine owl species used in this study [Wink et al., 2008] and figure 4.4B illustrates the similarity among the nine species based on a cluster analysis of the relative size of all visual brain structures. This dendrogram has two main clusters and it is clear that the species are not separated by their activity pattern. In one cluster, the northern saw-whet owl and the boobook owl, both nocturnal species, are grouped with the northern hawk owl, a diurnal species, and the great horned owl, a crepuscular species. In the other cluster, the nocturnal barn owl appears as the root branch to a group that includes three crepuscular species and one diurnal, the snowy owl (fig. 4.4B). The dendrogram also does not

resemble the phylogenetic relationships among species and therefore the relative size of the entire visual system does not reflect activity pattern or phylogeny.

4.3 Discussion

Overall, our study shows that there are clear differences in the relative size of the visual pathways among owl species. This is one of the few studies to evaluate relationships between retinal topography and RGC layer neuron numbers and the relative size of the brain visual pathways in any vertebrate. Previously, Kaskan et al. [2005] found that in mammals there is no correlation between rod:cone ratios and the relative size of cortical visual areas. Also, Collin and Pettigrew [1988a, b] suggested that in reef teleosts RGC topography is related to the relative size of the TeO.

4.3.1 Thalamofugal Pathway

On the basis of gross anatomy, Stingelin [1958] reported that the barn owl visual wulst appears much smaller than the wulst of strigid owls, mostly in that it does not extend completely to the lateral edge of the telencephalon. In agreement with this, Bravo and Pettigrew [1981] found that the peak density of RGCs projecting to the TeO was similar between the barn owl and the burrowing owl, but the peak density of RGCs projecting to the thalamofugal pathway was four times larger in the burrowing owl. Our findings that the barn owl has both the smallest DLL (fig. 4.2A) and wulst (fig. 4.2B) of all species sampled confirms the suggestion that the thalamofugal pathway is smaller in the barn owl compared to

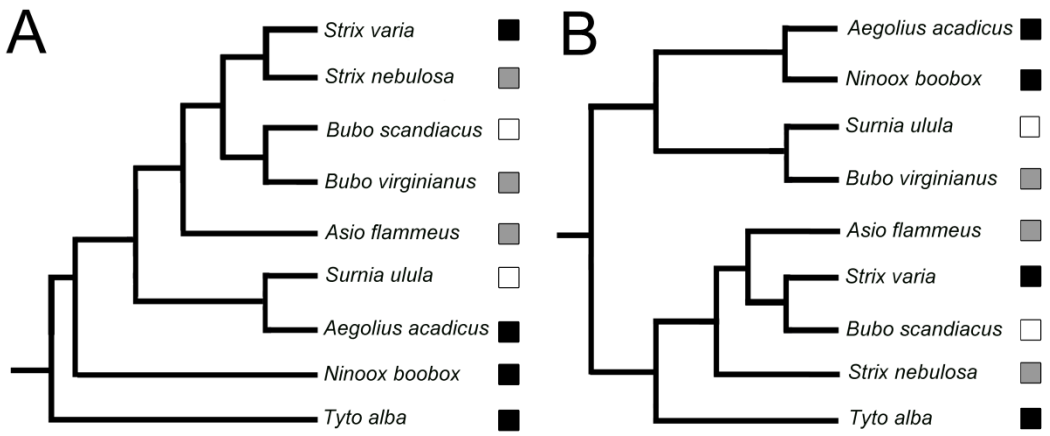

Figure. 4.4. Owls phylogeny and cluster analisis of the relative size of visual pathways. Comparison of owls phylogeny and cluster analysis of the relative volume of all visual brain structures. A Phylogenetic relationships among the nine species used in this study based on Wink et al. [2009]. B The similarity between species based on a cluster analysis of the relative size of all visual brain structures. The coloured squares indicate the activity pattern of each species: black = nocturnal, grey = crepuscular, white = diurnal.

strigid owls.

In both mammals [Barton, 2004] and birds [Iwaniuk et al., 2008], the relative size of the thalamofugal pathway is positively correlated with the size of the binocular visual field. Therefore, one may expect that because of the reduced thalamofugal pathway in the barn owl, there may also be differences in binocular overlap between the barn owl and other owl species, but this does not appear to be the case. The barn owl has neither less binocular overlap nor less convergent orbits than other owls [Iwaniuk et al., 2008]. We found that the barn owl also has a relatively small tectofugal pathway and, in fact, there is a positive correlation between the relative size of the thalamofugal and tectofugal pathway in all species (fig. 4.2F). This indicates that the barn owl does not have a specific reduction of the thalamofugal pathway, but an overall reduction of the visual pathways, which is most likely related to the relatively low number of RGCs in this species (see below; table 4.3). Why the barn owl is so different from strigid owls is not clear. The ecology and hunting behaviour of barn owls does not differ greatly from many strigid owls [König and Weick, 2008]. Tytonid owls do differ in several morphological aspects from strigid owls, such as the shape of the sternum and feet morphology [König and Weick, 2008], and several lines of evidence indicate a split between the two families dating back to the Neogene (23 mya) [Brown and Mindell, 2009], so these neuroanatomical differences could reflect aspects of this ancient diver gence. Given these apparent differences between strigid and tytonid owls, future studies should address whether the barn owl is typical of all tytonids

and whether there are differences in the retinal and brain morphology between *Tyto* and *Phodilus* , the two genera within the Tytonidae.

Our results confirm previous findings [Iwaniuk et al., 2006, 2008] that the tawny frogmouth has a relative wulst volume similar to that of owls (fig. 4.2B), and also show that this is true for DLL, which relays information from the retina to the visual wulst [Karten et al., 1973; Bagnoli et al., 1990]. We also found that the relative size of the tectofugal pathway is much larger in the tawny frogmouth than in any owls (fig.4.2 C–E). Because the tawny frogmouth has feeding habits and morphology very similar to owls [Cleere, 1998; Higgins, 1999], we expected this species to be closer to owls with respect to the relative size of the tectofugal pathway. While some studies have placed caprimulgiformes and the frogmouth as closely related to owls [Sibley and Ahlquist, 1990], several other studies place them as more closely related to hummingbirds and swifts [Cracraft et al., 2004; Davis, 2008; Hacket et al., 2008] and thus the common habits of owls and the frogmouths probably evolved independently and the difference in the relative size of the tectofugal pathway could reflect different evolutionary histories.

4.3.2 Auditory-Visual Trade-Off?

Although our results show no significant correlation between the relative size of visual and auditory pathways when all owl species are included, there is a significant negative correlation between these two sensory pathways when the northern saw-whet owl is excluded (see Results; fig. 4.3D). Why the northern

saw-whet owl escapes this trend of a trade-off between the relative size of auditory and visual regions is unclear. The northern saw-whet owl is peculiar among the asymmetrically eared species with enlarged auditory pathways because it is both strictly nocturnal and hunts mostly in woodlands. Other asymmetrically eared, nocturnal species (e.g. barn and shorteared owls) hunt primarily in open habitats [del Hoyo et al., 1999; König and Weick, 2008]. The northern sawwhet owl therefore hunts in an especially dim habitat that is full of obstacles and thus might require more visually guided prey capture and navigation than other asymmetrically eared species. Although this life history is not unique amongst all owls, the saw-whet owl was the only species that had all of these traits in our analyses. This possible trade-off between sensory modalities should be taken with caution as the inclusion of more species in the analysis, especially other nocturnal asymmetrically eared species that hunt primarily in woodlands (e.g. the mottled owl, *Ciccaba virgata* , and the boreal owl, *Aegolius funereus*) [Norberg, 1977; König and Weick, 2008] may show that the northern saw-whet owl is not an exception and that there I s no significant relationship between the relative sizes of the auditory and visual pathways.

Despite the caveats in this analysis, similar sensory system trade-offs have been reported in mammals. For example, Baron et al. [1996] found that there is a tradeoff between the relative sizes of auditory and visual structures in the mesencephalon in bats, and Eisenberg [1981] also suggested that a similar trade-off between visual and auditory pathways may occur in tenrecs, which use echolocation and have small eyes. In owls, the possible trade-off between the

visual and auditory pathways is likely driven by the increased capability of asymmetrically eared owls to use auditory cues to locate prey. Species like the barn owl and the northern saw-whet owl can locate sounds within 2°, and some asymmetrically eared species can hunt in complete darkness [Payne, 1971; Konishi, 1973]. An improved ability to locate prey using auditory cues could loosen the selective pressure on maintaining a well-developed visual system for visually guided prey capture and thus result in the reduction of the relative number of RGCs and relative size of the visual pathways.

4.3.3 Activity Pattern

In birds, and vertebrates in general, one of the adaptations of the visual system to scotopic environments is to increase retinal summation, *i.e.* an increase in the number of photoreceptors that converge onto one RGC [Warrant, 2004; Hall and Ross, 2007]. One consequence of this is a reduction in the number RGCs [Kay and Kirk, 2000, 2004; Hall et al., 2009]. In birds, there is evidence that this, in turn, results in a reduction of the tectofugal pathway [Martin et al., 2007; Iwaniuk et al., 2010b; Corfield et al., 2011]. Surprisingly, our results show that in owls there is no correlation between the relative size of the tectofugal pathway and activity pattern. First, we found no correlation between the relative size of the tectofugal (or the thalamofugal) pathway and H:V ratio (fig. 4.3A, B), which are correlated with activity pattern in owls [Lisney et al., 2012]. Second, in our cluster analysis (fig. 4.4B), species do not appear to be grouped by activity pattern, indicating that the relative size of visual pathways is not similar among species

with similar activity patterns. Also, in the boobook owl, a nocturnal species for which we did not have an H:V ratio, the size of the tectofugal pathway is relatively large compared to other owls (fig. 4.2C–E), further indicating that nocturnal owls do not have a reduced tectofugal pathway. Instead, our results show that the relative sizes of the visual pathways are correlated with the relative number of RGC layer neurons (fig. 4.3C), which, in turn, appears to be independent of activity pattern in the species examined. This is well exemplified by the northern saw-whet and barn owls. Both of these species are strictly nocturnal, but the northern saw-whet owl has almost three times as many neurons in the RGC layer, relative to brain size, as the barn owl (table 4.3). Previously, Hall et al. [2009] had found that there is no difference in the relative size of the optic foramen between diurnal and nocturnal owls, which also suggests that the number of RGCs is not correlated with activity pattern in owls. Thus, in owls, activity patterns are associated with differences in eye morphology [Lisney et al., 2012], rod:cone ratios and retinal topography [Oehme, 1961; Bravo and Pettigrew, 1981; Lisney et al., 2011, 2012], but not in the number of RGCs and the relative size of visual pathways. This is similar to what Kaskan et al. [2005] found in mammals where the relative size of cortical visual areas between diurnal and nocturnal species is not different despite a great variation in rod:cone ratios. One explanation for this lack of correlation between activity pattern and the relative size of visual pathways is that the amount of variation in the peripheral visual system related to changes in the activity pattern is enough to accommodate the changes in light available for vision resulting from a nocturnal to diurnal

transition (or vice versa) and therefore changes in the number of RGCs or the relative size of visual pathways are not necessary. Alternatively, it is possible that the number of RGCs, and hence the relative size of visual pathways, is constrained by evolutionary history. Regardless of whether they are diurnal or nocturnal, all owls have relatively large eyes [Brooke et al., 1999], convergent orbits and a broad binocular visual field [Martin, 1986; Iwaniuk et al., 2008] and a relatively small optic foramen [Hall et al., 2009] when compared to other birds. All these characteristics strongly suggest that owls are descended from a nocturnal ancestor and more diurnal activity patterns have evolved independently several times. This would be similar to what has been proposed in the evolution of the visual system of mammals, where a nocturnal 'bottleneck' seems to define several of the characteristics of the mammalian visual system, even in diurnal species [Heesy and Hall, 2010].

4.4 Conclusion

Our results show that there is little correlation between the relative size of visual pathways and activity pattern in owls, despite the fact that several characteristics of the peripheral visual system (e.g. eye shape and RGC distribution, see Introduction) do vary with the activity pattern of each species. Instead, our results strongly suggest that the relative size of all visual structures in the brain is related to the number of cells in the RGC layer relative to brain size. Interestingly, the relative sizes of the main visual pathways (tectofugal and thalamofugal) covary, even though they have different functions. This is similar to what we found in our study of the relative size of the auditory pathways of owls

[Gutiérrez-Ibáñez et al., 2011] where the relative size of two distinct auditory pathways, the intensity and time-delay pathways, are highly correlated. This is likely related to the hearing range of each species and therefore to the number of sensory cells in the periphery [Gutiérrez-Ibáñez et al., 2011]. Further, several other studies in vertebrates suggest that the number of sensory cells is the main driver of the relative size of sensory areas [e.g. Roth et al., 1992; Kotrschal et al., 1998]. Together, these points emphasize the need for future research in sensory ecology to study variation at *all* levels within a given sensory pathway.

Finally, we still need to consider why there is so much variation in the relative number of cells in the RGC layer (and therefore visual pathways) among owls. As stated before (see Discussion) a combination of both phylogenetic history and particular aspects of the ecology of each species may help to explain these differences. Part of the difficulty in interpreting our findings derives from a limited sampling of owl species. Even though this is the most extensive study of its kind in owls, several other groups are missing. For example, the study of other nocturnal and diurnal species of small owls in the tribe Surniinae [Wink et al., 2008] could help to clarify the uniqueness of the visual system of the northern saw-wet owl.

Table 4.1: Volumes of visual nuclei in owls. List of the owl species surveyed, sample size and volumes (in mm3) of the brain and all nuclei measured; optic tectum (**TeO**), nucleus rotundus (**Rt**), ectopallium **(E**), nucleus dorsolateralis anterior thalami, pars lateralis (**DLL**), **wulst**, ventral part of the lateral genicualte nucleus (**GLv**), nucleus of the basal optic root (**nBOR**), and nucleus lentiformis mesencephali (**LM**).

Common name	Species	n	activity pattern	Brain volume (mm3)	TeO (mm3)	Rt (mm3)	E (mm3)	Dll (mm3)	wulst (mm3)	Glv (mm3)	nBOR (mm3)	LM (mm3)
Barn Owl	*Tyto alba*	1	Nocturnal	5849.80	136.510	2.926	7.111	5.479	509.071	1.326	0.660	1.777
Saw-whet Owl	*Aegolius acadicus*	2	Nocturnal	2999.93	68.542	2.618	6.769	6.884	783.317	2.313	0.737	2.163
Short-eared Owl	*Asio flammeus*	1	Crepuscular	6221.04	99.163	3.860	12.583	8.345	795.418	1.593	0.779	1.882
Great Grey Owl	*Strix nebulosa*	1	Crepuscular	13433.39	161.304	6.250	26.655	16.421	1880.845	3.921	1.431	2.856
Barred Owl	*Strix varia*	1	Nocturnal	12727.12	166.642	7.248	24.206	13.908	2036.382	3.719	1.562	3.095
Great horned Owl	*Bubo virginianus*	3	Crepuscular	17199.09	277.015	9.711	34.883	18.545	2617.419	3.510	2.640	4.315
Snowy Owl	*Bubo scandiacus*	3	Diurnal	17345.97	286.041	12.158	58.802	26.475	3561.186	2.540	1.830	5.049
Hawk Owl.	*Surnia ulula*	1	Diurnal	9408.30	204.755	7.678	29.798	13.332	1544.342	1.907	1.182	2.285
Southern Boobook	*Ninox boobox*	1	Nocturnal	6338.80	148.150	5.503	15.800	10.499	1503.680	2.153	2.214	3.835
Tawny Frogmouth	*Podargus strigoides*	1	Nocturnal	5311	290.880	8.948	38.000	5.935	1226.890	1.320	2.561	1.914

Table 4.2: Retinal ganglion cells numbers and density for some the owl species surveyed. Retinal ganglion cells (RGCs) numbers, average density (cells/mm^2) and number of RGCs relative to brain volume (cells/mm^3) for some the owl species surveyed. RGCs numbers and density are from Lisney et al., [2012].

Common name	Species	n	Total RGCs	Average RGC density	RGCs number/ brain volume
Barn Owl	*Tyto alba*	1	1271450	6064	217.35
Saw-whet Owl	*Aegolius acadicus*	2	1948100	9840	619.85
Short- eared Owl	*Asio flammeus*	1	2451200	9682	394.02
Great Grey Owl	*Strix nebulosa*	1	5313825	13285	395.57
Barred Owl	*Strix varia*	1	6915200	12105	543.34
Great horned Owl	*Bubo virginianus*	3	6858000	7410	398.74
Snowy Owl	*Bubo scandiacus*	3	5973200	9967	344.36
Hawk Owl.	*Surnia ulula*	1	5920425	13855	629.28

Table 4.3: Regressions between H:V ratio and volume of visual pathways. Results of linear regression between H:V ratio (see methods) and the relative volume of the optic tectum (**TeO**), the nucleus rotundus (**nRt**), the ectostriatum **(E**), the nucleus dorsolateralis anterior thalami, pars lateralis (**DLL**), the **wulst**, the ventral part of the lateral genicualte nucleus (**GLv**), the nucleus of the basal optic root (**nBOR**), the nucleus lentiformis mesencephali (**LM**), the total volume of the tectofugal pathway (**TeO**+**nRt**+**E**) and the thalamofugal pathwya (**DLL**+**wulst**).

ff

nuclei	R2	F1, 8	p
Gld	0.0352	0.219	0.656
Wulst	0.252	2.698	0.139
Teo	0.0376	0.234	0.645
Rot	0.00246	0.0148	0.907
E	0.105	0.703	0.434
Tectofugal pathway	0.0793	0.517	0.499
Thalamofugal pathway	0.0000119	0.0000716	0.994

4.5 References

Bischof HJ, Watanabe S (1997): On the structure and function of the tectofugal visual pathway in laterally eyed birds. Eur J Morph 35: 246–254.

Bravo H, Pettigrew JD (1981): The distribution of neurons projecting from the retina and visual cortex to the thalamus and tectum opticum of the barn owl, *Tyto alba*, and burrowing owl, *Speotyto cunicularia*. J Comp Neurol 199:419–441.

Bagnoli P, Fontanesi G, Casini G, Porciatti V (1990): Binocularity in the little owl, *Athene noctua*. I. Anatomical investigation of the thalamo-Wulst pathway. Brain Behav Evol. 35:31-39.

Baron G, Stephan H, Frahm HD (1996): Comparative Neurobiology in Chiroptera. Basel, Birkhauser Verlag.

Baron J, Pinto L, Dias MO, Lima B, Neuenschwander S (2007): Directional responses of visual wulst neurones to grating and plaid patterns in the awake owl. Europ J Neurosci 26: 1950–1968.

Barton RA (1998): Visual specialization and brain evolution in primates. Proc R Soc Lond B 265:1933–1937.

Barton RA (2004): Binocularity and brain evolution in primates. Proc Nat Acad Sci USA 101:10113–10115

Brooke MdL, Hanley S, Laughlin SB (1999): The scaling of eye size with body mass in birds. Proc R Soc Lond B 266:405–12.

Brown JW, Mindell DP (2009): Owls (Strigiformes); In Hedges SB, Sumar S, (eds): The Timetree of Life. Oxford, University Press, pp 451-453.

Budzynski CA, Bingman VP (2004): Participation of the thalamofugal visual pathway in a coarse pattern discrimination task in an open arena. Behav Brain Res. 153:543-56.

Catania KC (2005): Evolution of sensory specializations in insectivores. Anat Rec A 287A:1038- 1050.

Clark RJ (1975): A field study of the short-eared owl, *Asio flammeus* (Pontoppidan), in North America. Wildl Monogr 47:1-67.

Cleere N (1998): Nightjars: a guide to the nightjars, nighthawks, and their relatives. Yale University Press, New Haven

Chen Y, Naito J (1999): A quantitative analysis of the cells in the ganglion cell layer of the chick retina. Brain Behav Evol 53:75–86.

Collin SP, Pettigrew JD (1988a): Retinal topography in reef teleosts. I. Some species with well-developed *areae* but poorly-developed streaks. Brain Behav Evol 31: 269-282.

Collin SP, PettigrewJ D (1988b): Retinal topography in reef teleosts. II. Some species with prominent horizontal streaks and high-density *areae*. Brain Behav Evol 3 1:283-295.

Corfield JR, Gsell AC, Brunton D, Heesy CP, Hall MI, Acosta ML, Iwaniuk AI (2011): Anatomical specializations for nocturnality in a critically endangered parrot, the kakapo (*Strigops habroptilus*). PLoS ONE 6:e22945.

Cracraft J, Barker FK, Braun M, Harshman J, Dyke GJ, et al. (2004): Phylogenetic relationships among modern birds (Neornithes): toward an

avian tree of life; In Cracraft J, Donoghue MJ (eds): Assembling the tree of life. New York, Oxford University Press. pp 468–489.

Davis KE (2008): Reweaving the tapestry: a supertree of birds. PhD Thesis, University of Glasgow, UK.

del Hoyo J, Elliott A, Sargatal J (eds) (1999): Handbook of the Birds of the World. Volume 5: Barn-owls to Hummingbirds. Barcelona, Lynx Editions.

Eisenberg JF (1981): The Mammalian Radiations. An Analysis of Trends of Evolution, Adaptation and Behavior. Chicago: University of Chicago Press.

Fischer QS, Kirby MA (1991): Number and distribution of retinal ganglion cells in anubis baboons (*Papio Anubis*). Brain Behav Evol 37:189-203.

Fite KV, Reiner A, Hunt SP (1981): Optokinetic nystagmus and the accessory optic systems of pigeon and turtle. Brain Behav Evol 16:192–202.

Hall MI, Ross CF (2007): Eye shape and activity pattern in birds. J Zool 271:437–444.

Hall MI, Gutiérrez-Ibáñez C, Iwaniuk AN (2009): The morphology of the optic foramen and activity pattern in birds. Anat Rec 292:1827-1845.

Hayes BP (1984): Cell populations of the ganglion cell layer: displaced amacrine and matching cells in the pigeon retina. Exp Brain Res 56:565-573.

Harmening WM, Wagner H (2011): From optics to attention: visual perception in barn owls. J Comp Physiol A 197:1031-1042.

Hackett SJ, Kimball RT, Reddy S, Bowie RCK, Braun EL, et al. (2008): A phylogenomic study of birds reveals their evolutionary history. Science 320: 1763–1768.

Heesy CP, Hall MI (2010): The nocturnal bottleneck and the evolution of mammalian vision. Brain Beahv Evol 75: 195-203.

Herculano-Houzel, S (2011): Not all brains are made the same: new views on brain scaling in evolution. Brain Behav Evol 78, 22–36.

Higgins PJ (Ed) (1999): *Handbook of Australian, New Zealand and Antarctic Birds*. Vol. 4 Parrots to Dollarbird. Melbourne, Oxford University Press

Husband S, Shimizu T (2001): Evolution of the avian visual system. In Cook RG (Ed) *Avian visual cognition* [On-line]. available:www.pigeon.psy.tufts.edu/avc/husband/

Gamlin PDR, Cohen DH (1988): Retinal projections to the pretectum in the pigeon (*Columba livia*). J Comp Neurol 269:1–17.

Gamlin PD, Reiner A, Erichsen JT, Karten HJ, Cohen DH (1984) The neural substrate for the pupillary light reflex in the pigeon (*Columba livia*). J Comp Neurol 226:523–543.

Garland T Jr, Harvey PH, Ives AR (1992): Procedures for the analysis of comparative data using phylogenetically independent contrasts. Syst Biol 41: 18–32.

Garland T Jr, Bennett AF, Rezende EL (2005): Phylogenetic approaches in comparative physiology. J Exp Biol 208: 3015–3035.

Gutiérrez-Ibáñez C, Iwaniuk AN, Wylie DR (2011): Relative size of auditory pathways in symmetrically and asymmetrically eared owls. Brain Behav Evol 87:286-301.

Iwaniuk AN, Hurd PL (2005): The evolution of cerebrotypes in birds. Brain Behav Evol 65:215-230.

Iwaniuk AN, Dean KM, Nelson JE (2005): Interspecific allometry of the brain and brain regions in parrots (Psittaciformes): comparisons with other birds and primates. Brain Behav Evol 65**:** 40-59.

Iwaniuk AN, Wylie DRW (2006): The evolution of stereopsis and the wulst in caprimulgiform birds: a comparative analysis. J Comp Physiol A 192:1313-1326.

Iwaniuk AN, Clayton DH, Wylie DR (2006): Echolocation, vocal learning, auditory localization and the evolution of the avian inferior colliculus (MLd). Behav Brain Res 167:305-317.

Iwaniuk AN, Wylie DRW (2007): Comparative evidence of a neural specialization for hovering in hummingbirds: hypertrophy of the pretectal nucleus lentiformis mesencephali. J Comp Neurol 500:211-221.

Iwaniuk AN, Hall MI, Heesy CP, Wylie DRW (2008): Neural correlates of orbit orientation in birds. J Comp Physiol A 194:267-282.

Iwaniuk AN, Heesy CP, Hall MI (2010a): Morphometrics of the eyes and orbits of the nocturnal swallow-tailed gull (*Creagrus furcatus*). Can J Zool 88:855-865.

Iwaniuk AN, Gutiérrez-Ibáñez C, Pakan JMP, Wylie DR (2010b): Allometric scaling of the tectofugal pathway in birds. Brain Behav Evol 75:122-137.

Karten, HJ (1969) The organisation of the avian telencephalon and some speculations on the phylogeny of the amniote telencephalon, *Ann. N.Y. Acad. SoL,* 167:167-179.

Karten H, Hodos W (1967): A Stereotaxic Atlas of the Brain of the Pigeon (*Columba livia*). Baltimore, Johns Hopkins University Press.

Karten HJ, Nauta WHJ (1968) Organization of retinothalamic projections in the pigeon and the owl, Anat. Rec 160:373.

Karten HJ, Hodos W, Nauta WHJ Revzin,AM (1973) Neural connections of the 'visual wulst' of the avian telencephalon. Experimental studies in the pigeon *(Columba livia)* and the owl *Speotyto cunicularia*), J. comp. Neurol., 150 (1973) 253-277.

Karten HJ, Fite KV, Brecha N (1977): Specific projection of displaced retinal ganglion cells upon the accessory optic system in the pigeon (Columba livia). Proc Natl Acad Sci U S A 74:1753–1756.

Karten, HJ, Konishi, M, Pettigrew JD, (1978): Somatosensory representation in the anterior Wulst of the owl (*Speotyto cunicularis*). Soc. Neurosci. Abstr., 4:554.

Kay RF, Kirk EC (2000): Osteological evidence for the evolution of activity pattern and visual acuity in primates. Am J Physical Anthropol 113:235–262.

Kirk EC, Kay RF (2004): The evolution of high visual acuity in the Anthropoidea; In: Ross CF, Kay RF (eds) Anthropoid origins: new visions. New York, Kluwer Academic/Plenum, pp 539–602.

Kaskan P, Franco C, Yamada E, Silveira LCL, Darlington RB, Finlay BL (2005): Peripheral variability and central constancy in mammalian visual system evolution. Proc R Soc Lond B 272:91–100.

Konishi M (1973): How the owl tracks its prey. Am Sci 61: 414–424.

König C, Weick F (2008): Owls of the World, Second Edition. London, Christopher Helm.Kotrschal K, van Straaden MJ. Huber R (1998): Fish brains: evolution and environmental relationships. Reviews in Fish Biology and Fisheries 8**:**373-408.

Lisney TJ, Rubene D, Rózsa J, Løvlie H, Håstad O, Ödeen A (2011): Behavioural assessment of flicker fusion frequency in chicken *Gallus gallus domesticus*. Vision Res 51:1324-1332.

Lisney TJ, Iwaniuk AN, Bandet MV, Wylie DR (2012): Eye shape and retinal topography in owls (Aves: Strigiformes). Brain Behav Evol 79:218-236

Matochik JA, Reems CN, Wenzel BM (1991): A brain atlas of the northern fulmar (*Fulmarus glacialis*) in stereotaxic coordinates. Brain Behav Evol 37:215–244.

Martin GR (1986): Sensory capacities and the nocturnal habit of owls (Strigiformes). Ibis 128:266–277.

Martin GR, Wilson KJ, Wild MJ, Parsons S, Kubke MF, Corfield J (2007): Kiwi forego vision in the guidance of their nocturnal activities. PLoS One 2:e198.

Maturana HR, Varela FJ (1982): Color-opponent responses in the avian lateral geniculate: a study in the quail (*Coturnix coturnix japonica*). Brain Res 247:227-41.

McKenna O, Wallman J (1985): Accessory optic system and pretectum of birds: comparisons with those of other vertebrates. Brain Behav Evol 26:91–116.

Nieder A, Wagner H (1999): Perception and neuronal coding of subjective contours in the owl. Nat Neurosci. 2:660-3.

Nieder A, Wagner H (2001): Encoding of both vertical and horizontal disparity in random-dot stereograms by Wulst neurons of awake barn owls. Vis Neurosci. 18:541-7.

Norberg RA (1977): Occurrence and independent evolution of bilateral ear asymmetry in owls and implications on owl taxonomy. Phil Trans R Soc Lond B 280: 375–408.

Nguyen AP, Spetch ML, Crowder NC, Winship IR, Hurd PL, Wylie DRW (2004): A dissociation of motion and spatial-pattern vision in the avian telencephalon: Implications for the evolution of "visual streams". Journal of Neuroscience 24:4962-4970.

Oehme H (1961): Vergleichend-histologische Untersuchungen an der Retina von Eulen. Zool Jb Anat 79:439-478.

Payne RS (1971): Acoustic location of prey by barn owls *(Tyto alba)*. J Exp Biol 54: 535–573.

Pettigrew JD (1979): Binocular visual processing in the owl's telencephalon. Proc R Soc Lond B Biol Sci. 204:435-54.

Pettigrew JD, Konishi M (1976): Neurons selective for orientation and binocular disparity in the visual Wulst of the barn owl (Tyto alba). Science. 193:675-8.

Puelles L, Martinez-de-la-Torre M, Paxinos G, Watson C, Martinez S (2007): The Chick Brain in Stereotaxic Coordinates: An Atlas Featuring Neuromeric Subdivisions and Mammalian Homologies. San Diego: Academic Press.

Rojas de Azuaje LM, Tai S, McNeil R (1993): Comparison of rod/cone ratio in three species of shorebirds having different nocturnal foraging strategies. Auk 110:141-145

Reiner A, Brecha N, Karten HJ (1979): A specific projection of retinal displaced ganglion cells to the nucleus of the basal optic root in the chicken. Neuroscience 4:1679-1688

Reiner A, Perkel DJ, Bruce LL, Butler AB, Csillag A, Kuenzel W, Medina L, Paxinos G, Shimizu T, Striedter G, Wild M, Ball GF, Durand S, Güntürkün O, Lee DW,Mello CV, Powers A, White SA, Hough G, Kubikova L, Smulders TV, Wada K, Dugas-Ford J, Husband S, Yamamoto K, Yu J, Siang C, Jarvis ED; Avian Brain Nomenclature Forum (2004): Revised nomenclature for avian telencephalon and some related brainstem nuclei. J Comp Neurol. 473(3):377-414.

Reynolds P, Gorman ML (1999): The timing of hunting in short-eared owls (*Asio flammeus*) in relation to the activity patterns of Orkney voles (*Microtus arvalis orcadensis*). J Zool 247:371-379.

Roth G. Dicke U, Nishikawa K (1992): How do ontogeny, morphology, and physiology of sensory systems constrain and direct the evolution in amphibians? Am Nat 139:S105–S124.

Sibley CG, Ahlquist JE (1990): Phylogeny and classification of birds. New Haven, Yale University Press.

Stokes TM, Leonard CM, Nottebohm F (1974): The telencephalon, diencephalon, and mesencephalon of the canary, *Serinus canaria*, in stereotaxic coordinates. J Comp Neurol 156:337-374.

Stone J, Keens J (1980): Distribution of small and medium-sized ganglion cells in the cat's retina. J Comp Neurol 192:235-246.

Stingelin W (1958): Vergleichend morphologische Untersungen an Vorderhirn der Vogel auf cytologischer and cytoarchitektonischer Grundlage. Basel, Helbing and Lichtenhahn.

Sun HJ, Frost BJ (1998): Computation of different optical variables of looming objects in pigeon nucleus rotundus neurons. Nat Neurosci 1:296–303.

Tansley K, Erichsen JT (1985) Vision; In: Campbell B, Lack E (eds): A dictionary of birds B.Poyser, Calton, pp 623-629.

Vega-Zuniga T, Campos L, Severin D, Marin G, Letelier J, Mpodozis J (2011): The avian ventral nucleus of the lateral Geniculate (GLv) has key role in the generation of visually guided gaze orientation movements. Program No. 272.17 2011 Neuroscience Meeting Planner. Washington, DC, Society for Neuroscience. Online.

Voous KH (1988): Owls of the Northern Hemisphere. Cambridge, The MIT Press.

Wagner H, Frost B (1994) Binocular responses of neurons in the barn owl's visual Wulst. J Comp Physiol. A 174:661-670,

Wallman, J, Pettigrew, JD (1985): Conjunctive and disjunctive saccades in two avian species with contrasting oculomotor strategies. J Neurosci 5:1418–1428.

Wang YC, Jiang S, Frost BJ (1993): Visual processing in pigeon nucleus rotundus: luminance, color, motion, and looming subdivisions. Vis Neurosci 10:21–30.

Wakita M, Watanabe S, Shimizu T, Britto LR (1992): Visual discrimination performance after lesions of the ventral lateral geniculate nucleus in pigeons (*Columba livia*). Behav Brain Res 51:211–215.

Warrant E (2004): Vision in the dimmest habitats on Earth. J Comp Physiol A 190:765-789.

Wathey JC, Pettigrew JD (1989): Quantitative analysis of the retinal ganglion cell layer and optic nerve of the barn owl *Tyto alba*. Brain Behav Evol 33:279–292

Wild JM, Kubke MF, J.L. Peña JL (2008) A pathway for predation in the brain of the barn owl (Tyto alba): Projections of the gracile nucleus to the "claw area" of the rostral wulst via the dorsal thalamus, The J Comp Neurol. 509: 156-166.

Wink M, Heidrich P, Sauer-Gurth H, Elsayed AA, Gonzalez J (2008): Molecular phylogeny and systematics of owls (Strigiformes); In: Konig C, Weick F (eds): Owls of the world. London, Christopher Helm, pp 42–63.

Chapter 5: **Functional Implications of Species Differences in the Size and Morphology of the Isthmo Optic Nucleus (ION) in Birds**

A version of this chapter has been published:

Gutiérrez-Ibáñez C, Iwaniuk AN, Lisney TJ, Faunes M, Marín G, and Wylie DR (2012): Functional Implications of Species Differences in the Size and Morphology of the Isthmo Optic Nucleus (ION) in Birds PLoS ONE 7(5): e37816. doi:10.1371/journal.pone.0037816.

In all major groups of vertebrates there are retinofugal visual fibers projecting from the brain to the retina (for a complete review see Reperant et al., 2006 and 2007]). Retinofugal visual fibers are particularly well developed in birds, as first described by Cajal [1888; 1889] and Dogiel [1895]. In birds, the majority of the cells giving rise to the retinofugal fibres are found in the isthmo optic nucleus (ION), a group of cells in the most dorso-caudal part of the isthmal region of the midbrain [see fig. 5.1B–D; O'Leary and Cowan, 1982, Weidner et al., 1987, 1989 Wolf-Oberhollenzer, 1987].

Despite a large number of anatomical, physiological and histochemical studies, the function of the retinofugal system in birds remains unclear and a wide range of hypotheses have been proposed [reviewed in Reperant et al., 2006 and Wilson and Lindstrom, 2010]. Some suggest the ION is involved in selective shifting of visual attention in the retina, either between relevant stimuli [Rogers and Miles 1972; Uchiyama 1989; Ward et al., 1991; Uchiyama and Barlow, 1994; Uchiyama et al., 1998] or between the ventral and dorsal parts of the retina [Wilson and Lindstrom, 2010; Casticas et al., 1987; Clarke et al., 1996]. Alternative hypotheses include: involvement in the saccadic suppression of retinal activity [Holden, 1968; Nickla et al., 1994], enhancement of peripheral vision [Marin et al., 1990] and modulation of temporal processing [Knipling, 1978]. In addition, the more complex organization and larger number of cells of the ION in pecking birds (and the smaller size in non-pecking birds) has led to the hypothesis that the ION is involved in ground feeding, either visually searching for small

objects or in the control of pecking behavior [Weidner, 1987; Shortess and Klose 1977; Reperant et al., 1989; Hahmann and Gunturkun 1992, Miceli et al., 1999].

In vertebrates, sensory specializations are often correlated with increases in the size of brain areas associated with that specialization (‘‘The principle of proper mass’’; Jerison, 1973]) This has been shown repeatedly among vertebrates in relation to not only sensory specializations, but also motor skills and ‘complex’ behaviors [e.g. Pubols et al., 1965; Pubols and Pubols 1972; Finger, 1975; Barton, 1998; Iwaniuk and Wylie 2007]. In most of these studies, the correlation between a structure and a behavior is established with an a priori knowledge that the structure is related to the generation of the behavior or sensory modality. In the case of the ION, the opposite strategy has been applied; the relative size and organization of the structure has driven some of the theories about its’ function. Although the ‘ground–feeding hypothesis’ is congruent with the published comparative data, the ION has only been described for a few orders and cell numbers are available for even fewer species. If comparative data is to be used to aid in determining the function of the retinofugal system, then a broad comparative analysis of the relative size and organization of the ION, comprising a diversity of bird species with different ecological niches and feeding habits, is required. In this study, we compared the cytoarchitectonic organization and relative volume of the ION in 81 species of birds belonging to 17 different orders to gain further insight on the function and evolution of the retinofugal pathway in birds. Because previous studies [e.g. Weidner et al., 1987; Reperant et al., 1989; Shortess and Klose 1975; Feyerabend et al., 1994] focused on cell counts as an

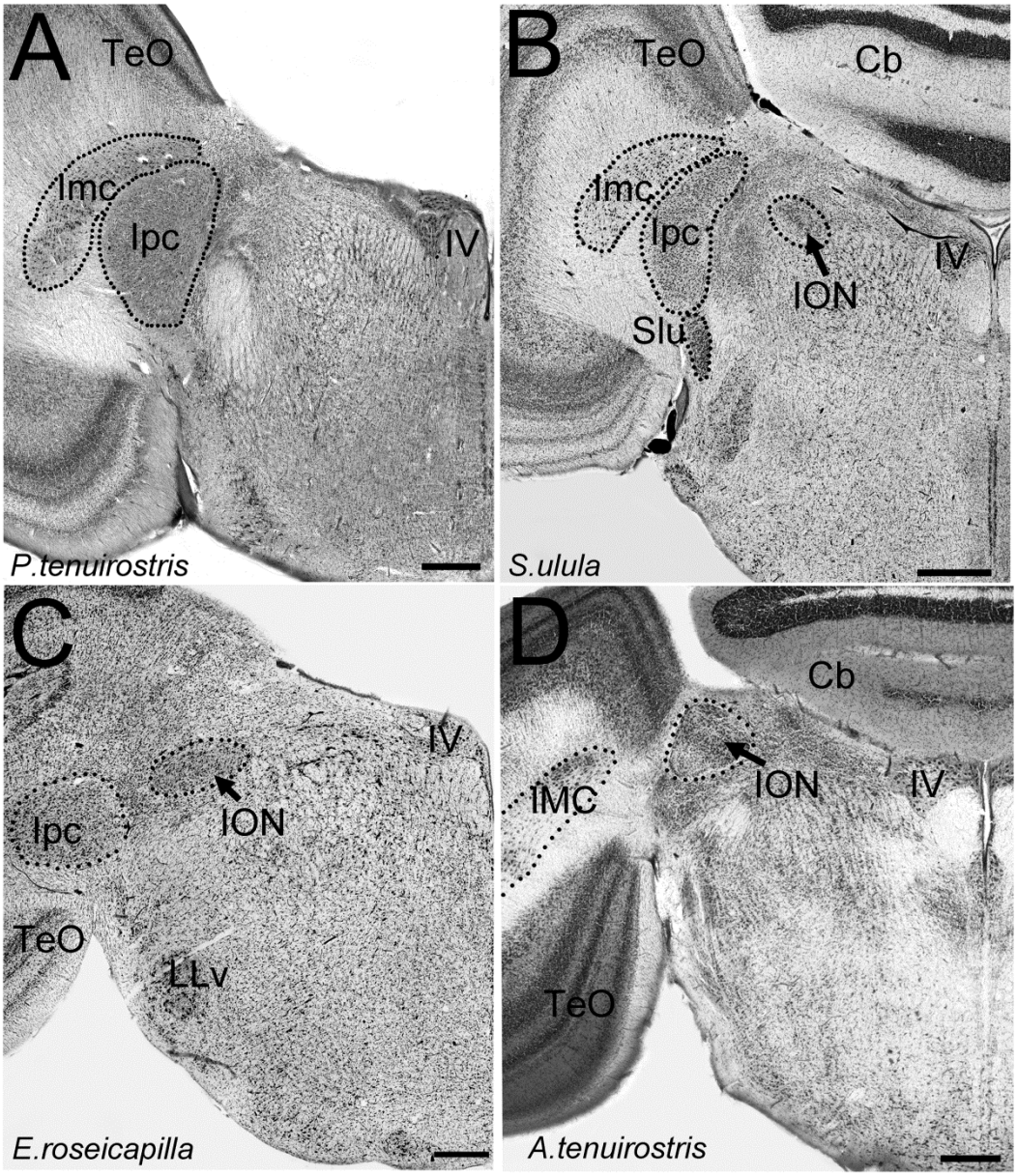
A
TeO
lmc
lpc
IV
P.tenuirostris
B
TeO
Cb
lmc
lpc
IV
ION
Slu
S.ulula
C
IV
ION
lpc
TeO
LLv
E.roseicapilla
D
Cb
ION
IV
lMC
TeO
A.tenuirostris

Figure 5.1. Location of the isthmo optic nucleus (ION) in the brainstem. Photomicrographs of coronal sections through the brainstem of different species of birds showing the location of the isthmo optic nucleus (**ION**). **A** shows the absence of ION in a seabird (Procellariiformes), the Short-tailed Shearwater (*Puffinus tenuirostris*). The coronal section is through the brainstem, at the level of the trochlear nucleus (**IV**), where the ION is usually found in other birds. **B** to D show the ION in (**B**) an owl (Strigiformes), the Northern Hawk Owl (*Surnia ulula*); (**C**) a parrot (Psittaciformes), the Galah (*Eolophus roseicapilla*); (**D**) a songbird (Passeriformes), the Eastern Spinebill (*Acanthorhynchus tenuirostris*). **Imc** = nucleus isthmi magnocellularis; **Ipc** = nucleus isthmi parvocellularis; **TeO** = optic tectum; **Cb** = Cerebellum; **LLv** = ventral part of the lateral lemniscus; Slu = nucleus semi lunaris. Scale bars in A and C= 400 μm, in B= 600 μm.

indicator of the ION size, we also counted the number of cells in 58 of these species to examine the number and density of cells in the ION among birds.

Using this broad, comparative dataset, we tested two of the theories regarding ION function. First, if the ground-feeding hypothesis is correct, we would expect that all ground-feeding birds, regardless of what order they belong to, will have enlarged ION volumes relative to brain volume and that the ION will contain a greater number of cells. Conversely, species that do not feed on the ground, such as hummingbirds, parrots and some songbirds and pigeons, are expected to have relatively smaller IONs with fewer cells. Second, Wilson and Lindstrom [2011] recently proposed that the ION is involved in the detection of aerial predators and predicted that the ION should be enlarged and have more cells in birds that are heavily predated upon by other birds. From a comparative perspective, we would predict that parrots, coots, pigeons, some songbirds, galliforms (*i.e.* quail, pheasant and relatives) and waterfowl, which are under significant predation pressure from aerial predators [Eddleman et al., 1985; Lindsey et al., 1994; Aumann, 2001], would have enlarged IONs containing more cells. The corollary of this theory is that groups that are rarely predated by other birds, amely owls, diurnal raptors (*i.e.*, hawks and falcons), woodpeckers, nightjars and seabirds should have relatively small IONs with fewer cells. Given the reported diversity of cell numbers and size of the ION among some avian orders, we also examined changes in the relative size and morphology of the ION across several phylogenetic trees to assess how the ION has evolved.

5.1 Materials and Methods

5.1.3 Ethics Statement

All specimens were provided to us dead by conservation authorities, wildlife veterinarians and museum staff and thus approval was not required by an institutional ethics committee to undertake this research.

5.1.3Measurements

We measured the relative volume, number of cells and cytoarchitecture of the ION in 83 specimens representing 81 species (Appendix B). In addition we examined the gross cytoarchitecture of several additional specimens loaned to us from museums. For these museum specimens, the volume and number of cells of the ION were not measured because of potential tissue shrinkage arising from long term storage of museum specimens in 70% ethanol. A complete list of these museum specimens is provided in Appendix C.

While we did report the cytoarchitectonic organization of the ION in the domestic chicken (*Gallus domesticus*; see results, Appendix A) we did not include this species in our volumetric or cells number analyzes because we have concerns relating to the domesticated nature of this species. Several studies [e.g. Ebinger and Lomer, 1987; Ebinger and Rhors 1995; Ebinger, 1995] have shown that domestication has profound effects on the relative size of different parts of the brain, as well as in the overall brain size, both in birds and other vertebrates.

For all specimens in which the ION volume was measured, the head was immersion-fixed in 4% paraformaldehyde in 0.1 M phosphate buffer. The brain was then extracted, weighed to the nearest milligram, cryoprotected in 30%

sucrose in phosphate buffer, embedded in gelatin and sectioned in the coronal or sagittal plane on a freezing stage microtome at a thickness of 40 μm. Sections were collected in 0.1 M phosphate buffered saline, mounted onto gelatinized slides, stained with thionin and coverslipped with Permount. The olfactory bulbs were intact in all of the specimens that we collected and sectioned. All brains were cut following bird brain atlases [e.g. Karten and Hodos, 1967; Puelles et al., 2007] in which the brainstem ends at the same rostrocaudal point as the cerebellum. In this manner, brain measurements were consistent among our specimens.

Photomicrographs of every second section were taken throughout the rostrocaudal extent of each nucleus using a Retiga EXi FAST Cooled mono 12-bit camera (Qimaging, Burnaby, BC, Canada) and OPENLAB Imaging system (Improvision, Lexington, MA, USA) attached to a compound light microscope (Leica DMRE, Richmond Hill, ON, Canada). Exceptions to this were four owl species in which photomicrographs were taken of every fourth section because the remaining series were required for an unrelated study. Measurements of all the nuclei were taken directly from these photos with ImageJ (NIH, Bethesda, MD, USA; http://rsb.info.nih.gov/ij/) and volumes were calculated by multiplying the area in each section by the thickness of the section (40 μm) and the sampling interval. For those species represented by more than one specimen (Appendix B), the average of the measurements was taken as the species' given value.

5.1.4 Borders of Nuclei

The ION lies in the dorsal isthmus, medial to the caudodorsomedial edge of the optic tectum, at the level of the trochlear nucleus (fig. 5.1A–D). Because no previous studies have described in detail the morphology and cytoarchitecture of the ION in a large groups of birds we provide detailed descriptions below. Briefly, the ION consists of a darkly stained group of cells that lies lateral and posterior to the root of the mesencephalic trigeminal nerve and medial to the parvocellular part of the nucleus isthmi, at the same level as the trochlear nucleus (fig. 5.1A–D).

5.1.5 Cells Counts

We counted the number of cells in the ION in 59 species for comparison with previous studies [Weidner et al., 1987; Reperant et al., 1989; Shortess and Klose 1975; Feyerabend et al., 1994; Sohal and Narayanan, 1975; Hirshberger, 1971]. In several specimens, cells counts were not obtained. Although the Nissl stain was of sufficient quality to establish the borders of the ION, it did not allow us to differentiate between the cell nuclei and nucleoli, and therefore precluded an accurate estimation of cell numbers. Cells were counted in the same sections used for volume estimation using an unbiased stereological method, the optical fractionator [West et al., 1991; Howard and Reed, 2005]. An unbiased counting frame [Gundersen, 1977] was positioned on the coordinates of a square lattice randomly superimposed on the section. Because of the large variation in absolute volume of the ION among the sampled species, both the size of the counting frame and the distance between the coordinates of the lattice were varied to assure

a minimum count of 80 cells. The area of the counting frame was either 0.00118 mm2 or 0.003 mm2, while the distance between the coordinates was between 0.2 and 0.1 mm along each axis. At each sampling point, the thickness of the sections was determined as the distance between that of the first particle coming into focus and the last particle going out of focus [West et al., 1991]. An unbiased brick-counting rule [Gundersen and Osterby, 1981; Howard et al., 1985] was used. That is, an unbiased counting frame was projected onto the thickness of the section resulting in a cuboid with the upper, top and left planes as acceptable surfaces and all others as unacceptable surfaces. Thus, if a cell contacted the lower, bottom or right planes, it was not counted. The height of the counting brick was two thirds of the total measured thickness. Nuclear profiles containing a nucleolus were counted using a 100X objective. At least 80 cells were counted per ION across all specimens. Coefficients of error were calculated using Scheaffer's estimator [Sheaffer et al., 1996; Schmitz and Hof, 2000] for non-homogeneous distributions of cells.

5.1.6 Statistical Analyses

To examine scaling relationships, we plotted the log10-transformed volume of each brain region against the log10- transformed brain volume minus the volume of each specific region [Deacon, 1990]. Allometric equations were calculated using linear least squares regressions using: (1) species as independent data points, and (2) phylogenetic generalized least squares (PGLS) to account for phylogenetic relatedness [Garland and Ives, 2000; Garland et al., 2005]. We

applied two models of evolutionary change as implemented in the MATLAB program Regressionv2.m [available from T. Garland, Jr., on request; Ives et al., 2007; Lavin et al., 2008]: Brownian motion (phylogenetic generalized least-squares or PGLS) and Ornstein–Uhlenbeck (OU) [Lavin et al., 2008; Swanson and Garland, 2009]. Akaike Information Criterion (AIC) was used to determine which model best fit the data. The model with the lowest AIC is considered to be the best fit [Lavin et al., 2008]. Models with AIC different by less than 2 units can also be considered as having substantial support [Burnham and Anderson, 2002; Duncan et al., 2007]. Because different phylogenetic trees can yield different results [Iwaniuk, 2004], we tested four models based on the trees provided in Cracraft et al., [2004], Livezey and Zusi [2007], Davis [2008], and Hackett et al. [2008]. Resolution within each order was provided by order- and family-specific studies [Brown and Toft, 1999; Johnson and Sorenson, 1999; Donne-Goussé et al., 2002; Barker et al., 2004; Driskell and Christidis, 2004; Wink and Sauer-Gürth, 2004; Pereira et al., 2007; Kimball and Braun, 2008; Wink et al., 2008; Wright et al., 2008], although this left several nodes unresolved. Phylogenetic trees, character matrices and phylogenetic variance-covariance matrices were constructed using Mequite/PDAP:PDTREE software [Midford et al., 2008; Maddison and Maddison, 2009] and the PDAP software package (available from T. Garland upon request). Because the phylogeny was constructed from multiple sources, branch lengths were all set at 1, which provided adequately standardized branch lengths when checked using the procedures outlined in Garland et al. (1992). Unresolved nodes were treated as soft polytomies, with branch lengths

between internal nodes set to zero [Purvis and Garland, 1993]. Allometric equations based on standard statistics, and the PGLS and OU models, calculated for each of the four trees, were calculated for: 1) ION volume against brain volume, (2) ION cell numbers against ION volume and (3) ION cell density against brain volume (Appendix D). We also included the avian orders and ION complexity categories (see results) as covariates in tree models to see if there is an effect of the orders or categories on the different variables. Currently there is no phylogenetically corrected pair wise comparison available and therefore Tukey HSD post hoc tests where only performed on non-phylogenetically corrected statistics. Because of the low number of species in some groups (e.g. woodpeckers), we also used the relative size of ION expressed as a percentage of the total brain volume in order to provide further comparisons between the different orders.

Non-phylogenetically corrected statistics and post-hoc tests were performed in the software JMP (JMP, Version 7. SAS Institute Inc., Cary, NC, 1989–2007). Additionally, we calculated phylogeny- corrected 95% prediction intervals using the PDAP module [Midford et al., 2008] of the Mesquite modular software package [Maddison and Maddison, 2009] to look for any significant outliers. To map the cytoarchitectonic organization of the ION on to an avian phylogeny, we constructed a phylogenetic tree of the orders used in this study (Appendix B) based on the phylogenetic relationships established by Hackett et al., (2008). While currently there is no consensus regarding the phylogenetic relationships among most orders of birds [e.g. Cracraft et al., 2004; Livezey and

Zusi, 2007; Davis, 2008; Sibley and Ahlquist 1990], the use of different phylogenies in this part of the analysis did not alter our general conclusion and therefore we present only one of the possible phylogenies.

5.2 Results

5.2.1 ION Morphology

Because we observed great variation in the cytoarchitectonic organization of the ION among species, we developed a categorical grading system to quantify the degree of complexity of ION organization. The grading system consists of 6 numerical categories (0–5) that differ from one another in how much of the ION as organized into distinct layers (laminae). In species with less complex IONs, most cells are evenly distributed throughout the nucleus. As the complexity increases (see below), more cells are organized in layers and the amount of neuropil (cell-free lamina) increases.

Categrory 0. This category is characterized by the absence of a recognizablegroup of cells that can be identified as theION.Species lacking an ION include the Chilean Tinamou (*Nothoprocta perdicaria*, Tinamiformes), seabirds (*i.e.*, shearwater and albatross, fig. 5.1A), the Australian Pelican (*Pelecanus conspicillatus* Pelecaniformes), and the Spotted Nightjar (*Eurostopodus argus*, Caprimulgiformes).

Category 1. In this category the ION is readily recognizable as an oval mass of evenly distributed cells. However, compared to other categories, the borders are somewhat indistinct (fig. 5.2A–C).

Category 2. In species within category 2, the border of ION is clearly defined and surrounded by a cell free neuropil (fig. 5.2D, E). Most cells are evenly distributed throughout the nucleus, although the beginnings of lamination are present, insofar as there is a layer along the outer edge of the ION. However, this layer does not encapsulate the ION. (For example, see the lateral edge of ION in fig. 5.2D and the medial edge in fig. 5.2E).

Category 3. Compared to category 2, ION in category 3 is characterized by a sharper border with a distinct layer of cells that encapsulates the rest of the nucleus (fig. 5.2F, G). Also, in the category, there is a suggestion of neuropil adjacent to this exterior cell layer. Otherwise the cells are evenly distributed throughout the ION in a reticular manner (fig. 5.2F, G).

Category 4. In category 4, a neuropil is clearly recognizable within the external layer of cells. Nonetheless, some cells still are distributed in a non-laminated fashion within the ION (fig. 5.3A–C).

Category 5. Finally, in category 5, all cells appear to be organized into distinct layers both peripherally and within the ION, with a clearly recognizable neuropil between the layers of cells. Also, both the cell layers and the neuropil are thicker than in the other categories (fig. 5.3D–F). These categories are widely spread among orders. In all diurnal raptors (fig. 5.2 A), owls (fig. 5.2B), hummingbirds (fig. 5.2C) and herons, the ION was classified as category 1. Inspection of several other hummingbird species and two swift species from museums (see Appendix C) demonstrated that a simple cytoarchitectonical organization of the ION is widespread in the Apodiformes. In waterfowl, all species belong to category 1

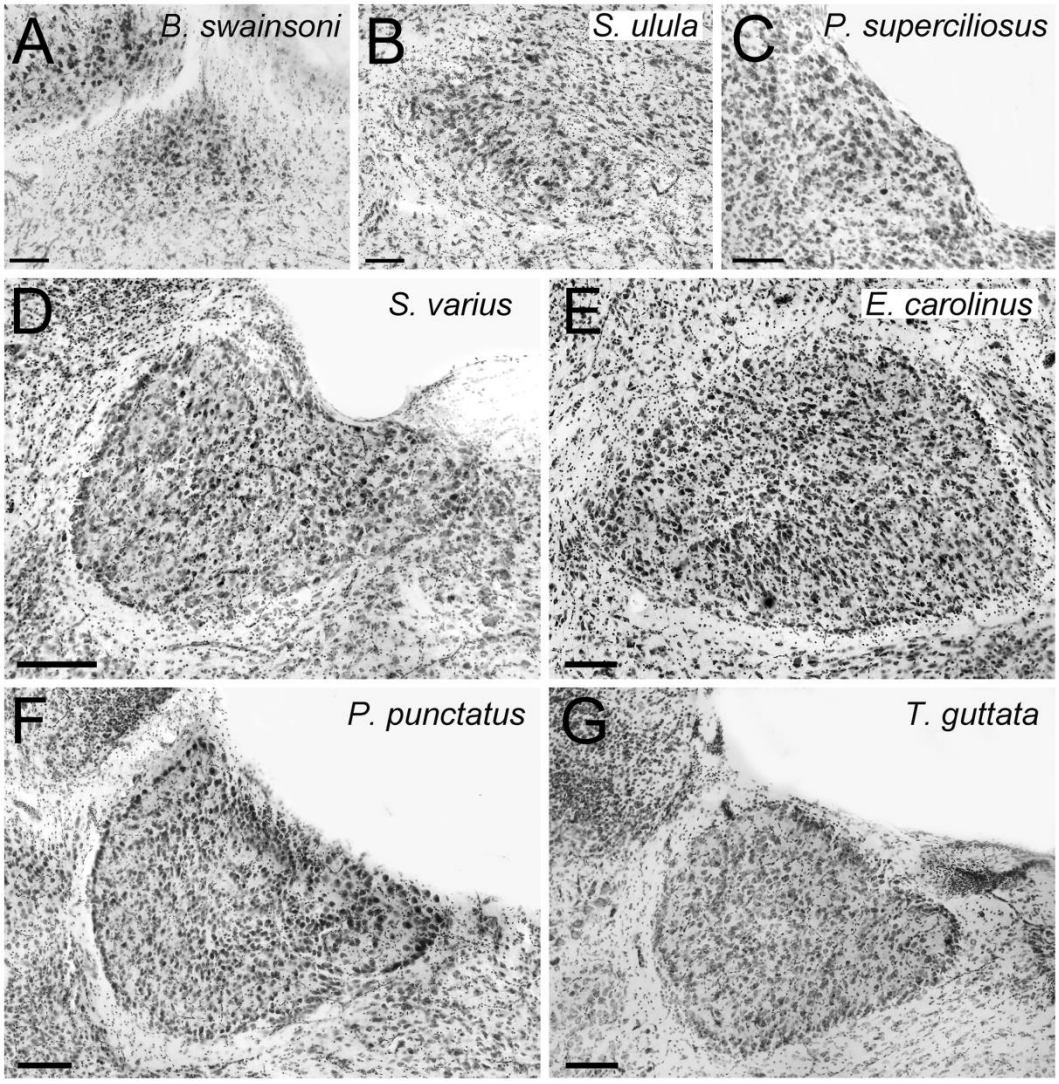
A
B. swainsoni
B
S. ulula
C
P. superciliosus
D
S. varius
E
E. carolinus
F
P. punctatus
G
T. guttata

Figure 5.2. Variation of the complexity of the cytoarchitectonic organization of ION: Categories 1–3. Photomicrographs of coronal sections through the isthmo optic nucleus (ION) showing the variation of the complexity of the cytoarchitectonic organization of ION in different species of birds. **A** to **C** shows species that belong to category 1 of ION complexity (see methods). **A**, a diurnal raptor (Falconiformes), the Swainson's Hawk (*Buteo swainsoni*); **B** an owl (Strigiformes), the Northern Hawk Owl, (*Surnia ulula*); **C** a hummingbird (Apodiformes), the Long-tailed Hermit (*Phaethornis superciliosus*); **D** and **E** shows species that belong to category 2 of ION complexity. **D** a woodpecker (Piciformes), the Yellow-bellied Sapsucker (*Sphyrapicus varius*); **E** a songbird (Passeriformes), the Rusty Blackbird (*Euphagus carolinus*); **F** and **G** shows species that belong to category 3 of ION complexity. **F** the Spotted Pardalote (*Pardalotus punctatus*); **G** the Zebra Finch (*Taeniopygia guttata*). **F** and **G** are both songbirds. Scale bars = 100 μm.

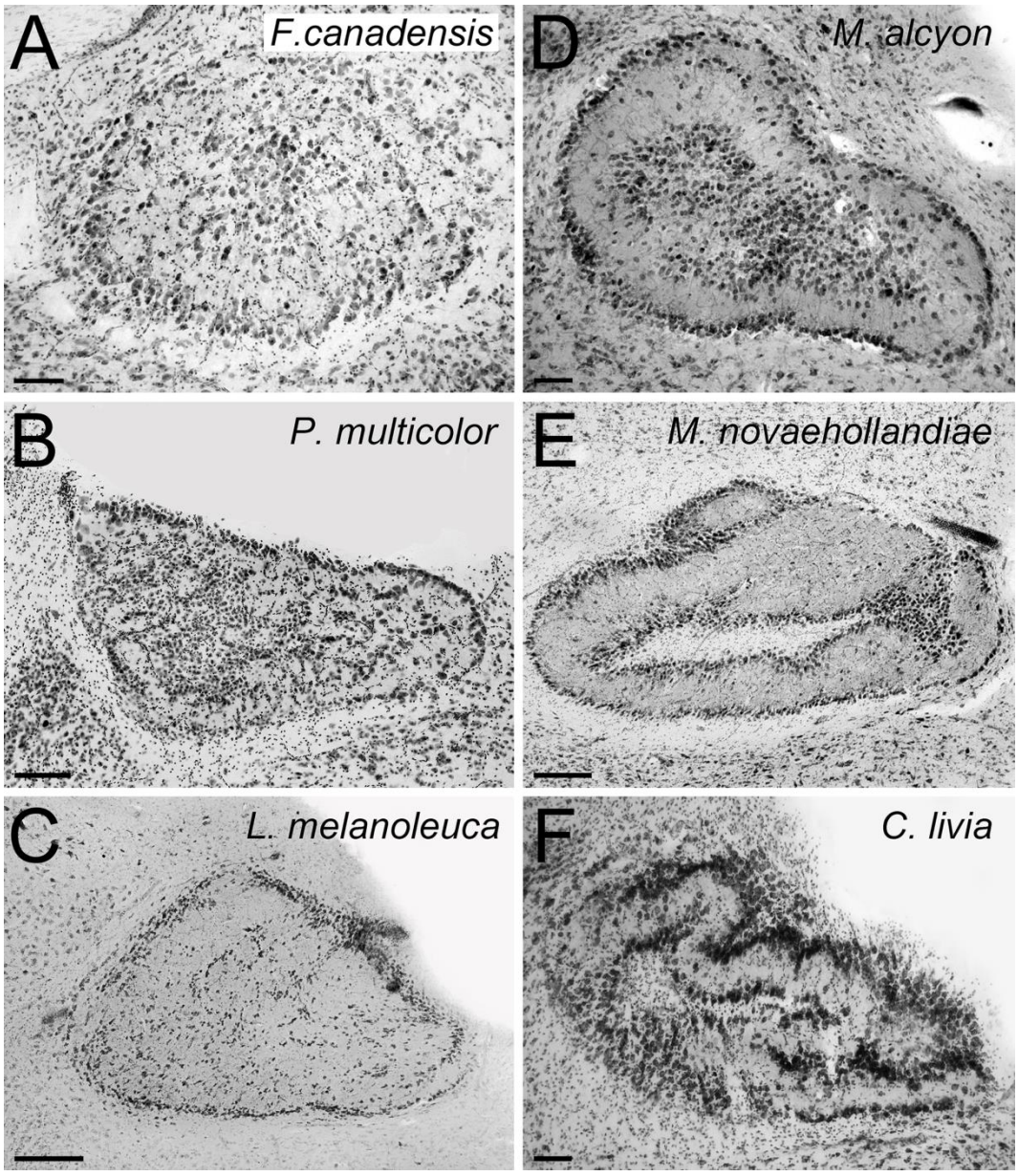
A
F.canadensis
D
M. alcyon
B
P. multicolor
E
M. novaehollandiae
C
L. melanoleuca
F
C. livia

Figure 5.3. Variation of the complexity of the cytoarchitectonic organization of ION: Categories 4 and 5. Photomicrographs of coronal sections through the isthmo optic nucleus (ION) showing the variation of the complexity of the cytoarchitectonic organization of ION in different species of birds (see methods). A to C shows species that belong to category 4 of ION complexity. **A** shows a Galliform, the Spruce Grouse (*Falcipennis canadensis*); **B** showa songbird, the Scarlet Robin (*Petroica multicolor*); C shows a Columbiform, the Wonga Pigeon (*Leucosarcia melanoleuca*); D to F shows species that belong to category 5 of ION complexity. **D** a Coraciiform, the Belted Kingfisher (*Megaceryle alcyon*); **E** a songbird, the Superb Lyrebird (*Menura novaehollandiae*); **F** the Rock Pigeon (*Columba livia*). Scale bars = 100 μm, in E and C= 200 μm.

except for the Lesser Scaup (*Aythya affinis*), which belongs to category 2. Among parrots, more than half of the species studied were classified as category 1 (5/8 species). The remaining three species were classified in category 2 (2 sp.) or 3 (Appendix B, fig. 5.4C). Shorebirds also have a less complex ION, with all species in categories 1 and 2. Coots and allies appear to have moderately complex IONs with species in categories 2 and 3. Pigeons and doves also show relatively uniform complexity of their IONs, with almost all species in categories 4 and 5 (Appendix B, fig. 5.3C, F, 5.4C). The exception is the Brush Bronzewing, Phaps elegans, (category 1). Within the order Piciformes, the Yellow-Bellied Sapsucker (*Sphyrapicus varius*) has an ION in category 2 (fig. 5.2D), but inspection of the museum specimens demonstrated that members of other families within the order have more complex IONs (Appendix C, fig. 5.4C). A similarly diverse range of ION morphologies occurs in the galliforms, where ION complexity ranges from categories 2 to 4 (fig. 5.3A, 4C). While not included in our volumetric analysis (see methods), inspection of a domestic chicken shows that this species has an ION in category 4 (Appendix A). An even broader range occurs in the kingfisher (Coraciiformes), even though they were only represented by two species. The Laughing Kookaburra (*Dacelo novaeguineae*) has a less complex ION (category 2) but the Belted Kingfisher (*Megaceryle alcyon*), has a very complex ION (category 5, fig. 3D). Finally, songbirds have the greatest variation in ION complexity of all of the orders that we examined, with species spanning categories 1 through 5 (fig. 5.2E–G, 5.3 B, E, 5.4C).

5.2.2 Relative Size of ION

ION varies greatly among taxa not only in morphology but also in relative size (fig. 5.4). A regression of ION volume against brain volume with orders as a covariate shows a significant effect of order on the relative size of ION. Based on AIC values, the OU approach yields the best fit for all phylogenies and corroborates the significant effect of order on the relative size of ION in the four phylogenies used (Appendix D). Tukey HSD post hoc comparisons indicated that pigeons, galliforms and songbirds have significantly larger relative ION volumes than waterfowl, parrots, owls and diurnal raptors. Also, the woodpecker, hummingbirds, non beakprobing shorebirds, coots, waterfowl and parrots have significantly larger relative ION volumes than owls and diurnal raptors. Pigeons and hummingbirds, for example, have relative ION volumes (expressed as a percentage of the total brain volume) that are about three times that of parrots and waterfowl and nine times that of diurnal raptors and owls (fig. 5.4C). Songbirds have, on average, IONs that are relatively smaller than those of pigeons and hummingbirds but which are still 8 times larger than those in diurnal raptors and owls. The Yellow Bellied Sapsucker (a woodpecker) has a relative ION volume between that of songbirds and galliforms. It is twice the size of parrots and waterfowl and more than 7 times that of diurnal raptors and owls. Also, galliforms and coots have IONs that are 5 to 6 times bigger than diurnal raptors and owls. Finally, beak-probing shorebirds, the frogmouth (a caprimulgiform) and the

Laughing Kookaburra have relative small ION volumes, similar to diurnal raptors and owls.

Not only are there large differences among orders but also substantial variation within some orders. For example, among songbirds, the relative size of ION (expressed as a percentage of the total brain volume) in the Brown Thornbill (*Acanthiza lineata*, 0.031) is three times that of other songbirds, like the Superb Lyrebird (*Menura novaehollandiae*, 0.0106) or the Australian Magpie (*Cracticus tibicen*, 0.0099). Similarly, within the order Charadriiformes, there is a clear difference in the relative size of ION between beak-probing shorebirds and non beak-probing shorebirds (gulls) (fig. 5.4A, C). As shown in Figure 5.4A, there is considerable scatter around the regression line depicting the relationship between ION and brain size. The correlation coefficients associated with the regression lines derived from conventional statistics and the phylogenetically corrected statistics using both models of evolutionary change (PGLS and OU) are all below 0.5 (Appendix D), indicating that brain size explains less than 50% of the variation in ION size. Phylogeny-corrected prediction intervals showed that only the Swainson's hawk (*Buteo swainsonii*) as an outlier and only when Davis' [2008] phylogeny is used. Not only does relative ION size vary among orders but also among our categories of cytoarchitectonic organization. Figure 5.4B shows the relative size of ION expressed as a percentage of the total brain volume grouped by ION complexity. Inclusion of ION categories as covariate in a regression shows that there is a significant effect of ION complexity on the

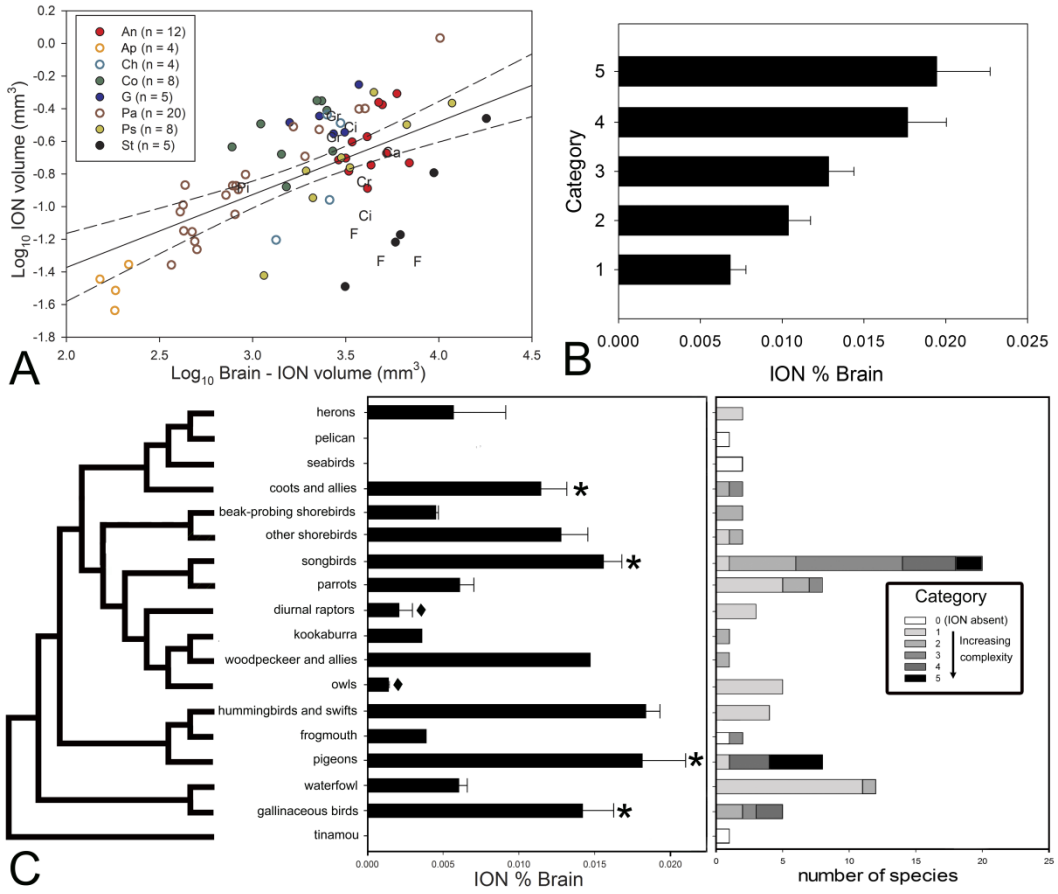
A
An (n = 12)
Ap (n = 4)
Ch (n = 4)
Co (n = 8)
G (n = 5)
Pa (n = 20)
Ps (n = 8)
St (n = 5)
Log10 ION volume (mm3)
Log10 Brain - ION volume (mm3)
B
Category
ION % Brain
C
herons
pelican
seabirds
coots and allies
beak-probing shorebirds
other shorebirds
songbirds
parrots
diurnal raptors
kookaburra
woodpeckeer and allies
owls
hummingbirds and swifts
frogmouth
pigeons
waterfowl
gallinaceous birds
tinamou
ION % Brain
number of species
Category
0 (ION absent)
Increasing complexity

Figure 5.4. Variation of relative volume of ION and relation to ION complexity. **A**, Scatterplot of the isthmo optic nucleus (ION) volume plotted as a function of brain minus ION volume for all species examined (see Appendix B). n indicates to the number of species measured in each order. **B**, Bar graph of the relative size of ION expressed as a percentage of total brain volume grouped by the ION cytoarchitectonical complexity categories; the error bars indicate standard error. **C**. Phylogenetic relations among orders of birds surveyed in this study based on Hackett et al. [2008]. The black bar graphs represent the relative size of ION expressed as a percentage of total brain volume for the different groups of birds. The error bars indicate standard error. The asterisk (*) indicates the groups in which a lower field myopia has been described. The black diamond (♦) indicates species where a lack of lower field myopia has been described. The colored bars represent the number of species that were examined of each ION cytoarchitectoncial organization complexity category in each order (see results, Appendix B, fig. 5.2). **An** = Anseriformes (red full circles); **Ap** = Apodiformes (empty orange circle); **Ca** = Caprimulgiforms; **Ch** = Charadriiforms (empty light blue circle); **Ci** = Ciconiiformes; **Co** = Columbiforms (dark green full circles); **Cr** = Coraciiforms; **F** = Falconiforms; **G** = Galliformes (dark blue full circle); **Gr** = Gruiformes; **Pa** = Passerifomes (empty brown circles); **Pi** = Piciforms; **Ps** = Psittaciformes (full yellow circle); **St** = Strigiforms (full black circle).

relative volume of ION (Appendix D). The evolutionary model with the lowest AIC (the OU model) corroborates the significant effect of ION category on the relative size of ION for all phylogenies used (Appendix D). Tukey HSD post hoc comparisons showed that species scored as having a more complex ION (categories 4 and 5) have relative ION volumes that are significantly larger than those in species scored as having category 1 IONs, but which are not significantly larger than those in species classified as having the others categories of ION. Although the other pair-wise comparisons are not statistically different, the general trend suggests that relative size of ION and its cytoarchitectonic organization is positively correlated (fig. 5.4B). We also found that ION complexity is not related to either absolute ION volume or brain volume (data not shown). We then mapped the distribution of ION relative size and complexity over one of the proposed phylogenies for birds fig. 5.4C). The results suggest that a relatively large ION has evolved independently several times, including: coots and allies, non beakprobing shorebirds, songbirds, woodpeckers, hummingbirds, pigeons and galliforms. Also our results show that a complex, laminated ION, with distinct cell layers and neuropil (categories 4–5, fig.5. 3) has evolved independently at least three times; in songbirds, pigeons and kingfishers (fig. 5.4C). Our results also suggest that ION has been 'lost' at least two times independently, in the nightjar (Caprimulgiformes) and in the clade that includes the pelican and seabirds (fig. 5.4C).

5.2.3 ION Cells Numbers and Cell Density

Cell numbers in the ION varied between 953 (CE = 0.0831) in the Swainson's Hawk to 23,760 (CE = 0.0808) in the Superb Lyrebird (Appendix B). The highest cell density was 117,439 cells/ mm^3 in the Spotted Pardalote (Pardalotus punctatus) and the lowest cell density was 8,448 cells/mm^3 in the Pacific Black Duck (*Anas superciliosa*; Appendix B). There is a significant positive correlation between ION cell numbers and ION absolute volume (fig. 5.5A), but this explains only between 50 and 60% of the variation in cell number (Appendix D). The inclusion of orders as a covariate yielded a significant effect of group on cell number for both conventional statistics and the evolutionary model with the lowest AIC (OU) (Appendix D). Tukey HSD post hoc comparisons demonstrated that songbirds have significantly more cells in the ION than hummingbirds, waterfowl, parrots, herons, diurnal raptors and owls (fig. 5.5B), after accounting for the size of the ION. Cell density (# cells/mm3) in the ION is also negatively correlated with the logarithm of brain volume (fig. 5.5C; Appendix D). Thus, cell numbers increase with the absolute size of ION but cell density decreases with absolute brain size. A regression of ION cell density against the brain volume with order as a covariate revealed a significant effect of order on cell density for both conventional statistics and the OU evolutionary model (Appendix D). Tukey HSD post hoc comparisons show that songbirds and owls have a significantly higher cell density in the ION than hummingbirds, waterfowl, parrots and herons, relative to brain size (fig. 5.5D). We found no

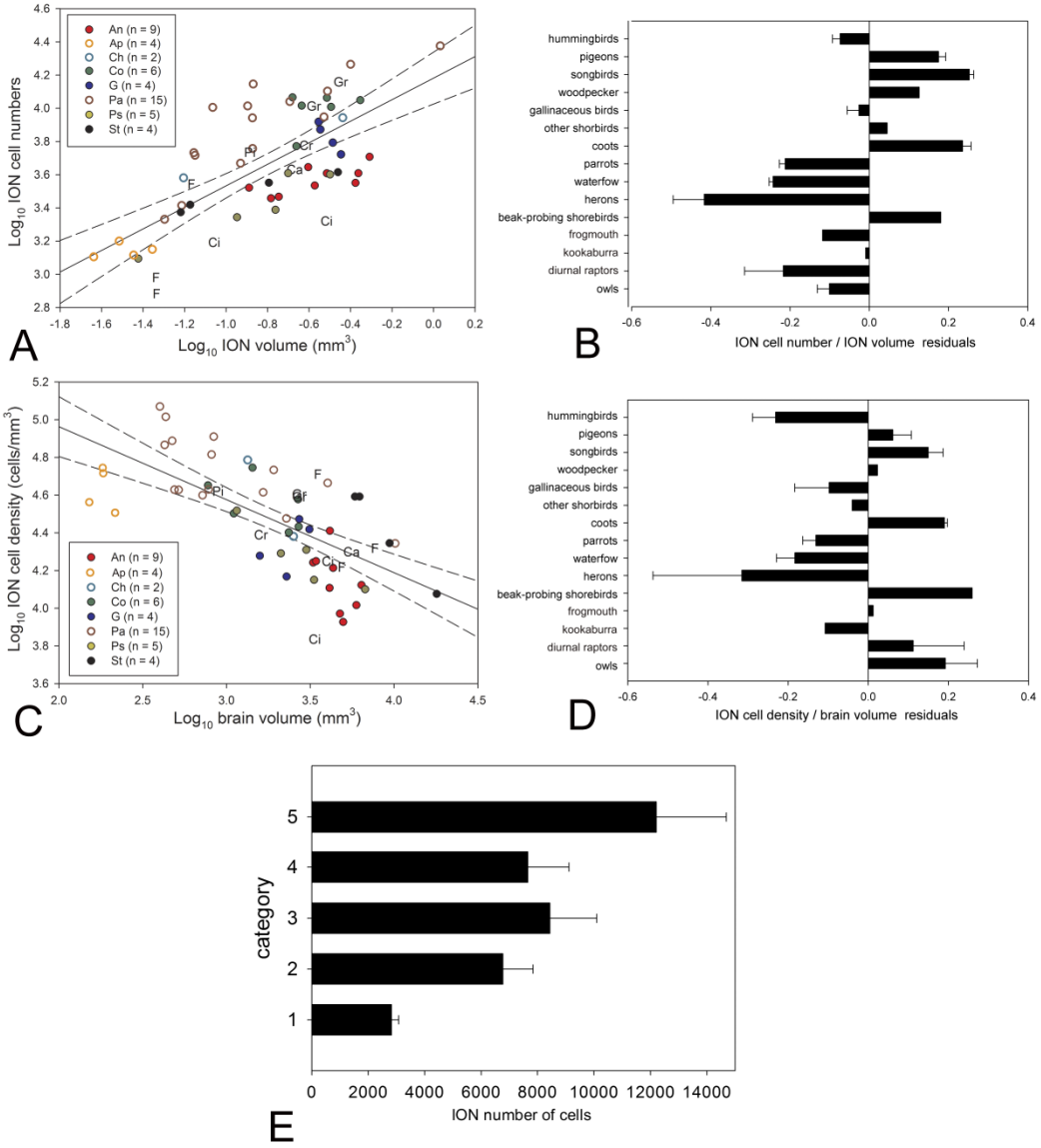
A
Log10 ION cell numbers
Log10 ION volume (mm3)
An (n = 9)
Ap (n = 4)
Ch (n = 2)
Co (n = 6)
G (n = 4)
Pa (n = 15)
Ps (n = 5)
St (n = 4)
B
hummingbirds
pigeons
songbirds
woodpecker
gallinaceous birds
other shorbirds
coots
parrots
waterfow
herons
beak-probing shorebirds
frogmouth
kookaburra
diurnal raptors
owls
ION cell number / ION volume residuals
C
Log10 ION cell density (cells/mm3)
Log10 brain volume (mm3)
D
ION cell density / brain volume residuals
E
category
ION number of cells

Figure 5.5. ION cells numbers and cells density variation among birds. A, Scatterplot of the cell numbers of ION plotted as a function of ION volume for all species examined (see Appendix B). The n between parentheses indicates the number of species measured in each order. B, Bar graph of the residuals of ION cell numbers against the ION volume (A) for different groups of birds; the error bars indicate standard error. C Scatterplot of the cell density (cells/mm^3) in the ION, plotted as a function of brain volume for all species examined (see Appendix B). D, Bar graph of the residuals of ION cell density against the brain volume (C) for different groups of birds; the error bars indicate standard error. E, Bar graph of ION absolute cells numbers grouped by the ION cytoarchitectonic complexity categories; the error bars indicate standard error. n indicates to the number of species measured in each order. An = Anseriformes (red full circles); Ap = Apodiformes (empty orange circle); Ca = Caprimulgiformes; Ch = Charadriiformes (empty light blue circle); Ci = Ciconiiformes; Co = Columbiformes (dark green full circles); Cr = Coraciiformes; F = Falconiformes; G = Galliformes (dark blue full circle); Gr = Gruiformes; Pa = Passerifomes (empty brown circles); Pi = Piciformes; Ps = Psittaciformes (full yellow circle); St = Strigiformes (full black circle).

effect of ION categories on the ION cell numbers relative to ION volume or cell density (data not shown). A one way ANOVA yielded a significant effect of ION complexity categories on the absolute number of cells (Appendix D; fig. 5.5E). The OU evolutionary model also shows a significant effect of ION complexity categories on the absolute number of cells (Appendix D). Tukey HSD post hoc comparisons showed that birds in category 1 have significantly fewer cells than birds in all other categories of ION complexity and species in category 5 have significantly more cells than species in category 2. We also found that the number of cells in the ION, relative to ION volume, varies significantly among categories (ANOVA, $F_{4,53}$ =13.63, p,0.001; fig. 5.5F). Tukey HSD post hoc comparisons indicated that species in category 1 have significantly fewer cells relative to ION volume than all other categories.

5.3 Discussion

This is the first major systematic, comparative analysis of relative size, cytoarchitecture and cell number in the ION, the principal origin of retinofugal fibres in birds. The present study expands greatly the number of orders and species in which ION is described and provides a broad phylogenetic base onto which functional hypothesis can be tested and revised.

5.3.1 ION Cytoarchitecture

In several species we found a lack of a recognizable assemblage of cells that could be classified as the ION (Appendix B). This is not the first time an ‘absence’ of the ION has been reported in birds. For example, the Brown Kiwi

[*Apteryx australis*; Craigie, 1930], the Wood Stork [*Mycteria americana*; Showers and Lyons, 1968], and the Ostrich [*Struthio camelus*; Verhaart, 1971] all reportedly lack a recognizable ION. It is not clear whether ION is truly absent in these species or whether the ION is just extremely small. Unfortunately it is not known whether there are isthmal cells that project to the retina in any of these species, which might indicate the presence of an ION. Crocodilians, the living vertebrates most closely related to birds [Janke et al., 2001], do have centrifugal projections to the retina from cells in the isthmal region [Kruger and Maxwell 1969; Ferguson et al., 1978; Medina et al., 2004]. However, these cells are more similar to the ectopic cells of birds and there is no evidence that crocodilians have an ION [Medina et al., 2004]. In birds, ectopic cells also project to the retina but to different targets and are thought to have a different function from that of cells in ION [see Reperant et al., 2006; Wilson and Lindstrom, 2011]. Interestingly, the Ostrich and the Kiwi, along with the Chilean Tinamou, all belong to the most ancestral group of birds, Paleognathae [Hacket et al., 2008]. The absence of a recognizable ION in Paleognathae and the crocodilians suggests that the ION may have evolved first in the more modern group of birds, Neognathae, and that Paleognathae are more similar to Crocodilians with only ectopic cells that project to the retina. Mapping the differences in cytoarchitectonic organization and relative size of ION on top of an avian phylogeny (fig. 5.4C) reveals a complex pattern and suggests that evolutionary changes in both the relative size and the cytoarchitectonic organization of the ION have occurred independent of phylogeny. For example, Figure 5.4C shows that an ION with obvious cell layers

and neuropils (fig. 5.3, categories 4, 5) has evolved independently at least 4 times. In addition, birds with a relatively large ION tend to have a more complex ION (fig.5. 4B), and birds with less complex ION organization (*i.e.*, category 1) have both fewer cells in both absolute and relative terms (see results). This suggests that the independent evolution of a complex laminated ION is associated with an enlarged ION, but also that a simple, reticular organization may be associated with fewer cells. This is well exemplified by hummingbirds; they have a large ION relative volume but have only around 1,000 cells and a simple ION organization (fig. 5.4C). Thus, our data suggest that as ION increases in terms of relative size and the absolute number of cells, a more laminar organization is necessary to maintain or generate specific connections and/or firing properties. The variation we observed in ION morphology is similar to the evolutionary transitions from a non-laminated to a laminated structure in other vertebrates (for a review see Striedter, 2005). Examples of this include the dorsal lateral geniculate nucleus in mammals [Sanderson, 1974; Kaas et al., 1978; Kahn et al., 2002] and the vagal lobe of cyprinid fish [Morita and Finger 1985]. Striedter [2005] proposed that one of the benefits of lamination is to reduce the length of neuronal connections thereby reducing transmission time and increasing processing power. In pigeons and galliforms, the dendrites of ION projection cells are directed towards the neuropil [Miceli et al., 1995; 1997] and both GABAergic interneurons and terminals from cells in the optic tectum, the main afferent of ION, lie exclusively in the neuropil [Crossland and Hughes 1978; Woodson et al., 1991; Uchiyama et al., 1996 Miceli et al., 1997]. This suggests that a more

laminar organization of ION could be essential to maintain the interaction of tectal terminals, GABAergic interneurons and ION cells dendrites, which in turn would maintain the firing properties of ION cells. In fact, in quail, which have a laminated ION, the ION cells have large suppressive surrounds that include almost all of the remaining visual field and these properties depend exclusively on the GABAergic interneurons within the ION [Uchiyama et al., 1998; Uchiyama, 1999]. Taken together this suggests that as the number of cells has increased in the ION, a more laminar organization has emerged to maintain the connections and response properties of ION cells.

5.3.2 Relative Volume and Cell Numbers

Based on the total number of cells and morphology of ION, previous studies reported three types of ION: (1) songbirds, galliforms and pigeons have a well-developed, laminated ION, with around 10,000 cells [Reperant et al., 1989], (2) waterfowl have a less differentiated, reticular ION with around 3,000 cells [; Sohal and Narayanan 1975; Reperant et al., 1989] and (3) owls, diurnal raptors and birds that feed on the wing have a poorly developed ION with close to 1,000 cells [Shortess and Klose 1977; Weidner et al., 1987; Reperant et al., 1989,; Feyerabend et al., 1994]. Based on a much larger number of species, our results confirm this pattern (fig. 5.4A, C) and add several taxa. Hummingbirds, coots and non-beak probing shorebirds have relatively large IONs, similar to songbirds and pigeons. Parrots, beak-probing shorebirds, herons and the kookaburra have medium sized IONs, similar to waterfowl. Our results also confirm the very small

IONs in owls and diurnal raptors (fig. 5.4C). Cell numbers in ION in species that have been previously studied, like the rock pigeon [*Columba livia*, Wolf-Oberhollenzer, 1987], the Common Blackbird (*Turdus merula*, Feyerabend et al., 1994) and the mallard duck (*Anas platyrhynchos*, Sohal and Narayanan, 1975) are very close to what we found. The one discrepancy is in the barn owl (*Tyto alba*), where Weidner et al. [1987] reported only 1,400 cells compared to the <2,500 we found. This discrepancy in the barn owl likely arises from a difference in counting methods because Weidner et al. [1987] did not use a rigorous stereological approach, as we did, to count cells. Although we found a correlation between ION volume and ION cell numbers, this only explained abut 50% of the variation in cell number (fig. 5.5A). In agreement with this, we found significant differences in cell density among birds, after accounting for the influence of brain size on cell density (fig. 5.5D). There seems to be a tendency for birds with large IONs to have higher cell density and birds with small IONs to have lower cell density, but this is not absolute. Among the groups with large IONs, galliforms and hummingbirds tend to have much lower relative cell densities. These differences in relative cell density may reflect differences in the functions or organization of the ION. For example, in galliforms the tectal projections to the ION arise from all parts of the tectum, whereas in pigeons, the projections largely arise from the ventral part of the tectum [Holden and Powel, 1972; Miles, 1972; Clarke and Whitteridge, 1976; Crossland and Hughes, 1978; Woodson et al., 1991; Miceli et al., 1995, 1997]. It is possible that these differences influence the relative number of cells and volume of ION, but there is no information on tectal efferents to ION

in any other groups of birds to test this hypothesis any further. To date, most comparative studies of brain regions have focused on comparisons of relative volume [e.g. Iwaniuk and Wylie 2007; Gutierrez-Ibanez et al., 2009]; but see Moore et al., 2001], but variations among species in the relative volume of a neural structure can be attributed to a variation (increases or decreases) in cell number and/or the number and complexity of dendritic trees and terminals within the nucleus. Thus, comparing not only the relative volume, but also cell numbers and density can provide important clues on to how neural structures evolve. In the case of our study, both the relative volume and cell numbers of ION are associated with the cytoarchitectonic organization the nucleus and thus have provided insight in to the evolutionary transition from an unlaminated to a laminated structure.

5.3.3 Control of Pecking Behavior

As mentioned before, the idea that the ION was larger in ground feeding and pecking birds (e.g., pigeons, songbirds and galliforms) and small in non-pecking birds (e.g., waterfowl, diurnal and nocturnal raptors) led various authors to propose that the ION is involved in the visual search of small objects or in the control of pecking behavior [Weidner, 1987; Shortess and Klose 1977; Reperant et al., 1989; Hahmann and Gunturkun 1992, Miceli et al., 1999]. Although several groups adhere to this general distinction (like coots and non-beak-probing shorebirds; fig. 5.4A–C), the data from other taxa casts doubt on the universality of this pattern. For example, the ION is relatively large in all of the songbirds and

pigeons we measured, even though some species in these groups are not ground feeders, like the Eastern Spinebill (Acanthorhynchus tenuirostris), which is nectarivorous [Higgins et al., 2002], or the Cedar Waxwing (Bombycilla cedorum) and the Torresian Imperial Pigeon (Ducula spilorrhoa) both of which feed largely on fruit in trees [Witmer, 1996; McConkey et al., 2004]. This would at least indicate that ground feeding and searching for small objects is not the main driving force of the relative size of the ION. Similarly, hummingbirds have a relatively large ION (fig. 5.4C) and they are highly specialized for feeding from flowers while hovering [Gass and Mongomerie, 1981], which is not similar in any way to ground feeding or pecking.

5.3.4 Aerial Predator Detection

Wilson and Lindstrom [2011] recently advanced the idea that the ION is involved in detecting images of shadows cast on the ground or on objects in the environment, which will then initiate a rapid and parallel search of the sky for a possible aerial predator. They based this on the anatomy and physiology of the retinofugal system, but also on the observation that ground-feeding birds have reportedly large IONs. Measuring the risk of aerial predation across the range of species we examined was not possible, but our results seem to be at odds with the aerial predation theory. For instance, we found that the ION is large and well developed in coots, which feed mostly in water bodies, and use similar nesting, feeding, brooding, and loafing sites as waterfowl [reviewed in Eddleman et al., 1985]. The same aerial predators prey upon both coots and waterfowl, but these

two groups have very different relative ION volumes (fig. 5.4C). Also contradictory with Wilson and Lindstrom's [2011] theory is the small size of ION in parrots In most environments, parrots are subjected to predation by diurnal raptors [e.g. Lindsey et al., 1994; Aumann, 2001] and respond with alarm calls to the presence of such predators [Wescott and Cockburn, 1988], so they should possess large rather than small IONs.

5.3.5 New Hypothesis

Based on our observations of species differences in both size and morphology of ION, we propose an alternative theory for ION function. Several taxa that have both relatively large and complex IONs also have a lower field myopia (fig. 5.4C). That is, asymmetries in the eye's optical structure result in the dorsal part of the eye being myopic while the ventral part of the eye is emmetropic in these species, thereby keeping the ground in focus on the dorsal retina at the same time that the horizon and sky are in focus on the ventral retina [Martin, 1993]. Birds that have been described as having a lower field myopia include: pigeons [Fitzke et al., 1985], songbirds [Martin, 1986], galliforms [Schaeffel et al., 1994] and coots [Murphy et al., 1995], all which have relatively large IONs (fig. 5.4C). Conversely, owls and diurnal raptors, both of which have small IONs, do not have a lower field myopia [fig. 5.4C; Hodos and Erichsen, 1990]. Additional support for our hypothesis is provided by comparison the observations of Kolmer [Kolmer, 1924] on the optics of the Common Kingfisher (*Alcedo atthis*). In this species, the temporal retina is extremely myopic in air and

only becomes emmetropic once it enters the water. Although we did not sample a Common Kingfisher, the Belted Kingfisher (fig. 5.3D), which is also a diving species, has a complex, laminated ION. In contrast, the closely related Laughing Kookaburra has a simpler ION morphology that is relatively small (fig. 5.4C) and is a terrestrial perch-hunting predator, similar to diurnal raptors in its foraging behavior and diet. Although we did not include the relative volume of ION in the Belted Kingfisher in our analyses because it is a museum specimen (see methods), the ION represented 0.015% of the total brain volume, which is much larger than that of the kookaburra and similar to that of galliforms and songbirds (fig. 5.4C), suggesting that this species has an enlarged ION.

We therefore suggest that the ION is involved in switching attention between two parts of the retina *i.e.* from an emmetropic to a myopic part of the retina. In most cases this would mean switching from close range to long range vision in the retina. In the case of the birds with a lower field myopia this would be between the dorsal and ventral parts of the retina, but in the kingfisher this would be between the temporal retina and the rest of the retina. Birds with large IONs feed close to the substrate, which can include the ground, flowers and tree trunks and in species with a lower field myopia it is the part of the visual field containing the substrate that is myopic. On the other hand, birds with smaller IONs appear to feed far from the substrate, or have non-visually guided foraging behaviors. This is certainly true for galliforms, songbirds and pigeons that feed by pecking on the ground, but also true for species in these orders that feed mostly on fruit or insects in trees. Although both coot species that we examined feed in the

water, they do so mostly by pecking, and while they ometimes submerge to feed [Desrocherbs and Ankney, 1986], the small size of the beak and trigeminal system in these birds [Gutierrez-Ibanez, et al., 2009], suggests that they depend on vision for the detection of prey, probably at close range. The one woodpecker we examined also adheres to this pattern because it feeds on sap or insects on tree trunks at close range [Tate, 1973]. The difference in the relative size of the ION between beak probing and non-beak probing shorebirds is also in agreement with this hypothesis. Beak probing shorebirds feed close to the substrate, but they use tactile rather than visual cues to guide their foraging and their visual fields are adapted to attend to their surroundings and not the bill while foraging [Martin, 1994]. The situation in parrots is somewhat similar; parrots cannot see in the region below the bill and instead have more comprehensive visual coverage above the head [Demery et al., 2007]. The apparent 'absence' of the ION in the nightjar further supports our hypothesis as they feed by hunting insects in the air [Holyoak, 2001], which is in accordance with the previous reports that birds that feed on the wing have a reduced ION [Fereyabend et al., 1994]. The reduced size of the ION in herons and the 'absence' of ION in seabirds and a pelican also fits our hypothesis; seabirds and pelicans usually dive into the water to catch fish, while herons have longs legs that keep them at a considerable distance from the ground when foraging [Martin and Katzir, 1994]. Finally, that owls and diurnal raptors also have small and simple IONs is consistent with their feeding habits, which generally involve either perch hunting or feeding in the air [Jaksic and Carothers, 1985]. Several studies have indicated that the effect of centrifugal

fibers on nearby retinal ganglion cells is excitatory [Uchiyama and Barlow, 1994; Galifret et al., 1971; Miles 1972; Pearlman and Hughes, 1976]. This, in turn, suggests that the ION switches attention between different parts of the retina by increasing the responses of retinal ganglion cells. The anatomy of the centrifugal system provides good support to the idea of differential activation of parts of the retina as there is a clear asymmetry between the dorsal and ventral retina. In pigeons and galliforms, the ION projects exclusively to the ventral part of the retina (*i.e.* the dorsal visual field; [Catsicas et al., 1987; Hayes and Holden, 1986; Woodson et al., 1995; Lindstrom et al., 2009]. In the ventral retina, terminals from the ION make synapses with target amacrine cells (TCs), which project to both the ventral and the dorsal retina [Catsicas et al., 1987; Uchiyama et al., 2004; Uchiyama and Stell, 2005; Lindstrom et al., 2010]. Although the major synapses of the ION fibers in the retina are the TCs, there is evidence that some terminals from the ION synapse with targets other than TCs in the ventral retina [Lindstrom et al., 2009; Chmielevski et al., 1988]. Therefore, the ION could enhance the responses of cells in the dorsal and ventral differentially; directly and through some TCs in the ventral retina, but only through TCs in the dorsal retina. Other authors [Wilson and Lindstrom, 2011] have proposed that the ION is involved in switching attention between the dorsal and ventral retina for the primary purpose of predator detection. Our results do not support the notion that avian predator detection is the primary function of the ION, but predator detection would be one of the behaviors supported by the ability to switch attention between different parts of the visual field. While we believe that our hypothesis is general enough to

explain the diversity of species with an enlarged ION, it is certainly true that the different hypotheses proposed so far are not mutually exclusive and that the ION could subserve different functions in different groups. Although our new functional hypothesis is based on a much broader sampling of bird species, it requires experimental testing. For example, if our hypothesis is correct, then birds with relatively large IONs, like hummingbirds, woodpeckers and non beakprobing shorebirds, should be myopic parts in some parts of their visual fields and this myopia should match their respective feeding behaviors. Further, electrophysiological confirmation that projections from the ION alternatively activate parts of the retina that subserve the upper and lower (i.e. emmetropic and myopic) parts of the visual field in pigeons or galliforms will be necessary.

5.4 References

Aumann T (2001): An intraspecific and interspecific comparison of raptor diets in the south-west of the Northern Territory, Australia. Wildl Res 28: 379–393.

Barton RA (1998): Visual specialization and brain evolution in primates. Proc Biol Sci 265: 1933–1937.

Brown DM, Toft CA (1999): Molecular systematics and biogeography of the cockatoos (Psittaciformes: Cacatuidae). Auk 116: 141–157.

Barker FK, Cibois A, Schikler P, Feinstein J, Cracraft J (2004): Phylogeny and diversification of the largest avian radiation. Proc Nat Acad Sci USA 101: 11040–11045.

Cajal SR (1888) Morfologia y conexiones de los elementos de la retina de las aves. Rev Trim Histol Norm Patol 2: 1–10.

Cajal SR (1889): Sur la morphologie et les connexions des e´le´ments de la re´tine des oiseaux. Anat Anz 4: 111–128.

Catsicas S, Catsicas M, Clarke PG (1987): Long-distance intraretinal connections in birds. Nature 326: 186–187.

Clarke PG, Whitteridge D (1976): The projection of the retina, including the 'red area' on to the optic tectum of the pigeon. Q J Exp Physiol Cogn Med Sci 61: 351–358.

Clarke PG, Gyger M, Catsicas S (1996): A centrifugally controlled circuit in the avian retina and its possible role in visual attention switching. Vis Neurosci 13:1043–1048.

Cracraft J, Barker FK, Braun M, Harshman J, Dyke GJ, et al. (2004): Phylogenetic relationships among modern birds (Neornithes): toward an avian tree of life. In: Assembling the tree of life. Cracraft J, Donoghue MJ, eds. New York: Oxford University Press. pp 468–489.

Craigie EH (1930): Studies on the brain of the kiwi (Apteryx australis). J Comp Neurol 49: 223–357. 80.

Chmielevski CE, Dorado ME, Quesada A, Genis-Galvez JM, Prada FA (1988): Centrifugal fibers in the chick retina. A morphological study. Arch Histol Embryol 17: 319–327.

Crossland WJ, Hughes CP (1978): Observations on the afferent and efferent connections of the avian isthmo-optic nucleus. Brain Res 145: 239–256.

Davis KE (2008): Reweaving the tapestry: a supertree of birds. PhD Thesis, University of Glasgow, UK.

Deacon TW (1990): Fallacies of progression in theories of brain-size evolution. Int J Primatol 11: 193–236.

Demery ZP, Chappell J, Martin GR (2011): Vision, touch and object manipulation in Senegal Parrots Poicephalus senegalus. Proc R Soc Lond B doi: 10.1098/rspb.2011.0374

Desrocherbs A, Ankney CD (1986): Effect of brood size and age on the feeding behavior of adult and juvenile American Coots (Fulica americana). Can J Zool 64: 1400–1406.

Dogiel AS (1895): Die Retina der Vo¨gel. Arch Mikrosk Anat 44: 622–648.

Donne-Gousse´ C, Laudet V, Ha¨nni C (2002): A molecular phylogeny of anseriformes based on mitochondrial DNA analysis. Mol Phylogenet Evol 23: 339–356.

Driskell AC, Christidis L (2004): Phylogeny and evolution of the Australo-Papuan honeyeaters Passeriformes, Meliphagidae). Mol Phylogenet Evol 31: 943–960.

Duncan RP, Forsyth DM, Hone J (2007): Testing the metabolic theory of ecology: allometric scaling exponents in mammals. Ecology 88: 324–333.

Eddleman WR, Patterson CT, Knopf FL (1985): Interspecific Relationships between American Coots and Waterfowl during Fall Migration. Wilson Bull 97: 463–472.

Ebinger P, Lo¨hmer R (1987): A volumetric comparison of brains between greylag geese (Anser anser L.) and domestic geese. J Hirnforsch 3: 291–299.

Ebinger P, Rohrs M (1995): Volumetric analysis of brain structures, especially of the visual system in wild and domestic turkeys (Meleagris gallopavo). J Brain Res 36: 219–228.

Ebinger P (1995): Domestication and plasticity of brain organization in mallards (Anas platyrhynchos). Brain Behav Evol 45: 286–300.

Ferguson JL, Mulvanny PJ, Brauth SE (1978): Distribution of neurons projecting to the retina of Caiman crocodilus. Brain Behav Evol 15: 294–306.

Feyerabend B, Malz CR, Meyer DL (1994): Birds that feed-on-the-wing have few isthmo-optic neurons. Neurosci Lett 182: 66–68.

Finger TE (1975): Feeding patterns and brain evolution in ostariophysean fishes. Acta Physiol Scand Suppl 638: 59–66.

Fitzke FW, Hayes BP, Hodos W, Holden AL, Low JC (1985): Refractive sectors in the visual field of the pigeon eye. J Physiol 369: 33–45.

Gass CL, Montgomerie RD (1981): Hummingbird foraging behavior: decision-making and energy regulation. In: AC InKamil, TD Sargent, editors. Editors. Foraging behavior: ecological, ethological and psychological approaches. New York: Garland STDP Press. pp. 159–194.

Garland T Jr., Harvey PH, Ives AR (1992): Procedures for the analysis of comparative data using phylogenetically independent contrasts. Syst Biol 41: 18–32.

Garland T Jr., Ives AR (2000): Using the past to predict the present: confidence intervals for regression equations in phylogenetic comparative methods. Am Nat 155: 346–364.

Garland T Jr., Bennett AF, Rezende EL (2005): Phylogenetic approaches in comparative physiology. J Exp Biol 208: 3015–3035.

Galifret Y, Condé-Courtine F, Repérant J, Servière J (1971): Centrifugal control in the visual system of the pigeon. Vision Res: Suppl 3185–200

Gundersen HJG (1977): Notes on the estimation of the n umerical density of arbitrary profiles: the edge effect. J Microsc 111: 219–223.

Gundersen HJ, Osterby R (1981): Optimizing sampling efficiency of stereological studies in biology: or ‘do more less well!’ J Microsc 121: 65–73.

Gutiérrez-Ibáñez C, Iwaniuk AN, Wylie DRW (2009): The independent evolution of the enlargement of the principal sensory nucleus of the trigeminal nerve (PrV) in three different groups of birds. Brain Behav Evol 74: 280–294 .

Hahmann U, Gunturkun O (1992): Visual-discrimination deficits after lesions of the centrifugal visual system in pigeons (Columba livia). Vis Neurosci 9: 225–233.

Hackett SJ, Kimball RT, Reddy S, Bowie RCK, Braun EL, et al. (2008): A phylogenomic study of birds reveals their evolutionary history. Science 320: 1763–1768.

Hirschberger W (1971): Vergleichend experimentellhistologische Untersuchung zur retinalen Repra¨ sentation in den prima¨ren visuellen Zentren einiger Vogelarten. Dissertation, Johan Wolfgang, Goethe-Universita¨ t, Frankfurt.

Higgins PJ, Peter JM, Steele WK (2002): Handbook of Australian, New Zealand and Antarctic birds, vol 5: tyrant-flycatchers to chats. New York: Oxford University Press. 1270 pp.

Holyoak DT (2001): Nightjars and their Allies. Oxford: Oxford University Press. 848 pp.

Hodos W, Erichsen JT (1990): Lower field myopia in birds: an adaptation that keeps the ground in focus. Vision Res 30: 653–659.

Holden AL (1968): The centrifugal system running to the pigeon retina. J Physiol (London) 197: 199–219.

Holden AL, Powell TPS (1972): The functional organization of the isthmo optic nucleus in the pigeon. J Physiol 223: 419–447.

Howard CV, Reed MG (2005): Unbiased Stereology. Three-Dimensional Measurement in Microscopy. New York: Springer. 277 pp.

Howard VS, Reid A, Baddeley A, Boyde A (1985): Unbiased estimation of particle density in the tandem scanning reflected light microscope. J Microsc 138: 203–212.

Ives AR, Midford PE, Garland T Jr. (2007): Within-species variation and measurement error in phylogenetic comparative methods. Syst Biol 56:252–270.

Iwaniuk AN (2004): Brood parasitism and brain size in cuckoos: A cautionary tale of the use of modern comparative methods. International J Comp Psychol 17: 17–33.

Iwaniuk AN, Wylie DRW (2007): Comparative evidence of a neural specialization for hovering in hummingbirds: hypertrophy of the pretectal nucleus lentiformis mesencephali. J Comp Neurol 500: 211–221.

Janke A, Erpenbeck D, Nilsson M, Arnason U (2001): The mitochondrial genomes of the iguana Iguana iguana) and the caiman (Caiman crocodylus): Implications for amniote phylogeny. Proc Biol Sci 268: 623–631.

Jerison HJ (1973): Evolution of the brain and intelligence. New York: Academic Press. 482 pp.

Johnson KP, Sorenson MD (1999): Phylogeny and biogeography of dabbling ducks (Genus: Anas): a comparison of molecular and morphological evidence. Auk 116: 792–805.

Kaas JH, Huerta MF, Weber JT, Harting JK (1978): Patterns of retinal terminations and laminar organization of the lateral geniculate nucleus of primates. J Comp Neurol 182: 517–553.

Kahn DM, Krubitzer L (2002): Retinofugal projections in the short-tailed opossum (Monodelphis domestica). J Comp Neurol 447: 114–127.

Karten H, Hodos W (1967): A Stereotaxic Atlas of the Brain of the Pigeon (Columba livia). Baltimore: Johns Hopkins University Press. 206 pp.

Kimball RT, Braun EL (2008): A multigene phylogeny of Gallifomes supportsa single origin of erectile ability in non-feathered facial traits. J Avian Biol 39: 438–445.

Knipling RR (1978): No deficit in near-field visual acuity of pigeons after transection of the isthmo-optic tract. Physiol Behav 21: 813–816.

Kolmer W (1924): Uber das Auge des Eisvogels (Alcedo' attis attis). Pfluegers Arch gesamte Physio Menschen Tiere 2: 266–274.

Kruger L, Maxwell DS (1969): Wallerian degeneration in the optic nerve of a reptile: an electron microscopic study. Am J Anat 125: 247–269.

Lavin SR, Karasov WH, Ives AR, Middleton KM, Garland TJr (2008): Morphometrics of the avian small intestine, compared with non-flying mammals: a phylogenetic approach. Physiol Biochem Zool 81:526-550.

Lindsey GD, Arendt WJ, Kalina J (1994): Survival and Causes of Mortality in Juvenile Puerto Rican Parrots (Supervivencia y Factores de Mortalidad en Juveniles de Amazona vittata) J Field Ornithol 65: 76–82.

Lindstrom SH, Nacsa N, Blankenship T, Fitzgerald PG, Weller C, et al. (2009): Distribution and structure of efferent synapses in the chicken retina. Vis Neurosci 26: 215–226.

Lindstrom SH, Azizi N, Weller C, Wilson M (2010): Retinal input to efferent target amacrine cells in the avian retina. Vis Neurosci 27: 103–118.

Livezey BC, Zusi RL (2007): Higher-order phylogeny of modern birds (Theropoda, Aves:Neornithes) based on comparative anatomy. II. Analysis and discussion. Zool J Linn Soc 49: 1–95.

Martin GR (1986): The eye of a passeriform bird, the European starling (Sturnus vulgaris): Eye movement amplitude, visual fields and schematic optics. J Comp Physiol A 159: 545–557.

Maddison WP, Maddison DR (2009): Mesquite: a modular system for evolutionary analysis. Version 2.6. Mesquite project website. Available: http://mesquiteproject.org/. Accessed 2012 May 1.

McConkey KR, Meehan HJ, Drake DR (2004): Seed dispersal by Pacific Pigeons (Ducula pacifica) in Tonga, Western Polynesia. EMU 104: 369–376.

Marin G, Letelier JC, Wallman J (1990): Saccade-related responses of centrifugal neurons projecting to the chicken retina. Exp Brain Res 82: 263–270.

Martin GR (1993): Producing the image. In: Zeigler HP, Bischof H-J, editors. Vision, Brain, and Behavior in Birds. Cambridge: MIT Press. pp. 5–24.

Martin GR (1994): Visual fields in woodcocks Scolopax rusticola Scolopacidae;Charadriiformes). J Comp Physiol A 174: 787–793.

Martin GR, Katzir G (1994): Visual fields and eye movements in herons (Ardeidae). Brain Behav Evol 44: 74–85.

Jaksić FM, Carothers JH (1985): Ecological, Morphological, and Bioenergetic Correlates of Hunting Mode in Hawks and Owls. Ornis Scandinavica 16: 165–172.

Médina M, Repérant J, Ward R, Miceli D (2004): Centrifugal visual system of Crocodylus niloticus: a hodological, histochemical, and immunocytochemical study. J Comp Neurol. 468: 65–85.

Midford PE, Garland T, Maddison WP (2008): PDAP: a MESQUITE translation of the PDTREE application of Garland, et al.'s phenotypic diversity analysis programs, version 1.14. Mesquite project website. Available: http:// mesquiteproject.org/pdap_mesquite/. Accessed 2012 May 1.

Miceli D, Repérant J, Rio JP, Médina M (1995): GABA immunoreactivity in the nucleus isthmo-opticus of the centrifugal visual system in the pigeon: a light and electron microscopic study. Vis Neurosci 12: 425–441.

Miceli D, Repérant J, Bavikati R, Rio JP, Volle M (1997): Brain-stem afferents upon retinal projecting isthmo-optic and ectopic neurons of the pigeon centrifugal visual system demonstrated by retrograde transneuronal transport of rhodamine β-isothiocyanate. Vis Neurosci 14: 213–224

Miceli D, Reperant J, Bertrand C, Rio JP (1999): Functional anatomy of the avian centrifugal visual system. Behav Brain Res 98: 203–210.

Miles FA (1972): Centrifugal control of the avian retina. II. Receptive field properties of cells in the isthmo-optic nucleus. Brain Research 48: 93–113.

Miles FA (1972): Centrifugal control of the avian retina: III. Effects of electrical stimulation of the isthmo-optic tract on the receptive field properties of retinal ganglion cells. Brain Res 48: 115–129.

Morita Y, Finger TE (1985): Topographic and laminar organization of the vagal gustatory system in the goldfish, Carassius auratus. J Comp Neurol 238: 187–201.

Moore JM, Székely T, Büki J, DeVoogd TJ (2011): Motor pathway convergence predicts syllable repertoire size in oscine birds. PNAS 108: 16440–16445.

Murphy CJ, Howland M, Howland HC (1995): Raptors lack lower field myopia. Vis Res 35: 1153–5.

Nickla DL, Gottlieb MD, Marin G, Rojas X, Brito LR, et al. (1994): The retinal targets of centrifugal neurons and the retinal neurons projecting to the accessory optic system. Vis Neurosci 11: 401–409.

O'Leary DD, Cowan WM (1982): Further studies on the development of the isthmo-optic nucleus with special reference to the occurrence and fate of ectopic and ipsilaterally projecting neurons. J Comp Neurol 212: 399–416.

Pereira SL, Johnson KP, Clayton DH, Baker AJ (2007): Mitochondrial and nuclear DNA sequences support a Cretaceous origin of Columbiformes and a dispersal-driven radiation in the Paleogene. Syst Biol 56: 656–672.

Pearlman AL, Hughes CP (1976): Functional role of efferents to the avian retina. II. Effects of reversible cooling of the isthmo-optic nucleus. J Comp Neurol 166: 123–132. .Hayes BP, Holden AL (1983): The distribution of centrifugal terminals in the pigeon retina. Exp Brain Res. 49: 189–197.

Pubols BH, Welker WI, Johnson JI (1965): Somatic sensory representation of forelimb in dorsal root fibers of raccoon, coatimundi, and cat. J Neurophysiol 28: 312–341.

Pubols BH, Pubols LM (1972): Neural organization of somatic sensory representation in the spider monkey. Brain Behav Evol 5: 342–366.

Puelles L, Martinez-de-la-Torre M, Paxinos G, Watson C, Martinez S (2007): The Chick Brain in Stereotaxic Coordinates: An Atlas Featuring Neuromeric Subdivisions and Mammalian Homologies. San Diego: Academic Press.

Purvis A, Garland T (1993): Polytomies in comparative analyses of continuous characters. Syst Biol 42: 569–575.

Reperant J, Miceli D, Vesselkin NP, Molotchnikoff S (1989): The centrifugal visual system of vertebrates: a century-old search reviewed. Int Rev Cytol 118: 115–171.

Reperant J, Ward R, Miceli D, Rio JP, Medina M, et al. (2006): The centrifugal visual system of vertebrates: A comparative analysis of its functional anatomical organization. Brain Research Reviews 52: 1–57.

Reperant J, Medina M, Ward R, Miceli D, Kenigfest NB, et al. (2007): The evolution of the centrifugal visual system of vertebrates. A cladistic analysis and new hypotheses. Brain Res Rev 53: 161–97.

Rogers LJ, Miles FA (1972): Centrifugal control of the avian retina: V. Effects of lesions of the isthmo-optic nucleus on visual behaviour. Brain Res 48: 147–156.

Schaeffel F, Hagel G, Eikerman J, Collett T (1994): Lower-field myopia and astigmatism in amphibians and chickens. J Opt Soc Am A 11: 487–495.

Scheaffer RL, Mendenhall W, Ott L (1996): Elementary Survey Sampling. 5th edition. Boston: Duxbury Press, Wadsworth Publishing. 464 p.

Schmitz C, Hof PR (2000): Recommendations for straightforward and rigorous methods of counting neurons based on a computer simulation approach. J Chem Neuroanat 20: 93–114.

Striedter GF (2005): Principles of brain evolution. In: Sunderland , editor. Mass. Sinauer Associates. 436 pp.

Sanderson KJ (1974): Lamination of the dorsal lateral geniculate nucleus in carnivores of the weasel (Mustelidae), raccoon (Procyonidae), and fox (Canidae) families. J Comp Neurol 153: 239–266.

Sibley CG, Ahlquist JE (1990): Phylogeny and classification of birds. New

Showers MJ, Lyons P (1968) Avian nucleus isthmi and its relations to hippus. J Comp Neurol 132: 589–616.

Shortess GK, Klose EF (1975): The area of the nucleus isthmoopticusin the american kestrel (Falco sparverius) and the redtailed hawk (Buteo jamaicensis). Brain Res 88: 525–531.

Shortess GK, Klose EF (1977): Effects of lesions involving efferent fibers to the retina in pigeons (Columba livia). Physiol Behav 18: 409–414.

Sohal GS, Narayanan CH (1975): Effects of optic primordium removal on the development of the isthmo-optic nucleus in the duck. Exp Neurol 46: 521–533.

Swanson DL, Garland T Jr. (2009): The evolution of high summit metabolism and cold tolerance in birds and its impact on present-day distributions. Evolution 63: 184–194.

Tate J (1973): Methods and Annual Sequence of Foraging by the Sapsucker. Auk 90: 840–856.

Uchiyama H (1989): Centrifugal pathways to the retina: influence of the optic tectum. Vis Neurosci 3: 183–206. retina using two fluorescent markers. Neurosci Lett 73: 16–20.

Uchiyama H (1999): The isthmo-optic nucleus: A possible neural substrate for visual competition. Neurocomputing 26–27: 565–571.

Uchiyama H, Aoki K, Yonezawa S, Arimura F, Ohno H (2004): Retinal target cells of the centrifugal projection from the isthmo-optic nucleus. J Comp Neurol 476: 146–153.

Uchiyama H, Barlow RB (1994): Centrifugal inputs enhance responses of retinal ganglion cells in the Japanese quail without changing their spatial coding properties. Vis Res 34: 2189–2194.

Uchiyama H, Yamamoto N, Ito H (1996): Tectal neurons that participate in centrifugal ontrol of the quail retina: a morphological study by means of retrograde labeling with biocytin. Vis Neurosci 13: 1119–1127.

Uchiyama H, Nakamura S, Imazono T (1998): Long-range competition among the neurons projecting centrifugally to the quail retina. Vis Neurosci 15: 417–423.

Uchiyama H, Stell WK (2005): Association amacrine cells of Ramon y Cajal: Rediscovery and reinterpretation. Vis Neurosci 22: 881–891.

Verhaart WJ (1971): Forebrain bundles and fibre systems in the avian brain stem. J Hirnforsch 13: 39–64.

Ward R, Repe´rant J, Miceli D (1991): The centrifugal visual system: what can comparative anatomy tell us about its evolution and possible function? In: Bagnoli P, Hodos W, eds. The Changing Visual System. New York: Plenum Press. pp 61–76.

Weidner C, Repe´rant J, Desroches AM, Miceli D, Vesselkin NP (1987): Nuclear origin of the centrifugal visual pathways in birds of prey. Brain Res 43:153–160.

Weidner C, Desroches AM, Repe´rant J, Kirpitchnikova E, Miceli D (1989): Comparative study of the centrifugal visual system in the pigmented and glaucomatous albino quail. Biol Struct Morphol 2: 89–93.

West MJ, Slomianka L, Gundersen HJ (1991): Unbiased stereological estimation of the total number of neurons in the subdivisions of the rat hippocampus using the optical fractionator. Anat Rec 231: 482–497.

Westcott DA, Cockburn A (1988): Flock Size and Vigilance in Parrots. Aust J Zool 36: 335–349.

Wilson M, Lindstrom SH (2011): What the bird's brain tells the bird's eye: the function of descending input to the avian retina Vis Neurosci 28: 337–50.

Wink M, Sauer-Gu¨rth H, Fuchs M (2004): Phylogenetic relationship in owls based on nucleotide sequences of mitochondrial and nuclear marker genes.

In: Chancelor RD, Meyburg B-U,editors. Raptors worldwide. Berlin: WWGBP. pp 517–526.

Wink M, Heidrich P, Sauer-Gu¨rth H, Elsayed AA, Gonzalez J (2008): Molecular phylogeny and systematics of owls (Strigiformes); in Konig C, Weick F, editors. Owls of the World. London: Christopher Helm. pp 42–63.

Witmer MC (1996): Annual Diet of Cedar Waxwings Based on U.S. Biological Survey Records (1885–1950) Compared to Diet of American Robins: Contrasts in Dietary Patterns and Natural History. Auk 113: 414–430.

Wolf-Oberhollenzer F (1987): A study of the centrifugal projections to the pigeon retina using two fluorescent markers. Neurosci Lett 73: 16–20.

Woodson W, Reiner A, Anderson K, Karten HJ (1991): Distribution, laminar location, and morphometry of tectal neurons projecting to the isthmo-optic nucleus and nucleus isthmi, pars parvocellularis in the pigeon (Columba livia) and chick (Gallus domesticus): a retrograde labelling study. J Comp Neurol 305: 470–488

Woodson W, Shimizu T, Wild JM, Schimke J, Cox K, et al. (1995): Centrifugal projections upon the retina: an anterograde tracing study in the pigeon (Columba livia). J Comp Neurol 362: 489–509.

Wright TF, Schirtzinger EE, Matsumoto T, Eberhard JR, Graves GR, et al. (2008): A multilocus molecular phylogeny of the parrots (Psittaciformes): support for a Gondwanan origin during the Cretaceous. Mol Biol Evol 25: 2141–2156.

Chapter 6: **Mosaic and concerted evolution in the visual system of birds**

In recent years, there has been an increased interest in understanding the principles and processes that govern brain evolution [Striedter, 2005]. A major goal has been to understand how differences in the absolute and relative size of different neural structures evolve and two models have been proposed to explain this. In the concerted evolution model, developmental constraints cause different parts of the brain to vary in size in a coordinated manner [Finlay and Darlington, 1995; Finlay et al., 2001]. Thus, if there is selective pressure to increase the size of a specific brain region the rest of the brain will increase in size as well. In the mosaic evolution model, there are no such constraints and individual brain structures can vary in size independently of each other. Most studies to date have tested these models at an anatomically crude level, comparing variation of the relative size of large subdivision of the brain, such as telencephalon, thalamus, cerebellum and brainstem. The results of these analyses support either model of evolutionary change depending upon which clade is being examined [e.g. Barton, and Harvey, 2000; Iwaniuk, and Hurd, 2005; Gonzalez-Voyer et al., 2009; Yopak et al., 2010]. A possible drawback of the use of major subdivisions of the brain is that they do not represent functional units; each region contains multiple independent motor and sensory pathways. This means that the size of these different regions of the brain is the result of a complex combination of multiple selection pressures and constraints affecting several motor and sensory pathways. There is plenty of evidence that individual nuclei within these pathways can vary greatly through evolution (see below), but little attention has been given to how this affects variation in nuclei down- or upstream. Analysis of more constrained,

functionally homogeneous and interconnected structures are needed to reveal fine details of the correlated evolution of neural structures.

Several studies have shown hypertrophy of specific neural structures related to sensory [e.g. Barton, 1998; Kubke et al., 2004a; Gutiérrez-Ibáñez et al., 2009; Iwaniuk, and Wylie, 2007], and motor [e.g. Pubols et al., 1965; Dobson, and Sherwood, 2011] specializations. Unfortunately, the majority of these studies are restricted to one structure and therefore it is unclear if functionally and anatomically related nuclei evolve according to a concerted or mosaic model of evolutionary change. While some recent studies have suggested concerted evolution in some sensory pathways of birds (e.g. [Iwaniuk et al., 2010; Gutiérrez-Ibáñez et al., 2011; Gutiérrez-Ibáñez et al., 2013]), no study has specifically set out to test these two models at the level of specific neural pathways.

The visual system of birds is a good candidate to study the covariation of the relative size of nuclei that belong to the same pathway or sensory modalities. In birds, like in all vertebrates, projections from the retina go to several retinorecipient nuclei, which give rise to several parallel visual pathways. The main retinorecipient structure is the optic tectum (TeO), a multilayered structure that in pigeons receives more than 90% of retinal projections and forms part of the tectofugal pathway [Fig 6.1A; Hunt, and Webster, 1975; Mpodozis et al., 1995; Remy, and Güntürkün, 1991]. The tectofugal pathway is also comprised of the nucleus rotundus (nRt) in the thalamus and the entopallium (E) in the telencephalon. This pathway is involved in processing brightness, colour, pattern

discrimination, simple motion and looming stimuli [Wang et al., 1993; Bischof, and Watanabe, 1997; Sun, and Frost, 1998; Husband, and Shimizu, 2001; Nguyen et al., 2004]. A second pathway is the thalamofugal pathway, which includes the dorsal thalamus and the Wulst (also known as the hyperpallium, [Karten et al., 1973; Reiner et al., 2004]). Other retinorecipient nuclei in birds include the nucleus lentiformis mesencephali (LM) and the nucleus of the basal optic root [nBOR; Karten et al., 1977; Fite et al., 1981; McKenna, and Wallman, 1985; Gamlin, and Cohen, 1988a] both of which are involved in the generation of the optokinetic response [Frost et al., 1994], and the ventral lateral geniculate nucleus (GLv), whose function remains largely unclear [see Maturana, and Varela, 1982; Gamlin et al., 1984; Gioanni et al., 1991; Wakita et al., 1992; Vega-Zuniga et al., 2011 for some proposed functions]. Besides all receiving retina projections, these nuclei are all interconnected with one another. For example, GLv and LM receive projections from TeO [Hunt, and Künzle, 1976; Crossland, and Uchwat, 1979; Hunt, and Brecha, 1984; Gamlin, and Cohen, 1988b] and LM and nBOR have massive reciprocal projections [Wylie et al., 1997]. The isthmo optic nucleus (ION), a small nucleus in the isthmal region, receives projections from the tectum and sends projection to the retina, thus creating a loop between retina, TeO and ION [reviewed in [Wilson, and Lindstrom, 2011]. Another group of nuclei interconnected with TeO is the isthmal complex, which is composed of the magnocellular and parvocellular parts of the nucleus isthmi (Imc and Ipc) and the nucleus semilunaris (SLu). Each of these nuclei receives a prominent, retinotopically organized visual projection from the ipsilateral TeO, specifically

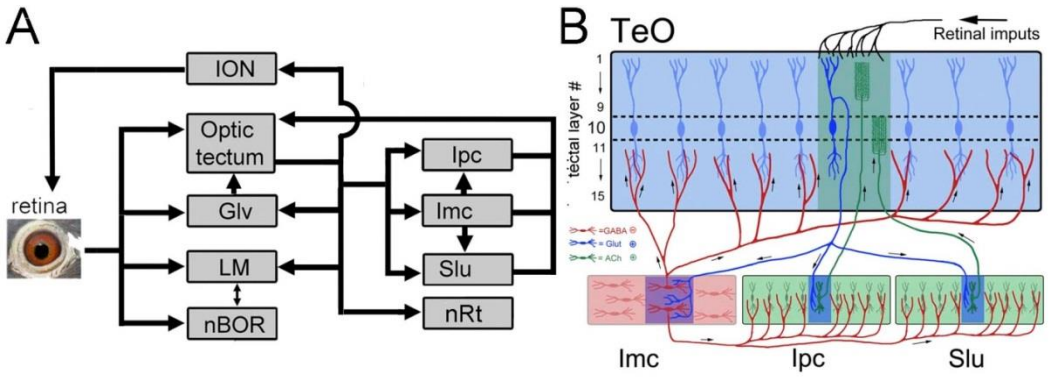

Figure 6.1. Connectivity of the avian visual system and the isthmo-tectal circuit. A, illustrates some of the connectivity in the visual pathways in birds. The black arrows show the projections from one structure to the other. The optic tectum (TeO), the nucleus of the basal optic root (nBOR), the nucleus lentiformis mesenscephali (LM), the ventral geniculate nucleus (GLv) all receive projections from the contralateral retina. The isthmo-optic nucleus (ION), which projects to the retina, GLv, LM, the nucleus rotundus (nRt), the magnocellular and parvocellular portions of nucleus isthmi (Imc, Ipc) and the nucleus semilunaris (SLu) all receive projections from TeO. Several of the nuclei are also interconnected, like LM and nBOR or Imc, Ipc, and SLu. B, illustrates in detail the isthmo-tectal circuit. Imc, Ipc and SLu receive a topographic, excitatory projection from cells in layer 10 of the TeO (blue cells). Ipc and SLu send back excitatory projections to TeO in a topographic manner (green cells). Imc neurons on the other hand are GABAergic [Granda and Crossland 1989, Tömböl and Németh 1995] and send a so call antitopographic projection to either Ipc, SLu or to the deep layers of TeO [Wang et al., 2004].

from ‘shepherd’s crook’ neurons [Hunt, and Künzle, 1976; Brecha, 1978; Güntürkün, and Remy, 1990; Hellmann et al., 2001; Wang et al., 2006]. Ipc and SLu neurons are cholinergic [Fig 6.1B; Sorenson et al., 1989; Medina, and Reiner, 1994] and project back to TeO in a precise homotopic fashion [fig. 6.1B; Hunt, and Künzle, 1976; Brecha, 1978; Remy, and Güntürkün, 1991; Hellmann et al., 2001; Wang et al., 2006]. Imc neurons are GABAergic [fig. 6.1B; Granda, and Crossland, 1989; Tömböl, and Németh, 1998] and send an anti-topographic projection to Ipc, SLu or to the deep layers of TeO [fig. 6.1B; Wang et al., 2004]). By anti-topographic we mean that Imc neurons project broadly to the TeO, Ipc and SLu, except to the locus from which they receive projections (fig. 6.1B).

Several comparative studies have shown great variation in the relative size of visual neural structures in birds, both among and within orders [Iwaniuk, and Wylie, 2006; Iwaniuk, and Wylie, 2007; Iwaniuk et al., 2008; Gutiérrez-Ibáñez et al., 2013]. For example, Iwaniuk and Wylie [2007] showed that LM, but not GLv, nBOR or TeO, is greatly enlarged in hummingbirds. Similar volumetric studies have shown a reduction in size of the TeO and the rest of the tectofugal pathway in in owls, parrots and waterfowls compared to other birds [Iwaniuk et al., 2010] and great variation in the relative size of the ION between and within orders [Gutierrez-Ibanez et al., 2012]. The heavily interconnected circuitry (fig. 6.1) and known variation in the relative size of some of the nuclei therefore makes the visual system a perfect candidate to study the principles underlying the evolution of relative size differences in sensory pathways. Here, we examine the relative size of 9 different visual nuclei in 98 species of birds belonging to 16 different

orders. This includes data on interspecific variation in the cytoarchitecture and relative size of the isthmal nuclei (Ipc, Imc, SLu), which has not been previously reported. Specifically, we tested for interspecific differences in Imc related to cytoarchitectural differences. In the chick (*Gallus domesticus*), Imc is composed of two different cells types; one cell type projects to Ipc and SLu, and the other cells project to TeO [fig. 6.1B; Wang et al., 2004; Wang et al., 2006]. Recently, Faunes et al., [2013] showed that in the zebra finch (*Taeniopygia guttata*), these two cells types are segregated in two subdivisions, which are identified as the external (Imc-ex) and internal (Imc-in) Imc (e.g. fig. 6.2A-C). Further, these authors showed that this segregation is likely present in all songbirds, but not in most other birds with the exception of coots (Gruiformes) and woodpeckers and allies (Piciformes) (fig. 6.2B-C). In vertebrates, lamination has evolved in several neural structures [for a review see Striedter, 2005] and this is likely related to an increase in the size of the structure but also to a necessity to minimize connection lengths and thus increase processing power. Recently, we have shown that in the ION the occurrence of a clearly segregated cell layer and neuropil is related to an increase in the relative size of this nucleus [Gutiérrez-Ibáñez et al., 2012]. In this sense, it is possible that groups that have a segregated Imc have a relatively larger Imc than birds with non-segregated Imc.

In addition to the descriptions and measurements of the isthmal nuclei, we used a novel combination of statistical analyses to test if visual nuclei evolve in a concerted or mosaic manner: i) phylogenetically corrected principal component analysis and, ii) evolutionary rates of change, on the absolute and relative size of

the nine visual nuclei. Previous studies [Barton, and Harvey, 2000; Whiting, and Barton, 2003] suggested that covariation in the size of different neural structures is related to their functional connectivity to one another. We therefore expected heavily interconnected and functionally related nuclei, such as the isthmal nuclei or LM and nBOR, to vary in relative size in a more concerted manner with each other than with other nuclei.

6.1 Materials and Methods

6.1.1 Ethics Statement

Most specimens were provided to us dead by conservation authorities, wildlife veterinarians and museum staff and thus approval was not required by an institutional ethics committee for the use of those specimens. Some of the songbird specimens in this study were captured in Tippecanoe County, Indiana, USA using mist-nets and live traps. The Purdue Animal Care and Use Committee (protocol #09-018) approved all capturing and handling of the birds, and the experimental procedures the birds were involved in. Birds were housed indoors in cages (0.9 m x 0.7 m x 0.6 m) with 1-3 other individuals of the same species prior to tissue collection. They were kept on a 14:10 hour light:dark cycle and an ambient temperature of approximately 23°C. Food (millet, sunflower seeds and thistle seeds) and water was always provided *ad libitum*, and supplemented with mealworms (*Tenebrio molitor*) which were also provided to each cage daily. Tissue collection began by euthanizing birds via carbon dioxide asphyxiation,

followed by immediate removal of the head for preservation in 4% paraformaldehyde.

6.1.2 Measurements

We measured the relative volume of Ipc, Imc, SLu, ION, LM, GLv, nBOR, nRt and TeO in 100 specimens representing 98 species (Appendix E). Some of the values reported in this study, including the volume for ION in 81 of the species and volume for LM, nBOR, GLv, nRt and TeO in some of the species have been reported in previous work [Iwaniuk, and Wylie, 2007; Iwaniuk et al., 2010; Gutiérrez-Ibáñez et al., 2012; Gutiérrez-Ibáñez et al., 2013]. For all specimens, the head was immersion-fixed in 4% paraformaldehyde in 0.1 M phosphate buffer. The brain was then extracted, weighed to the nearest milligram, cryoprotected in 30% sucrose in phosphate buffer, embedded in gelatin and sectioned in the coronal or sagittal plane on a freezing stage microtome at a thickness of 40 µm. Sections were collected in 0.1 M phosphate buffered saline, mounted onto gelatinized slides, stained with thionin and coverslipped with Permount (Fisher Scientific, Fair Lawn, New Jersey, USA). The olfactory bulbs were intact in all of the specimens that we collected and sectioned. All brains were cut following bird brain atlases [Karten, and Hodos, 1967; Puelles et al., 2007] in which the brainstem ends at the same rostrocaudal point as the cerebellum. In this manner, brain measurements were consistent among our specimens.

Photomicrographs of every second or every fourth section were taken throughout the rostrocaudal extent of each nucleus using a Retiga EXi *FAST* Cooled mono 12-bit camera (Qimaging, Burnaby, BC, Canada) and OPENLAB Imaging system (Improvision, Lexington, MA, USA) attached to a compound light microscope (Leica DMRE, Richmond Hill, ON, Canada). For some brains, images of full sections were obtained with a digital slide scanner (Leica SCN400 , Richmond Hill, ON, Canada) with a 20x objective.

Measurements of all the nuclei were taken directly from these photos with ImageJ (NIH, Bethesda, MD, USA; http://rsb.info.nih.gov/ij/) and volumes were calculated by multiplying the area in each section by the thickness of the section (40 µm) and the sampling interval. For those species represented by more than one specimen (Appendix E), the average of the measurements was taken as the species' given value.

6.1.3 Borders of nuclei

In all birds, Imc, Ipc and SLu were readily identifiable in Nissl stained sections. Imc and Ipc lie ventral and lateral to the ventricle and they are surrounded by fibers coming from the TeO. Ipc is medial and dorsal to Imc and is characterized by small densely packed cells. In contrast, Imc is characterized by larger and more loosely arranged cells (fig. 6.2). SLu is similar to Ipc, with small, darkly stained cells. It is ventral and medial to the posterior ventral tip of Ipc (fig. 6.2) and lateral to the ventrolateral lemniscal nuclei. For the rest of the nuclei measured, we followed the same borders described in previous studies [fig. 6.3, Iwaniuk, and Wylie, 2007; Iwaniuk et al., 2010; Gutiérrez-Ibáñez et al., 2012].

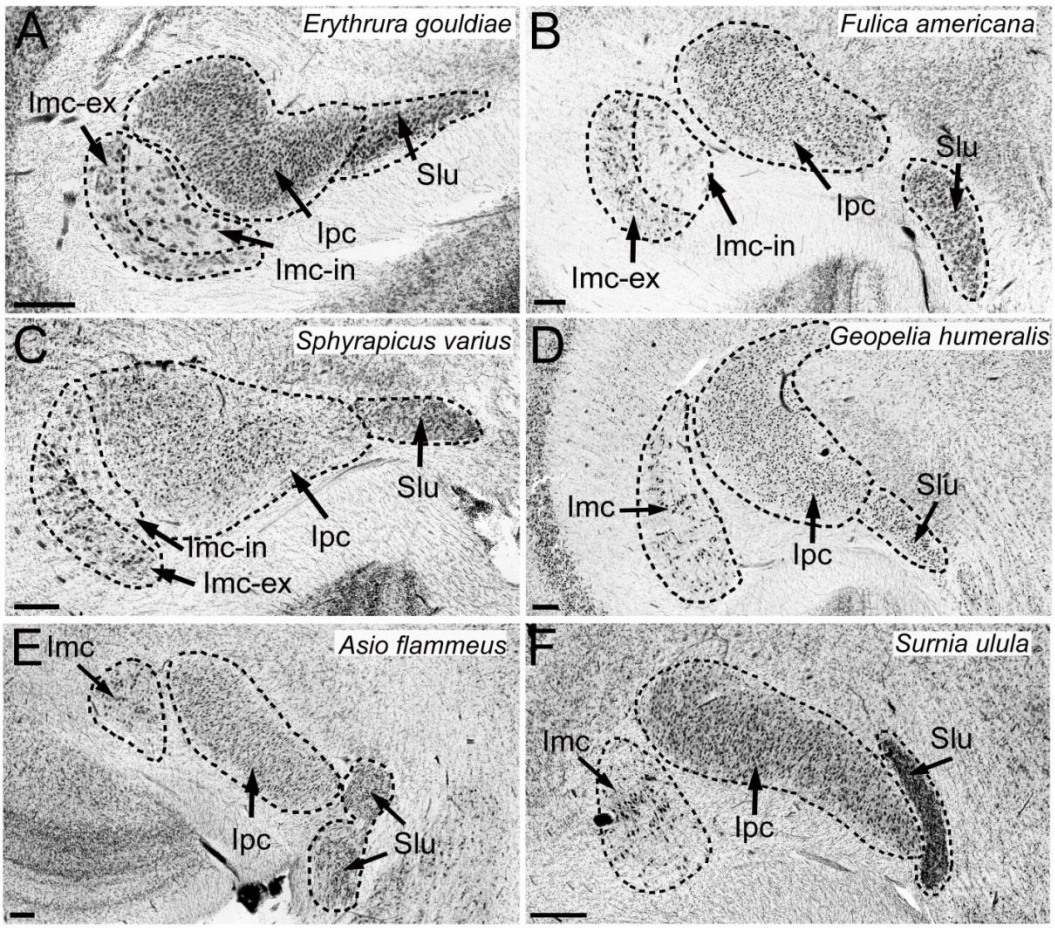
A
Erythrura gouldiae
lmc-ex
Slu
lpc
lmc-in
B
Fulica americana
Slu
lpc
lmc-in
lmc-ex
C
Sphyrapicus varius
Slu
lmc-in
lpc
lmc-ex
D
Geopelia humeralis
lmc
Slu
lpc
E
lmc
Asio flammeus
lpc
Slu
F
Surnia ulula
lmc
Slu
lpc

Figure 6.2. Location, borders and cytoarchitecture of the isthmal complex. Photomicrographs showing the location and borders of the three isthmal nuclei, the magnocellular and parvocellular portions of nucleus isthmi (**Imc**, **Ipc**) and the nucleus semilunaris (**SLu**) in four species of birds. **A**-**C** show the isthmal complex in the three different groups of birds that exhibited a Imc segregated in two layers, the internal subdivision of the Imc (Imc-in) and the external subdivision of the Imc (Imc-ex). **A** shows a songbird (Passeriformes), the Gouldian Finch (*Erythrura gouldiae*). **B** shows a Gruiform, the American Coot (*Fulica Americana*). **C** shows a woodpecker (Piciformes), the Yellow-bellied Sapsucker (*Sphyrapicus varius*); **D** shows a pigeon (Columbiformes), the Bar-shouldered Dove (*Geopelia humeralis).* **E** and **F** show two species of owls (Strigiformes), the Short-eared Owl (*Asio flammeus*) and the Northern Hawk Owl (*Surnia ulula*).

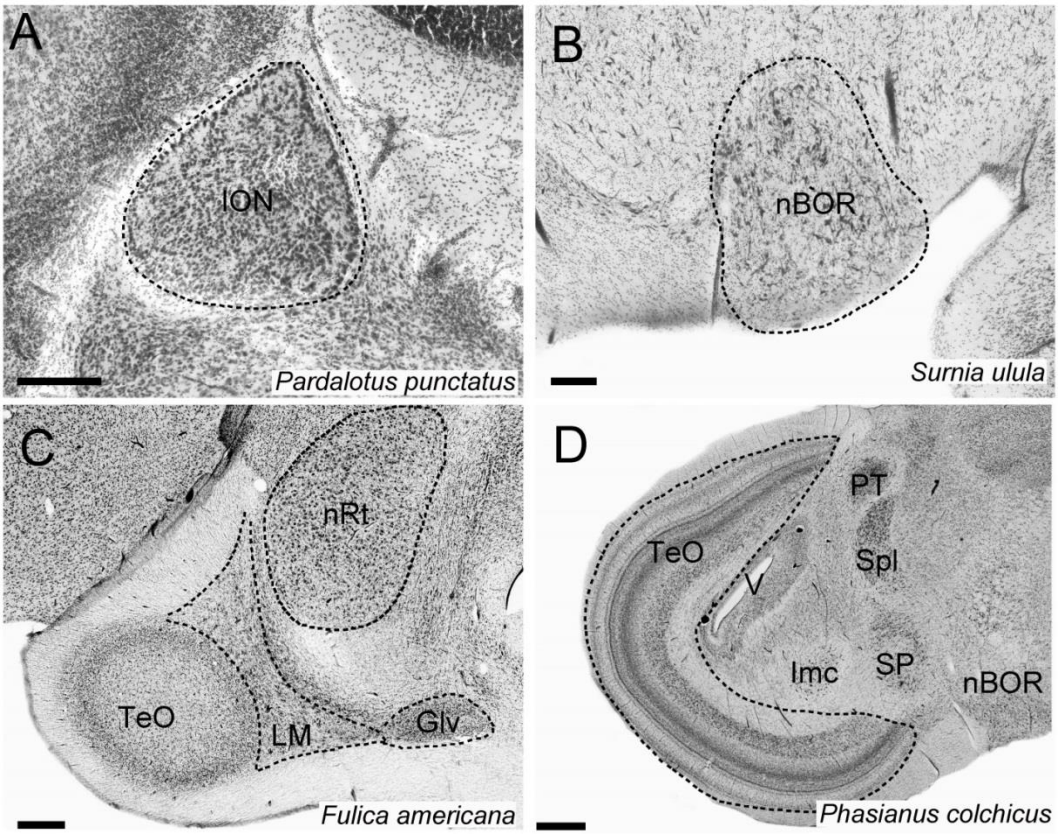

Figure 6.3. Location, borders and cytoarchitecture of other visual nuclei. Photomicrographs of coronal sections showing the location and borders of the different visual nuclei in birds. A, show the isthmo optic nucleus (ION) in a songbird (Passeriformes) the Spotted Pardalote (*Pardalotus punctatus*). B shows the nucleus of the basal optic root (nBOR) in an owl (Strigiformes), the Northern Hawk Owl (*Surnia ulula*). C shows the nucleus lentiformis mesencephali (LM), the ventral part of the geniculate nucleus (GLv) and the nucleus rotundus (nRt) in a Gruiform, the American Coot (*Fulica americana*). D shows the optic tectum (TeO) in a gallinaceous bird (Galliformes) the Ring-necked Pheasant (*Phasianus colchicus*). PT = nucleus pretectalis. SP =nucleus subpretectalis. SPl =nucleus spiriformis lateralis

6.1.4 Statistical analyses

To examine scaling relationships, we plotted the $\log_{10}$-transformed volume of each brain region against the $\log_{10}$-transformed brain volume minus the volume of each specific region [Deacon, 1990]. Because of the close anatomical and functional relationship of the isthmal nuclei with the TeO (see introduction), we also examined the scaling relationships of these nuclei against the TeO.

Allometric equations were calculated with linear least squares regressions using: (1) species as independent data points, and (2) phylogenetic generalized least squares (PGLS) to account for phylogenetic relatedness [Garland Jr, and Ives, 2000; Garland et al., 2005]. We applied two models of evolutionary change as implemented in the MATLAB program Regressionv2.m [available from T. Garland, Jr on request; Ives et al., 2007; Lavin et al., 2008]: Brownian motion (phylogenetic generalized least-squares or PGLS) and Ornstein–Uhlenbeck (OU) [Lavin et al., 2008; Swanson, and Garland, 2009]. Because different phylogenetic trees can yield different results [Iwaniuk, 2004] we tested two models based on the trees provided in Livezey and Zusi [2007], and Hackett et al. [2008]. Resolution within each order was provided by order- and family-specific studies [Brown, and Toft, 1999; Johnson, and Sorenson, 1999; Donne-Goussé et al., 2002; Barker et al., 2004; Driskell, and Christidis, 2004; Wink, and Sauer-Gürth, 2004; Pereira et al., 2007; Kimball, and Braun, 2008; Wink et al., 2009; Wright et al., 2008] Phylogenetic trees, character matrices and phylogenetic variance-covariance matrices were constructed using Mequite/PDAP:PDTREE software [Midford et al., 2008; Maddison, and Maddison, 2010] and the PDAP software

package (available from T. Garland, Jr., upon request). Because the phylogeny was constructed from multiple sources, branch lengths were all set at 1, which provided adequately standardized branch lengths when checked using the procedures outlined in Garland et al. [1992]. Unresolved nodes were treated as soft polytomies, with branch lengths between internal nodes set to zero [Purvis, and Garland, 1993]. Allometric equations based on standard statistics, and the PGLS and OU models, for each of the two trees, were calculated for: (1) visual nuclei volume against brain volume; and (2) Ipc, Imc and SLu volume against TeO volume (table 6.2). We also performed regression models that included the avian orders and presence of two layers in Imc [Faunes et al., 2013] as covariates in regression models of the volume of Ipc, Imc and SLu against both the brain and TeO volume. Currently, there is no phylogenetically corrected pair wise comparison available and therefore Tukey HSD post hoc tests were only performed on non-phylogenetically corrected statistics.

Non-phylogenetically corrected statistics and post-hoc tests were performed using the software JMP (JMP, Version 10. SAS Institute Inc., Cary, NC, 1989-2007). Additionally, we calculated phylogeny-corrected 95% prediction intervals [Garland Jr, and Ives, 2000] using the PDAP module [Midford et al., 2008] of the Mesquite modular software package [Maddison, and Maddison, 2010] to look for any significant outliers.

6.1.5 Phylogenetic multivariate allometry analyses

To compare patterns of evolution among the different nuclei, we used maximum likelihood values for the lambda (λ) and alpha (α) parameters [Pagel, 1999]. These parameters test for departure from a Brownian motion model of evolution where trait divergence accumulates in time in a stochastic manner. In the λ parameter test, a λ equal to 1 means a null Brownian motion model [Pagel, 1999]. The α model is based on an OU process and estimates the strength of selection acting on the trait; the higher the value of α, the stronger the selective regime. As α becomes small the OU model is eventually reduced to a Brownian process. As α tends towards 1, the process will reduce to a model with one selective optimum but with no accelerated accumulation of divergence [Hansen, 1997; Butler, and King, 2004]. P-values were obtained by comparing the models with the λ and α parameters to a null model of unconstrained Brownian motion with the log-likelihood statistic. The GEIGER [Harmon et al., 2013] package in R [R Core Team, 2013] was used to estimate the values.

To test how the relative size of the nuclei vary with respect to each other, we used a correlation based principal components approach taking into account the phylogenetic relationships among species using the PHYTOOLS [Revell, 2009] package in R. A multivariate allometric analysis has advantages over other methods, such as multiple regressions, in that it avoids problems with the adequate control of size when analyzing inter-correlation between structures, as well as problems of multicolinearity, which can arise because structure volumes are usually highly correlated with one another [Freckleton, 2002; Deaner et al.,

2007; Schoenemann, 2003]. In any principal component analysis (PCA) where all variables are correlated with a size variable (in this case brain size), the first principal component corresponds to a size variable, in this case absolute brain size [Klingenberg, 1996]. In this sense, all other principal components will correspond to variance in the size of the different structures independent of brain size. The ratio between the loadings of any pair of variables in the first principal component (PC1) corresponds to the bivariate allometric coefficient of those variables [Klingenberg, 1996]. Bivariate allometric coefficients close to 1 indicate isometry between two nuclei (*i.e.* both nuclei vary equally in size with changes in absolute size). Bivariate allometric coefficients that depart from 1 indicate positive or negative allometry between a pair of nuclei indicating that one nucleus changes in size disproportionally with respect to the other with changes in absolute size. Therefore, isometry between nuclei can be interpreted as indicative of concerted evolution between those nuclei. In addition to running multivariate analysis on the absolute volume of the visual nuclei, we also performed a phylogenetically corrected PCA of the relative size of the nuclei. For this analysis, we used residuals from a least squares regression analysis, while controlling for non-independence due to phylogenetic relatedness. The residuals were also calculated using the PHYTOOLS package in R. As with the previous analyses, we used two different phylogenies [Livezey, and Zusi, 2007; Hackett et al., 2008]. Because variation of the relative size of some of the nuclei departs from a Brownian motion evolutionary model (see results) we assumed both a Brownian motion and

Pagel's λ [Pagel, 1999] evolutionary model when performing the PCA analysis with the residuals.

All multivariate analyses included 94 of the 98 species because four species did not have a recognizable ION [see Appendix E; Gutiérrez-Ibáñez et al., 2012] and the R function used to calculate the different parameters could not handle missing values.

6.2 Results

6.2.1 Isthmal nuclei cytoarchitecture

The cytoarchitectonics of the Ipc is similar across all birds that we examined (fig. 6.2). The same is true for Imc with the exception of songbirds, Gruiformes (coots and allies) and Piciformes (woodpeckers and allies) in which Imc cells are organized in two distinct layers as reported by Faunes et al.[2013] (fig. 6.2A-C). We examined the cytoarchitectonical organization of Imc in 14 additional species of birds (13 songbirds and one Piciform) to the ones reported by Faunes et al. [2013], all of which had two distinct layers of cells (Appendix E). We also found that owls have a distinct cytoarchitectonical organization of SLu. In 8 out of the 9 owl species in this study (the exception being the Northern Hawk Owl, *Surnia ulula*), SLu is divided into dorsal and ventral portions that are separated by a bundle of fibers that courses dorsal to Ipc, but ventral to the lateral part of the mesencephalic reticular formation, towards the brachium conjunctivum (fig. 6.2E-F).

6.2.2 Isthmal nuclei relative size

The three isthmal nuclei (Imc, Ipc and SLu) scale with negative allometry against brain volume (Appendix F, fig. 6.4A, C; fig. 6.5A). When order is included as a covariate, we found a significant effect of order on the relative size of Imc and Ipc, but not SLu (Appendix G). Pairwise comparisons using Tukey's HSD test showed that herons, pigeons and gallinaceous birds (*i.e.*, quail, pheasant and relatives) have significantly smaller Imc and Ipc volumes than parrots and owls (fig. 6.4B,D), relative to brain size. We also tested if species with two layers in Imc (see above, [Faunes et al., 2013]) have relatively larger isthmal nuclei than species with one layer. Species were scored as having a one or two layered Imc, which resulted in two groups: songbirds, Gruiforms and Piciforms (two layers) and all other species (one layer). No significant differences in the relative size of Imc were found between the two groups (Appendix G).

We also examined the size of the isthmal nuclei relative to the size of the TeO. Imc and Ipc scaled with isometry or positive allometry with the TeO, while SLu scaled with isometry with TeO (fig. 6.4E, G; fig. 6.5C). This means that as the absolute volume of TeO increases, the size of Imc, Ipc and SLu do so proportionally or slightly more than TeO. When order is included as a covariate, we found a significant effect of orders in the three isthmal nuclei. In the case of Imc and Ipc, songbirds and coots have significantly larger nuclei with respect to the TeO than parrots and hummingbirds (fig. 6.4F, H). SLu, however, is larger relative to TeO in owls than most other orders (fig. 6.5D).

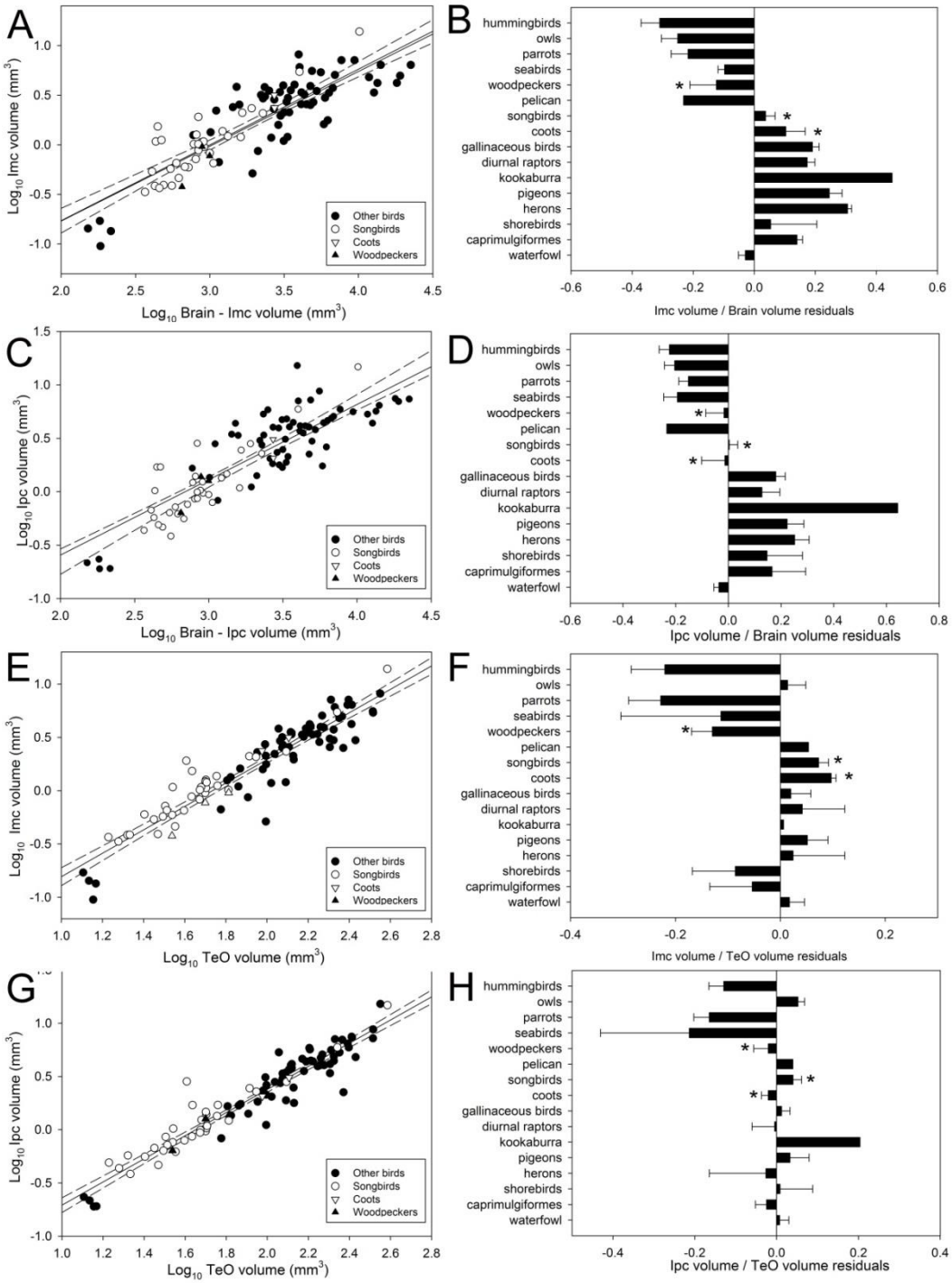
A
B
C
D
E
F
G
H
Log10 lmc volume (mm3)
Log10 Brain - lmc volume (mm3)
lmc volume / Brain volume residuals
Log10 lpc volume (mm3)
Log10 Brain - lpc volume (mm3)
lpc volume / Brain volume residuals
Log10 lmc volume (mm3)
Log10 TeO volume (mm3)
lmc volume / TeO volume residuals
Log10 lpc volume (mm3)
Log10 TeO volume (mm3)
lpc volume / TeO volume residuals
Other birds
Songbirds
Coots
Woodpeckers
hummingbirds
owls
parrots
seabirds
woodpeckers
pelican
songbirds
coots
gallinaceous birds
diurnal raptors
kookaburra
pigeons
herons
shorebirds
caprimulgiformes
waterfowl

Figure 6.4. Relative size of the magnocellular and parvocellular portions of nucleus isthmi. Scatterplot of log-transformed volume of the magnocellular and parvocellular portions of nucleus isthmi (Imc or Ipc) plotted as a function of either the log-transformed brain volume minus the volume of the respective nuclei (Imc, **A**; Ipc, **C**) or the log-transformed volume of the optic tectum (TeO; Imc, E; Ipc, G) for all species examined (see Appendix E). The bar graph shows the relative size of each nuclei relative to the brain (Imc, **B**; Ipc, **D**) or the TeO (Imc, F; Ipc ,**H**). Values shown in the bar graphs are the means of the residuals derived from the respective regressions show in **A**, C, **E** and **G.**

6.2.3 Variation in the relative size of other visual nuclei

Order also had a significant effect on the relative size of all of the other visual nuclei. Differences in the relative size of ION among orders were not different from those previously reported [fig. 6.6A, B; see [Gutiérrez-Ibáñez et al., 2012]. GLv and nBOR are significantly larger in gallinaceous birds than most other orders (fig. 6.6C-F). Pairwise comparisons show that in the case of LM, hummingbirds and gallinaceous birds have significantly larger LM than parrots, songbirds and the pelican, but not other orders (fig.6.6G, H). Nevertheless, when these two groups are tested against all other species grouped together, they both have significantly larger LM (fig. 6.6G, H). Results for TeO and nRt are similar to those reported before [Iwaniuk et al., 2010] with owls and waterfowl having a significantly smaller TeO, relative to brain size, than most other orders (fig. 6.7A-B). Parrots had a TeO significantly smaller than pigeons, but no other orders, and a nRT significantly smaller than pigeons, herons and gallinaceous birds.

6.2.4 Multivariate allometry analysis

We first tested whether the evolutionary rate of change of the $\log_{10}$-transformed volumes of each visual nucleus departs significantly from a Brownian motion model using maximum likelihood estimates of α and λ. When the absolute size of the visual nuclei was used, none of them differed significantly from a Brownian model of evolutionary change (Appendix H). We then performed a multivariate PCA with the $\log_{10}$-transformed volume of the visual nuclei using the same two phylogenies as in the regressions (see methods).

Although there were some minor differences in the loadings between the two phylogenies (see below, table 1, S5), the overall pattern was similar. The first component of the PCA explained around 80% of the total variance in volume of the different visual nuclei (table 1, S5). All structures loaded strongly and in the same direction in PC1, and species scores for PC1 were significantly correlated with brain size (PGLS using Livezey, and Zusi, [2007]; R^2= 0.836, $F_{1,93}$ = 470.2, P = >0.0001). This strongly suggests that PC1 describes variance in the different structures' volumes resulting from differences in brain size. In other words, evolutionary changes in brain size explain about 80% of the variance in the absolute size of the visual nuclei. TeO, nRt Imc, Ipc and SLu had the largest loadings in PC1, which indicates a strong correlation between the volumes of these structures and overall brain size. In contrast, the lower loadings of the other visual nuclei, particularly GLv and ION, suggest a weaker correlation between the volume of these two nuclei and whole brain size. PC2 explained around 7% total variance (table 6.1). In PC2 GLv has the strongest loading followed by LM. PC3 accounted for 5% of the total variance and ION had a strong positive loading, while GLv and LM loaded weakly in the same direction.

Using the loadings of each nucleus in PC1 we calculated bivariate allometric coefficients (table 6.2). Bivariate allometric coefficients show that TeO varies closely to isometry with respect to the isthmal nuclei (Imc = 1.00, Ipc = 1.00, and SLu =1.05) and nRt (0.99), but TeO has positive allometry with respect to other nuclei (table 6.2). Similarly, nRt varies close to isometry with respect to the

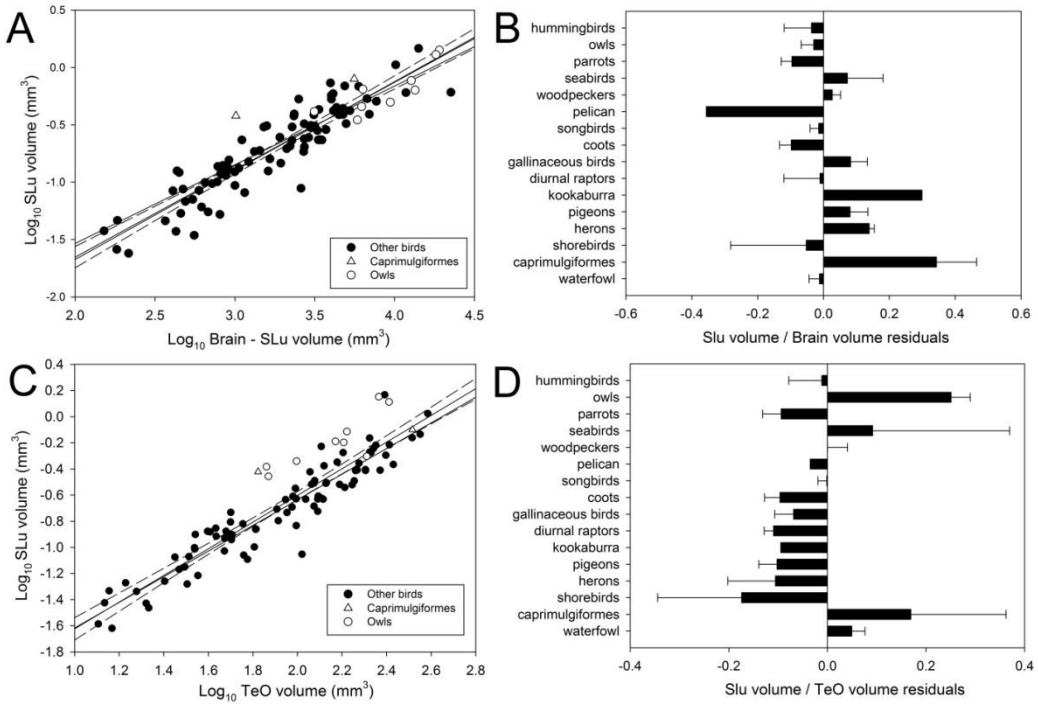

Figure 6.5. Relative size of nucleus semilunaris. Scatterplot of log-transformed volume of nucleus semilunaris (SLu) plotted as a function of the log-transformed brain volume minus the SLu volume (**A**) or the log-transformed volume of the optic tectum (**TeO; B**) for all species examined (see Appendix E). The bar graph shows the relative size of SLu relative to the brain (**B**) or the TeO (**C**). Values shown are the means of the residuals derived from the respective regressions show in **A** and C.

isthmal nuclei (Imc = 1.01, Ipc = 1.01, and SLu = 1.05) but positive allometry with respect to other visual nuclei (table 6.2). Bivariate allometric coefficients also indicated that the isthmal nuclei vary with isometry with each other, but positive allometry with respect to other visual nuclei (table 6.2). LM and nBOR also varied with positive allometry with respect to ION and GLv, but close to isometry with each other (0.97) and that GLv and ION also vary with isometry with each other (0.99).

We then performed the same analysis as above, but using the relative size of each nucleus expressed as the phylogenetically corrected residuals against the brain. In this case, the evolutionary rate differed significantly from a Brownian motion model for some of the nuclei (table 6.3). The relative size of SLu, LM and GLv clearly show a significant departure form Brownian motion as both the α and λ Ln likelihood estimates are significantly different from that of the Brownian motion model (table 6.3). In the case of nBOR and TeO only the α Ln likelihood estimates are significantly different from that of the Brownian motion model. The evolutionary rate of change of the relative size of ION, Imc, Ipc and nRt, however, are not significantly different from a Brownian motion model.

Because the relative size of some of the nuclei departs from Brownian motion evolutionary model, we performed a PCA using both a Brownian motion model and Pagel's λ model of evolutionary change. We found no major differences in the estimated values between the two models with either of the phylogenies used (table 6.1, S5). When relative size of the nuclei was used in the

PCA to remove the effect of absolute brain size, the PC1 explained around 45 % of the variance. All of the nuclei were positively loaded on PC1, but not with the same strength. Imc, Ipc, TeO and SLu loaded strongly (loadings > 0.7) while LM, GLv and ION had loadings well below 0.5 (table 6.1, S5). PC1 values were significantly correlated with the size of the brain (PGLS using Hackett et al. 2008; R^2= 0.109 , $F_{1,93}$ = 11.33, P = 0.001), suggesting that the size correction removed most, but not all, effects of variation in brain size. PC2 explains about 15 % of the variance with a strong loading of GLv and LM. Finally, PC3 explained about 10.5% of the variance with a strong loading of ION.

6.3 Discussion

This is the first study to assess variation of the relative size of the isthmal nuclei in birds. In recent years, the isthmotectal system has received increased attention, especially in birds, as a model to study visual spatial attention and competitive stimulus selection [Sereno, and Ulinski, 1987; Marín et al., 2005; Salas et al., 2007; Marín et al., 2012; Gruberg et al., 2006; Asadollahi et al., 2010; Asadollahi et al., 2011; Mysore et al., 2011; Knudsen, 2011]. We found the differences in relative size of Ipc and Imc between orders closely matches that of the TeO (fig. 6.6J) and the principal component and evolutionary rate analyzes further support that Imc and Ipc evolve in a concerted manner with TeO (table 6.1, 6.2,6.3; see below). Recently Faunes et al. [2013] showed that Imc is segregated in two distinct layers in at least three different orders; songbirds, woodpeckers and coots, and that these layers correspond, at least in songbirds, to

two types of projecting cells in Imc (see introduction). Our results show that Imc is not relatively larger in any these three groups compared to other birds. Therefore, the segregation of neurons within Imc is not related to an increase in relative size of the nucleus. Our results do show that there is a significant difference between songbirds, woodpeckers and coots, and the rest of the species in the size of Imc and Ipc relatively to the TeO (fig. 6.4E-H; Appendix G), but woodpeckers do not show a relative large Imc and Ipc respect to TeO (fig. 6.4E-H). Therefore, the difference in Imc and Ipc size relative to TeO is not entirely due to this separation of two cell layers in Imc. As Faunes et al. [2013] pointed out, the segregation of Imc has evolved independently three times, but the groups that presented this segregation share little in their ecology or visual behaviors, making it difficult to determine the possible functional consequences of this segregation. Lamination of a structure is thought to enhance the separation of information within a neural pathway [Walls, 1953], but that seem to be only partially true in this case. Imc only receives projections from one type of cell in TeO [Wang et al., 2004] and even though the segregated cells project to different targets (TeO vs. Ipc/SLu), both inhibit the surrounding of a locus being activated in the TeO and Ipc/SLu [Salas et al., 2007; Wylie, 2013]. Experiments comparing fine differences in the response of the two types of cells segregated in the Imc may be need it to pinpoint the functional consequences of this segregation.

Our results indicate that evolutionary changes in the size of SLu are distinct from that of the other isthmal nuclei. Although bivariate allometric coefficients and loadings of SLu in PC1 of the relative size PCA suggest that the

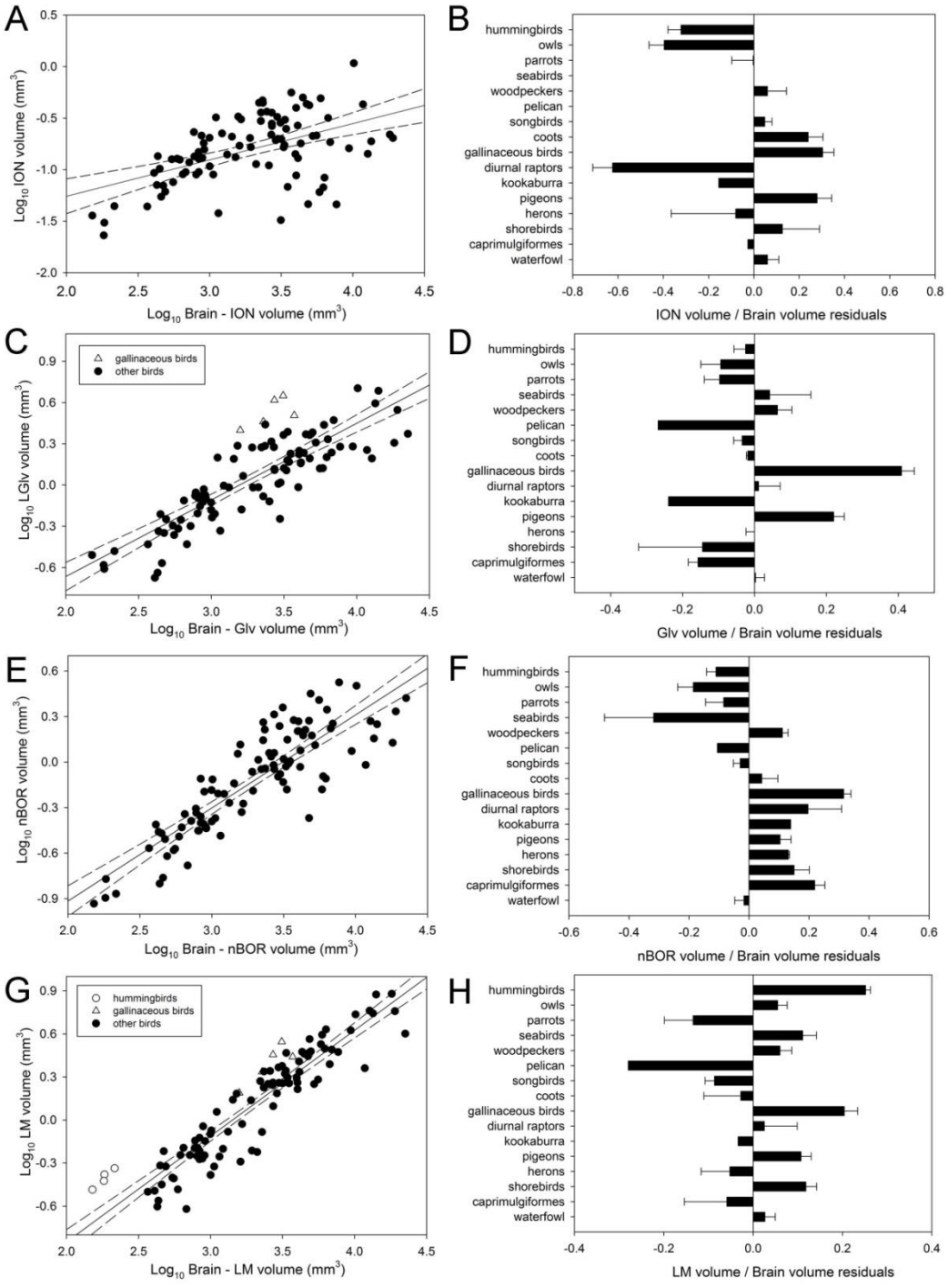
A
B
C
D
E
F
G
H
Log10 ION volume (mm3)
Log10 Brain - ION volume (mm3)
ION volume / Brain volume residuals
Log10 LGlv volume (mm3)
Log10 Brain - Glv volume (mm3)
Glv volume / Brain volume residuals
Log10 nBOR volume (mm3)
Log10 Brain - nBOR volume (mm3)
nBOR volume / Brain volume residuals
Log10 LM volume (mm3)
Log10 Brain - LM volume (mm3)
LM volume / Brain volume residuals
hummingbirds
gallinaceous birds
other birds
owls
parrots
seabirds
woodpeckers
pelican
songbirds
coots
gallinaceous birds
diurnal raptors
kookaburra
pigeons
herons
shorebirds
caprimulgiformes
waterfowl

Figure 6.6. Relative size of other visual nuclei. Scatterplot of log-transformed volume of different nuclei plotted as a function of the log-transformed brain volume minus the volume of the respective nuclei (**A**, **C**, **E**, **G** and **I**). The bar graphs show the relative size each nuclei relative to the brain represented as the mean of the residuals derived from the respective regressions (**B**, **D**, **F**, **H** and **K**). **A-B**, Scatterplot and bar graph for the isthmo optic nucleus (**ION**). **C-D**. Scatterplot and bar graph for the ventral geniculate nucleus (**GLv**). The white triangles correspond to gallinaceous birds. Black circles to all other birds studied. **E-F**, Scatterplot and bar graph for the nucleus of the basal optic root (**nBOR**). **G-H**, Scatterplot and bar graph for the nucleus lentiformis mesencephali (**LM**). The white triangles correspond to gallinaceous birds. Open circles correspond to hummingbirds. Black circles to all other birds species studied**.**

relative size of SLu varies more closely with Imc, Ipc, TeO and nRt, other lines of evidence suggest that the relative size of SLu is more independent. First, we found significant differences between orders in the relative size of Imc and Ipc, and these closely follow the differences in relative size of TeO and nRt among orders, but we found no differences among orders in the relative size of SLu, suggesting the variation of the relative size of SLu is different from that of Imc and Ipc (and TeO/nRt). Second, while the evolutionary rate of the relative size of Imc, Ipc, TeO and nRt do not differ significantly from a Brownian motion model (see below), that of SLu clearly does (table 6.3). The difference in evolutionary patterns between Ipc and SLu is surprising given the similarities between these two nuclei. Both are cholinergic, have reciprocal topographic projections with the TeO, and also receive an anti-topographic projection from Imc, presumably from collaterals of axons going to Ipc [fig. 6.1B; Wang et al., 2006]. This suggests that, like Ipc, SLu takes part in a stimulus selection mechanism in the TeO but with different tectal outputs. Ipc projects mainly to the retinorecipient layers of TeO, whereas SLu project to deeper layers [Wang et al., 2006]. Within the TeO, Ipc terminals make connections with type I tectal ganglion cells (TGCs), which then project to the nucleus rotundus [nRt; Karten et al., 1997; Manns et al., 2004]. In contrast, Wang et al. [2006] suggested that SLu cells are likely to make contact with type II TGCs, which have dendritic fields in the deep layers of TeO and project to a different subdivision of nRt than type I TGCs. Recently, Marin et al., [2012] found that blocking activity in SLu produce no changes in the activity of nRt and proposed that SLu probably makes contact with TGCs that give rise to

descending tectal projections, the tectopontine and crossed tectobulbar pathways [Reiner, and Karten, 1982]. In either case, Ipc and SLu seem to contact different population of TeO cells and this difference in connectivity between them suggest they differ slightly in function. Our results show that while both nuclei seem to covary in some degree with TeO, they also differ markedly in their evolutionary patterns. This would corroborate that they are functionally differences between Ipc and SLu.

Interestingly, while we found no differences in size of SLu relative to the brain among orders (fig. 6.5B), we found owls have a greatly enlarge SLu relative to the size of TeO when compared to almost all other orders (Fig 6.5C-D). As already mentioned (see above), SLu sends projections to the deep layers of TeO, which are the same layers that in owls receive auditory projections from the external part of the inferior colliculus [Knudsen, and Knudsen, 1983], which then results in an auditory spatial map in register with the visual map of the TeO [Knudsen, 1982]. Owls have enlarge auditory nuclei compared to other birds [Kubke et al., 2004b; Iwaniuk et al., 2006] and thus the particular large size of SLu relative to the TeO may be related to the largely bimodal nature of the TeO in owls.

6.3.2 Other visual nuclei

In both PCAs we found that in the second principal component, which explained around 15% of the variation in the size corrected PCA, GLv and LM load in the same direction, suggesting they vary in relative size together and

therefore may have shared functions. Groups like gallinaceous birds and pigeons, which have relatively large LM and GLv, have likely driven this covariation of LM and GLv sizes. In a previous study, Iwaniuk and Wylie [2007] showed, using a smaller sample of species, that hummingbirds and other semi hovering species have a large LM compared to other species. Our results confirm these findings, but also show that gallinaceous birds have enlarged LM compared to other birds. This difference between the two studies is likely related to the species sampling. Iwaniuk and Wylie [2007] only had one species of gallinaceous birds while we sampled 5, allowing for statistical comparisons with other groups. As mentioned before, the function of GLv remains unknown, but many functions have been proposed (see Introduction). Interestingly, Gioanni et al. [1991] showed that in pigeons, lesions of GLv had a marked effect on the gain of the horizontal, but not the vertical, optokinetic nystagmus, especially in the temporal to nasal direction. nBOR and LM are both involved in generating the optokinetic responce [Fite et al., 1981; Gioanni et al., 1983a; Gioanni et al., 1983b] and have similar response properties [Burns, and Wallman, 1981; Morgan, and Frost, 1981; Winterson, and Brauth, 1985], but cells in LM respond preferentially to motion in the temporal-nasal direction. Our results suggesting some covariation of the relative size of LM and GLv would then support the idea that GLv is involved in regulating the optokinetic response, particularly in the temporal-nasal direction. A possible caveat is that projections from nBOR to LM course through or immediately dorsal to GLv [Wylie et al., 1997] and therefore lesions of GLv may also lesion this pathway. Inhibition of nBOR has a profound effect on the spatio-temporal tuning

of LM cells [Crowder et al., 2003] and therefore the effect of lesioning GLv upon the optokinetic response may be solely to the interruption of the nBOR-LM pathway.

The covariation of LM and GLv may be partially related to the cytoarchitectonical and hodological similitudes between the two nuclei. Gamlin and Cohen [1988a,b] noted that the medial part of LM (LMm) is almost contiguous with the external, retinorecipient lamina, of GLv. Further, these same authors notice that the external layer of GLv, which is not retinorecipient, is continuous with the nucleus laminaris precommissuralis (LPC), which lies medial to LMm thought the anteroposterior extend of LM and is also not retinorecipient. These suggest that the relationship between LMm and LPC may be equivalent to that of the external and internal laminae of GLv, further supporting the affinity between these two nuclei. Fine detail studies of the afferent and efferent of GLv and its relation to LM are needed to further clarify the relationship between these two nuclei.

Our results on the variation in the relative size of the TeO and nRt among orders were similar to what has been reported before [Iwaniuk et al., 2010]. Owls and waterfowl have the smallest TeO and nRt relative size, while diurnal raptors, herons, pigeons and gallinaceous birds have a relatively large TeO and nRt (fig. 6.6I-J). Previously we found that parrots have a TeO relatively smaller than most other orders [Iwaniuk et al., 2010] but we found that the TeO of parrots is only significantly smaller than that of pigeons. These differences are probably related to different species sampling between the two studies. For example, in Iwaniuk et

al. [2010] 24 species of parrots were sampled whereas in the present study only 8 were sampled. Fewer species were sampled in our study because it was not always possible to measure the size of all regions of interest due to the quality of the tissue and staining in some of the specimens. It has been extensively shown that sampling can affect the slope and intercept of allometric relationships [Harvey, and Pagel, 1991; Striedter, 2005] and therefore affect the residuals of different groups. In fact the slope for the relationship between TeO and brain size is 0.663 in the current study but was 0.756 in Iwaniuk et al. [2010]. Nonetheless, our results still suggest that parrots have a relatively small tectofugal pathway compared to other birds [Striedter, and Charvet, 2008].

6.3.3 Statistical analysis

Previous studies that tested between mosaic and concerted models of evolutionary change in the brain did so by examining allometric scaling trends [e.g. Barton, and Harvey, 2000; Yopak et al., 2010]. Although allometric approaches reveal some important information on brain structure evolution, they are clearly insufficient to adequately assess covariation among structures, particularly covariation in relative size. The use of a combination of statistical approaches; phenotypic evolutionary rates of changes and phylogenetically corrected PCA (pPCA) provides a robust way to asses covariation of the relative size of neural structures. In our study, the concerted variation of isthmal nuclei and TeO and the more independent variation of other visual nuclei was supported

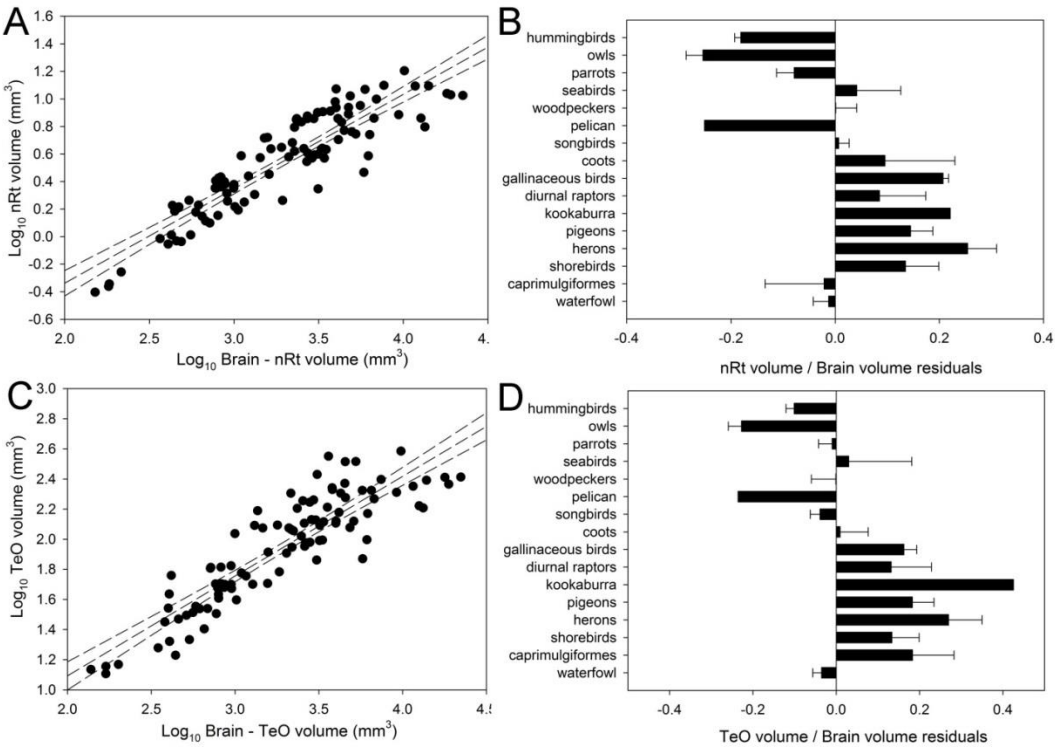

Figure 6.7. Relative size of optic tectum and nucleus rotundus. Scatterplot of log-transformed volume of structures of the tectofugal pathway plotted as a function of the log-transformed brain volume minus the volume of the respective nuclei (**A** and **C**). The bar graphs show the relative size each nuclei relative to the brain represented as the mean of the residuals derived from the respective regressions (**B** and **D**). **A-B**, Scatterplot and bar graph for the nucleus rotundus (**nRt**). **C-D**. Scatterplot and bar graph for the optic tectum (**TeO**).

by differences/similarities in evolutionary rates of change, bivariate allometric coefficients and the loadings of each structures in different principal components.

Our study also examined both absolute sizes and phylogenetically corrected relative sizes whereas previous studies have only examined one or the other [Gonzalez-Voyer et al., 2009; Smaers, and Soligo, 2013] in their pPCAs. As shown above, both methods provide different information. In the pPCA with absolute volume, PC1 provides the amount of variation explained by variation in absolute brain size (78-79 % in this case, see table 6.1, appendix I), and therefore a proxy for the amount of concerted evolution vs. mosaic evolution present (see below). In the pPCA with the size corrected values, while most PCs are very similar to the other analysis, the PC1 revealed a brain size independent covariation of the visual nuclei not shown in the other analysis (see results). Future studies should use a combination of these analyses, in addition of changes in evolutionary rate to properly assess the evolution of brain morphology as they provide multiple, independent means of testing the covariation of different neural structures.

6.3.4 Multivariate allometric analysis.

Striedter (2005) proposed a probabilistic approach to asses if mosaic or concerted evolution explains the variation in the size of different neural structures where variable amount of mosaic evolution operate over a background of concerted evolution. In studies where concerted evolution has been proposed to be the main driver of changes in the size of different brain regions, more than 90 %

of variance in the size of different neural structures is explained by variation in the absolute size of the brain [e.g. Finlay and Darlington 1995; Powel and Leal 2012]. Our results show that between 78 and 79 % of the variance in the size of visual structures in birds is explained by variation in the absolute size of the brain (table 6.1, appendix I). This is lower than any other previous studies, even those where mosaic evolution has been propose to play an important role in the evolution of neural structures [Finlay and Darlington 1995; Yopak et al., 2010; Gonzalez-Voyer et al., 2011; Powell and Leal; 2012]. Therefore we propose that mosaic evolution has had a major role in the evolution of the visual system of birds. Our results suggest that not all nuclei are under mosaic evolution but rather that some nuclei tend to vary in size in a coordinated manner with each other and the absolute size of the brain while other vary more independently. Across the 98 species of birds we examined, the relative size of the isthmal nuclei (particularly Imc and Ipc) and components of the tectofugal pathway (TeO and nRT) vary together, but the relative volumes of ION, nBOR and GLv vary independently of one another in more of a mosaic manner. This pattern is supported by several lines of evidence. First, the bivariate allometric coefficients between Imc, Ipc, SLu, TeO and nRt are all close to 1 (table 6.2), indicating there is an isometric relationship among the isthmal nuclei, and also between the isthmal nuclei and the tectofugal pathway. In contrast, most of the bivariate allometric coefficients calculated between all other nuclei tend to be different from 1 (table 6.2), indicating a departure from isometry. While an isometric relationship between any pair of nuclei implies they evolve in a concerted manner, departure from it does

not necessarily imply the contrary, mosaic evolution. Nonetheless, departure from isometry suggests that structures grow or shrink more independently of changes in size of other structures. Second, in PC1 of the size corrected PCA (table 6.1), Imc Ipc, TeO and nRt and to a lesser degree SLu, load strongly in the same direction while all other nuclei, even though still load in the same direction, have far weaker loadings. In the same analysis, GLv and LM load strongly in PC2, ION is the only structure to load strongly in PC3 in both PCAs and nBOR is the only nucleus with a strong loading on PC4. Taken together, this strongly indicates that the relative size of each of these nuclei vary independently from one another or at most as a pair (e.g., LM and GLv). Third, the differences in the relative size of Ipc and Imc among orders is very similar (fig. 6.4A-D) and closely follow the differences in relative size of TeO and nRt among orders (fig. 6.7A-D), further suggesting that these nuclei vary in a concerted manner. Note, however, that this is not the case for SLu (fig. 6.5B; see above). Finally, the evolutionary rates of change of the different nuclei also support this claim. In concerted evolutionary models, one would expect nuclei that vary in size together to evolve at the same rate. Our results show that changes in relative size of Imc and Ipc, nRt and TeO do not differ significantly from a Brownian motion model, but GLv, LM, nBOR and SLu do. While the TeO does differ from a Brownian motion model when compared to an OU process, this may not truly indicate departure from Brownian motion. The OU model is an extension of the Brownian motion model and characters with small departures from Brownian motion may produce higher likelihood values when their evolution is modeled by an OU process [Butler and

King, 2004]. Thus, when comparing between models of evolutionary change, the value of α is critically important [Butler and King, 2004]. With respect to TeO, α is relatively low, which suggests that the evolutionary rate of change in the relative size of TeO does not depart strongly from Brownian motion and is similar to that of Imc, Ipc and nRt (table 6.3).

The low degree of covariation in the relative sizes of GLv, nBOR and LM from TeO suggested by our results is somewhat surprising given that all three nuclei receive projections from the retina. Iwaniuk et al. [2010] suggested that the relative size of the tectofugal pathway is correlated with the relative amount of retinal ganglion cells (RGCs) and subsequent studies appear to support this idea. Owls and waterfowl, which have relatively smaller tectofugal pathways, have relatively fewer RGCs compared to other birds [Lisney et al., 2012, 2013], and in owls, the relative size of the tectofugal pathway is correlated with the relative number of RGCs [Gutiérrez-Ibáñez et al., 2013]. Our results show that other retinorecipient nuclei do not vary in relative size along with the TeO and this could suggest that the number of RGCs is unlikely to be associated with the sizes of nBOR, GLv or LM. Support for this hypothesis is provided by the pattern of retinal projections to these nuclei; afferents of each nucleus arise from independent populations of RGCs. For example, nBOR receives projections from a subpopulation of retinal ganglion cells found in the amacrine cell layer, known as the displaced ganglion cells [DGCs; Karten et al., 1977; Fite et al., 1981]. LM receive projections from a sub population of RGCs [Bodnarenko et al., 1988] and possibly some DGCs [see Woodson et al., 1995]; D.R Wylie unpublished

observations], and it is possible that some of the RGCs projections are collaterals from RGCs projecting to the TeO. GLv receives projections from RGCs that send collaterals to TeO, but this probably represents only a small proportion of the total retinal ganglion cell population [Britto et al., 1989]. So is possible that while the total number of RGCs or relative size of TeO increases, the numbers of cells that project to these different nuclei remain unchanged or vary independently of total number of RGCs.

Previous studies have suggested that functionally and anatomically related neural structures should vary together [Barton, and Harvey, 2000; Whiting, and Barton, 2003]. On the one hand, the concerted variation of the size of the isthmal nuclei and TeO seems to support this notion. The isthmal nuclei and TeO are heavily interconnected (see introduction) and the isthmal nuclei all participate in a circuit related to stimulus selection in the TeO [Marín et al., 2005; Salas et al., 2007; Mysore et al., 2011]. On the other hand, the independent variation of LM and nBOR, which are also heavily interconnected [Brecha et al., 1980; Wylie et al., 1997] and functionally related [Gioanni et al., 1983a; Gioanni et al., 1983b; Frost et al., 1994; Wylie, 2013], seems to reject the concerted model. This contradictory pattern may be at least partially explained by the diversity of connections of the retinorecipient nuclei. The isthmal nuclei are connected to a much smaller number of other brain regions when compared to the retinorecipient nuclei in this study. Imc only receives projections from TeO and projects to TeO, Ipc and SLu, while Ipc and SLu only receive projections from TeO and Imc [reviewed in Wylie et al., 2009]. So while only a small fraction of cells in TeO

project to the isthmal nuclei, cells in the isthmal nuclei only project to either the TeO or other isthmal nuclei, forming a closed network. This is also supported by the close variation of relative size of three components of the tectofugal pathway (TeO, nRt and entopallium), which was previously suggested by Iwaniuk et al. [2010] and seems largely confirmed by our results showing that TeO and nRt evolve in a concerted manner. nRt receives projection only from TeO, the nucleus subpretectalis [Mpodozis et al., 1996] and maybe SLu [Hellmann et al., 2001] and projects exclusively to the entopallium which only has one other afferent [Karten, and Hodos, 1970; Krützfeldt, and Wild, 2005]. In contrast, in addition to receiving projections from the retina and each other, LM and nBOR receive projections from the visual Wulst, the TeO and other structures [Miceli et al., 1979; Rio et al., 1983]. LM and nBOR also have a diversity of efferent targets that includes the inferior olive, cerebellum, oculomotor regions, pontine nuclei and ventral tegmentum, among other structures [Gamlin, and Cohen, 1988b; Wylie et al., 1997; Brecha et al., 1980; Wild, 1989], and these projections emerge from distinct neuronal populations within nBOR and LM [Pakan et al., 2006; Wylie et al., 2007]. Similarly, GLv also has several inputs and outputs; Beside efferents from the retina and TeO [Reperant, 1973; Hunt, and Künzle, 1976; Crossland, and Uchwat, 1979], GLv receives projections from the Wulst [Miceli et al., 1987; Ehrlich et al., 1989] and projects to the dorsal thalamus [Wylie et al., 1998] and the TeO [Brecha, 1978; Crossland, and Uchwat, 1979]. Therefore, our results suggest that the covariation of different neural structures depends not only on the functional connectivity of each nucleus but on the “exclusivity” or diversity of the

connections between them. We think our study further emphasizes the need for future research to consider variation of neural pathways as a whole and not isolated neural structures, particularly when the relative size of a neural structures in being correlated with a particular ecology or behavior. Our study shows that a combination of multivariate statistics and rates of evolution are constitute a robust method to study patterns of evolutionary change in neural pathways.

Table 6.1. Results of Principal component analysis. Loadings, eigenvalues and cumulative amount of variation explained by four of the components (PC's) obtained from a PCA analysis using the log-transformed volume or the relative size (residuals, see methods) of nine visual nuclei. Values obtained using Hackett et al., [2008] phylogeny are shown. Values obtained with two different evolutionary models (Brownian motion and pagel's lambda) are also shown for the relative size PCA. For complete values with both phylogenies used in this study see Appendix I.

Hackett et al., [2008]														
log-volume (BM)	PC1	PC2	PC3	PC4	Resid. (BM)	PC1	PC2	PC3	PC4	Resid. (λ)	PC1	PC2	PC3	PC4
Imc	-0.95	0.20	0.03	-0.06		0.84	0.27	0.03	0.15		-0.86	0.20	-0.04	0.07
Ipc	-0.95	0.21	0.06	-0.02		0.90	0.21	0.08	0.04		-0.91	0.21	-0.09	0.06
SLu	-0.91	0.14	0.04	-0.07		0.72	0.06	0.03	0.04		-0.74	0.18	0.02	0.25
ION	-0.72	-0.15	-0.68	0.02		0.28	-0.18	-0.93	-0.09		-0.31	-0.23	0.91	-0.10
GLv	-0.76	-0.58	0.19	0.07		0.29	-0.83	0.15	-0.13		-0.27	-0.82	-0.15	-0.14
nBOR	-0.88	0.05	0.08	0.44		0.57	-0.04	0.14	-0.77		-0.62	-0.06	-0.19	-0.69
LM	-0.87	-0.30	0.09	-0.22		0.43	-0.73	0.08	0.31		-0.35	-0.76	-0.13	0.34
nRt	-0.96	0.11	0.00	-0.02		0.82	0.12	-0.09	0.05		-0.86	0.04	0.09	-0.03
Tectum	-0.95	0.15	0.07	-0.10		0.87	0.08	0.07	0.17		-0.89	0.08	-0.07	0.13
eigenvalues	7.08	0.59	0.52	0.26		4.13	1.39	0.94	0.78		4.31	1.43	0.93	0.71
% variance	78.68	6.53	5.82	2.93		45.88	15.49	10.47	8.65		47.88	15.86	10.28	7.93

Table 6.2. Visual nuclei bivariate allometric coefficients. Coefficients of the bivariate allometric relationship between visual nuclei calculated from the loading of each nucleus in the first principal component of a phylogenetically corrected PCA performed with Hacket et al., [2008] phylogeny (see Methods for calculations details).

ff

	Ipc	SLu	ION	GLv	nBOR	LM	nRt	TeO
Imc	1	0.96	0.78	0.8	0.93	1.93	1.01	1
Ipc		0.1	0.77	0.8	0.93	1.93	1.01	1
SLu			0.81	0.84	0.97	1.97	1.05	1.05
ION				1.03	1.2	1.19	1.3	1.29
GLv					1.16	1.16	1.26	1.25
nBOR						1	1.09	1.08
LM							1.09	1.08
nRt								0.99

Table 6.3. Maximum likelihood estimates of the evolutionary parameters. Maximum likelihood estimators for the λ and α for the relative size (see methods) of nine visual nuclei. *P* values for the λ and α parameters were determined from likelihood ratio tests against an unconstrained Brownian motion model. Hackett et al. [2008] phylogeny was used in this case (see Appendix H for values with other phylogeny and values obtained with the log-transformed volume of each nuclei).

Hackett et al. [2008] /residuals	Brownian	Lambda			Alpha		
Brain structure	Ln likelihood	λ	Ln likelihood	p	α	Ln likelihood	p
Imc	35.92	1.00	35.92	1.0	0.05	36.16	0.486
Ipc	31.58	1.00	31.58	1.0	0.14	33.38	0.057
Slu	33.03	0.47	39.12	0.0005	0.61	46.08	> 0.0001
ION	14.29	1.00	14.29	1.0	0.07	14.92	0.263
Glv	39.10	0.87	41.77	0.021	0.22	42.32	0.011
nBOR	40.82	0.89	42.70	0.052	0.25	44.33	0.008
LM	53.12	0.71	59.89	0.0002	0.23	57.51	0.003
Rt	64.21	1.00	64.21	1	0.07	64.87	0.250
TeO	53.80	0.92	54.82	0.152	0.20	56.99	0.011

6.4 References

Asadollahi A, Mysore SP, Knudsen EI. (2010):. Stimulus-driven competition in a cholinergic midbrain nucleus. Nature neuroscience 13:889–95.

Asadollahi A, Mysore SP, Knudsen EI. (2011):. Rules of competitive stimulus selection in a cholinergic isthmic nucleus of the owl midbrain. J neurosci: 31:6088–97.

Barker FK, Cibois A, Schikler P, Feinstein J, Cracraft J. (2004): Phylogeny and diversification of the largest avian radiation. PNSA 101:11040–5.

Barton R a, Harvey PH. (2000): Mosaic evolution of brain structure in mammals. Nature 405:1055–8.

Barton R a. (1998): Visual specialization and brain evolution in primates. Proc R Soc Lond B 265:1933–7.

Bischof HJ, Watanabe S. (1997): On the structure and function of the tectofugal visual pathway in laterally eyed birds. European journal of morphology 35:246–54.

Bodnarenko SR, Rojas X, McKenna OC. (1988): Spatial organization of the retinal projection to the avian lentiform nucleus of the mesencephalon. J Comp Neurol 269:431–47.

Brecha N, Karten HJ, Hunt SP. (1980): Projections of the nucleus of the basal optic root in the pigeon: an autoradiographic and horseradish peroxidase study. J Comp Neurol 189:615–70.

Brecha NC. (1978): Some observations on the organization of the avian optic tectum: Afferent nuclei and their tectal projections.

Britto LRG, Hamassaki DE, Keyser KT, Karten HJ. (1989): Neurotransmitters , receptors , and neuropeptides in the accessory optic system : An immunohistochemical survey in the pigeon (Columba livia). Visual Neuroscience:463–475.

Brown D, Toft C. (1999): Molecular systematics and biogeography of the cockatoos (Psittaciformes: Cacatuidae). The Auk 116:141–157.

Burns S, Wallman J. (1981): Relation of single unit properties to the oculomotor function of the nucleus of the basal optic root (accessory optic system) in chickens. Experimental brain research 42:171–80.

Butler M, King A. (2004): Phylogenetic comparative analysis: a modeling approach for adaptive evolution. The American Naturalist 164:683–695.

Crossland WJ, Uchwat CJ. (1979): Topographic projections of the retina and optic tectum upon the ventral lateral geniculate nucleus in the chick. The J Comp Neurol. 185:87–106.

Crowder NA, Lehmann H, Parent MB, Wylie DRW. (2003): The accessory optic system contributes to the spatio-temporal tuning of motion-sensitive pretectal neurons. Journal of neurophysiology 90:1140–51.

Deacon TW. (1990): Fallacies of progression in theories of brain-size evolution. International Journal of Primatology 11:193–236.

Deaner RO, Isler K, Burkart J, Van Schaik C. (2007): Overall brain size, and not encephalization quotient, best predicts cognitive ability across non-human primates. Brain behav evol 70:115–24.

Dobson SD, Sherwood CC. (2011): Correlated evolution of brain regions involved in producing and processing facial expressions in anthropoid primates. Biology letters 7:86–88.

Donne-Goussé C, Laudet V, Hänni C. (2002): A molecular phylogeny of anseriformes based on mitochondrial DNA analysis. Molecular phylogenetics and evolution 23:339–356.

Driskell A, Christidis L. (2004): Phylogeny and evolution of the Australo-Papuan honeyeaters (Passeriformes, Meliphagidae). Molecular phylogenetics and evolution 31:943–960.

Ehrlich D, Stuchbery J, Zappia J. (1989): Organisation of the hyperstriatal projection to the ventral lateral geniculate nucleus in the chick (Gallus gallus). Neuroscience Letters 104:1–6.

Faunes M, Fernández S, Gutiérrez-Ibáñez C, Iwaniuk AN, Wylie DR, Mpodozis J, Karten HJ, Marín G. (2013): Laminar segregation of GABAergic neurons in the avian nucleus isthmi pars magnocellularis: a retrograde tracer and comparative study. J Comp Neurol . 521:1727–42.

Finlay BL, Darlington RB. (1995): Linked regularities in the development and evolution of mammalian brains. Science 268:1578–1584.

Finlay BL, Darlington RB, Nicastro N. (2001): Developmental structure in brain evolution. The Behavioral and brain sciences 24:263–78; discussion 278–308.

Fite K V, Brecha N, Karten HJ, Hunt SP. (1981): Displaced ganglion cells and the accessory optic system of pigeon. J Comp Neurol. 195:279–88.

Freckleton R. (2002): On the misus of residuals in ecology: regression of residuals vs. multiple regression. J Anim Ecol 71:542–545.

Frost BJ, Wylie DR, Wang YC. (1994): The analysis of motion in the visual systems of birds. In: Perception and motor control in birds. Springer. p 248–269.

Gamlin PD, Cohen DH. (1988a): Retinal projections to the pretectum in the pigeon (Columba livia). J Comp Neurol 269: 1–17.

Gamlin PDR, Cohen DH. (1988b): Projections of the retinorecipient pretectal nuclei in the pigeon (Columba livia). J Comp Neurol. 269: 18–46.

Gamlin PDR, Reiner A, Erichsen JT, Karten HJ, Cohen DH. (1984): The neural substrate for the pupillary light reflex in the pigeon (Columba livia). J Comp Neurol. 226: 523–543.

Garland Jr T, Ives AR. (2000) Using the past to predict the present: confidence intervals for regression equations in phylogenetic comparative methods. Amer Natur 155: 346–364.

Garland T, Bennett AF, Rezende EL. (2005): Phylogenetic approaches in comparative physiology. J Expl Biol 208: 3015–3035.

Garland T, Harvey P, Ives A. (1992): Procedures for the analysis of comparative data using phylogenetically independent contrasts. Syst Biol 41: 18–32.

Gioanni H, Palacios A, Sansonetti A, Varela F. (1991): Role of the nucleus geniculatus lateralis ventralis (GLv) in the optokinetic reflex: a lesion study in the pigeon. Exp Brain Res 86: 601–607.

Gioanni H, Rey J, Villalobos J. (1983a): Optokinetic nystagmus in the pigeon (Columba livia) II. Role of the pretectal nucleus of the accessory optic system (AOS). Exp Brain Res 50: 237–247.

Gioanni H, Villalobos J, Rey J, Dalbera A. (1983b): Optokinetic nystagmus in the pigeon (Columba livia) III. Role of the nucleus ectomamillaris (nEM): interactions in the accessory optic system (AOS). Exp Brain Res. 50: 248-58.

Gonzalez-Voyer A, Winberg S, Kolm N. (2009): Brain structure evolution in a basal vertebrate clade: evidence from phylogenetic comparative analysis of cichlid fishes. BMC Evol Biol 9.

Granda RH, Crossland WJ. (1989); GABA-like immunoreactivity of neurons in the chicken diencephalon and mesencephalon. J Comp Neurol 287:455–69

Gruberg E, Dudkin E, Wang Y. (2006) Influencing and interpreting visual input: the role of a visual feedback system. J Neurosci 26:10368–10371.

Güntürkün O, Remy M. (1990): The topographical projection of the nucleus isthmi pars parvocellularis (Ipc) onto the tectum opticum in the pigeon. Neurosc Lett 111:18–22.

Gutiérrez-Ibáñez C, Iwaniuk AN, Lisney TJ, Faunes M, Marín GJ, Wylie DR. (2012): Functional implications of species differences in the size and morphology of the isthmo optic nucleus (ION) in birds. PloS one 7:e37816.

Gutiérrez-Ibáñez C, Iwaniuk AN, Lisney TJ, Wylie DR. (2013):. Comparative study of visual pathways in owls (aves: strigiformes). Brain behav evol 81:27–39.

Gutiérrez-Ibáñez C, Iwaniuk AN, Wylie DR. (2009): The independent evolution of the enlargement of the principal sensory nucleus of the trigeminal nerve in three different groups of birds. Brain behav evol 74:280–94.

Gutiérrez-Ibáñez C, Iwaniuk AN, Wylie DR. (2011): Relative size of auditory pathways in symmetrically and asymmetrically eared owls. Brain behav evol 78:286–301.

Hackett SJ, Kimball RT, Reddy S, Bowie RCK, Braun EL, Braun MJ, Chojnowski JL, Cox WA, Han K-L, Harshman J, et al. (2008): A phylogenomic study of birds reveals their evolutionary history. Science 320:1763–8.

Hansen T. (1997): Stabilizing selection and the comparative analysis of adaptation. Evolution 51:1341–1351.

Harmon AL, Weir J, Brock C, Challenger W, Hunt G, Harmon ML. (2013): Package " geiger ."

Harvey PH, Pagel M. (1991):. Comparative method in evolutionary biology. Oxford: Oxford University Press.

Hellmann B, Manns M, Güntürkün O. (2001): Nucleus isthmi, pars semilunaris as a key component of the tectofugal visual system in pigeons. J Comp Neurol. 436:153–166.

Hunt SP, Brecha N. (1984): The avian optic tectum: a synthesis of morphology and biochemistry. Comparative neurology of the optic tectum New York: Plenum Press p:619–648.

Hunt SP, Künzle H (1976) Observations on the projections and intrinsic organization of the pigeon optic tectum: an autoradiographic study based on

anterograde and retrograde, axonal and dendritic flow. J Comp Neurol. 170:153–172.

Hunt SP, Webster KE. (1975) The projection of the retina upon the optic tectum of the pigeon. J Comp Neurol 162:433–45.

Husband S, Shimizu T. (2001): Evolution of the avian visual system. In: Cook RG, editor. Avian Visual Cognition. . [On–line]. Available: www.pigeon.psy.tufts.edu/avc.

Ives AR, Midford PE, Garland T. (2007): Within-species variation and measurement error in phylogenetic comparative methods. Systematic Biology 56:252–270.

Iwaniuk A. (2004): Brood parasitism and brain size in cuckoos: a cautionary tale on the use of modern comparative methods. Inter J Comp Psychol 17:17–33.

Iwaniuk AN, Clayton DH, Wylie DRW. (2006): Echolocation, vocal learning, auditory localization and the relative size of the avian auditory midbrain nucleus (MLd). Behav Brain Res 167:305–17.

Iwaniuk AN, Gutierrez-Ibanez C, Pakan JMP, Wylie DR. (2010): Allometric scaling of the tectofugal pathway in birds. Brain Behav Evol 75:122–37.

Iwaniuk AN, Heesy CP, Hall MI, Wylie DRW. (2008): Relative Wulst volume is correlated with orbit orientation and binocular visual field in birds. J Comp Physiol A 194: 267–82.

Iwaniuk AN, Hurd PL. (2005): The evolution of cerebrotypes in birds. Brain, Behav Evol 65: 215–30.

Iwaniuk AN, Wylie DRW. (2006): The evolution of stereopsis and the Wulst in caprimulgiform birds: J Comp Physiol A 192: 1313–26.

Iwaniuk AN, Wylie DRW. (2007): Neural specialization for hovering in hummingbirds: hypertrophy of the pretectal nucleus Lentiformis mesencephali. J Comp Neurol 500:211–21.

Johnson K, Sorenson M. (1999): Phylogeny and biogeography of dabbling ducks (genus: Anas): a comparison of molecular and morphological evidence. The Auk 116: 792–805.

Karten HJ, Cox K, Mpodozis J. (1997): Two distinct populations of tectal neurons have unique connections within the retinotectorotundal pathway of the pigeon (Columba livia). J Comp Neurol 387: 449–65.

Karten HJ, Hodos W, Nauta WJ, Revzin AM. (1973): Neural connections of the "visual wulst" of the avian telencephalon. Experimental studies in the piegon (Columba livia) and owl (Speotyto cunicularia). J Comp Neurol 150:253–78.

Karten HJ, Hodos W. (1967) A Stereotaxic Atlas of the Brain of the Pigeon:(Columba Livia). Baltimore: Johns Hopkins Press.

Karten HJ, Hodos W. (1970) Telencephalic projections of the nucleus rotundus in the pigeon (Columba livia). J Comp Neurol 140:35–51.

Karten JH, Fite K V, Brecha N. (1977) Specific projection of displaced retinal ganglion cells upon the accessory optic system in the pigeon (Columbia livia). PNAS 74:1753–6.

Kimball R, Braun E. (2008): A multigene phylogeny of Galliformes supports a single origin of erectile ability in non-feathered facial traits. J Avian Biol. 39: 438–445.

Klingenberg CP. (1996) Multivariate Allometry. Nato Asi Series a Life Sciences 284: 23–50.

Knudsen EI, Knudsen PF. (1983) Space-mapped auditory projections from the inferior colliculus to the optic tectum in the barn owl (Tyto alba). J Comp Neurol 218: 187–96.

Knudsen EI. (2011): Control from below: the role of a midbrain network in spatial attention. Europ J Neurosci 33: 1961–72.

Knudsen I. (1982): Auditory and visual maps of space in the optic tectum of the owl.J Neurosci. 2: 1177–1194.

Krützfeldt NOE, Wild JM. (2005): Definition and novel connections of the entopallium in the pigeon (Columba livia). J Comp Neurol 490:40–56

Kubke M, Massoglia D, Carr C. (2004): Bigger brains or bigger nuclei? Regulating the size of auditory structures in birds. Brain Behav Evol 2004:169–180.

Lavin S, Karasov W, Ives A. (2008): Morphometrics of the avian small intestine compared with that of nonflying mammals: a phylogenetic approach. Physiol Biochem Zool 81:526–550.

Lisney TJ, Iwaniuk AN, Kolominsky J, Bandet M V, Corfield JR, Wylie DR. (2012): Interspecifc variation in eye shape and retinal topography in seven species of galliform bird (Aves: Galliformes: Phasianidae). J Comp Physiol A 198: 717–31.

Lisney TJ, Stecyk K, Kolominsky J, Schmidt BK, Corfield JR, Iwaniuk AN, Wylie DR. (2013): Ecomorphology of eye shape and retinal topography in waterfowl (Aves: Anseriformes: Anatidae) with different foraging modes. J of Comp Physiol A 199: 385–402.

Livezey BC, Zusi RL. (2007): Higher-order phylogeny of modern birds (Theropoda , Aves : Neornithes) based on comparative anatomy . II . Analysis and discussion. Zool J Linn Soc:1–95.

Maddison W, Maddison D. (2010):. Mesquite: a modular system for evolutionary analysis. Version 2.6. 2009. Available at mesquiteproject org/mesquite/mesquite.

Manns M, Hellmann B, Gu O. (2004):. Tectal Mosaic: Organization of the Descending Tectal Projections in Comparison to the Ascending Tectofugal. J Comp Neurol 410: 395–410.

Marín G, Mpodozis J, Mpdozis J, Sentis E, Ossandón T, Letelier JC. (2005):. Oscillatory bursts in the optic tectum of birds represent re-entrant signals from the nucleus isthmi pars parvocellularis. J Neurosci 25: 7081–9.

Marín GJ, Dura E, Morales C, González-cabrera C, Sentis E, Mpodozis J, Letelier JC. (2012): Attentional Capture ? Synchronized Feedback Signals from the Isthmi Boost Retinal Signals to Higher Visual Areas. J Neurosci 32: 1110–1122.

Maturana HR, Varela FJ. (1982): Color-opponent responses in the avian lateral geniculate: A study in the quail (*Coturnix coturnix japonica*). Brain Res 247: 227–241.

McKenna OC, Wallman J. (1985): Accessory Optic System and Pretectum of Birds: Comparisons with those of other Vertebrates (Part 1 of 2). Brain Behav Evol 26:91–103.

Medina L, Reiner A. (1994): Distribution of choline acetyltransferase immunoreactivity in the pigeon brain. J Comp Neurol 342:497–537.

Miceli D, Gioanni H, Reperant J, Peyrichoux J. 1979. The avian visual Wulst: I. An anatomical study of afferent and efferent pathways. II. An electrophysiological study of the functional properties of single. In: Granda A, Maxwel J, editors. Neural mechanisms of behavior of the pigeon. New York: Plenum Press. p 223–354.

Miceli D, Repérant J, Villalobos J, Dionne L. (1987): Extratelencephalic projections of the avian visual Wulst. A quantitative autoradiographic study in the pigeon Columbia livia. Journal für Hirnforschung 28:45–57.

Midford P, Garland Jr T, Maddison W. (2008): PDAP: a Mesquite translation of the PDTREE application of Garland et al.'s phenotypic diversity analysis programs, version 1.14. See http://mesquiteproject org/pdap_mesquite.

Morgan B, Frost BJ. (1981): Visual response characteristics of neurons in nucleus of basal optic root of pigeons. Exp Brain Res 42:181–8.

Mpodozis J, Cox K, Shimizu T, Bischof HJ, Woodson W, Karten HJ. (1996): GABAergic inputs to the nucleus rotundus (pulvinar inferior) of the pigeon (columba livia). J Comp Neurol 374:204–22.

Mpodozis J, Letelier J, Concha ML. (1995) Retino-tectal and retino-thalamic Visual phatways of the pigeon (Columba livia). Int J Neurosci 81:123–136.

Mysore SP, Asadollahi A, Knudsen EI. (2011): Signaling of the strongest stimulus in the owl optic tectum. J Neurosci. 31: 5186–96.

Nguyen AP, Spetch ML, Crowder NA, Winship IR, Hurd PL, Wylie DRW. (2004):. A dissociation of motion and spatial-pattern vision in the avian telencephalon: implications for the evolution of “visual streams”. J Neurosci 24: 4962–70.

Pagel M. (1999): Inferring the historical patterns of biological evolution. Nature 401: 877–84.

Pakan JMP, Krueger K, Kelcher E, Cooper S, Todd KG, Wylie DRW, Tg A. (2006): Projections of the Nucleus Lentiformis Mesencephali in Pigeons (Columba livia): A Comparison of the Morphology and Distribution of Neurons with Different Efferent Projections. J Comp Neurol 99:84–99.

Pereira SL, Johnson KP, Clayton DH, Baker AJ. (2007): Mitochondrial and Nuclear DNA Sequences Support a Cretaceous Origin of Columbiformes and a Dispersal-Driven Radiation in the Paleogene. Sys Biol 56 :656–672.

Pubols BH, Welker WI, Johnson JI, others. (1965): Somatic sensory representation of forelimb in dorsal root fibers of raccoon, coatimundi, and cat. J Neurophysiol 28:312–341.

Puelles L, Paxinos G, Watson C, Martinez S, Martinez-de-la-Torre M. (2007): The chick brain in stereotaxic coordinates: an atlas based on neuromeres. Amsterdam: Academic Press.

Purvis A, Garland T. (1993): Polytomies in comparative analyses of continuous characters. Syst Biol 42:569–575.

R Core Team. (2013): R: A Language and Environment for Statistical Computing. Available from: http://www.r-project.org/

Reiner a, Karten HJ. 1982. Laminar distribution of the cells of origin of the descending tectofugal pathways in the pigeon (Columba livia). J Comp Neurol 204:165–87.

Reiner A, Perkel DJ, Bruce LL, Butler AB, Csillag A, Kuenzel W, Medina L, Paxinos G, Shimizu T, Striedter G, et al. (2004): Revised nomenclature for avian telencephalon and some related brainstem nuclei. J Comp Neurol 473:377–414.

Remy M, Güntürkün O. (1991): Retinal afferents to the tectum opticum and the nucleus opticus principalis thalami in the pigeon. J Comp Neurol 305:57–70.

Reperant J. (1973): New data on visual projections in the pigeon (Columba livia). J Hirnforsch 14:151–187.

Revell LJ. (2009): Size-correction and principal components for interspecific comparative studies. Evolution 63: 3258–68.

Rio J, Villalobos J, Miceli D, Reperant J. (1983): Efferent projections of the visual wulst upon the nucleus of the basal optic root in the pigeon. Brain Res 8: 145-51.

Salas C, Sentis E, Rojas X, Letelier JC, Mpodozis J. (2007): A Cholinergic Gating Mechanism Controlled by Competitive Interactions in the Optic Tectum of the Pigeon. J Neurosci 27: 8112–8121.

Schoenemann P. (2004): Brain size scaling and body composition in mammals. Brain Behav evol .63: 47-60.

Sereno M, Ulinski P. (1987): Caudal topographic nucleus isthmi and the rostral nontopographic nucleus isthmi in the turtle, Pseudemys scripta. J Comp Neurol. ;261: 319-46.

Smaers JB, Soligo C. (2013): Brain reorganization, not relative brain size, primarily characterizes anthropoid brain evolution. Proc. R. Soc. B 280:20130269.

Sorenson EM, Parkinson D, Dahl JL, Chiappinelli V a. (1989): Immunohistochemical localization of choline acetyltransferase in the chicken mesencephalon. J Comp Neurol 281:641–57.

Striedter GF, Charvet CJ. (2008): Developmental origins of species differences in telencephalon and tectum size: morphometric comparisons between a parakeet (Melopsittacus undulatus) and a quail (Colinus virgianus). J Comp Neurol 507:1663–75.

Striedter GF. (2005): Principles of Brain Evolution. Sunderland: Sinauer Associates.

Sun H, Frost BJ. (1998): Computation of different optical variables of looming objects in pigeon nucleus rotundus neurons. Nature neuroscience 1:296–303.

Swanson DL, Garland Jr T. (2009): The evolution of high summit metabolism and cold tolerance in birds and its impact on present-day distributions. Evolution 63:184–194.

Tömböl T, Németh A. (1998): GABA-immunohistological observations, at the electron-microscopical level, of the neurons of isthmic nuclei in chicken, Gallus domesticus. Cell Tiss Res 291:255–266.

Vega-Zuniga T, Campos L, Severin D, Marin G, Letelier J, Mpodozis J. (2011):. The avian ventral nucleus of the lateral Geniculate (GLv) has key role in the generation of visually guided gaze orientation movements. In: Program No. 272.17 2011 Neuroscience Meeting Planner. Washington, DC: Society for Neuroscience. Online.

Wakita M, Watanabe S, Shimizu T, Britto LRG. (1992): Visual discrimination performance after lesions of the ventral lateral geniculate nucleus in pigeons (*Columba livia*). Behav Brain Res 51: 211–215.

Walls G. (1953): The lateral geniculate nucleus and visual histophysiology. University of California Publications in Physiology 9:1–100.

Wang Y, Luksch H, Brecha NC, Karten HJ. (2006): Columnar projections from the cholinergic nucleus isthmi to the optic tectum in chicks (Gallus gallus): a possible substrate for synchronizing tectal channels. J Comp Neurol 494:7–35.

Wang Y, Major DE, Karten HJ. (2004): Morphology and connections of nucleus isthmi pars magnocellularis in chicks (Gallus gallus). J Comp Neurol 469:275–97.

Wang YC, Jiang S, Frost BJ. (1993): Visual processing in pigeon nucleus rotundus: luminance, color, motion, and looming subdivisions. Vis Neurosci 10:21–30.

Whiting B., Barton R. (2003): The evolution of the cortico-cerebellar complex in primates: anatomical connections predict patterns of correlated evolution. J Hum Evol 44:3–10.

Wild JM. (1989): Avian somatosensory system: II. Ascending projections of the dorsal column and external cuneate nuclei in the pigeon. J Comp Neurol 287:1–18.

Wilson M, Lindstrom SH. (2011): What the bird's brain tells the bird's eye: the function of descending input to the avian retina. Vis Neurosci 28:337–50.

Wink M, Sauer-gürth H, Gonzalez J. (2009): Molecular Phylogeny of Owls (Strigiformes) Inferred from DNA Sequences of the Mitochondrial Cytochrome b and the Nuclear RAG-1 gene Molecular phylogeny of owls (Strigiformes) inferred from DNA sequences of the mitochondrial cytochrome b and the nuclea. Ardea 97:581–591.

Wink M, Sauer-Gürth H. (2004): Phylogenetic relationships in diurnal raptors based on nucleotide sequences of mitochondrial and nuclear marker genes. In: Chancelo R, Meyburg B-U, editors. Raptors worldwide. Berlin: WWGBP. p 517–526.

Winterson BJ, Brauth SE. (1985): Direction-selective single units in the nucleus lentiformis mesencephali of the pigeon (Columba livia). Exp Brain Research 60:215–26.

Woodson W, Shimizu T, Wild JM, Schimke J, Cox K, Karten HJ. (1995): Centrifugal projections upon the retina: an anterograde tracing study in the pigeon (Columba livia). J Comp Neurol 362:489–509.

Wright T, Schirtzinger E, Matsumoto T, Eberhard JR, Graves .Gary R., Sanchez JJ, Capelli S, Müller H, Scharpegge J, Chambers GK, et al. (2008): A multilocus molecular phylogeny of the parrots (Psittaciformes): support for

a Gondwanan origin during the Cretaceous. Molecular biology and evolution 25:2141–2156.

Wylie DR, Glover RG, Lau KL. (1998): Projections from the accessory optic system and pretectum to the dorsolateral thalamus in the pigeon (Columbia livia): a study using both anteretrograde and retrograde tracers. J Comp Neurol 391:456–69

Wylie DR, Linkenhoker B, Lau KL. (1997): Projections of the nucleus of the basal optic root in pigeons (Columba livia) revealed with biotinylated dextran amine. J Comp Neurol 384:517–36.

Wylie DR. (2013): Processing of visual signals related to self-motion in the cerebellum of pigeons. Behavioral Neuroscience 7:1–15.

Wylie DRW, Gutierrez-ibanez C, Pakan JMP, Iwaniuk AN. (2009): The Optic Tectum of Birds : Mapping Our Way to Understanding Visual Processing. Canadian Journal of Experimental Psychology 63:328–338.

Wylie DRW, Pakan JMP, Elliott CA, Graham DJ, Iwaniuk AN. (2007): Projections of the nucleus of the basal optic root in pigeons (Columba livia): A comparison of the morphology and distribution of neurons with different efferent projections. Visual Neuroscience 24:691–707.

Yopak KE, Lisney TJ, Darlington RB, Collin SP, Montgomery JC, Finlay BL. (2010): A conserved pattern of brain scaling from sharks to primates. PNAS 107:12946–51.

Chapter 7: Summary and Future Directions

A broad of approach has been used to unveil the principles behind brain evolution, from variation of the absolute and relative size of the brain to variation in individual nuclei. Despite these efforts, many questions remain unanswered.

Using birds as a model, the current dissertation adds greatly to our knowledge of the forces that drive differences in morphology and cytoarchitecture of the brain between different species. Several common patterns emerge from the different chapters. For instance, in Chapter 2 we showed that PrV has increased in size independently of phylogeny at least three times, and in Chapter 3 we showed that the enlargement of auditory nuclei related to the presence of ear asymmetry has also occurred in at least three unrelated linages. Similarly, ION has also become larger in several groups independent of phylogeny. Changes in the cytorchitectonic organization of some structures, like the appearance of cell layer and neuropil in ION (Chapter 4) and the separation of different cells types in two distinct layers in Imc [Faunes et al., 2012; Chapter 6] also occurs largely independent of phylogeny. This is similar to the dorsal lateral geniculate nucleus of mammals where and organization in several layers has occurred independently at least three times [Striedter, 2005].

The repeated changes in cytoarchitectonic organization or the increase in the relative size of a specific nuclei suggest that these changes are not "hard" to evolve *i.e.* they rely on small changes in an existing developmental mechanism. For example, when a nucleus increases in size through evolution (and therefore

number of neurons), changes in the timing and duration of neurogenesis are likely responsible [Charvet and Striedter, 2008, 2009; Striedter and Charvet, 2008].

Several studies have shown variation of individual sensory nuclei between species [e.g. Barton, 1998; Kubke et al., 2004; Gutiérrez-Ibáñez et al., 2009; Iwaniuk, and Wylie, 2007], however very little attention has been paid to how components within the same sensory pathway vary. That is, it was previously unknown how variation of one neural structure would affect other structures further downstream within the same sensory pathway. Results from this dissertation show that neural structures belonging to functionally distinct parallel pathway tend to vary in size together within an order (Chapter 3, 4) but at a more macroevolutinary level, nuclei that belong to the same sensory modality, but have distinct functions, can vary in size independently of each other (Chapter 6). Our results in Chapter 6 suggest that the amount of covariation of neural structures depends on the diversity of afferents and efferents of each nucleus. The relationship between number of targets and covariation of neural structures may also be related to the developmental mechanisms of neural pathways, such as developmental cell death and trophic interactions between afferent and efferent targets [Finlay et al., 1987; Linden 1994].

The different chapters of this dissertation show that the comparative method still constitutes a powerful tool to study the brain. They also show that in order to understand the principles and forces that drive brain evolution, we have to approach it from many different levels. This dissertation further suggests that we cannot assume straight forward correlations between behaviour, ecology and the size of isolated neural structures, and that developmental constrains,

phylogenetic contingencies and functional pathways as a whole should be considered when comparing the variation in the size of neural structures.

7.1 Summary of Chapters

This dissertation consists of 5 studies that used the comparative method to study variation of the different brain structures at different levels with the aim of understanding the different factors that determine changes in brain morphology and architecture during evolution.

In Chapter 2 the relative volume of the principal nucleus of the trigeminal nerve (PrV) was compared among 73 species of birds. In birds PrV receives somatosensory information from the orofacial region, mainly from the trigeminal nerve which innervates the beak [Dubbeldam and Karten, 1978]. Previous studies suggested that species that depend heavily on tactile input when feeding have an enlarged PrV [Stingelin, 1961, 1965; Boire, 1989; Dubbeldam, 1998], but no broad systematic analysis across species had been carried out. We found that PrV is enlarged in three groups of birds; waterfowl, beak-probing shorebirds and parrots. These three groups are not closely related to each other [see figure 1.3; Hackett et al., 2008], and therefore our results suggest that the enlargement of PrV has occurred independently at least three times. We related the enlargement of PrV in these three groups with increased necessity of somatosensory information from the orofacial region, concomitant to the particular feeding mechanism of each group. For example, beak-probing shorebirds use pressure information from the tip of the beak to find buried prey in soft substrates [Gerritsen and Meiboom,

1986; Zweers and Gerritsen, 1997; Piersma et al., 1998], whereas waterfowl, especially filter-feeding ducks, use information from the beak, palate, and tongue when feeding [Zweers et al., 1977; Tome and Wrubleski, 1988; Kooloos et al., 1989]. Finally, parrots likely require increased somatosensory information from the tongue to manipulate food items.

After showing a correlation between a single sensory nucleus and ecology we wanted to study variation at the level of sensory pathways, restricted to one order. For this we chose owls (Strigiforms) as they show great variation in ecology and therefore different sensory requirements and specializations. In chapter 3 we investigated differences in the auditory pathway of owls related to the presence of vertically asymmetrical ears. Within owls, these asymmetries have evolved independently several times [Norberg, 1978]. Vertical asymmetry of the ear openings facilitates localization of sound in elevation as they create interaural level differences (ILD) between the two ears when the sound source is above or below the head [Knudsen and Konishi, 1979, 1980; Moiseff and Konishi, 1981; Moiseff, 1989]. In barn owls, azimuth and elevation are computed using interaural time differences (ITDs) and ILDs respectively [Knudsen and Konishi, 1979, 1980; Moiseff and Konishi, 1981; Moiseff, 1989] and ITDs and ILDs are processed independently along two separate pathways from the cochlear nuclei to the external part of inferior colliculus (ICx)[see figure 2.1; Moiseff and Konishi, 1983; Takahashi et al., 1984; Takahashi and Konishi, 1988a, b; Adolphs, 1993; Mazer, 1998]. We compared the relative size of 11 auditory nuclei in both the ITD and the ILD pathways of 8 species of symmetrically and asymmetrically eared owls. Additionally we compared the number of cells in the three cochlear

nuclei (nucleus angularis, nucleus magnocelularis and nucleus laminaris) between these species. We found that both the ILD and ITD pathways are equally enlarged in asymmetrically eared species (fig. 3.5, 3.6). Additionally, we found that nuclei not directly involved in binaural comparisons, such as the superior olive or nucleus lemnisci lateralis, pars ventralis, are also enlarged in asymmetrically eared owls (fig. 3.6). We suggested that the hypertrophy of auditory nuclei in asymmetrically eared owls likely reflects both an improved ability to precisely locate sounds in space and an expansion of the hearing range. Additionally, our results suggest that the hypertrophy of nuclei that compute space may have preceded that of the expansion of the hearing range. Finally, our results suggest that changes in the relative size of nuclei within the auditory pathways of owls occurred independently of phylogeny.

In addition to the variation in the presence or absence of vertically asymmetrical ears, owls also vary greatly in their activity patterns. Some species are nocturnal but others are more active during dawn and dusk (crepuscular), and other are active during the day (diurnal)[del Hoyo et al., 1999]. In Chapter 4, we compared the relative size of 8 visual nuclei in 9 species of owls (and one Caprimulgiform) with different activity patterns. This included the two main visual pathways, the tectofugal and thalamofugal pathways, as well as other retinorecipient nuclei, like ventral lateral gesticulate nucleus (Glv), the nucleus lentiformis mecensephali (LM) and the nucleus of the basal optioc root (nBOR). Several studies have shown that differences in the activity pattern are reflected in eye morphology and retinal organization both in birds in general, and in owls [see Lisney et al., 2011; Oehme, 1961; Bravo and Pettigrew, 1981]. Specifically,

Lisney et al., [2012] showed that in owls the distribution of retinal ganglion cells (RGCs) varies with activity pattern such that diurnal species have well-defined, elongated visual streaks, while more nocturnal species have a poorly defined visual streak and exhibit a more radially symmetrical retinal topography pattern. We found marked differences in the relative size of all visual structures among the species studied, both in the tectofugal and the thalamofugal pathway, as well in other retinorecipient nuclei [fig. 4.2]. We found that although there is no relationship between activity pattern and the relative size of either the tectofugal or the thalamofugal pathway, there is a positive correlation between the relative size of both visual pathways and the relative number of cells in the retinal ganglion layer [fig. 4.3]. Our results also suggest a trade-off between the relative size of auditory and visual pathways [fig. 4.3], similar to what has previously been suggested for the relative size of auditory and visual areas in the mesencephalon of bats [Baron et al., 1996]. This was one of the first studies to assess the relationship between retinal topography, RGC layer neuron numbers, and the relative size of the visual pathways in any vertebrate. Together with the results in Chapter 3, which suggests that the relative size of the auditory pathways in owls is also related to the number of sensory cells in the periphery, our studies seem to confirm previous suggestions that the number of sensory cells is the main driver of the relative size of sensory areas [e.g. Roth et al., 1992; Kotrschal et al., 1998].

In chapter 5 we use the comparative method to cast new light on the function of the isthmo optic nucleus (ION), a visual nuclei in the brain of birds which has been studied extensively but whose function remains largely unknown

[reviewed in Reperant et al., 2006, 2007; Wilson and Lindstrom 2011]. In all vertebrates there are retinofugal visual fibers projecting from the brain to the retina. These are particularly well developed in birds, where they arise from cells in the ION which lies in the isthmal region of the midbrain [O'Leary and Cowan, 1982; Weidmer et al., 1987; 1989]. Despite a large number of anatomical, physiological and histochemical studies, the function of this retinofugal system remains unclear. Several functions have been proposed including: gaze stabilization, dark adaptation, shifting attention, and detection of aerial predators [Rogers and Miles, 1972; Catsicas et al., 1987; Uchiyama, 1989; Ward et al., 1991; Uchiyama and Barlow, 1994; Woodson et al., 1995; Clarke et al., 1996; Uchiyama et al., 1998]. Additionally, some functional theories have been proposed based on differences in the number of cells in ION in different species. Birds that feed by pecking (like pigeons, chickens and songbirds) have a larger number of cells compared to non pecking birds (diurnal raptors and owls), and this led to the proposal that ION is involved in ground feeding [Shortess and Klose, 1977; Weidner et al., 1987; Reperant et al., 1989; Hahmann and Gunturkun, 1992; Miceli et al., 1999]. In chapter 5, we compared the cytoarchitectonic organization and relative volume of the ION in 81 species of birds belonging to 17 different orders. Additionally, we also counted the number of cells in 58 of these species. We found marked differences in the cytoarchitectonic organization, relative size and number of cells of ION among birds [fig. 5.4, 5.5]. We found ION to vary in the complexity of its cytoarchitectonical organization, such that some species have less complex IONs, with most cells evenly distributed throughout the nucleus while other have

variable degrees of cells organized in layers and a clear neuropil (cell-free lamina)(see figure 5.2, 5.3).We also showed that several orders of birds (other than those previously reported) have a large, well-organized ION, including hummingbirds, woodpeckers, coots and allies, and kingfishers [fig. 5.4]. At the other end of the spectrum, parrots, herons, waterfowl, owls and diurnal raptors have relatively small ION volumes [fig. 5.4]. ION also appears to be absent or unrecognizable is several taxa, including one of the most basal avian groups, the tinamous, which suggest that the ION may have evolved only in the more modern group of birds, Neognathae (see figure 1.2). We also showed that evolutionary changes in the relative size and the cytoarchitectonic organization of ION have occurred largely independent of phylogeny [fig. 5.4]. The large relative size of the ION in orders with very different lifestyles and feeding behaviors suggests there is no clear association with pecking behavior or predator detection as previously suggested [see above; Wilson and Lindstrom 2011]. Instead, our results suggest that the ION is more complex and enlarged in birds that have eyes that are emmetropic in some parts of the visual field and myopic in others. We therefore proposed that the ION is involved in switching attention between two parts of the retina i.e. from an emmetropic to a myopic part of the retina.

In chapter 6 we aimed to understand how several nuclei that belong to the same sensory modality vary in relative size with respect to each other in a large sample of species. Two main models have been proposed to explain how the relative size of neural structures varies through evolution. In the mosaic evolution model individual brain structures vary in size independently of each other [Barton and Harvey 2000], whereas in the concerted evolution model developmental

constraints result in different parts of the brain varying in size in a coordinated manner [Finlay and Darlington, 1995; Finlay et al., 2001]. Several studies have shown variation of the relative size of individual nuclei in the brain of vertebrates [e.g Barton 1998; Iwaniuk and Wylie, 2007; Kubke et al., 2004], but it is currently not known if nuclei belonging to the same functional pathway vary independently of each other or in a concerted manner. We examined the relative size of 9 different visual nuclei in 98 species of birds. This included data on interspecific variation in the cytoarchitecture and relative size of the isthmal nuclei, a group of thee nucleus (the magnocellular and parvocellular parts of the nucleus isthmi, Imc and Ipc respectivly, and the nucleus semilunaris, SLu) which are heavily interconnected with each other and the TeO, and are thought to be implicated in visual stimulus selection [e.g. Marin et al., 2005; 2007]. This is the first study to assess variation of the relative size of these nuclei among birds. We also used a combination of statistical analyses, phylogenetically corrected principal component analysis and evolutionary rates of change on the absolute and relative size of the 9 nuclei to test if visual nuclei evolve in a concerted or mosaic manner. Our results strongly indicate a combination of mosaic and concerted evolution (in the relative size of 9 nuclei) within the avian visual system. Specifically, the relative size of the isthmal nuclei and parts of the tectofugal pathway covary across species in a concerted fashion, whereas the relative volume of the other visual nuclei measured vary independently of one another, such as that predicted by the mosaic model. Our results suggest the covariation of different neural structures depends not only on the functional connectivity of each nucleus but on the diversity of afferents and efferents of each nucleus.

7.2 Future directions

There are many interesting questions that can be addressed as an extension of the work presented in this dissertation. A natural progression from Chapter 2 would be to examine the variation of the relative size of the nucleus basalis in the telencephalon, which receives a direct projection form PrV [Dubbeldam et al., 1981]. Our results in chapter 3 and 4 suggest that the number of sensory cells in the periphery is important in driving the size of sensory pathways. Several studies have shown that waterfowl, parrots and beak-probing shorebirds have high concentration of mechanoreceptors in the beak [e.g Berkhoudt, 1980; Demery et al., 2011; Gerritsen and Meiboom, 1986; Gottschaldt, 1985; Gottschaldt and Lausmann, 1974; Nebel and Thompson, 2005; Piersma et al., 1998], but no study has either compared the number or density of these cells between species, or tried to correlate this with variation in the relative size of the trigeminal pathway. Also, several studies have shown that other groups of birds, like kiwis (Apterygidae) and ibis (Threskiornithidae) present a large concentration of mechanoreceptors in their beak, liekly related to beak-probing behaviors [Bolze, 1968; Cunningham et al., 2007; Cunningham et al., 2010]. Further, other birds, like flamingos [Phoenicopteridae; Zweers et al., 1995] and Antarctic prions [Procellariidae; Morgan and Ritz, 1982; Harper, 1987;Klages and Cooper, 1992] also filter their food in a manner similar to waterfowls. It would be very interesting to evaluate if these groups have also independently evolved an enlarged PrV.

Complementary to Chapter 3 would be a study assessing the variation of ILDs and ITDs produced by ear morphology in different asymmetrically-eared species ofowls. Currently this data is only available for the barn owl [Knudsen et al., 1977, 1979; Knudsen and Konishi, 1978a; Coles and Guppy, 1988]. Ear asymmetry has evolved independently several times, based on a variety of anatomical adaptations [Kelso, 1940; Norberg, 1977, 1978], and therefore is likely that the manner in which ILDs and ITDs vary with space is different in each species. Particularly interesting would be to assess how much spatial resolution is provided by more subtle ear asymmetries, like that of the barred owl where the right ear opening in the skin is slightly larger than the left and is a few millimeters higher [Voous, 1964; Norberg, 1978]. Similarly, auditory spatial resolution in azimuth and elevation, assessed behaviorally, is only available for a few species (barn owl [Kundsen and Konishi, 1979] and northern saw-whet owl [Frost et al., 1989]). Further quantification of other species would be important to assess how precisely they can locate sounds, and see if this correlates with variation in the relative size of the auditory pathways. Finally, it would be important to study the properties of space-specific neurons in ICx of different species. In the barn and northern saw-wet owl, receptive fields of neurons in ICx are highly restricted in elevation [Kudnsen and Konishi 1978a,b; Wise et al., 1988] but in the long-eared owl the receptive fields are much less restricted in elevation [Volman and Konishi, 1990]. This suggests that different ear morphologies can results in different auditory spatial resolution and this could be correlated with the relieve size of auditory nuclei.

A continuation of Chapter 4 would be to asses if the relative number of RGCs in the retina correlates with the relative size of visual pathways in other orders. Recently, the number and distribution of RGCs have been made available for several gallinaceous birds and waterfowl species [Lisney et al., 2012, 2013] where this correlation could be tested. A study of the distribution and number of RGCs in the frogmouth would also be important as it could explain the differences in the relative size of the tectofugal pathway found between this species and owls. It would also be interesting to further explore the possible trade-off between the size of the visual and auditory pathways in owls. Our results suggested that there is an inverted correlation between the relative size of the visual and auditory pathways in some species, where particularly the northern saw-wet owls seem to depart from this trend (see figure 4.3). A larger data set, especially from species in the tribe Surniinae to which the northern saw-wet owls belongs [Wink et al., 2008], and other species in the genus *strix* could help to clarify is this tradeoff truly exists.

In chapter 5, we proposed that the presence of a relatively large ION in birds is related to the presence of eyes that are emmetropic in some parts of the visual field and myopic in others. Coots, gallinaseous birds, pigeons and songbirds have been shown to have a lower field myopia [Fitzke et al., 1985; Martin, 1986, 1993; Schaeffel et al., 1994] but it is not known if other species with large ION (like hummingbirds, some shorebirds and woodpeckers) present emmetropic and myopic parts of the retina. Furthermore, the presence of myopic parts of the retina has only been shown in one or two species of each order. Conversely the absence of a ventral field myopia has only been shown in diurnal

raptors and owls [Murphy et al., 1995] and is not known if other species with a relatively small ION, like herons, waterfowls and parrots, lack a lower field myopia. We also reported that ION is absent in several species including a tinamou, which belongs to the more basal group of modern birds, palaeognathae. This led us to propose that ION may be an evolutionary novelty present only in the more derived group of modern birds, neognathae. Labeling retina-projecting cells by means of intraocular injections of neural tracers is needed to test if birds like the tinamou indeed lack cells that resemble ION neurons, or if they are present but not organized in a recognizable cluster of cells.

In chapter 6 we evaluated the covariation of the relative size of different visual nuclei in a large sample of birds using multivariate methods. While this comprised most of the retinorecipient nuclei found in birds, we were not able to assess variation in the relative size of the thalamufugal pathway, which is involved in stereopsis [e.g. Pettigrew and Konishi, 1976; Pettigrew, 1979; Wagner and Frost, 1994; Nieder and Wagner, 2001] and includes the retinorecipient nucleus nucleus dorsolateralis anterios thalami (DLL) and the Wulst in the telencephalon. In Chapter 4 we showed that the relative size of this pathway correlates with that of the tectofugal pathway in owls but is not known if this is true in other birds. The visual Wulst is greatly enlarged in owls compared to other birds [Iwaniuk et al., 2008] but the tectofugal pathway is reduced in owls compared to most other birds [Chapter 6; Iwaniuk et al., 2010] which would seem to suggest that relative size of these two pathways evolves independently of each other.

Our results from Chapter 3 and 4 suggest that, at least in owls, there could be a tradeoff between the relative size of auditory and visual pathways. Also, as mentioned above, waterfowl and parrots have enlarged PrV but also a reduced tectofugal pathway [Chapter 6; Iwaniuk et al., 2010]. Sensory trade-offs between the relative size of auditory and visual nuclei[Esingberg 1981; Baron 1996], but also between the olfactory and visual system [Barton et al., 1995] have been previously suggested in mammals. The addition of the relative size of auditory, somatosensory and olfactory structures to the already extensive data set of visual structures in birds would provide a unique opportunity to test, using the same multivariate approach, if there are indeed sensory trade-offs in birds.

7.3 Conclusion

Comparative studies among different species, like those in this dissertation, are useful in determining some of the ultimate causes of interspecific differences in brain morphology, like activity pattern or feeding behavior, but fail to reveal the proximate causes of these differences. In other words, large comparative studies tell us nothing about the mechanisms that generate the differences in the size and organization of neural system between species. One of these proximate causes is differences in the development between species.

It has long been recognized that evolutionary changes in morphology are the results of evolutionary changes in ontogeny, and this is not different in neural systems. In recent years, several studies have shown that some of the differences in relative size between brain regions can be explained by differences in

developmental process, such as the timing of neurogenesis, cell cycle rates, and brain patterning [see Charvet et al., 2011 for a review]. In birds, the telencephalon of parrots and songbirds is enlarge compared to other birds [Portmann, 1947; Boire and Baron, 1994; Iwaniuk and Hurd, 2005]. Accordingly, the zebra finch and the parakeets (*Melopsittacus undulatus*) show delayed neurogenesis in the telencephalon compared to gallinaseous birds [Charvet and Striedter, 2008, 2009; Striedter and Charvet, 2008]. Alternatively, in the case of TeO, differences in the relative size between parrots and gallinaseous birds (parrots have smaller TeO, see Iwaniuk et al., 2010; Chapter 6), can be explained by differences in the amount of tissue allocated to become TeO at the time of brain regionalization in each species [Striedter and Charvet, 2008].

Another important proximal cause that has been largely overlooked in the study of vertebrate brain evolution has been at the micro-evolutionary scale, i.e. variation of brain size and morphology within a species. This is despite intraspecific variation being one of the cornerstones of evolutionary theory. Only recently have studies emerged showing that there is indeed variation of relative brain size and morphology within a species [e.g. Ishikawa et al., 1999, Karlen and Krubitzer, 2006; Kolm, et al., 2009]. These studies have shown that factors similar to those that affect brain size variation at the macro-evolutionary level (see chapter 1), such as parental care [Kotrschal et al., 2012] or environmental complexity [Roth and Pravosudov, 2009], also affect brain size at the species level.

Adaptive variation at the species level is usually due to two processes, either local adaptation, where natural selection acts upon heritable phenotypic

variation [e.g. Kawecki and Ebert 2004] or phenotypic plasticity, wherein different phenotypes can develop from the same genotype [e.g. Pigliucci, 2001]. Variation of relative size and cell numbers in different regions due to phenotypic plasticity has been shown extensively in vertebrates [reviewed in Gonda et al., 2013]. Increasing evidence shows that traits that result from phenotypic plasticity can be assimilated, become heritable and highly adaptive [see Badyaev, 2009; Lande 2009; Wund 2012]. While there is no yet evidence of this in neural systems, it is very likely that phenotipic plasticity and subsequent assimilation plays an important role in the evolution of the brain. Future research should aim to integrate changes in developmental mechanisms, intraspecific variation due to local adaptation or phenotipic plasticity, and macroevolutionary changes in brain morphology.

Birds have become powerful models for a variety of endevours in neuroscience. For example, owls have been used extensively to understand auditory and visual processing, the development of these sensory systems and how they interact with each other (e.g. Knudsen, 2002). Also, songbirds (and parrots and hummingbirds), learn their vocalizations and thus have become models for understanding the behavioral and neurobiological mechanisms that underlie learning and processing of human language (Knudsen and Gentner, 2010). Additionally, several groups of birds have relatively large brains and outstanding cognitive abilities, comparable to primates (Emery, 2006), and thus have become models to understand the evolution of brain enlargement and increased cognitive abilities. Therefore, research such as that in this dissertation is

of vital importance, not only to understand more about the evolution of birds' brains but vertebrates in general, including humans.

7.4 References

Adolphs R (1993): Acetylcholinesterase staining differentiates functionally distinct auditory pathways in the barn owl. J Comp Neurol 329: 365–377.

Badyaev AV (2009): Evolutionary significance of phenotypic accommodation in novel environments: an empirical test of the Baldwin effect. Philosophical Transactions of the Royal Society B: Biological Sciences, *364*(1520), 1125-1141.

Baron G, Stephan H, Frahm HD (1996): Comparative Neurobiology in Chiroptera. Basel, Birkhäuser Verlag.

Barton RA, Purvis A, Harvey PH (1995): Evolutionary radiation of visual and olfactory brain systems in primates, bats and insectivores. Proc R Soc Lond B, *348*: 381-392.

Barton RA (1998): Visual specialization and brain evolution in primates. Proc R Soc Lond B 265:1933–7.

Berkhoudt H (1980): The morphology and distribution of cutaneous mechanoreceptors (Herbst and Grandry corpuscles) in bill and tongue of the mallard *(Anas platyrhynchos L.).* Neth J Zool 50: 1–34.

Bravo H, Pettigrew JD (1981): The distribution of neurons projecting from the retina and visual cortex to the thalamus and tectum opticum of the barn owl,

Tyto alba , and burrowing owl, *Speotyto cunicularia* . J Comp Neurol 199: 419–441.

Boire D (1989): Comparaison quantitative de l'encéphale de ses grades subdivisions et de relais visuals, trijumaux et acoustiques chez 28 espèces. PhD Thesis, Université de Montréal, Montréal.

Boire D, Baron G (1994): Allometric comparison of brain and main brain subdivisions in birds. J Hirnforsch 35: 49–66.

Bolze G (1968): Anordnung und Bau der Herbstchen Körperchen in Limicolenschnabeln im Zusammenhang mit der Nahrungsfindung. Zool Anz 181: 313–355.

Clarke PG, Gyger M, Catsicas S (1996): A centrifugally controlled circuit in the avian retina and its possible role in visual attention switching. Vis Neurosci 13: 1043–1048.

Catsicas S, Catsicas M, Clarke PG (1987): Long-distance intraretinal connections in birds.Nature 326: 186–187.

Charvet CJ, Striedter GF (2008): Developmental species differences in brain cell cycle rates between bobwhite quail *(Colinus virginianus)* and parakeets *(Melopsittacus undulatus):*implications for mosaic brain evolution. Brain Behav Evol 72: 295–306.

Charvet CJ, Striedter GF (2009a): Developmental origins of mosaic brain evolution: morphometric analysis of the developing zebra finch brain. J Comp Neurol 514: 203–213.

Charvet CJ, Striedter GF, Finlay, BL (2011): Evo-devo and brain scaling: Candidate developmental mechanisms for variation and constancy in vertebrate brain evolution. Brain, behavior and evolution, *78*(3), 248-257.

Coles RB, Guppy A (1988): Directional hearing in the barn owl *(Tyto alba)*. J Comp Physiol A 163: 117–133.

Cunningham S, Castro I, Alley M (2007): A new prey-detection mechanism for kiwi (*Apteryx* spp.) suggests convergent evolution between paleognathous and neognathous birds. J. Anat 211: 493–502.

Cunningham SJ, Alley MR, Castro I, Potter MA, Cunningham M, Pyne MJ (2010): Bill morphology of ibises suggests a remote-tactile sensory system for prey detection.The Auk. 127: 308-316.

del Hoyo J, Elliott A, Sargatal J (eds) (1999):Handbook of the Birds of the World, vol 5: Barn Owls to Hummingbirds. Barcelona, Lynx Editions.

Demery ZP., Chappell J, Martin GR (2011): Vision, touch and object manipulation in Senegal parrots Poicephalus senegalus. Proc R Soc Lond B, *278:* 3687-3693.

Dubbeldam JL, Brauch CS, Don A. (1981): Studies on the somatotopy of the trigeminal system in the mallard, Anas platyrhynchos L. III. Afferents and organization of the nucleus basalis. J Comp Neurol. 196: 391-405.

Dubbeldam JL (1998): The sensory trigeminal system in birds: input, organization and effects of peripheral damage. A review. Arch Physiol Biochem 106: 338–345.

Dubbeldam JL, Karten HJ (1978): The trigeminal system in the pigeon (Columba livia). I. Projections of the gasserian ganglion. J Comp Neurol 180: 661–678.

Eisenberg JF (1981): The Mammalian Radiations: an Analysis of Trends of Evolution, Adaptation and Behavior. Chicago, University of Chicago Press.

Finlay B, Wikler K, Sengelaub D (1987): Regressive Events in Brain Development and Scenarios for Vertebrate Brain Evolution (Part 1 of 2). Brain, behavior and evolution. 30(1-2):102-17.

Finlay BL, Darlington RB (1995): Linked regularities in the development and evolution of mammalian brains. *Science.* 268:1578–1584.

Finlay BL, Darlington RB, Nicastro N (2001): Developmental structure in brain evolution. The Behavioral and brain sciences 2001, 24:263–78; discussion 278–308.

Fitzke FW, Hayes BP, Hodos W, Holden AL, Low JC (1985): Refractive sectors in the visual field of the pigeon eye. J Physiol 369: 33–45.

Frost BJ, Baldwin J, Csizy M (1989): Auditory localization in the saw-whet owl *Aegolius acadicus* . Can J Zool 67: 1955–1959.

Gerritsen AFC, Meiboom A (1986) The role of touch in prey density estimation by *Calidris alba* . Neth J Zool 36: 530–562.

Gonda A, Herczeg G, Merilä J (2013): Evolutionary ecology of intraspecific brain size variation: a review.*Ecology and Evolution*. Article first published online: 26 JUN 2013

Gottschaldt KM (1985): Structure and function of avian somatosensory receptors. In: Form and function in birds Vol. 3. (King AS, McLelland J, eds), pp 375–461. London: Academic Press.

Gottschaldt KM, Lausmann S (1974): The peripheral morphological basis of tactile sensibility in the beak of geese. Cell Tissue Res 153: 477–496.

Hackett SJ, Kimball RT, Reddy S, Bowie RCK, Braun EL, Braun MJ, Chojnowski JL, Cox WA, Han KL, Harshman J, Huddleston CJ, Marks BD, Miglia KJ, Moore WS, Sheldon FH, Steadman DW, Witt CC, Yuri T (2008): A phylogenomic study of birds reveals their evolutionary history. Science 320: 1763–1768.

Hahmann U, Güntürkün O (1992): Visual-discrimination deficits after lesions of the centrifugal visual system in pigeons (Columba livia). Vis Neurosci 9: 225–233.

Iwaniuk AN, Wylie DRW (2007): Neural specialization for hovering in hummingbirds: hypertrophy of the pretectal nucleus Lentiformis mesencephali**.** J Comp Neurol **500**:211–21.

Iwaniuk AN, Hall MI, Heesy CP, Wylie DRW (2008): Neural correlates of orbit orientation in birds. J Comp Physiol A 194: 267–282.

Iwaniuk AN, Gutiérrez-Ibáñez C, Pakan JMP,Wylie DR (2010): Allometric scaling of the tectofugal pathway in birds. Brain Behav Evol 75: 122–137.

Kelso L (1940): Variation of the external earopening in the Strigidae. Wilson Bull 52: 24–29.

Klages NTW, Cooper J (1992): Bill morphology and the diet of filter-feeding seabird: the Broad-billed Prion *Pachyptila vittata* at South Atlantic Gough Island. J Zool Lond 227: 385–396.

Knudsen EI, Konishi M, Pettigrew JD (1977): Receptivefields of auditory neurons in the owl.Science 198: 1278–1280.

Knudsen EI, Konishi M (1978a): A neural map of auditory space in the owl. Science 200: 795–797.

Knudsen EI, Konishi M (1978b): Space and frequency are represented separately in auditory midbrain of the owl. J Neurophysiol 41:870–884.

Knudsen E, Konishi M (1979): Mechanisms of sound localization in the barn owl *(Tyto alba)*. J Comp Physiol 133: 13–21.

Knudsen EI, Konishi M (1980): Monaural occlusion shifts receptive-field locations of auditory midbrain units in the owl. J Neurophysiol44: 687–695.

Kooloos JGM, Kraaijeveld AR, Langenbach GEJ (1989): Comparative mechanics of filter feeding in *Anas platyrhynchos* , *Anas clypeata* and *Aythya fuligula* (Aves , Anseriformes) Zoomorphology 108: 269–290.

Kotrschal K, van Straaden MJ, Huber R (1998): Fish brains: evolution and environmental relationships. Rev Fish Biol Fisheries 8: 373–408.

Kubke MF, Massoglia DP, Carr CE (2004): Bigger brains or bigger nuclei? Regulating the size of auditory structures in birds**.** Brain Behav Ev, **63**:169–80.

Lande, R. (2009): Adaptation to an extraordinary environment by evolution of phenotypic plasticity and genetic assimilation. Journal of evolutionary biology, *22*(7), 1435-1446.

Lisney TJ, Iwaniuk AN, Kolominsky J, Bandet M V, Corfield JR, et al. (2012): Interspecifc variation in eye shape and retinal topography in seven species of galliform bird (Aves: Galliformes: Phasianidae). Journal of comparative physiology A, Neuroethology, sensory, neural, and behavioral physiology 198: 717–731.

Linden R (1994): The survival of developing neurons: A review of afferent control. Neuroscience 58:671–682.

Lisney TJ, Stecyk K, Kolominsky J, Schmidt BK, Corfield JR, et al. (2013): Ecomorphology of eye shape and retinal topography in waterfowl (Aves: Anseriformes: Anatidae) with different foraging modes. Journal of comparative physiology A, Neuroethology, sensory, neural, and behavioral physiology 199: 385–402.

Lisney TJ, Iwaniuk AN, Bandet MV, Wylie DR (2012): Eye shape and retinal topography in owls (Aves: Strigiformes). Brain Behav Evol 79: 218–236.

Lisney TJ, Rubene D, Rózsa J, Løvlie H, Håstad O, Ödeen A (2011): Behavioural assessment of flicker fusion frequency in chicken *Gallus gallus domesticus* . Vision Res 51: 1324–1332.

Martin GR (1986): The eye of a passeriform bird, the European starling (Sturnus vulgaris):Eye movement amplitude, visual fields and schematic optics. J Comp Physiol A 159:545–557.

Mazer JA (1998): How the owl resolves auditory coding ambiguity. Proc Natl Acad Sci USA 95: 10932–10937.

Miceli D, Repérant J, Bertrand C, Rio JP (1999): Functional anatomy of the avian centrifugal visual system. Behav Brain Res 98: 203–210

Moiseff A (1989): Bi-coordinate sound localization by the barn owl. J Comp Physiol A 64:637–644.

Moiseff A, Konishi M (1981): Neuronal and behavioral sensitivity to binaural time differences in the owl. J Neurosci 1: 40–48.

Moiseff A, Konishi M (1983): Binaural characteristics of units in the owl's brainstem auditory pathway: precursors of restricted spatial receptive fields. J Neurosci 12: 2553–2562.

Morgan WL, Ritz DA (1982): Comparison of the feeding apparatus in the Mutton-bird, *Puffinus tenuirostris* (Temminck) and the Fairy Prion, *Pachyptila turtur* (Kuhl) in the relation to the capture of krill, *Nyctyphanes australis* . J Exp Mar Biol Ecol 59: 61–76.

Murphy CJ, Howland M, Howland HC (1995): Raptors lack lower field myopia. Vis Res 35: 1153–5.

Nebel S, Jackson DL, Elner RW (2005): Functional association of bill morphology and foraging behaviour in calidrid sandpipers.*Animal Biology*, *55*(3), 235-243.

Nieder A, Wagner H (2001): Encoding of both vertical and horizontal disparity in randomdot stereograms by Wulst neurons of awake barn owls. Vis Neurosci 18: 541–547.

Norberg RA (1977): Occurrence and independent evolution of bilateral ear asymmetry in owls and implications on owl taxonomy. Phil Trans R Soc Lond B 280: 375–408.

Norberg RA (1978): Skull asymmetry, ear structure and function, and auditory localization in Tengmalm's owl, *Aegolius funereus* (Linné). Phil Trans R Soc Lond B 282: 325–410.

Oehme H (1961): Vergleichend-histologische Untersuchungen an der Retina von Eulen.Zool Jb Anat 79: 439–478.

O'Leary DD, Cowan WM (1982): Further studies on the development of the isthmo-optic nucleus with special reference to the occurrence and fate of ectopic and ipsilaterally projecting neurons. J Comp Neurol 212: 399–416.

Oppenheim R (1985): Naturally occurring cell death during neural development. Trends in Neurosciences 8:487–493.

Oppenheim R (991): Cell death during development of the nervous system. Annual review of neuroscience 14:453–501.

Pettigrew JD (1979): Binocular visual processing in the owl's telencephalon. Proc R Soc Lond B Biol Sci 204: 435–454.

Pettigrew JD, Konishi M (1976): Neurons selective for orientation and binocular disparity in the visual Wulst of the barn owl *(Tyto alba).* Science 193: 675–678.

Piersma T, van Aelst R, Kurk K, Berkhoudt H, Maas LRM (1998): A new pressure sensory mechanism for prey detection in birds: the use of seabed-dynamic principles? Proc R Soc Lond B 265: 1377–1383

Portmann A (1947): Étude sur la cérébralisation chez les oiseaux. 2. Les indices intracérébraux. Alauda 15: 1–15.

Repérant J, Miceli D, Vesselkin NP, Molotchnikoff S (1989): The centrifugal visual system of vertebrates: a century-old search reviewed. Int Rev Cytol 118: 115–171.

Repérant, J, Ward R, Miceli D, Rio JP, Medina M, et al. (2006): The centrifugal visual system of vertebrates: A comparative analysis of its functional anatomical organization. Brain Research Reviews 52: 1–57.

Repérant J, Médina M, Ward R, Miceli D, Kenigfest NB et al. (2007): The evolution of the centrifugal visual system of vertebrates. A cladistic analysis and new hypotheses. Brain Res Rev 53:161-97.

Rogers LJ, Miles FA (1972): Centrifugal control of the avian retina: V. Effects of lesions of the isthmo-optic nucleus on visual behaviour. Brain Res 48: 147–156.

Roth G, Dicke U, Nishikawa K (1992): How doo ntogeny, morphology, and physiology of sensory systems constrain and direct the evolution in amphibians? Am Nat 139:S105–S124.

Stingelin W (1961): Grössenunterschiede des sensiblen Trigeminuskerns bei verschiedenen Vögeln. Rev Suisse Zool 68: 247–251.

Schaeffel F, Hagel G, Eikerman J, Collett T, (1994): Lower-field myopia and astigmatism in amphibians and chickens. J Opt Soc Am A 11: 487–495.

Shortess GK, Klose EF (1977): Effects of lesions involving efferent fibers to the retina in pigeons (Columba livia). Physiol Behav 18: 409–414.

Striedter GF, Charvet CJ (2008): Developmental origins of species differences in telencephalon and tectum size: morphometric comparisons between a

parakeet *(Melopsittacus undulatus)* and a quail (*Colinus virgianus*). J Comp Neurol 507: 1663–1675.

Takahashi TT, Konishi M (1988a): Projections of nucleus angularis and nucleus laminaris to the lateral lemniscal nuclear complex of the barn owl. J Comp Neurol 274: 212–238.

Takahashi TT, Konishi M (1988b): Projections of the cochlear nuclei and nucleus laminaris to the inferior colliculus of the barn owl. J Comp Neurol 274: 190–211.

Takahashi TT, Moiseff A, Konishi M (1984): Time and intensity cues are processed independently in the auditory system of the owl. J Neurosci 4: 1781–1786.

Tome MW, Wrubleski DA (1988): Underwater foraging behavior of canvasbacks, lesser scaups, and ruddy ducks. Condor 90: 168–172.

Uchiyama H (1989): Centrifugal pathways to the retina: influence of the optic tectum. Vis Neurosci 3: 183–206.

Uchiyama H, Barlow RB (1994): Centrifugal inputs enhance responses of retinal ganglion cells in the Japanese quail without changing their spatial coding properties. Vis Res 34: 2189–2194.

Uchiyama H, Nakamura S, Imazono T (1998): Long-range competition among the neurons projecting centrifugally to the quail retina. Vis Neurosci 15: 417–423.

Volman SF, Konishi M (1990): Comparative physiology of sound localization in four species of owls. Brain Behav Evol 36: 196–215.

Wagner H, Frost B (1994): Binocular responses of neurons in the barn owl's visual Wulst. J Comp Physiol A 174: 661–670.

Ward R, Repérant J, Miceli D (1991): The centrifugal visual system: what can comparative anatomy tell us about its evolution and possible function? In: Bagnoli P, Hodos W, Editors. The Changing Visual System. New York: Plenum Press. pp. 61–76.

Weidner C, Repérant J, Desroches AM, Micel, D, Vesselkin NP (1987): Nuclear origin of the centrifugal visual pathways in birds of prey. Brain Res 43: 153–160.

Weidner C, Desroches, A.M, Repérant J, Kirpitchnikova E, Miceli D (1989): Comparative study of the centrifugal visual system in the pigmented and glaucomatous albino quail. Biol Struct Morphol 2: 89–93.

Wink M, Heidrich P, Sauer-Gurth H, Elsayed AA, Gonzalez J (2008): Molecular phylogeny and systematics of owls (Strigiformes); in Konig C, Weick F (ed): Owls of the World. London, Christopher Helm, pp 42–63.

Wise LZ, Frost BJ, Shaver SW (1988): The representation of sound frequency and space in the mid brain of the saw-whet owl. Neurosci Abstr 14: 1095.

Wilson M, Lindstrom SH (2011): What the bird's brain tells the bird's eye: the function of descending input to the avian retina Vis Neurosci 28: 337-50.

Woodson W, Shimizu T, Wild JM, Schimke J, Cox K, Karten HJ, (1995): Centrifugal projections upon the retina: an anterograde tracing study in the pigeon (Columba livia). J Comp Neurol 362: 489–509.

Wund, M. A. (2012): Assessing the impacts of phenotypic plasticity on evolution. Integrative and comparative biology, 52: 5-15.

Zweers GA, Gerritsen AFC, Van Kranenburg-Vood PJ (1977): Mechanics of feeding o the Mallard (*Anas platyrhynchos L* .; Aves, Anseriformes) Contrib Vertebr Evol 3: 1–109.

Zweers G, de Jong F, Berkhoudt H, Vanden Berge JC (1995): Filter feeding in flamingos *(Phoenicopterus ruber)*. Condor 97: 297–324.

Zweers GA, Gerritsen AFC (1997): Transition from pecking to probing mechanisms in waders. Neth J Zool 47: 161–208.

Appendix A Photomicrograph of a coronal section through the isthmo optic nucleus (ION) of a domestic chicken (*Gallus domesticus*). Scale bar= 100 μm.

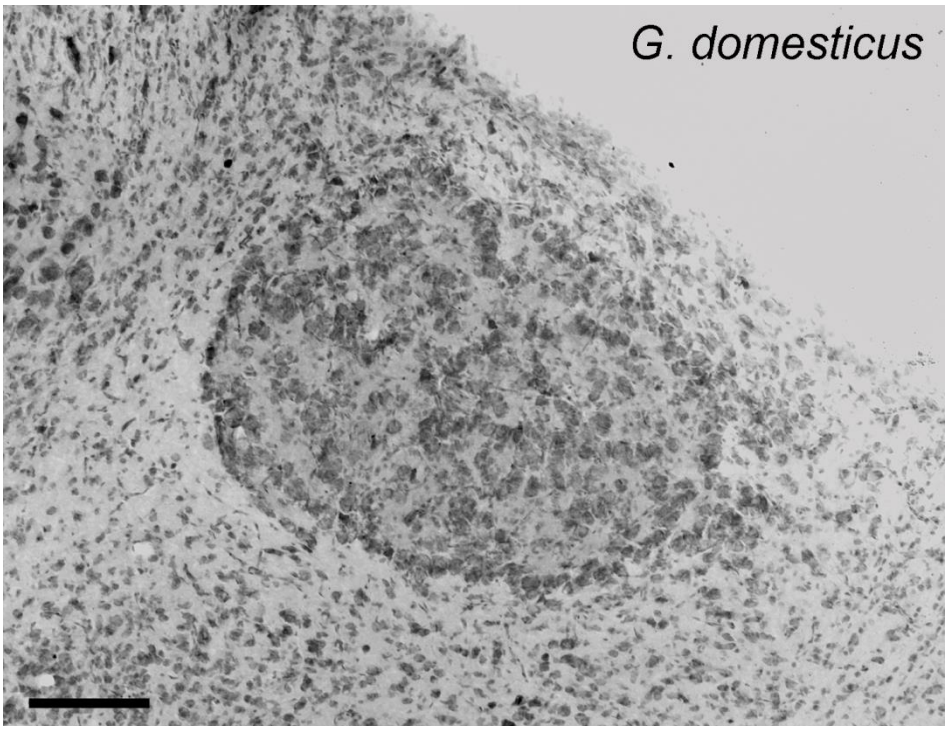

Appendix B. List of the Species Surveyed, Sample Sizes, Volumes (mm^3), Number of Cells, Coefficients of Error (CE), and Cell Density (in cells/mm^3) of the isthmo optic nucleus (ION). Brain Volumes (mm^3) for each species are also included.

ff

Order	Common name	Species	n	ION	Brain	ION N cells	CE	ION cell density	ION cytorchitecture
Anseriformes	Green-winged Teal	Anas carolinensis	1	0.198	3165.83				1
	Chestnut Teal	Anas castanea	1	0.249	3424.71	4422.703	0.1018	17776.14	1
	Northern Shoveller	Anas clypeata	1	0.165	3288.51	2873.016	0.0676	17450.29	1
	Blue-winged Teal	Anas discors	1	0.193	2895.75				1
	Mallard duck	Anas platyrhynchos	1	0.185	6949.81	4057.627	0.0930	13264.55	1
	Pacific Black Duck	Anas superciliosa	1	0.420	4973.94	3552.301	0.0779	8448.206	1
	Lesser Scaup	Aythya affinis	1	0.129	4141.89	3323.478	0.0672	25739.45	2
	Redhead	Aythya americana	1	0.212	5245.17				1
	Bufflehead	Bucephala albeola	1	0.268	4122.97	3427.739	0.0899	12805.36	1
	Common Goldeneye	Bucephala clangula	1	0.492	5961.39	5102.61	0.1217	10377.91	1
	Australian Wood Duck	Chenonetta jubata	1	0.180	4329.15	2934.413	0.1045	16345.88	1
	Red-breasted Merganser	Mergus serrator	1	0.434	4754.34	4064.046	0.0741	9358.986	1
Caprimulgiformes	Spotted Nightjar	Eurostopodus argus	1		1013				0 (absent)

	Tawny Frogmouth	Podargus strigoides	1	0.214	5585.91	4264.234	0.0621	19889.15	3
Charadriiformes	Silver Gull	Chroicocephalus novaehollandiae	1	0.324	2968.15				1
	Bonaparte's Gull	Chroicocephalus philadelphia	1	0.365	2512.55	3811.152	0.0901	61076.15	2
	Short-billed Dowitcher	Limnodromus griseus	1	0.062	1338.03	8771.799	0.0928	24024.43	2
	Eurasian Woodcock	Scolopax rusticola	1	0.110	2593.63				2
Ciconiiformes	Nankeen Night Heron	Nycticorax caledonicus	1	0.305	3360.04	1550.763	0.0714	17686.62	1
	Cattle Egret	Bubulcus ibis	1	0.088	4025.1	2085.959	0.0990	6836.519	1
Columbiformes	White-headed Pigeon	Columba leucomela	2	0.444	2355.21	11191.43	0.1104	25224.11	4
	Rock Pigeon	Columba livia	1	0.388	2508.93	11574.51	0.1067	37795.57	5
	Torresian Imperial Pigeon	Ducula spilorrhoa	1	0.218	2697.88	5909.324	0.1234	27077.18	4
	Bar-shouldered Dove	Geopelia humeralis	1	0.321	1106.18	10199.52	0.1157	31809.87	5
	Peaceful Dove	Geopelia placida	1	0.232	776.062	10377.11	0.1354	44821.65	5
	Wonga Pigeon	Leucosarcia melanoleuca	1	0.445	2217				4
	Brush Bronzewing	Phaps elegans	1	0.132	1517.37				1
	Spotted Dove	Streptopelia chinensis	1	0.209	1430.5	11630.59	0.0600	55659.42	5
Coraciiformes	Laughing Kookaburra	Dacelo novaeguineae	1	0.141	3970.08				2
Falconiformes	Collared Sparrowhawk	Accipiter cirrocephalus	1	0.046	4875.48	761.5132	0.1271	16468.71	1
	Swainson's Hawk	Buteo swainsoni	1	0.046	7694.02	953.0021	0.0831	20753.53	1

	Merlin	Falco columbarius	1	0.068	3509.65	3482.408	0.0656	51211.88	1
Galliformes	Chukar Partridge	Alectoris chukar	1	0.358	2284.75	5273.065	0.1326	14725.94	2
	Ruffed Grouse	Bonasa umbellus	1	0.285	3124.9	7450.48	0.1301	26175.1	2
	Spruce Grouse	Falcipennis canadensis	1	0.279	2720	8287.376	0.1098	29665.58	4
	Grey Partridge	Perdix perdix	1	0.327	1582.2	6206.134	0.1267	18976.68	4
	Common Pheasant	Phasianus colchicus	1	0.559	3721.7				3
Gruiformes	American Coot	Fulica americana	1	0.357	2718.92	14372.66	0.0828	40246.03	3
	Dusky Moorhen	Gallinula tenebrosa	1	0.265	2726.54	10295.78	0.0981	38904.85	2
Passeriformes	Brown Thornbill	Acanthiza pusilla	1	0.135	434.363	14002.28	0.0725	103567.2	4
	Eastern Spinebill	Acanthorhynchus tenuirostris	1	0.061	489.382	2598.557	0.0867	42515.66	4
	Cedar Waxwing	Bombycilla cedrorum	1	0.089	805.3				3
	White-throated Treecreeper	Cormobates leucophaea	1	0.134	781.853	5719.855	0.1101	42609.17	5
	Australian Magpie	Cracticus tibicen	1	0.398	4017.37	18393.58	0.0744	46168.62	3
	Painted Firetail	Emblema pictum	1	0.044	366.795				2
	Eastern Yellow Robin	Eopsaltria australis	1	0.127	838.803	10325.34	0.0988	81276.33	3
	Gouldian Finch	Erythrura gouldiae	1	0.071	427.606	5208.527	0.0890	73483.73	2
	Rusty Blackbird	Euphagus carolinus	1	0.308	1656.56	12682.39	0.0891	41155.22	2
	Magpie-lark	Grallina cyanoleuca	1	0.396	3731.66				1

	White-plumed Honeyeater	Lichenostomus penicillatus	1	0.157	916.988				2
	Noisy Miner	Manorina melanocephala	1	0.296	2278.96	8871.08	0.1269	29921.34	3
	Superb Lyrebird	Menura novaehollandiae	1	1.077	10163.1	23760.38	0.0808	22059.18	5
	Spotted Pardalote	Pardalotus punctatus	2	0.102	424.228	10127.94	0.1097	117439	3
	Scarlet Robin	Petroica multicolor	1	0.070	473.938	5398.523	0.1234	77209.99	4
	Black-capped Chickadee	Poecile atricapillus	1	0.134	814.479	8759.452	0.1066	65330.04	3
	Diamond Firetail	Stagonopleura guttata	1	0.117	720.077	4666.459	0.1061	39734.83	3
	Double-barred Finch	Taeniopygia bichenovii	1	0.093	409.266				4
	Zebra Finch	Taeniopygia guttata	1	0.055	502.51	2143.779	0.1373	42400.7	3
	Common Blackbird	Turdus melura	1	0.203	1914.09	10972.73	0.1079	54084.82	2
Pelecaniformes	Australian Pelican	Pelecanus conspicillatus	1		22500				0 (absent)
Piciformes	Yellow-bellied Sapsucker	Sphyrapicus varius	1	0.130	888.4	5414.347	0.1012	41572.08	2
Procellariiformes	Short-tailed Shearwater	Puffinus tenuirostris	1		4757.72				0 (absent)
	Black-browed Albatross	Thalassarche melanophrys	1		14129.3				0 (absent)
Psittaciformes	Australian King Parrot	Alisterus scapularis	1	0.501	4478.76				1
	Long-billed Corella	Cacatua tenuirostris	1	0.430	11778				1
	Galah	Eolophus roseicapilla	1	0.317	6723.94	3993.969	0.1363	12594.5	1
	Purple-crowned Lorikeet	Glossopsitta porphyrocephala	1	0.165	1939.19				2

	Budgerigar	Melopsittacus undulatus	1	0.038	1151.54	1243.332	0.0759	32927.21	2
	Cockatiel	Nymphicus hollandicus	1	0.113	2111	2207.132	0.0883	19539.05	1
	Superb Parrot	Polytelis swainsonii	1	0.199	2996.14	4066.512	0.1047	20414.22	1
	Rainbow Lorikeet	Trichoglossus haematodus	1	0.173	3333.98	2447.665	0.0943	14138.54	3
Strigiformes	Northern Saw-whet Owl	Aegolius acadicus	1	0.032	3142.86				1
	Short-eared Owl	Asio flammeus	1	0.067	6221.04	2626.059	0.0949	39078.26	1
	Great Horned Owl	Bubo virginianus	1	0.346	17994.2	4122.411	0.0700	11906.22	1
	Northern Hawk-Owl	Surnia ulula	1	0.161	9408.3	3560.759	0.0943	22122.01	1
	Barn Owl	Tyto alba	1	0.060	5849.81	2363.641	0.1137	39081.37	1
Trochiliformes	Anna's Hummingbird	Calypte anna	1	0.031	183.88	1273.757	0.1061	55284.58	1
	Long-tailed Hermit	Phaethornis superciliosus	1	0.044	216.15	1585.969	0.0999	51896.88	1
	Rufous-tailed Hummingbird	Amazilia tzacatl	1	0.023	182.19	1412.858	0.1065	31994.08	1
	Rufous Hummingbird	Selasphorus rufus	1	0.036	151.641	1305.641	0.0971	36429.73	1
Tinamiformes	Chilean Tinamou	Nothoprocta perdicaria	1						0

Appendix C. List of species in which museum specimens where used to describe the cytoarchitecture of ION.

Order	Common name	Species	ION cytorchitecture	Specimen number*
Apodiformes	Glossy Swiftlet	*Collocalia esculenta*	1	FMNH SEA132
	Pygmy Swiftlet	*Collocalia troglodytes*	1	FMNH SEA133
	Speckled hummingbird	*Adelomyia melanogenys*	1	LSUMZ 129494, 129491
	Green-fronted lancebill	*Doryfera ludoviciae*	1	FMNH 320498
	Magnificent hummingbird	*Eugenes fulgens*	1	LSUMZ64774
	Rufous-breasted hermit	*Glaucis hirsuta*	1	USNM 616825
	Giant hummingbird	*Patagona gigas*	1	LSUMZ 123075
	Green-backed firecrown	*Sephanoides sephanoides*	1	FMNH 316786, 316784
	Fork-tailed woodnymph	*Thalurania furcata*	1	LSUMZ 123339
Coraciiformes	Belted Kingfisher	*Megaceryle alcyon*	5	USNM430744
Piciformes	Scaly-throated Honeyguide	*Indicator variegatus*	4	USNM638140
	Yellow-rumped Tinkerbird,	*Pogoniulus bilineatus*	3	USNM632982
	Emerald Toucanet	*Aulacorhynchus prasinus*	2	USNM540590

*Specimen numbers refer to the following institutions: USNM, National Museum of Natural History (Washington, DC); FMNH, Field Museum of Natural History (Chicago, IL); and LSUMZ, Louisiana State University Museum of Natural Science (Baton Rouge, LA).

Appendix D Results of least-squares linear regression performed on the ION volume against brain volume, ION cell numbers against ION volume and ION cell density against brain volume are provided for ION using both species as independent data points ('no phylogeny') and two models of evolutionary change, Brownian motion (PGLS) and Ornstein-Uhlenbeck (OU [Garland and Ives, 2000; Garland et al., 2005]) with four different phylogenetic trees.

	Model	Regression					Group Effect				Category Effect			
ION volume / brain volume		d .f.	F	slope	r2	AIC	d.f.	F	p	AIC	d.f.	F	p	AIC
No phylogeny		1, 74	31.83	0.425	0.301	35.27	13, 61	10.55	< 0.0001	-28.29	4, 71	5.91	< 0.0001	21.51
Cracraft et al., 2004 [57]	PGLS	1, 74	39.95	0.581	0.350	14.72	13, 61	1.98	>0.05	14.03	4, 71	1.27	0.288	17.38
	OU	1, 74	39.23	0.553	0.346	13.06	13, 61	9.56	< 0.0001	-26.29	4, 71	3.93	>0.05	11.731
Davis, 2008 [59]	PGLS	1, 74	53.42	0.629	0.419	4.77	13, 61	1.51	0.136	9.87	4, 71	0.96	0.429	8.67
	OU	1, 74	51.96	0.607	0.412	4.03	13, 61	9.48	< 0.0001	-26.29	4, 71	3.44	>0.05	5.38
Livezey and Zusi, 2007 [58]	PGLS	1, 74	46.66	0.638	0.386	4.32	13, 61	1.56	0.119	8.87	4, 71	0.49	0.737	10.19
	OU	1, 74	45.47	0.612	0.381	3.29	13, 61	9.47	< 0.0001	-26.29	4, 71	3.10	>0.05	6.02
Hackett et al., 2008 [60]	PGLS	1, 74	41.16	0.599	0.357	13.32	13, 61	2.16	>0.05	10.48	4, 71	1.28	0.285	15.95
	OU	1, 74	41.37	0.571	0.358	10.10	13, 61	9.53	< 0.0001	-26.29	4, 71	3.47	>0.05	9.05

ION cell N/ ION vol		d.f.	F	slope	r2	AIC	d.f.	F	p	AIC	
No phylogeny		2, 56	53.01	0.649	0.481	7.10	12, 44	12.01	< 0.0001	-53.16	
Cracraft et al., 2004 [57]	PGLS	2.56	71.77	0.557	0.561	-39.49	12, 44	1.80	0.076	-29.99	
	OU	2, 56	73.28	0.568	0.566	-38.04	12, 44	7.11	< 0.0001	-50.83	
Davis, 2008 [59]	PGLS	2, 56	77.28	0.582	0.579	-35.18	12, 44	1.16	0.336	-27.83	
	OU	2, 56	77.40	0.587	0.581	-33.80	12, 44	6.91	< 0.0001	-50.83	
Livezey and Zusi, 2007 [58]	PGLS	2. 56	84.87	0.582	0.602	-37.41	12, 44	0.73	0.708	-24.48	
	OU	2, 56	84.39	0.583	0.601	-35.64	12, 44	6.83	< 0.0001	-50.84	
Hackett et al., 2008 [60]	PGLS	2, 56	79.74	0.597	0.587	-32.39	12, 44	1.76	0.084	-32.15	
	OU	2, 56	79.83	0.605	0.587	-31.48	12, 44	3.31	< 0.05	-50.90	
ION cell den/ brain vol		d.f.	F	slope	r2	AIC	d.f.	F	P	AIC	
No phylogeny		2, 56	45.17	-0.388	0.444	-13.05	12, 44	5.74	< 0.0001	-44.92	
Cracraft et al., 2004 [57]	PGLS	2.56	21.75	-0.353	0.279	-24.27	12, 44	1.46	0.173	-17.76	
	OU	2, 56	24.97	-0.344	0.308	-29.27	12, 44	5.31	< 0.0001	-42.91	
Davis, 2008 [59]	PGLS	2, 56	25.39	-0.345	0.311	-25.81	12, 44	0.87	0.576	-15.59	
	OU	2, 56	29.05	-0.353	0.342	-28.89	12, 44	5.20	< 0.0001	-42.91	
Livezey and Zusi, 2007 [58]	PGLS	2, 56	28.30	-0.356	0.335	-27.67	12, 44	0.61	0.817	-12.59	
	OU	2, 56	31.87	-0.363	0.362	-29.70	12, 44	5.04	< 0.0001	-42.91	

Hackett et al., 2008 [60]	PGLS	2, 56	24.24	-0.351	0.302	-24.30	12, 44	1.06	0.406	-16.58	
	OU	2, 56	28.83	-0.355	0.339	-29.28	12, 44	4.57	< 0.0001	-42.91	

Absolut ION cell numbers		d.f	F	p	AIC
No phylogeny		4, 53	10.81	< 0.0001	1121.03
Cracraft et al., 2004 [57]	PGLS	4.53	3.49	< 0.05	1132.27
	OU	4, 53	7.71	< 0.0001	1122.23
Davis, 2008 [59]	PGLS	4, 53	2.81	< 0.05	1133.1
	OU	4, 53	7.28	< 0.0001	1122.1
Livezey and Zusi, 2007 [58]	PGLS	4, 53	1.69	0.164	1116.12
	OU	4, 53	7.46	< 0.0001	1117.99
Hackett et al., 2008 [60]	PGLS	4, 53	3.49	< 0.05	1134.18
	OU	4, 53	7.53	< 0.0001	1121.88

Appendix E List of the species surveyed, sample sizes and volumes (mm^3) of the magnocellular and parvocellular portions of nucleus isthmi (Imc, Ipc), the nucleus semilunaris (SLu), the isthmo optic nucleus (ION), the ventral part of the geniculate nucleus (Glv), the nucleus of the basal optic root (nBOR), the nucleus lentiformis mesencephali, the optic tectum (TeO) and the Brain for each species in Chapter 6.

Order	Common name	Species	n	Imc	Ipc	Slu	ION	Glv	nBOR	LM	nRt	Tectum	Brain
Anseriformes	Green-winged Teal	Anas carolinensis	1	2.122	2.481	0.309	0.198	1.327	1.048	1.804	3.97	134.19	3165.83
	Chestnut Teal	Anas castanea	1	2.126	2.132	0.235	0.249	1.472	0.977	1.980	3.71	98.74	3424.71
	Northern Shoveller	Anas clypeata	1	2.719	3.098	0.283	0.165	1.279	0.935	2.104	4.32	97.93	3288.51
	Blue-winged Teal	Anas discors	1	1.585	2.334	0.245	0.193	1.020	0.801	1.534	3.72	95.47	2895.75
	Mallard duck	Anas plathyrinchus	1	5.054	5.070	0.391	0.185	2.964	1.792	3.095	9.95	185.44	6949.81
	Pacific Black Duck	Anas supercilliosa	1	2.691	2.969	0.324	0.420	2.413	1.495	3.011	5.77	119.49	4973.94
	Lesser Scaup	Athya affinis	1	3.369	4.141	0.420	0.129	1.461	1.193	2.164	5.06	131.66	4141.89
	Redhead	Athya americana	1	3.488	3.797	0.421	0.212	2.035	1.292	1.779	5.55	131.70	5245.17
	Bufflehead	Bucephala albeola	1	2.564	3.692	0.592	0.268	1.439	0.929	2.558	7.20	127.91	4122.97

	Common Goldeneye	Bucephala clangula	1	2.975	4.427	0.685	0.492	2.740	0.807	3.927	11.72	210.87	5961.39
	Australian Wood Duck	Chemonneta jubata	1	3.205	3.550	0.449	0.180	1.716	1.498	2.985	6.77	150.79	4329.15
	Red-breasted Merganser	Mergus serrator	1	3.909	4.034	0.440	0.434	2.309	1.872	2.782	7.76	188.89	4754.34
Caprimulgiformes	Spotted Nightjar	Eurostopodus argus	1	5.381	8.742	0.795	0.214	1.320	2.561	1.914	1.65	66.54	5585.91
	Tawny Frogmouth	Podargus strigoides	1	1.337	1.361	0.379		0.580	0.769	0.845	8.95	328.05	1013.00
Charadriiformes	Silver Gull	Chroicocephalus novaehollandiae	1	3.393	3.941	0.301	0.324	0.567	1.727	2.323	7.19	176.08	2968.15
	Bonaparte's Gull	Chroicocephalus philadelphia	1	3.511	5.843	0.531	0.365	0.759	1.146	1.785	6.80	160.31	2512.55
	Eurasian Woodcock	Scolopax rusticola	1	1.178	2.041	0.088	0.110	2.072	1.086	2.198	4.36	104.92	2593.63
Ciconiiformes	Cattle Egret	Bubulcus ibis	1	6.058	7.070	0.531	0.088	1.775	1.598	1.640	11.80	213.76	4025.10
	Nankeen Night Heron	Nycticorax caledonicus	1	4.968	4.796	0.431	0.305	1.439	1.404	1.932	8.07	269.32	3360.04
Columbiformes	White-headed Pigeon	Columba leucomela	1	3.071	3.388	0.393	0.444	2.755	0.908	2.178	7.19	201.90	2355.21
	Rock Pigeon	Columba livia	1	3.813	5.325	0.378	0.470	1.925	1.636	1.685	7.08	113.89	2343.44
	Torresian Imperial Pigeon	Ducula spilorrhoa	1	2.295	1.832	0.185	0.218	1.886	0.955	1.753	0.00	89.79	2697.88
	Bar-shouldered Dove	Geopelia humeralis	1	2.208	2.806	0.234	0.321	1.583	0.620	1.140	3.86	108.92	1106.18

	Peaceful Dove	Geopelia placida	1	1.251	1.662	0.101	0.232	0.835	0.493	0.635	2.25	64.00	776.06
	Wonga Pigeon	Leucosarcia melanoleuca	1	3.175	3.022	0.206	0.445	1.880	0.897	1.865	4.81	118.75	2217.00
	Brush Bronzewing	Phaps elegans	1	3.834	4.367	0.303	0.132	1.931	1.133	1.528	5.19	154.58	1517.37
	Spotted Dove	Streptopelia chinensis	1	2.393	3.448	0.189	0.209	1.550	0.724	1.383	3.74	123.37	1430.50
Coraciiformes	Laughing Kookaburra	Dacelo novaeguineae	1	8.131	15.165	0.733	0.141	0.962	1.598	1.964	9.52	355.42	3970.08
Falconiformes	Collared Sparrowhawk	Accipiter cirrocephalus	1	5.547	7.218	0.690	0.046	2.361	2.824	3.661	10.50	327.20	4875.48
	Swainson's Hawk	Buteo swainsoni	1	7.116	5.914	0.507	0.046	1.899	3.348	2.978	12.53	249.25	7694.02
	Merlin	Falco columbarius	1	3.542	4.045	0.234	0.068	1.691	1.014	1.803	4.29	130.46	3509.65
Galliformes	Chukar Partridge	Alectoris chukar	1	2.928	2.742	0.304	0.358	2.893	1.827	2.166	6.22	115.86	2284.75
	Ruffed Grouse	Bonasa umbellus	1	3.959	4.721	0.387	0.285	4.470	2.287	3.512	7.97	182.33	3124.90
	Spruce Grouse	Falcipennis canadensis	1	2.860	4.016	0.323	0.279	4.151	2.059	2.854	7.19	179.87	2720.00
	Grey Partridge	Perdix perdix	1	2.536	3.370	0.310	0.327	2.504	1.303	1.547	5.25	118.69	1582.20
	Common Pheasant	Phasianus colchicus	1	4.032	4.455	0.287	0.559	3.210	1.888	2.758	8.15	163.03	3721.70
Gruiformes	American Coot	Fulica americana	1	3.159	3.090	0.239	0.357	1.307	1.148	1.824	7.50	127.65	2718.92

	Dusky Moorhen	Gallinula tenebrosa	1	2.365	2.064	0.203	0.265	1.285	0.898	1.249	4.05	94.62	2726.54
Passeriformes	Brown Thornbill	Acanthiza pusilla	1	1.080	1.022	0.125	0.135	0.461	0.158	0.274	1.68	34.81	434.36
	Eastern Spinebill	Acanthorhynchus tenuirostris	1	0.392	0.465	0.068	0.061	0.564	0.240	0.475	0.92	29.46	489.38
	Red-winged Blackbird	Agelaius phoeniceus	1	1.198	1.083	0.125	0.171	0.663	0.467	0.512	2.83	50.83	1614.86
	Tufted Titmouse	Baeolophus bicolor	1	1.017	0.993	0.117	0.148	0.701	0.437	0.533	2.71	47.15	837.26
	Cedar Waxwing	Bombycilla cedrorum	1	0.717	0.855	0.052	0.089	0.620	0.352	0.561	1.42	31.98	805.30
	American Goldfinch	Carduelis tristis	1	0.386	0.384	0.034	0.076	0.433	0.268	0.391	1.03	21.52	555.89
	White-throated Treecreeper	Cormobates leucophaea	1	1.017	1.216	0.137	0.134	0.881	0.461	0.718	2.55	64.87	781.85
	Australian Magpie	Cracticus tibicen	1	1.221	1.470	0.185	0.140	0.959	0.538	0.828	8.63	219.43	4017.37
	Gray Catbird	Dumetella carolinensis	1	0.333	0.435	0.046	0.044	0.370	0.270	0.316	2.02	50.18	1324.32
	Painted Firetail	Emblema pictum	1	1.909	2.839	0.131	0.127	0.831	0.777	0.752	0.97	18.96	366.80
	Eastern Yellow Robin	Eopsaltria australis	1	0.384	0.572	0.037	0.071	0.230	0.346	0.249	2.70	40.52	838.80
	Gouldian Finch	Erythrura gouldiae	1	2.104	2.449	0.160	0.308	1.164	0.531	0.937	1.03	20.94	427.61
	Rusty Blackbird	Euphagus carolinus	1	5.440	5.923	0.571	0.398	1.673	1.853	1.823	4.34	82.10	1656.56

House Finch	Haemorhous mexicanus	1	0.651	0.791	0.133	0.089	0.616	0.427	0.474	1.56	39.49	1058.98
Dark-eyed Junco	Junco hyemalis	2	1.060	1.030	0.114	0.214	0.753	0.392	0.539	2.51	50.54	879.05
White-plumed Honeyeater	Lichenostomus penicillatus	1	0.952	0.968	0.156	0.157	0.805	0.366	0.713	1.81	50.08	916.99
Noisy Miner	Manorina melanocephala	1	2.075	2.275	0.232	0.296	0.826	1.392	0.824	4.17	88.50	2278.96
Song Sparrow	Melospiza melodia	1	1.077	1.233	0.133	0.181	0.846	0.375	0.567	2.06	47.79	908.78
Superb Lyrebird	Menura novaehollandiae	1	13.848	14.742	1.055	1.077	5.058	3.182	5.441	16.01	384.66	10163.13
Spotted Pardalote	Pardalotus punctatus	1	1.527	1.701	0.121	0.102	0.613	0.339	0.482	1.53	43.19	447.88
Indigo Bunting	Passerina cyanea	1	0.462	0.619	0.061	0.125	0.558	0.371	0.569	1.69	35.76	618.53
Pacific Robin	Petroica multicolor	1	1.113	1.704	0.087	0.070	0.448	0.311	0.606	1.64	57.40	473.94
Black-capped Chickadee	Poecile atricapillus	1	1.264	1.393	0.119	0.134	0.801	0.353	0.638	2.67	50.44	814.48
Carolina Chickadee	Poecile carolinensis	1	0.599	0.558	0.055	0.095	0.370	0.208	0.240	1.30	25.35	680.02
White-breasted nuthatch	Sitta carolinensis	1	0.827	0.938	0.094	0.108	0.657	0.406	0.414	2.38	47.01	1000.00
Chipping Sparrow	Spizella passerina	2	0.654	0.718	0.085	0.129	0.485	0.326	0.336	1.50	32.59	595.99
Field Sparrow	Spizella pusilla	1	0.572	0.635	0.071	0.126	0.508	0.262	0.396	1.83	31.20	544.11

	Diamond Firetail	Stagonopleura guttata	1	0.592	0.760	0.097	0.117	0.503	0.409	0.569	1.25	34.59	720.08
	Double-barred Finch	Taeniopygia bichenovii	1	0.536	0.672	0.084	0.093	0.211	0.387	0.321	0.88	28.19	409.27
	Zebra Finch	Taeniopygia guttata	1	0.367	0.490	0.053	0.055	0.270	0.173	0.355	0.93	16.94	458.34
	Common Blackbird	Tordus merula	1	2.331	2.816	0.247	0.203	1.874	0.863	1.372	4.44	124.05	1914.09
	House Wren	Troglodytes aedon	1	0.880	0.863	0.140	0.095	0.801	0.397	0.608	2.29	42.98	839.09
	White-throated Sparrow	Zonotrichia albicollis	1	1.370	1.344	0.151	0.225	0.989	0.617	0.629	2.75	56.88	1220.37
Pelecaniformes	Australian Pelican	Pelecanus conspicillatus	1	6.381	7.365	0.608		2.358	2.640	3.995	10.58	258.77	22500.00
Piciformes	Lesser Honeyguide	Indicator minor	1	0.377	0.636	0.099	0.090	0.771	0.454	0.639	1.40	34.51	649.61
	Downy Woodpecker	Picoides pubescens	1	0.772	1.262	0.123	0.204	0.745	0.654	0.798	2.25	50.09	997.53
	Yellow-bellied Sapsucker	Sphyrapicus varius	1	0.957	1.381	0.138	0.130	0.931	0.638	0.903	2.40	65.10	888.40
Procellariiformes	Black-browed Albatross	Thalassarche melanophrys	1	6.388	6.424	1.468		4.842	1.774	7.486	12.40	246.40	14129.34
	Short-tailed Shearwater	Puffinus tenuirostris	1	2.517	2.246	0.389		1.561	0.428	2.915	8.67	235.01	4757.72
Psittasiformes	Australian King Parrot	Alisterus scapularis	1	2.560	4.134	0.387	0.501	2.338	1.629	2.892	5.90	202.14	4478.76
	Long-billed Corella	Cacatua tenuirostris	1	4.798	5.319	0.604	0.430	1.796	0.957	2.297	12.39	224.85	11777.99

	Galah	Eolophus roseicapilla	1	3.738	4.874	0.535	0.317	1.722	1.664	2.450	7.24	211.06	6723.94
	Purple-crowned Lorikeet	Glossopsitta porphyrocephala	1	0.513	1.104	0.147	0.165	0.957	0.648	0.612	1.83	60.62	1939.19
	Budgerigar	Melopsittacus undulatus	1	0.666	0.828	0.081	0.038	0.464	0.327	0.556	1.78	59.64	1151.54
	Cockatiel	Nymphicus hollandicus	1	0.866	1.412	0.196	0.113	0.962	1.034	0.598	3.79	80.82	2111.00
	Superb Parrot	Polytelis swainsonii	1	1.960	1.782	0.312	0.199	1.041	0.834	1.818	3.92	134.88	2996.14
	Rainbow Lorikeet	Trichoglossus haematodus	1	1.199	1.886	0.234	0.173	1.511	0.660	2.211	4.37	123.42	3333.98
Strigiformes	Northern Saw-whet Owl	Aegolius acadicus	1	1.094	1.684	0.413	0.032	2.313	0.737	2.379	2.22	72.59	3142.86
	Short-eared Owl	Asio flammeus	1	1.768	2.623	0.456	0.067	1.593	0.779	3.138	3.86	99.16	6221.04
	Snowy Owl	Bubo scandiacus	1	4.209	7.459	1.295	0.219	2.029	1.341	7.573	10.93	257.72	18127.41
	Great Horned Owl	Bubo virginianus	1	4.968	6.984	1.419	0.203	3.515	2.156	5.733	10.69	231.98	19073.36
	Southern Boobook	Ninok boobook	1	3.342	4.632	0.646	0.084	2.153	2.214	4.281	5.50	148.15	6338.80
	Geat Grey Owl	Strix nebulosa	1	4.197	5.660	0.636	0.188	3.921	1.431	5.537	6.25	161.30	13433.40
	Barred Owl	Strix varia	1	3.360	4.381	0.769	0.142	1.562	1.862	5.783	7.25	166.64	12727.12
	Northern Hawk-Owl	Surnia ulula	1	7.118	5.600	0.498	0.161	1.907	1.182	4.213	7.68	204.75	9408.30

	Barn Owl	Tyto alba	1	1.611	1.740	0.349	0.060	1.326	0.660	3.374	2.93	74.09	5849.81
Trochiliformes	Rufous-tailed Hummingbird	Amazilia tzacatl	1	0.171	0.233	0.026	0.023	0.262	0.127	0.376	0.43	12.77	182.19
	Anna's Hummingbird	Calypte anna	1	0.095	0.189	0.046	0.031	0.245	0.170	0.417	0.45	14.28	183.88
	Long-tailed Hermit	Phaethornis superciliosus	1	0.134	0.191	0.024	0.044	0.330	0.135	0.461	0.55	14.72	216.15
	Rufous Hummingbird	Selasphorus rufus	1	0.143	0.216	0.038	0.036	0.309	0.117	0.327	0.39	13.63	151.64

Appendix F Results of least-squares linear regression performed on the log-transformed volume the magnocellular and parvocellular portions of nucleus isthmi (Imc, Ipc), the nucleus semilunaris (SLu), the isthmo optic nucleus (ION), the ventral part of the geniculate nucleus (Glv), the nucleus of the basal optic root (nBOR), the nucleus lentiformis mesencephali, the nucleus rotundus (nRt) and the optic tectum (TeO) against the log-transformed brain volume minus the volume of the respective nuclei are provided using both species as independent data points ('no phylogeny') and two models of evolutionary change, Brownian motion (PGLS) and Ornstein-Uhlenbeck (OU; [Garland and Ives, 2000; Garland et al., 2005]) with two different phylogenetic trees.

	model			Imc				model			Glv		
		d .f.	F	slope	r2	AIC			d .f.	F	slope	r2	AIC
No phylogeny		1,96	284.08	0.765	0.747	-18.72	No phylogeny		1,96	217.54	0.567	0.694	-50.98
Livezey and Zusi, 2007	PGLS	1,96	247.92	0.914	0.721	-57.95	Livezey and Zusi, 2007	PGLS	1,96	79.94	0.512	0.454	-60.71
	OU	1,96	251.29	0.896	0.724	-58.49		OU	1,96	115.05	0.538	0.545	-69.18
Hackett et al., 2008	PGLS	1,98	238.39	0.911	0.713	-53.51	Hackett et al., 2008	PGLS	1,96	85.66	0.522	0.472	-62.18
	OU	1,98	237.71	0.890	0.712	-54.21		OU	1,96	116.29	0.542	0.548	-70.16
	model			Ipc				model			nBOR		
		d .f.	F	slope	r2	AIC			d .f.	F	slope	r2	AIC
No phylogeny		1,96	298.88	0.747	0.757	-28.30	No phylogeny		1,96	277.01	0.614	0.743	-59.34
Livezey and Zusi, 2007	PGLS	1,96	247.92	0.914	0.721	-57.95	Livezey and Zusi, 2007	PGLS	1,96	161.54	0.697	0.627	-69.38

	OU	1,96	251.29	0.896	0.724	-58.49		OU	1,96	189.17	0.664	0.663	-76.70
Hackett et al., 2008	PGLS	1,96	191.38	0.853	0.666	-44.89	Hackett et al., 2008	PGLS	1,96	159.87	0.690	0.625	-68.69
	OU	1,96	205.31	0.816	0.681	-49.87		OU	1,96	183.04	0.656	0.656	-75.45
	model			Slu				model			LM		
		d .f.	F	slope	r2	AIC			d .f.	F	slope	r2	AIC
No phylogeny		1,96	506.08	0.762	0.841	-75.85	No phylogeny		1,98	537.69	0.741	0.849	-87.26
Livezey and Zusi, 2007	PGLS	1,96	154.63	0.617	0.748	-50.93	Livezey and Zusi, 2007	PGLS	1,96	173.86	0.618	0.644	-99.93
	OU	1,96	364.08	0.760	0.791	-76.53		OU	1,96	244.27	0.659	0.718	-106.76
Hackett et al., 2008	PGLS	1,96	204.57	0.863	0.681	-50.31	Hackett et al., 2008	PGLS	1,96	180.86	0.626	0.653	-99.75
	OU	1,96	221.55	0.829	0.698	-54.86		OU	1,96	248.13	0.663	0.721	-107.26
	model			ION				model			TeO		
		d .f.	F	slope	r2	AIC			d .f.	F	slope	r2	AIC
No phylogeny		1,96	20.74	0.313	0.178	62.51	No phylogeny		1,96	371.01	0.663	0.794	-70.18
Livezey and Zusi, 2007	PGLS	1,96	59.25	0.681	0.382	24.52	Livezey and Zusi, 2007	PGLS	1,96	176.58	0.663	0.648	-84.78
	OU	1,96	53.61	0.634	0.358	24.43		OU	1,96	234.84	0.669	0.710	-94.38
Hackett et al., 2008	PGLS	1,96	49.28	0.647	0.339	33.93	Hackett et al., 2008	PGLS	1,96	166.41	0.652	0.634	-80.81
	OU	1,96	44.09	0.588	0.315	31.12		OU	1,96	218.69	0.658	0.695	-90.14
	model			nRt									
		d .f.	F	slope	r2	AIC							
No phylogeny		1,96	418.27	0.686	0.813	-77.73							

Livezey and Zusi, 2007	PGLS	1,96	288.34	0.759	0.750	-109.95			
	OU	1,96	315.77	0.746	0.766	-113.67			
Hackett et al., 2008	PGLS	1,96	272.65	0.745	0.739	-105.73			
	OU	1,96	294.06	0.735	0.753	-109.51			

Appendix G Results of least-squares linear regression performed on the log-transformed volume the magnocellular and parvocellular portions of nucleus isthmi (Imc, Ipc), the nucleus semilunaris (SLu), the isthmo optic nucleus (ION), the ventral part of the geniculate nucleus (Glv), the nucleus of the basal optic root (nBOR), the nucleus lentiformis mesencephali, the nucleus rotundus (nRt) and the optic tectum (TeO*)* against the log-transformed brain volume minus the volume of the respective nuclei with the order of each species as a covariate. Results are provided using both species as independent data points ('no phylogeny') and two models of evolutionary change, Brownian motion (PGLS) and Ornstein-Uhlenbeck (OU) with two different phylogenetic trees. Values for regression of the log-transformed volume of Imc, Ipc and Slu against the log-transformed TeO volume are also provided.

Covariates		Imc				Ipc				SLu			
Brain / order	Model	d .f.	F	p	AIC	d.f.	F	p	AIC	d.f.	F	p	AIC
No phylogeny		15, 81	8.58	< 0 .0001	-81.95	15,81	6.83	< 0 .0001	78.39	15,81	2.21	< 0.05	-79.46
Livezey and Zusi, 2007	PGLS	15, 81	3.16	< 0.001	-73.28	15,81	3.25	< 0.001	-66.52	15,81	1.14	0.34	-39.69
	OU	15, 81	3.92	< 0 .0001	-87.78	15,81	3.75	< 0 .0001	-82.53	15,81	1.68	0.07	-77.48
Hackett et al., 2008	PGLS	15, 81	3.48	< 0.001	-72.32	15,81	3.25	< 0.01	-65.55	15,81	1.13	0.34	-39.69
	OU	15, 81	4.34	< 0 .0001	-87.77	15,81	4.27	< 0 .0001	-82.61	15,81	1.67	0.07	-77.48
TeO / order	Model	d.f.	F	p	AIC	d.f.	F	p	AIC	d.f.	F	p	AIC
No phylogeny		15, 81	4.24	< 0 .0001	-115.39	15,81	2.86	< 0.01	-138.67	15,81	4.55	< 0.0001	-115.68
Livezey and Zusi, 2007	PGLS	15, 81	0.63	0.84	-64.39	15,81	0.54	0.91	-94.86	15,81	0.68	0.80	-53.93

	OU	15, 81	4.13	< 0 .0001	-113.39	15,81	2.31	< 0.01	-136.67	15,81	4.54	< 0.0001	-113.68
Hackett et al., 2008	PGLS	15, 81	0.66	0.81	-63.73	15,81	0.58	0.88	-94.69	15,81	0.70	0.78	-53.10
	OU	15, 81	4.13	< 0 .0001	-113.39	15,81	2.28	< 0.01	-136.66	15,81	4.54	< 0.0001	-113.68
Brain / Imc layers	Model	d .f.	F	p	AIC	d.f.	F	p	AIC	d.f.	F	p	AIC
No phylogeny		1,95	1.67	0.199	-18.43	1,95	0.0005	0.98	-26.30	1,95	0.84	0.36	-74.71
Livezey and Zusi, 2007	PGLS	1,95	0.46	0.501	-56.42	1,95	3.36	0.07	-51.72	1,95	0.50	0.48	-49.44
	OU	1,95	0.15	0.700	-56.53	1,95	1.75	0.19	-53.82	1,95	0.69	0.41	-75.26
Hackett et al., 2008	PGLS	1,95	0.11	0.744	-51.62	1,95	0.11	0.74	-43.00	1,95	0.00	0.95	-45.94
	OU	1,95	0.30	0.587	-52.64	1,95	0.01	0.92	-47.87	1,95	0.58	0.45	-74.14
TeO / Imc layers	Model	d .f.	F	p	AIC	d.f.	F	p	AIC	d.f.	F	p	AIC
No phylogeny		1,95	15.62	> 0.001	-101.46	1,95	6.49	0.01	-131.42	1,95	0.14	0.71	-83.98
Livezey and Zusi, 2007	PGLS	1,95	0.80	0.372	-82.43	1,95	0.21	0.64	-113.72	1,95	0.29	0.59	-70.61
	OU	1,95	8.07	0.006	-103.70	1,95	3.00	0.09	-133.58	1,95	0.05	0.83	-89.28
Hackett et al., 2008	PGLS	1,95	0.43	0.515	-80.85	1,95	0.009	0.92	-112.63	1,95	0.03	0.86	-69.17
	OU	1,95	8.45	0.005	-103.14	1,95	3.517	0.06	-133.81	1,95	0.08	0.77	-89.19
Brain / Imc layers	Model	d .f.	F	p	AIC	d.f.	F	p	AIC	d.f.	F	p	AIC
		ION				Glv				nBOR			
Brain / order	Model	d .f.	F	p	AIC	d.f.	F	p	AIC	d.f.	F	p	AIC
No phylogeny		15, 81	17.52	< 0 .0001	-49.17	15,81	7.14	< 0 .0001	-103.56	15,81	7.20	< 0 .0001	-112.37
Livezey and Zusi, 2007	PGLS	15, 81	4.16	< 0 .0001	-1.49	15,81	1.58	0.10	-55.92	15,81	1.29	0.22	-60.37
	OU	15, 81	16.58	< 0 .0001	-47.17	15,81	7.13	< 0 .0001	-101.56	15,81	7.09	< 0 .0001	-110.37
Hackett et al., 2008	PGLS	15, 81	5.27	< 0 .0001	-2.79	15,81	1.45	0.14	-55.43	15,81	1.43	0.15	-61.75

	OU	15, 81	16.35	< 0 .0001	-47.17	15,81	7.13	< 0 .0001	-101.56	15,81	7.05	< 0 .0001	-110.37
		LM				nRt				TeO			
Brain / order	Model	d .f.	F	p	AIC	d.f.	F	p	AIC	d.f.	F	p	AIC
No phylogeny		15, 81	6.67	< 0 .0001	-136.06	15,81	10.60	< 0 .0001	-154.19	15,81	7.72	< 0 .0001	-127.21
Livezey and Zusi, 2007	PGLS	15, 81	1.02	0.44	-86.89	15,81	2.90	< 0.01	-122.13	15,81	2.52	< 0.01	-92.26
	OU	15, 81	6.67	< 0 .0001	-134.06	15,81	6.05	< 0 .0001	-152.75	15,81	4.47	< 0 .0001	-125.21
Hackett et al., 2008	PGLS	15, 81	1.01	0.45	-86.63	15,81	3.41	< 0.001	-123.69	15,81	2.88	< 0.01	-92.70
	OU	15, 81	6.67	< 0 .0001	-134.06	15,81	6.29	< 0 .0001	-152.87	15,81	4.94	< 0 .0001	-125.21

Appendix H. Maximum likelihood estimators for the λ and α for the the log-transformed volume and the relative size (residuals, see methods) of nine visual nuclei using two different phylogenies. *P* values for the λ and α parameters were determined from likelihood ratio tests against an unconstrained Brownian motion model. Values for the relative size using Hackett et al., [2008] phylogeny are shown in table 6.1.

Hackett et al., (2008)/log-volume	brownian	Lambda			Alpha	
brain structure	Ln likelihood	lambda	Ln likelihood	p	alpha	Ln likelihood	p
Imc	-31.75	1.00	-31.75	1.00	0.13	-30.90	0.194
Ipc	-28.27	1.00	-28.27	1.00	0.12	-27.37	0.180
Slu	-19.26	0.91	-18.60	0.25	0.09	-18.62	0.258
ION	-15.90	1.00	-15.90	1.00	0.21	-13.19	0.020
Glv	9.65	0.94	10.21	0.29	0.02	9.70	0.739
nBOR	-9.62	0.81	-8.38	0.11	0.11	-9.08	0.296
LM	2.56	0.89	3.07	0.31	0.01	2.57	0.874
Rt	-12.21	1.00	-12.21	1.00	0.05	-11.95	0.478
Tectum	-8.57	1.00	-8.57	1.00	0.04	-8.45	0.620

Livezey and Zusi (2007)/log-volume	brownian	Lambda			Alpha		
brain structure	Ln likelihood	lambda	Ln likelihood	p	alpha	Ln likelihood	p
Imc	-32.43	1.00	-32.43	1.00	0.15	-30.98	0.089
Ipc	-29.03	1.00	-29.03	1.00	0.15	-27.49	0.080
Slu	-19.63	1.00	-19.62	0.92	0.11	-18.60	0.153
ION	-17.38	1.00	-17.38	0.54	0.22	-14.07	0.010
Glv	9.35	0.98	9.54	0.93	0.03	9.42	0.704
nBOR	-9.73	1.00	-9.72	0.52	0.14	-8.67	0.145
LM	1.91	0.97	2.11	0.52	0.02	1.95	0.765
nRt	-11.38	1.00	-11.38	1.00	0.085	-10.87	0.312
Tectum	-8.99	1.00	-8.99	1.00	0.09	-8.43	0.287

Livezey and Zusi (2007)/residuals	brownian	Lambda			Alpha		
brain structure	Ln likelihood	lambda	Ln likelihood	p	alpha	Ln likelihood	p
Imc	33.29	1.00	33.29	1.00	0.05	33.52	0.4990
Ipc	27.89	1.00	27.89	1.00	0.16	29.73	0.0553
Slu	30.96	0.086	36.34	0.0010	0.81	45.40	> 0.0001
ION	8.68	1.00	8.68	1.00	0.11	10.60	0.0498
Glv	39.63	0.87	42.75	0.01	0.22	42.82	0.0115

nBOR	40.41	0.85	43.73	0.01	0.26	43.90	0.0082
LM	53.02	0.55	63.33	> 0.0001	0.24	57.66	0.0023
nRt	64.24	1.00	64.24	1.00	0.07	64.96	0.230
Tectum	51.01	0.91	51.79	0.21	0.21	54.40	0.0092

Appendix I. Loadings, eigenvalues and cumulative amount of variation explained by four of the components (PC's) obtained from a PCA analysis using the log-transformed volume or the relative size (residuals, see methods) of nine visual nuclei. Values obtained using Livezey and Zusi [2007] phylogeny are shown.

Livezey and Zusi (2007)														
log-volume (BM)	PC1	PC2	PC3	PC4	Resid. (BM)	PC1	PC2	PC3	PC4	Resid. (λ)	PC1	PC2	PC3	PC4
Imc	-0.95	0.20	-0.03	-0.06		0.83	0.28	-0.07	0.13		-0.86	0.23	0.06	0.05
Ipc	-0.95	0.22	0.03	-0.02		0.90	0.23	0.04	0.03		-0.90	0.22	-0.06	0.05
Slu	-0.91	0.15	0.02	-0.06		0.70	0.06	0.04	0.03		-0.72	0.16	0.01	0.24
ION	-0.73	-0.30	-0.61	0.02		0.21	-0.33	-0.91	-0.07		-0.27	-0.35	0.89	-0.10
Glv	-0.76	-0.54	0.29	0.06		0.28	-0.82	0.19	-0.11		-0.26	-0.81	-0.18	-0.15
nBOR	-0.88	0.06	0.07	0.44		0.56	-0.06	0.13	-0.79		-0.61	-0.10	-0.22	-0.67
LM	-0.88	-0.25	0.15	-0.23		0.44	-0.69	0.18	0.33		-0.37	-0.71	-0.19	0.41
nRt	-0.96	0.11	-0.03	-0.02		0.81	0.11	-0.10	0.04		-0.85	0.07	0.06	-0.05
TeO	-0.95	0.17	0.04	-0.10		0.87	0.09	0.08	0.17		-0.88	0.08	-0.05	0.12
eigenvalues	7.11	0.60	0.48	0.26		4.02	1.42	0.95	0.79		4.21	1.43	0.92	0.73
% variance	79.02	6.71	5.37	2.93		44.68	15.77	10.50	8.79		46.77	15.88	10.18	8.11